Copyright is owned by the Author of the thesis. Permission is given for a copy to be downloaded by an individual for the purpose of research and private study only. The thesis may not be reproduced elsewhere without the permission of the Author.

Improving Granular Fertiliser Aerial Application for Hill Country Farming

A thesis presented in partial fulfilment of the requirements for the degree of

Doctor of Philosophy

In

Agricultural Engineering

At Massey University, Palmerston North, New Zealand



Sue Chok

2017

Abstract

Soil fertility and pasture productivity varies significantly over hill country farms. Therefore conventional aerial fertiliser application of a single application rate is inefficient. Automation of the aircraft hopper door increases control of fertiliser application. This includes the ability to achieve variable rate application, where multiple application rates can be applied over the farm. Ravensdown Limited has installed variable rate application technology (VRAT) on their Pacific Aerospace Cresco (PAC) 600 aircraft to improve the aerial application of granular fertiliser to hill country farms. The objective of this study was to measure and improve the performance of the VRAT system. Various aspects of the system's performance were examined; including hopper flow dynamics, control of the hopper door, estimation of a fertiliser particle's landing position from a known release point, collection of field data, and prediction of wind effects on the ground fertiliser distribution.

Performance trials, bench testing and static hopper flow tests were used to improve the VRAT system. Three performance trials were carried out. Each had a different sampling configuration: grid, nested grid and line. Sampling configuration varied because the objective of each trial differed, and there were advantages and disadvantages to each configuration. Accuracy, precision, level of off-target application, and capability of the VRAT system to vary application rate was measured. The trials observed accurate application rates, and improved precision when compared to pilot operated hopper doors. Off-target application occurred because the buffer was insufficiently sized, and did not consider the forward motion of particles, wind effects, and the mechanical/hydraulic limitations of the VRAT system. Bench testing, modelling and field trials can be used to improve the sizing of buffers under varying field conditions. Statistical tests showed the VRAT system was capable of applying different application rates to application zones.

While some parts of aerial topdressing can be controlled, there are other factors that cannot be controlled and are a source of variation. Several factors are discussed. Particle bounce out of the collectors was observed after the second performance trial. This issue under-estimated the field application rate in the first two performance trials. Additional trials were completed to improve the capture efficiency by 38% for superphosphate, and provided correction factors for DAP and urea.

Wind contributes to variability in aerial applications, and automation of the hopper door is unlikely to significantly mitigate its effects. Ravensdown Limited wished to develop a wind

displacement calculator tool. The calculator uses a single particle granular fertiliser ballistics model to predict the displacement of the transverse spread pattern and swath width by wind. To achieve this, the ballistics model was validated for superphosphate, urea, di-ammonium phosphate (DAP), and a 70% superphosphate/30% Flexi-N blend.

The model was validated from two data sets for each fertiliser type. From the first data set, the propeller wash component was excluded because fertiliser particles leave the hopper door in a mass flow. Therefore in the initial time steps, the particles are not singular and the propeller wash does not significantly influence their motion. There was good agreement between the field and modelled transverse spread patterns. Additionally, the Kolmogorov-Smirnov test statistically showed that the two distributions were similar. The development of the wind displacement calculator tool and production of wind displacement look up tables is described. From a limited number of inputs, the calculator predicts the displacement of the peak mass in a transverse spread pattern. To decrease modelling time, wind displacement look up tables were created from the tool for superphosphate, urea and DAP.

In conclusion, the VRAT system will improve fertiliser application to hill country. However, aerial topdressing is highly variable and some factors cannot be controlled. Ballistics modelling can be used to minimise these factors and improve understanding of the variability. The model and wind displacement calculator should be used with care, as they are based on assumptions, which may not be completely representative of field conditions.

Acknowledgements

Many people contributed to the success of this project. Firstly, I would like to thank my supervisors Professor Ian Yule and Dr. Miles Grafton for their advice and guidance throughout this project. I am grateful to them for giving me the opportunity to complete this PhD.

Next, I would like to thank the incredible team at the New Zealand Centre of Precision Agriculture, who helped me with my trials and provided sound advice in troubled times. In particular, I would like to acknowledge Kate Saxton for her work in organising staff and the logistics of the trials. I have also enjoyed my time with my fellow PhD students. They have not only provided entertainment and encouragement, but also voluntarily participated in my trials. Additionally, I would like to thank John Edwards for his years of advice and kindness in the lab, and Ray Watson (Comtel Limited) for being an amazing problem solver.

I am thankful for the funding provided by Callaghan Innovation and Ravensdown Limited. This project could not have been completed without the support of Ravensdown and their staff. I want to thank Michael White and Michael Manning for mentoring me and giving me the opportunity to learn more about Ravensdown. I would like to acknowledge Grant Lennox and Mark Tocher, who operated their aircraft for my trials and co-operated with my ideas.

Lastly, I would have not made it without the love and support of my family and friends. My parents have continued to support all my endeavours, and I am eternally grateful for their encouragement and advice.

Table of Contents

Abstract 1
Acknowledgements 3
Table of Contents 5
List of Tables 9
List of Figures 11
Chapter 1 – Introduction 17
1.1. Introduction 17
1.2. Specific Objectives 18
1.3. Aerial Topdressing 19
1.4. Variability in Aerial Topdressing 22
1.4.1. Fertiliser Characteristics 23
1.4.2. Fertiliser Transportation and Storage 28
1.4.3. Wind 29
1.4.4. Altitude 30
1.4.5. Topography 31
1.4.6. Aircraft Velocity 31
1.4.7. Spreaders 31
1.4.8. Swath width 32
1.5. Variable Rate Application Technology 33
1.6. Ballistics Modelling for Aerial Topdressing 37
1.6.1. Mass Flow Prediction 40
1.7. Sampling Methods 42
1.7.1. Geo-statistics 44
1.8. Main Points 47
1.9. Structure of Thesis 48
Chapter 2 - Ballistics Modelling for Aerial Topdressing of Granular Fertiliser 49
2.1. Introduction 49
2.2. Method 51
2.2.1. Validation Trial 1 51
2.2.2. Validation Trial 2 54
2.2.3. Validation Trial 3 56
2.2.4. Pre – Processing 57
2.3. Initial Model Program Set Up 61

2.3.1. Particle Size Distribution 61
2.3.2. Wind Power Law 64
2.3.3. Particle Sphericity 65
2.3.4. Initial Discharge Variables 65
2.4. Validation Results and Discussion 67
2.4.1. Trial 1 68
2.4.2. Trial 2 74
2.4.3. Trial 3 79
2.4.4. Model Accuracy 82
2.5. Wind Displacement Calculator 86
2.5.1. Python script 87
2.5.2. GIS Tool 87
2.5.3. Wind Displacement Look Up Tables 90
2.6. Conclusion 94
Chapter 3 - Methods and Evaluation of Sampling for Aerial Topdressing Performance Trials 97
3.1. Introduction 97
3.2. Trial 4 – Grid Sampling 98
3.3. Trial 5 – Nested Grid Sampling 101
3.4. Trial 6 – Pickwick Trial 103
3.4.1. Objective 1 105
3.4.2. Objective 2 116
3.4.3. Objective 3 117
3.4.4. Objective 4 118
3.5. Collector Improvement 119
3.5.1. Initial Collector Study 119
3.5.2. Trial 7 – Collector Trial 123
3.6. Trial 8 – Line Sampling 126
3.7. Conclusion 131
Chapter 4 - Performance of an Aerial Variable Rate Application System 133
4.1. Introduction 133
4.2. Results and Discussion of Performance Trials 134
4.2.1. Accuracy 134
4.2.2. Precision 135
4.2.3. Capability 137

4.3. Bench Testing 142
4.3.1. Method 143
4.3.2. Results and Discussion 146
4.4. Static Hopper Flow Calibration 155
4.5. Trial 8 163
4.6. Static Hopper Flow Calibration Re-test 168
4.7. Conclusion 172
Chapter 5 - Variability in Aerial Topdressing 175
5.1. Introduction 175
5.2. Part 1: Release of Fertiliser Particle from Aircraft 179
5.2.1. Hopper Flow Characteristics 179
5.2.2. Future Work 181
5.3. Part 2: Fertiliser Particle Motion through Air 183
5.3.1. Wind and topography 183
5.3.2. Future Work 185
5.4. Part 3: Fertiliser Placement and Measurement 185
5.4.1. Data Collection 185
5.4.2. Collector Efficiency 185
5.4.3. Collector Placement 187
5.4.4. Future Work 190
5.5. Implications of Research 192
5.6. Improvements to Research Methodology 194
5.7. Conclusion 196
Chapter 6 - Summary 199
6.1. Summary 199
6.2. Concluding Remarks 202
6.3. Publications 204
References 205
Appendix 213

List of Tables

Table 1.1: Standard SGN and UI values set by Spreadmark (NZFQC, 2016b). 25
Table 2.1: Target application rate, swath width and hopper door opening for Trial 1. 54
Table 2.2: Target application rate, swath width and hopper door opening for Trial 2. 56
Table 2.3: Particle size distribution from the bulk pile for Trial 1..... 58
Table 2.4: Particle density, size guide number (SGN) and uniformity index (UI) of particles from the bulk pile of Trial 1. 58
Table 2.5: Particle size distribution from the bulk pile for Trial 2..... 58
Table 2.6: Particle density, size guide number (SGN) and uniformity index (UI) of particles from the bulk pile of Trial 2. 59
Table 2.7: Particle size distribution from the bulk pile for Trial 3..... 59
Table 2.8: Inputs for the Beverloo equation. 60
Table 2.9: Image analysed particle size distribution from Trial 1 for DAP and urea. 63
Table 2.10: Air velocity in a nine duct spreader at an aircraft velocity of 62 m s^{-1}..... 66
Table 2.11: Pacific Aerospace Cresco 600 aircraft parameters. 66
Table 2.12: Input values for the hopper door when a spreader is not attached for the application. 66
Table 2.13: Input values for a Transland spreader. 67
Table 2.14: Input values for a FarmAir spreader. 67
Table 2.15: Application rates and swath widths from Trial 1 for each collector row. 70
Table 2.16: Application rates and swath widths from Trial 2 for each collector row. 76
Table 2.17: Image analysed particle size distribution from Trial 2 for urea. 78
Table 2.18: Application rates and swath widths from Trial 3 for each collector row. 79
Table 2.19: Comparison of ballistics model and Beverloo flow rates for Trial 1 and 2. 82
Table 2.20: Comparison of ballistics model and Beverloo flow rates for Trial 3. 83
Table 2.21: Comparison of intended, trial and model application rate and swath width for Trial 1-3. The difference (%) is between the trial and model application rate. 84
Table 2.22: P and D values from the Kolmogorov-Smirnov test for Trial 1 and 2. 84
Table 2.23: P and D values from the Kolmogorov-Smirnov test for Trial 3 for a 70% Superphosphate and 30% Flexi-N fertiliser blend. 85
Table 2.24: The wind velocity, wind angle and flow required to produce a transverse spread pattern for DAP in Trial 2 that rejected the null hypothesis when tested with the K-S test. 86
Table 3.1: Level settings for swath width, intended application rate and aircraft groundspeed for Trial 6. 106
Table 3.2: ANOVA and interaction test results for urea in Trial 6. 107
Table 3.3: Using Figure 3.7, Figure 3.8 and Figure 3.9 equations to predict field application rate from Longview validation trials (Trial 1 and 2). 110
Table 3.4: Percentage of particles bouncing out of a collector and their average particle strength. 119
Table 3.5: Height required to reach terminal velocity for three fertiliser types. 120
Table 3.6: Average masses collected from the three fertiliser collectors in Trial 7. 126
Table 3.7: Percentage difference in masses between collector types in Trial 7..... 126
Table 4.1: Summary of collector data for Trial 4 (Limestone Downs) and Trial 5 (Longview).. 135
Table 4.2: ANOVA test for collector distance and application rate from Trial 5. 136

Table 4.3: Percentage of correct hopper door openings for bench tested prescription maps of different sizes. 151
Table 4.4: Two-way ANOVA test comparing hopper door opening and the aircraft velocity to the distance the hopper door closes in relation to the application zone boundary. 152
Table 4.5: Comparison of parameters determined by linear regression for Beverloo equation and original coefficients. 162
Table 4.6: Comparison of field results with calculated clam shell door openings. Linear and Beverloo equation application rates were calculated using an aircraft velocity of 59 m s^{-1}. ... 163
Table 4.7: Summary of collector data for Trial 8. 166
Table 4.8: One way ANOVA test comparing the applications rates in the 250 kg ha^{-1} and 500 kg ha^{-1} application zones at a 95% confidence interval. 166
Table 4.9: Comparison of field results with calculated cantilever door openings for superphosphate. Linear and Beverloo equation application rates were calculated using an aircraft velocity of 59 m s^{-1}. 172
Table 5.1: Summary of trials undertaken in this study. 176
Table 5.2: Original results from Trial 4 and 5. The samples were not adjusted for bounce out of the collectors. 186

List of Figures

Figure 1.1: Example of Spreadmark calculating the average field mass from the transverse spread pattern and set swath width (i.e. 15 m). The blue line represents the distribution created from a racecourse (round and round) flight path, and the purple is for a to and fro flying pattern..... 21
Figure 1.2: Factors that affect the transverse spread pattern in aerial granular fertiliser application. 24
Figure 1.3: Examples of the relationship between UI and SGN sourced from NZFQC (2016b). The images represent fertiliser in a sieve box, where the x axis is the mesh size in mm..... 26
Figure 1.4: Chemical compatibility of common New Zealand fertilisers (Fertiliser Association, 2007). 27
Figure 1.5: Port side image of an 11 duct spreader that is attached to the hopper door on an aircraft. 32
Figure 1.6: Predicted field scale application on a 25 ha site where the hopper door is pilot operated and there is no GPS guidance (Murray, 2007). The application rates were modelled using Jones et al. (2008) and recorded aircraft data. 35
Figure 1.7: Predicted field scale application using an automated GPS guided hopper door. Murray (2007) produced this image from Figure 1.6 by removing all points outside the application area except when it was within 45 m of an application area. 35
Figure 1.8: Collector developed by Laslett (1994). 43
Figure 1.9: Collectors used by the New Zealand Agricultural Aviation Association. 43
Figure 1.10: Example of a semi-variogram adapted from Bohling (2005). 45
Figure 2.1: Pacific Aerospace Cresco 600. 49
Figure 2.2: Pre-determined location of collectors for Trial 1 in ArcGIS 10.1. 52
Figure 2.3: Trial 1 set up..... 52
Figure 2.4: Wind anemometer that records wind velocity and direction. 53
Figure 2.5: The wind velocity and direction over the trial period in Trial 1. True north is denoted by 0 degrees. 53
Figure 2.6: Pre-determined location of collectors for Trial 2 in ArcGIS 10.1. 54
Figure 2.7: Trial 2 set up..... 55
Figure 2.8: The wind velocity and direction over the trial period in Trial 2. True north is denoted by 0 degrees. 55
Figure 2.9: Trial 3 set up..... 56
Figure 2.10: The wind velocity and direction over the trial period in Trial 3. True north is denoted by 0 degrees. 57
Figure 2.11: A riffler used to equally divide a fertiliser sample. 58
Figure 2.12: Example of Mapstar 8 output for Trial 2. The green outline represents the application area. Blue lines are flight lines, where the hopper is closed, and the red rectangles are the flight lines where the hopper door is open. The width of each individual rectangle represents the set swath width. 60
Figure 2.13: Image analysis of a collected DAP sample using a New Zealand 50 cent coin as a size reference. 62
Figure 2.14: Cumulative particle size distribution of bulk and collected samples for DAP in Trial 1. 63

Figure 2.15: Cumulative particle size distribution of bulk and collected samples for urea in Trial 1. 63
Figure 2.16: Trial 1 spread patterns collected from the nine rows for superphosphate. 68
Figure 2.17: Trial 1 spread patterns collected from the nine rows for DAP. 69
Figure 2.18: Trial 1 spread patterns collected from the nine rows for urea. 69
Figure 2.19: Comparison of Murray (2007) model and Trial 1 spread patterns for superphosphate. For this spread pattern, the aircraft was travelling at a heading of 92°, aircraft velocity of 69 m s^{-1} and an altitude of 34.2 m. The wind direction was 158.62° and wind speed was 0.1 m s^{-1}. The modelled flow rate of superphosphate out of the hopper was 1261 kg min^{-1}. 71
Figure 2.20: Comparison of model and Trial 1 spread patterns for superphosphate. For this spread pattern, the aircraft was travelling at a heading of 92°, aircraft velocity of 69 m s^{-1} and an altitude of 34.2 m. The wind direction was 158.62° and wind speed was 0.1 m s^{-1}. The modelled flow rate of superphosphate out of the hopper was 1261 kg min^{-1}. 72
Figure 2.21: Comparison of model and Trial 1 spread patterns for DAP. For this spread pattern, the aircraft was travelling at a heading of 92°, aircraft velocity of 62 m s^{-1} and an altitude of 32.5 m. The wind direction was 149.15° and wind velocity was 0.214 m s^{-1}. The modelled flow of DAP out of the hopper was 1300 kg min^{-1}. 72
Figure 2.22: Comparison of model and Trial 1 spread patterns for urea. For this spread pattern, the aircraft was travelling at a heading of 92°, aircraft velocity of 65 m s^{-1} and an altitude of 34.4 m. The wind direction was 178° and wind speed was 0.58 m s^{-1}. The modelled flow rate of urea out of the hopper was 551 kg min^{-1}. 73
Figure 2.23: Trial 2 spread patterns collected from six rows for superphosphate. 74
Figure 2.24: Trial 2 spread patterns collected from six rows for DAP. 75
Figure 2.25: Trial 2 spread patterns collected from six rows for urea. 75
Figure 2.26: Comparison of model and Trial 2 spread patterns for superphosphate. For this spread pattern, the aircraft was travelling at a heading of 273°, aircraft velocity of 59 m s^{-1} and altitude of 33.3 m. The wind direction was 77° and wind speed was 1.6 m s^{-1}. The modelled flow rate of superphosphate out of the hopper was 982 kg min^{-1}. 77
Figure 2.27: Comparison of model and Trial 2 spread patterns for DAP. For this spread pattern, the aircraft was travelling at a heading of 273°, aircraft velocity of 58 m s^{-1} and altitude of 32.5 m. The wind direction was 81° and wind velocity was 1.44 m s^{-1}. The modelled flow rate of DAP out of the hopper was 1490 kg min^{-1}. 77
Figure 2.28: Cumulative particle size distribution of bulk and collected samples for urea in Trial 2. 78
Figure 2.29: Comparison of model and Trial 2 spread patterns for urea. For this spread pattern, the aircraft was travelling at a heading of 273°, aircraft velocity of 63 m s^{-1} and altitude of 41.8 m. The wind direction was 85° and wind velocity was 2.57 m s^{-1}. The modelled flow rate of urea out of the hopper was 845 kg min^{-1}. 79
Figure 2.30: Trial 3 spread patterns collected from Flight 1 for the 70% superphosphate/30% Flexi-N blend. 80
Figure 2.31: Trial 3 spread patterns collected from Flight 2 for the 70% superphosphate/30% Flexi-N blend. 80
Figure 2.32: Comparison of model and Trial 3 spread pattern for Flight 1. For this spread pattern, the aircraft was travelling at a heading of 251°, aircraft velocity of 67 m s^{-1} and altitude

of 18.6 m. The wind direction was 185° and wind speed was 0.4 m s^{-1}. The flow rate of the blend out of the hopper was 684 kg min^{-1}..... 81
Figure 2.33: Comparison of model and Trial 3 spread pattern for Flight 2. For this spread pattern, the aircraft was travelling at a heading of 251°, aircraft velocity of 69 m s^{-1} and altitude of 11.6 m. The wind direction was 184° and wind velocity was 0.215 m s^{-1}. The flow rate of the blend out of the hopper was 822 kg min^{-1}..... 82
Figure 2.34: Comparison of model and Trial 2 row 6 spread pattern for DAP. For this spread pattern, the aircraft was travelling at a heading of 273°, aircraft velocity of 58 m s^{-1} and altitude of 32.5 m. The wind direction was 88.2° and wind speed was 1.8 m s^{-1}. The modelled flow rate of superphosphate out of the hopper was 1090 kg min^{-1}. 86
Figure 2.35: Example vector diagram of the wind offset calculated for a wind speed of 0.75 m s^{-1} at 300°..... 89
Figure 2.36: Example of application area and its offset when the average wind speed is 0.75 m s^{-1}, wind direction is 300° and aircraft heading is 10°. This was modelled for superphosphate. 89
Figure 2.37: Peak lateral mass displacement for wind direction of 180°, 270° and 340°, and wind velocity for superphosphate with no spreader..... 91
Figure 2.38: Swath width for wind direction of 180°, 270° and 340°, and wind velocity for superphosphate with no spreader..... 92
Figure 2.39: Peak lateral mass displacement for wind direction of 180°, 270° and 340°, and wind velocity for urea with an 11 duct spreader..... 93
Figure 2.40: Swath width for wind direction of 180°, 270° and 340°, and wind velocity for urea with an 11 duct spreader..... 93
Figure 3.1: Sampling configuration for Trial 4. 99
Figure 3.2: Sampling configuration for Trial 5. 102
Figure 3.3: Wind velocity and direction over the trial period in Trial 5. True north is denoted by 0 degrees..... 103
Figure 3.4: Wind velocity and direction over the trial period in Trial 6. True north is denoted by 0 degrees..... 105
Figure 3.5: Sample areas for Trial 6. 106
Figure 3.6: Trial set up in Area 3 in Trial 6. 107
Figure 3.7: The relationship between the measured field application rate and hopper door opening for urea in Trial 6. The dashed lines are the confidence interval (CI) of the linear equation..... 109
Figure 3.8: The relationship between the measured field application rate and hopper door opening for superphosphate in Trial 6. The dashed lines are the confidence interval (CI) of the linear equation..... 109
Figure 3.9: The relationship between the measured field application rate and hopper door opening for DAP in Trial 6. The dashed lines are the confidence interval (CI) of the linear equation..... 110
Figure 3.10: Relationship between intended and measured field application rate in Trial 6. Lines representing 1:1, 1:1.5 and 1:2 are included to illustrate the magnitude of difference between the two application rates..... 111
Figure 3.11: The relationship between the measured field application rate and swath width for urea in Trial 6. 112

Figure 3.12: The relationship between the measured field application rate and swath width for superphosphate in Trial 6. 113
Figure 3.13: The relationship between the measured field application rate and swath width for DAP in Trial 6. 113
Figure 3.14: Relationship between the measured field application rate and the recorded aircraft velocity for urea in Trial 6. 115
Figure 3.15: Relationship between the measured field application rate and the recorded aircraft velocity for superphosphate in Trial 6. 115
Figure 3.16: Relationship between the measured field application rate and the recorded aircraft velocity for DAP in Trial 6. 116
Figure 3.17: Comparison of the field application rate and the field Beverloo equation for Trial 6. 116
Figure 3.18: Distance fertiliser particles were found from the boundary for different edge time settings in Trial 6. A positive distance from the boundary indicates the particle landed within the application area and vice versa. 118
Figure 3.19: Image still of a video taken at 500 frames per second recorded at Pickwick farm of superphosphate taken at Trial 6. 119
Figure 3.20: Set up for terminal velocity of 9 m height. 120
Figure 3.21: Comparison of calculated and measured terminal velocities for various superphosphate particle sizes. Calculations were made using Haider and Levenspiel (1989). 121
Figure 3.22: Comparison of calculated and measured terminal velocities for various urea particle sizes. Calculations were made using Haider and Levenspiel (1989). 121
Figure 3.23: Comparison of calculated and measured terminal velocities for various DAP particle sizes. Calculations were made using Haider and Levenspiel (1989). 122
Figure 3.24: Sampling configuration for Trial 7. 124
Figure 3.25: Collector set up for Trial 7 on trial day. 124
Figure 3.26: Wind velocity and direction over the trial period in Trial 7. True north is denoted by 0 degrees. 125
Figure 3.27: Collectors set up with the bubble wrap liner in Trial 8. 127
Figure 3.28: Collectors set up in a line with replicates in Trial 8. The collectors travel over one hill and up one hill. 128
Figure 3.29: Sample configuration and application zones for Trial 8. 129
Figure 3.30: Wind velocity and direction over the trial period in Trial 8. True north is denoted by 0 degrees. 130
Figure 4.1: Comparison of application rate with the collector's proximity to the nearest treatment boundary line for Trial 4. A positive distance means the collector was in the 250 kg ha^{-1} application zone. 137
Figure 4.2: Comparison of application rate to the collector's proximity to the nearest treatment boundary line for Trial 5. A positive distance means the collector was in the 162 kg ha^{-1} application zone. 137
Figure 4.3: Semi-variogram of aircraft data from Trial 4 (A) and Trial 5 (B). The y-axis is the semi-variance and the x-axis is the lag distance (m). 138
Figure 4.4: Semi-variogram of collector data from Trial 4 (A) and Trial 5 (B). The y-axis is the semi-variance and the x-axis is the lag distance (m). 139
Figure 4.5: Proof of release (A) and placement (B) maps for Trial 4. 140

Figure 4.6: Proof of release (A) and placement (B) maps for Trial 5. 140
Figure 4.7: Error between predicted values and recorded aircraft values for Trial 4 (A) and Trial 5 (B). The y-axis is the predicted application rate (kg ha^{-1}) that was found using kriging, and the x-axis is the aircraft application rate (kg ha^{-1})..... 141
Figure 4.8: Error between predicted values and collector data for Trial 4 (A) and Trial 5 (B). The y-axis is the predicted application rate (kg ha^{-1}) that was found using kriging, and the x-axis is the field application rate (kg ha^{-1})..... 141
Figure 4.9: Prediction standard error maps for collector data for Trial 4 (A) and Trial 5 (B). .. 142
Figure 4.10: Aircraft hopper door in closed position. 144
Figure 4.11: Aircraft hopper door in the open position..... 144
Figure 4.12: Mechanical set up of variable rate bench testing unit. 145
Figure 4.13: Satloc user interface with simulated flight example. Blues lines represent a closed hopper and bold green lines are an open hopper. The red square is the application area. 145
Figure 4.14: Example of 1000 m by 1000 m application zone displayed in Mapstar 8. 147
Figure 4.15: Distance to/from boundary against the edge on/off setting for a dual accumulator. 147
Figure 4.16: An example of a prescription map and flight lines for Part 3 displayed in Mapstar 8. This shows a 50 m gap. The green line represents the application area. Flight lines are represented by the blue (fully closed hopper) and red lines (open hopper). 148
Figure 4.17: An example of a prescription map and flight lines from Part 4 displayed in Mapstar 8. This polygon is angled 20 degrees. 149
Figure 4.18: An example of a prescription map and flight lines for Part 5 displayed in Mapstar 8. This polygon has 100 vertices. 150
Figure 4.19: An example of a prescription map that consists of adjacent polygons (250 and 500 kg ha^{-1}), exclusion zones (0 kg ha^{-1}) and different application rates (200, 350, 400 kg ha^{-1}). This is displayed in Mapstar 8. 153
Figure 4.20: Two polygons separated by a gap of 50 m, where no application should occur. Application rates in the polygons are 200 and 400 kg ha^{-1}. This is displayed in Mapstar 8. 153
Figure 4.21: Simulated response of Figure 4.20 from the bench VRAT system in Mapstar 8 based on 'edge on' setting of 0.5 s and 'edge off' of 1.6 s. Entry into the application zone is denoted by the black arrows. The system did not react as intended. 154
Figure 4.22: Large farm prescription map for variable rate application..... 154
Figure 4.23: Response from creating an exclusion application zone displayed in Mapstar 8. Entry into the application area is denoted by black arrows. The red strips represent an open hopper door. 155
Figure 4.24: Hopper door was manually opened using the lever and, in this case, the flow rate of superphosphate was being measured..... 157
Figure 4.25: Static PAC hopper with clamshell doors operated by a lever (on left). A Mettler Toledo display is fixed on the front (centre of picture). 157
Figure 4.26: Example of funnel flow regime for a powder, courtesy of John Maber (Grafton, 2010). The angle of the standard PAC hopper allowed the hopper to empty and ratholing did not occur. 158
Figure 4.27: Flow rate out of the clamshell hopper door against time for three door openings (0.025 m, 0.046 m and 0.075 m)..... 159

Figure 4.28: Relationship between flow rate and the clam shell hopper door opening with linear regression for superphosphate. 159
Figure 4.29: Relationship between flow rate and the clam shell hopper door opening with linear regression for DAP. 160
Figure 4.30: Relationship between flow rate and the clam shell hopper door opening with linear regression for urea. 160
Figure 4.31: Relationship of flow rate to the 2/3 power and the clam shell hopper door opening with linear regression for superphosphate. 161
Figure 4.32: Relationship of flow rate to the 2/3 power and the clam shell hopper door opening with linear regression for DAP. 161
Figure 4.33: Relationship of flow rate to the 2/3 power and the clam shell hopper door opening with linear regression for urea. 162
Figure 4.34: Flight points recorded every 0.2 s on VRAT system. Hopper door opening in 1/16th inches are labelled. 164
Figure 4.35: Field application rate across the line of bubble wrap lined collectors from the west to east direction. Replicate lines are included. The location of the replicate line is denoted in the legend as north or south of the main center line. AZ stands for application zone. 165
Figure 4.36: Categorised application rate from collectors at each location. Yellow coloured points represent the target application rate range for the 250 kg ha^{-1} zone and red is the target range of application rates for the 500 kg ha^{-1} zone. 167
Figure 4.37: Particle size distribution comparison between the bulk and field samples for Trial 8. 168
Figure 4.38: Comparison of the intended hopper door opening and the measured hopper door opening. 169
Figure 4.39: Flow rate out of the cantilever hopper door against time for three door openings (0.032 m, 0.047 m and 0.066 m). 170
Figure 4.40: Open cantilever hopper door illustrating the main door opening and the smaller opening. 170
Figure 4.41: Relationship between average flow rate and the cantilever hopper door opening with linear regression for superphosphate. 171
Figure 4.42: Relationship of flow rate to the 2/3 power and the cantilever hopper door opening with linear regression for superphosphate. 172
Figure 5.1: Factors that affect the transverse spread pattern in aerial granular fertiliser application. 178
Figure 5.2: Top view of the cantilever hopper door with door hinges annotated. 179
Figure 5.3: Flow rate out of a 0.0254 m cantilever hopper door opening against time for superphosphate 180
Figure 5.4: Aircraft flight lines recorded every 0.2 s by the VRAT system for Trial 4. 188

Chapter 1 – Introduction

1.1. Introduction

Aerial topdressing is used in New Zealand to apply over 1.65 million tonnes of granular fertiliser to hill country (Statistics New Zealand, 2012). The current practice is to uniformly apply one application rate over an area. The extent of the application area is controlled by the pilot, where boundaries are visually reconciled and the pilot must take timely actions to control the hopper door. This is completed while the aircraft is operating at approximately 200 km h^{-1} and 35 m above varied terrain.

Within New Zealand's hill country farms, soil fertility and pasture productivity varies considerably. Slope, aspect, soil erosion, environmental conditions and fertiliser use have been identified as factors that affect pasture production, and therefore the stocking rate (Gillingham and During, 1973; Gillingham et al., 1998; Suckling, 1959). Thus, hill country is far more variable than New Zealand's other farming systems. Clearly the fertiliser requirements within farms will be highly variable, and it is beyond the scope of a pilot operating an aircraft manually to achieve a variable rate application. A variable rate application technology (VRAT) system will be required to recognise boundaries automatically, and reduce or eliminate off-target application.

In order to provide a controllable application rate, the hopper door must be able to compensate for changes in aircraft velocity as it varies during flight. The system is linked to GPS (Global Positioning System) in order to provide information on velocity and location. If variable rate technology is to be employed then variable rate application maps must be provided. Ballistics modelling can be deployed to account for dynamic issues surrounding the release of fertiliser from the aircraft and calculate the approximate landing point, especially in the presence of wind. Based on the application map, the VRAT system will select the hopper door opening from the recorded aircraft position, and control its closing and opening around wind compensated boundaries.

Ravensdown Limited, through Ravensdown Aerowork Limited, own and operate topdressing aircraft, and are developing and installing VRAT systems. While aspects of their performance have been partially studied, the overall field operational performance of such systems has not been studied. Some of the previous work has also been subject to only partial measurement with a number of assumptions made about the consistency of performance (Grafton et al., 2012; Morton et al., 2016).

The scope of this project includes the validation of a single particle ballistics model formulated by Jones et al. (2008), but developed for a different aircraft (Gippsland Aeronautics GA-200C). This study validated the model for a Pacific Aerospace Cresco (PAC) 600, with the intention to create a wind displacement calculator tool that can be used to recalculate aircraft flying pattern according to the average wind conditions. This wind displacement calculator tool gives the operators information to avoid off-target application.

As an introduction, this literature review discusses previous studies, explains key concepts and provides relevant background information. Topics include:

- Aerial topdressing
- Variability in aerial topdressing
- Variable rate application technology
- Ballistics modelling
- Sampling methods

The work presented in this thesis is linked to a Primary Growth Partnership (PGP) project called 'Pioneering to Precision – Application of Fertiliser in Hill Country', which seeks to create variable rate application fertiliser plans from remotely sensed data (Ministry of Primary Industries, 2017). The intention is for a fertiliser application plan to be pre-loaded into an aircraft before an application, so that there is automated control of the aircraft hopper door. In addition to addressing the requirements for more accurate fertiliser application and to improve the ability of delivering the prescribed application rate, the VRAT system has been developed to minimise some of the safety and off-target application issues encountered by aerial spreaders. The objective is to have a safer, more accurate, and easy to operate system that delivers benefits to both the applicator and farmer.

1.2. Specific Objectives

1. Validate the particle ballistics model formulated by Jones et al. (2008) for three common New Zealand fertiliser types: superphosphate, urea and di-ammonium phosphate.
2. Validate the particle ballistics model for a superphosphate/Flexi-N blend of a particular composition.
3. Create a Geographical Information Systems (GIS) tool that considers average wind speed and direction, using the ballistics model when planning on-farm flights. This tool is named the 'wind displacement calculator'.

4. Determine appropriate methods of field fertiliser collection in aerial application trials in order to evaluate spreading efficiency. This includes an examination of the efficacy of current field collectors.
5. Measure the performance of a variable rate application system on a fixed wing agricultural aircraft.

1.3. Aerial Topdressing

The temperate New Zealand climate allows medium to steep hill country to grow pasture and support all year grazing. In order to maintain and optimise pasture growth, good farm management is required. Fertiliser is one part of that equation. Previous studies have illustrated that withholding superphosphate on hill country farms negatively effects pasture production, plant species quality, and animal production (Gillingham et al., 1998; Lambert et al., 1990; O'Connor et al., 1990). However, due to the significant variations in hill country topography, fertiliser cannot be applied by truck. A cost effective solution is to use fixed wing aircraft and helicopters to topdress these pastures.

The first known aerial application was carried out by a hot air balloon applying seed. Aerial topdressing was developed in New Zealand in the 1940s as a means to apply granular fertiliser on to hill country (Geelen, 1983). This was completed because nutrient levels within hill country were becoming depleted, resulting in poor performance. Shortly after, this was adopted by other countries, such as Australia, United States and the United Kingdom. Globally, aerial topdressing is primarily used in the spraying of liquid fertilisers and insecticides/fungicides for crops. It is also used in applying seed, granular fertilisation of pasture, in commercial forests, and for pest control. However, the majority of fixed wing aircraft hours in New Zealand are spent topdressing hill country farms with granular material.

Topdressing by aircraft is common for hill country pasture. In New Zealand, the Pacific Aerospace Fletcher (PAF) and Cresco (PAC) are popular fixed wing aircraft used for spreading. The PAC hoppers have a capacity of 2 m^3. Flow out of the hopper is gravity fed with the application rate controlled by the hopper door aperture. In a pilot operated system, the pilot adjusts a lever in the cockpit to set the hopper door opening. Pilots often carry out an on-farm calibration flight for each job to ensure the hopper door is correctly set to apply the required application rate. This is completed by recording the time required for the hopper to fully empty at a hopper door opening, and is repeated until the correct application rate is reached. This method of determining the correct field application rate assumes that the flow out of the hopper is constant and therefore the application rate for the flight is consistent. Calibration is

important because aircraft, hopper, hopper door design and environmental conditions vary, which will affect the field application rates. Pilots also need to complete calibration as they move to different jobs since fertiliser physical characteristics will vary and will affect flow from the hopper.

Approximately 15 million hectares of land is used for agriculture and forestry in New Zealand. In 2009, 66% of this land was utilised for sheep and beef farming making it the dominant agricultural land user (Ministry for Primary Industries, 2012). A significant quantity of fertiliser is required to maintain the productivity of this land. Common granular fertilisers applied by aircraft to pasture are single superphosphate, di-ammonium phosphate (DAP), urea, lime and micronutrients. To ensure these are applied responsibly, Spreadmark was developed as a voluntary quality assurance programme by the New Zealand Fertiliser Quality Council (NZFQC, 2016b). It provides guidelines on how to apply fertiliser aerially and by ground based vehicles for optimal pasture growth, and how to minimise its environmental impact. An operator certified under this programme is trained, and their equipment is independently assessed. The programme therefore assures a farmer that fertiliser is applied at an appropriate rate and distribution pattern.

Aerial Spreadmark (NZFQC, 2016b) has different test methods to ground based vehicle testing. Aerial Spreadmark uses the fertiliser transverse distribution pattern in fly over tests to determine the certification swath width for an aircraft. Bout or swath width is the distance between two parallel flight lines. An aircraft is certified to a maximum bout width that will achieve the minimum standard of performance prescribed. A minimum of three rows of collectors are required to calculate the average and standard deviation of the application rate. Spreadmark calculates the average field application rate by overlapping the collected transverse spread pattern by the set swath width (Figure 1.1). It assumes that the collected transverse spread pattern is the same for each parallel swath width completed by the aircraft. In areas where the parallel spread patterns overlap, the masses are combined. It calculates the average field application rate by converting the average mass using the area of the collector (i.e. 0.25 m^2) (Equation 1.1).

$$Application\ Rate\ \left(\frac{kg}{ha}\right) = \frac{Average\ Mass\ (kg)}{Area\ (m^2)\ x\ 0.0001\left(\frac{ha}{m^2}\right)} \quad (1.1)$$

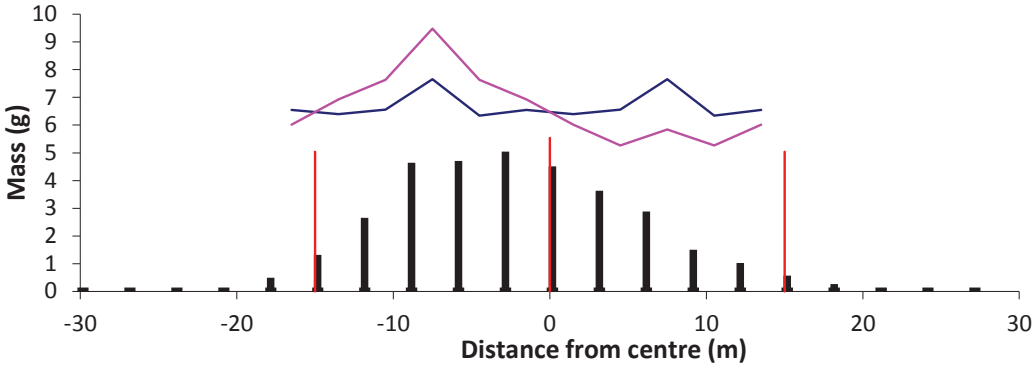


Figure 1.1: Example of Spreadmark calculating the average field mass from the transverse spread pattern and set swath width (i.e. 15 m). The blue line represents the distribution created from a racecourse (round and round) flight path, and the purple is for a to and fro flying pattern.

Each row needs a sufficient number of collectors so that the entire transverse spread pattern is obtained, and this is dependent on the wind conditions and the observed swath width. The collectors can be a maximum of 3 m apart. The transverse spread pattern from an aerial application is normally distributed (Akesson and Yates, 1964). Variations in the transverse spread pattern occur for a number of reasons, including local wind conditions and the use of 'fishtail' ram air spreaders. Spreaders are attached to the hopper door opening to increase the lateral distance fertiliser particles travel. The resulting distribution is normal with a large standard deviation. Some spreaders create an M shape distribution. Wind will skew the distribution depending on its direction relative to the aircraft's heading, and it is important to take this in to consideration to minimise off-target application.

Spreadmark calculates the coefficient of variation (CV), which quantifies the precision of a fertiliser application. It is the standard deviation of the application rate divided by the average rate. The Spreadmark certification test will establish the bout width required so that the overlap in the transverse spread pattern can achieve a CV of 15% for nitrogenous fertiliser and 25% for all other fertilisers. This is a set guideline based on the International Organization of Standardization (1985). Spreadmark also states that accuracy is achieved when the average field application rate is within 30% of the intended application rate. These tests are carried out when the wind speed is less than 4.2 m s^{-1} and the wind direction is ± 15° to the plane's heading. Therefore the CVs achieved in the Spreadmark tests are completed in close to ideal conditions.

In the field, fertiliser applications will have a starting CV of 15 – 25%. Failures in the aircraft operation and maintaining the bout width will increase variance, and therefore the CV. The CV

calculated from field data is referred to as the field CV (Grafton et al., 2012). So far the CV has only been estimated by assuming a consistent swath width and repeatable transverse spread pattern.

Calibration and testing of aerial topdressing in North America is done in accordance with ASAE S386.2 (ASAE, 1999). ASAE S386.2 was used to develop Spreadmark so they are similar. The main differences between ASAE S386.2 and Spreadmark are about how calibration tests should be carried out. For example, ASAE dictates that pilots need to complete three replicates of the calibration flight. This ensures that the swath width is repeatable. With Spreadmark, the pilot is only required to complete one flight and they have unlimited attempts to achieve the maximum swath width. ASAE S386.2 also requires that the collection of the transverse spread pattern should occur at least 100 m after the hopper door opens and 100 m before the hopper closes. This is to ensure an equilibrated flow rate is collected. Spreadmark does not dictate a distance. Another difference is the distance collectors are placed from each other with Spreadmark dictating 3 m, while the ASAE standard is 1 m. Spreadmark has standards on the accuracy of an application, while ASAE does not. Both assess the spread pattern and coefficient of variation for precision.

Additionally, there may be greater benefit if a spread pattern is assessed for robustness, which is a value based on the average CV over a range of swath widths. A robust pattern is expected to produce a suitable application over a range of swath widths. Grift (2000) proposed this assessment criteria, and suggested that spread patterns with a robustness factor under 5% are robust. Initial studies determined that a Gaussian/normal distribution were the most robust for a ground application. The robustness of aerial spread patterns was investigated in Grift et al. (2000). Four hundred spread patterns from 1992 – 1997 were assessed, using the Spatial Pattern Analysis Tool (SPAT). The study found approximately 70% of spread patterns had a robustness factor of 5 – 15%, which suggests that there is a need to improve how fertiliser is aerially applied. The authors discussed the necessity in redesigning spreading equipment and procedures to achieve higher quality applications.

1.4. Variability in Aerial Topdressing

This section discusses factors that influence the aerial application of granular fertiliser. There are three basic mechanisms by which fertiliser are energised during spreading. In spinning disc land based applications, fertiliser is accelerated by centrifugal forces and flung off a vane on the disc. This is common for urea and compound fertiliser applications. These applicators are often characterised as being European styled machines. Fertiliser can also be impacted off the

disc with shorter more aggressive vanes. This is more common in the application of superphosphate and lime. In aerial application, particles gain their energy by being dropped through the hopper door into a fast flowing stream of air under the aircraft, while it is operating at approximately 200 km h^{-1}. Figure 1.2 illustrates the many factors that influence the field application rate in aerial topdressing.

Since there are significantly more studies on ground based vehicle fertiliser application, some pertinent information will be referenced. There are noticeable differences between a truck and aerial application, such as the fertiliser's initial velocity, direction and the effect of wind on small particles. However, some conclusions are applicable to both. For example, the effect of particle characteristics on the accuracy and precision of a truck fertiliser application is applicable to an aerial application, as they are governed by the same fundamental laws of motion.

1.4.1. Fertiliser Characteristics

Particle size distribution, sphericity, particle strength and density are important fertiliser characteristics that influence aerial application. Single superphosphate is the primary source of added phosphorus and sulphur to hill country, and is New Zealand's most commonly applied fertiliser. It is manufactured within New Zealand by two fertiliser companies. Single superphosphate is not a uniform product, which introduces difficulty during application (Chok et al., 2014). Superphosphate is produced in batch processes by combining sulphuric acid and phosphate rock, which is sourced from a number of countries. The elemental composition (i.e. phosphate, cadmium, aluminium) of the phosphate rock will differ across sources and time. Therefore, each batch of superphosphate will have slight variations in particle strength, elemental composition and particle size. A drum granulator is used at the end of the manufacturing process to produce particles in the ideal size range. However, the particle size distribution can be inconsistent. Although manufacturers try their best to ensure uniformity, this is not always achievable. Despatch, transportation and storage are also inconsistent, which increases the potential for the spreading performance to be affected. Therefore during fertiliser application, the fertiliser distribution leaving the aircraft varies.

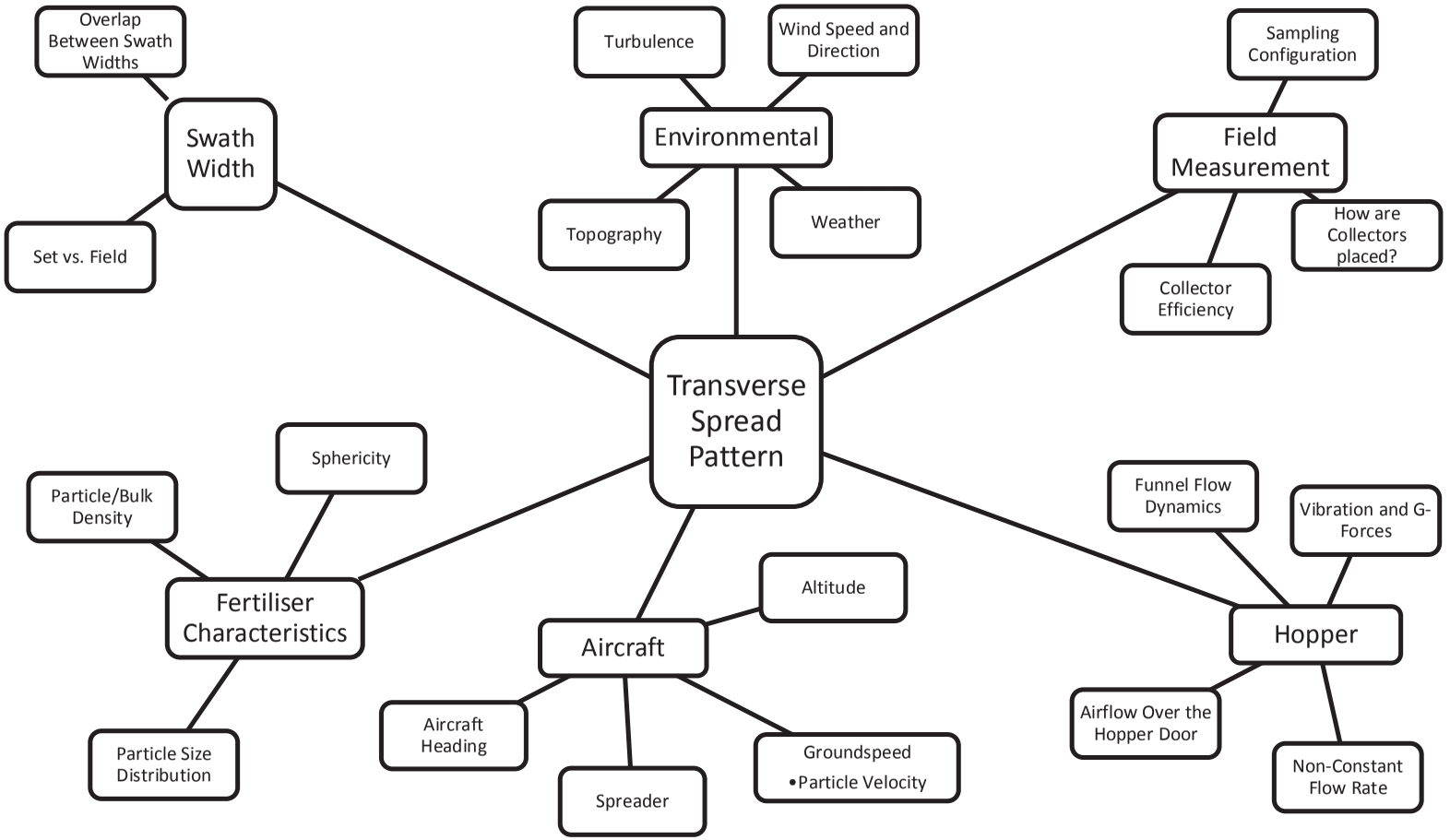


Figure 1.2: Factors that affect the transverse spread pattern in aerial granular fertiliser application.

Variations in particle characteristics make it difficult to predict the transverse spread pattern. Particle size has an effect on the distance a particle will travel. Larger particles tend to travel further in the direction of flight since they have greater initial momentum. The particle size distribution, which is found by sieving a representative fertiliser sample, has an effect on the shape of the transverse spread pattern. The benefit of having a particle size distribution with larger particles is a lower CV. Yule (2011) showed that an increase in the fines fraction (< 1.0 mm) increases the field CV for truck application. However, this effect is only significant if the percentage of fines is greater than 15%. A benefit of having a wide particle size distribution is that different particle sizes will have different fall times (i.e. time it takes for a fertiliser particle to reach the ground). This helps in achieving a normally distributed transverse spread pattern.

Spreadmark provides guidelines on particle size and uniformity (NZFQC, 2016b). The size guide number (SGN) expresses the average particle size of a fertiliser sample. It is calculated by multiplying the average particle diameter in millimetres by 100. The uniformity index (UI) is the ratio of small particles to large particles. It quantifies the particle size range, and is calculated by determining the percentage of fertiliser in each sieve range (Figure 1.3). A UI of 100 represents a sample with a uniform particle size, while a UI of 50 represents a well granulated particle range. SGN and UI for New Zealand fertilisers can be 95 – 475 and 5 – 68, respectively. Bulk density is another fertiliser characteristic that should be considered, since it affects a particle's ballistic properties. Table 1.1 shows typical SGN, UI and bulk density values for superphosphate, DAP and urea.

Table 1.1: Standard SGN and UI values set by Spreadmark (NZFQC, 2016b).

Product	Size Guide Number	Uniformity Index	Bulk Density
Superphosphate	245 – 300	11	1030 – 1280
Di-ammonium phosphate	265 – 335	55	900 – 1000
Urea	290 – 340	60	700 – 800

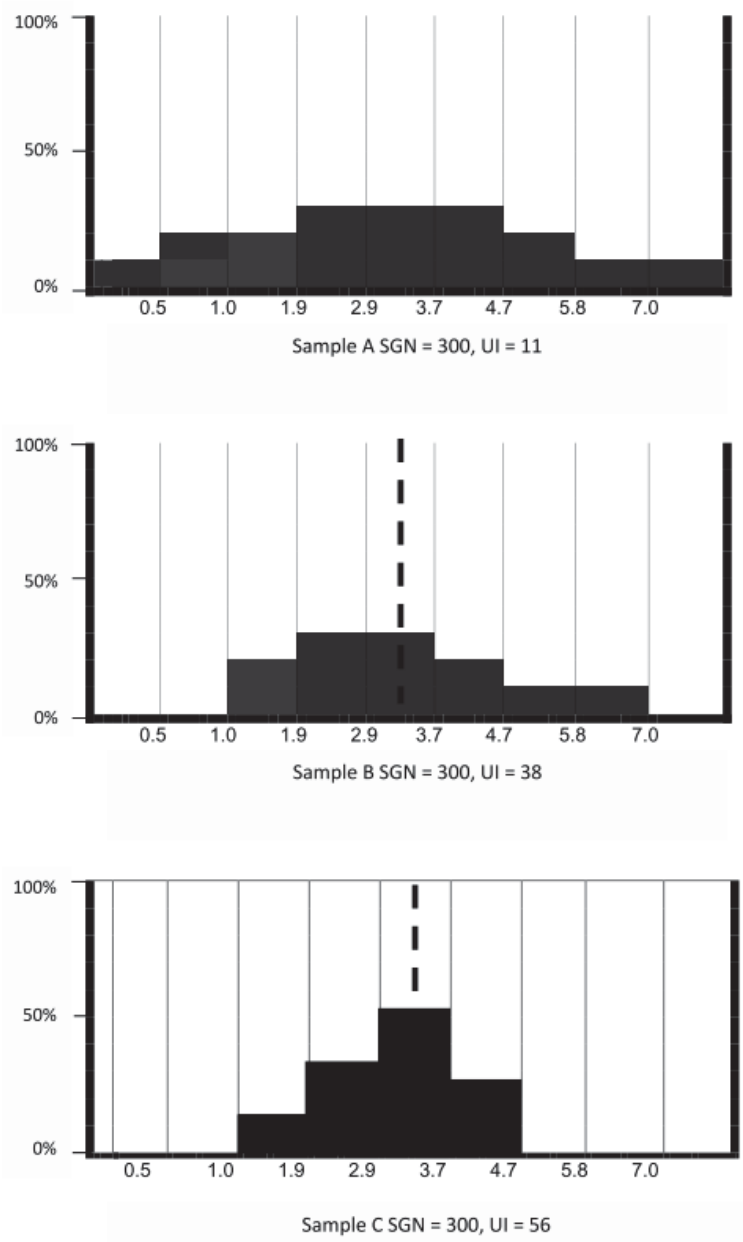


Figure 1.3: Examples of the relationship between UI and SGN sourced from NZFQC (2016b). The images represent fertiliser in a sieve box, where the x axis is the mesh size in mm.

There are three general guidelines used to interpret SGN and UI (NZFQC, 2016b).

- A SGN lower than 150 and UI less than 20 could result in an inaccurate distribution. The product may have a large percentage of fines.
- A SGN of 250 – 350 and UI of 20 – 60 should result in an even application if the applicator is operating correctly.
- If the SGN and UI are greater than 350 and 50, respectively, the material is likely to be coarse and spreading will be difficult.

SGN and UI can also be used to determine if two products can be blended and applied together. Spreadmark (NZFQC, 2016b) states that if the difference between the two SGN or UI values is less than 10, segregation of the two products is unlikely to occur. Differences of 11 – 20 show moderate compatibility where some segregation is expected. Blending products with differences over 20 should be avoided. These guidelines were developed around ground spreaders, and will differ in aerial topdressing due to different conditions (i.e. particle exit velocities). Limited work has been done to determine if these guidelines are suitable for aerial spreading, so care should be taken when using them. Chemical compatibility of the two fertiliser types should also be considered, since some fertiliser types react to each other. Figure 1.4 shows the chemical compatibility of common New Zealand fertilisers that could be blended together to create a fertiliser mix.

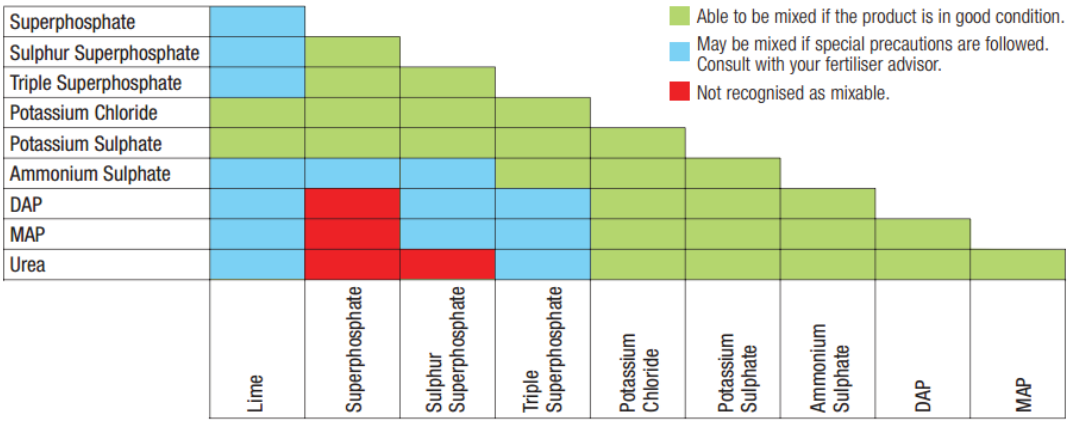


Figure 1.4: Chemical compatibility of common New Zealand fertilisers (Fertiliser Association, 2007).

Research has mainly been completed on spreading blended fertilisers using twin disc centrifugal spreaders, where the initial conditions from the spreader are different (Miserque et al., 2008; Virk et al., 2013; Yule and Pemberton, 2009). Little research has been completed on the aerial topdressing of blended materials. However, the effects of uneven topdressing have been observed in the field when blended products were used.

Sphericity is a measure of how much an object resembles a sphere. Wadell (1932) defined sphericity as the surface area of a sphere of the same volume as the particle, divided by the actual particle's surface area. A particle's sphericity affects its motion through air and is related to the drag coefficient (Grift et al., 1997). Spherical particles have a lower drag coefficient, which improves their aerodynamics allowing them to travel further. Superphosphate is not a perfect sphere. In comparison, urea and DAP are more spherical in shape.

The study by Hoffmeister et al. (1964) found that particle size, and therefore the particle size distribution, has the most significant impact on the transverse spread pattern. A triple superphosphate potassium chloride blend was applied with a fan type spreader in a truck application. The percentage of potassium chloride (KCl) particles was found to decrease with distance due to its smaller average particle size. In contrast, Yule and Pemberton (2009) found that KCl particles retained in the 2 mm and 2.8 mm sieve range was applied further than larger particle sizes. They also completed a truck spreading trial with a 30% potassium chloride and 70% superphosphate blend, comparing two mixing methods. The two superphosphate samples were found to produce different spread patterns. This was because the two samples had different SGN values (182 compared with 141). Hedderwick and Will (1982) compared superphosphate with a diameter of 5 – 10 mm and 0 – 5 mm in an aerial application and it showed that larger particles travelled further. This is because larger, heavier particles have higher terminal velocities than smaller, lighter particles. Particle density is therefore another significant factor.

Miserque et al. (2008) found that particle density had a significant effect on the spread pattern when applying a 50/50 blend of two materials, using a centrifugal truck spreader. At 16 m from the centreline, the proportion of the blend was 70/30 with analysis showing that heavier particles travelled further. On the other hand, Walker et al. (1997) found that particle shape significantly influenced a particle's landing position when aerially applied. Due to the complexity of aerial application, most studies focus on one factor. However, the factors are interconnected and the interaction effects require analysis.

To complement Spreadmark, the Fertmark code of practice (NZFQC, 2016a) was developed to ensure that there is a standard for fertiliser quality in New Zealand. Fertmark sets standards for nutrient and heavy metal content. For fertiliser physical characteristics, it monitors granule strength, granule degradation and the particle size distribution. The code of practice also sets out guidelines for production, transportation and storage.

1.4.2. Fertiliser Transportation and Storage

Fertiliser transportation and storage further complicates particle size and distribution variations. In New Zealand, fertiliser is transported from manufacturing sites to the distribution stores by truck or train. When required on farm, the fertiliser is transported from the stores by truck. Therefore, fertiliser can travel hundreds of kilometres before being applied. Superphosphate has low granule strength and will experience attrition during transportation. This increases the percentage of fine particulates (< 1.0 mm) and could

decrease the precision of an aerial application. Fertiliser age and its exposure to moisture will also have an effect on particle hardness and aerodynamic qualities (Adams and Merz, 1929).

Segregation, environmental exposure, and treatment are issues in fertiliser storage. Fertiliser is stored in covered sheds as large piles. Depending on the storage capacity of the shed, these piles can be over 8 m in height. Hoffmeister et al. (1964) observed that, on average, large particles will migrate down the outside of a fertiliser storage pile. This is an issue because fertiliser is first removed from one face of the pile. Therefore over a large fertiliser application there will be a change in the fertiliser particle size distribution. Front-end loaders are sometimes used to shift the fertiliser piles into trucks. Large stores use conveyor belts and hopper systems. Some particles are crushed as they are loaded. Although the crushed fertiliser is removed and sold as non-conforming material, some remain and increase the fines fraction of the particle size distribution.

Although these stores and sheds are covered, they are not fully enclosed. Therefore, the stored fertiliser is still exposed to humidity and temperature changes. This can negatively affect fertilisers depending on their hygroscopy (extent the material absorbs and holds moisture from the air) (Adams and Merz, 1929). Fertilisers with high hygroscopicity, such as superphosphate, will soften and become sticky, which reduces particle strength. This simultaneously leads to the formation of fine particles and large conglomerates. The stickiness negatively affects the spreading equipment and increases the chance of clogging. These issues are further exacerbated when fertiliser is stored at a distribution centre for a few months. Although manufacturers practice ‘Just in Time’ production, application delays occur during the winter season when fertiliser that has been ordered is produced, but not applied because conditions are too wet. These issues are prevented by maintaining a dry environment and reducing the time between manufacture and application when possible, so that there is not a significant change in fertiliser properties.

1.4.3. Wind

Wind conditions significantly contribute to the variability in the ground fertiliser distribution. Hedderwick and Will (1982) found in their study of aerial application to forests that superphosphate granules less than 2 mm were more affected by wind. Displacement of these small particles can negatively affect the evenness of the application and create off-target application.

Macfarlane et al. (1987) investigated the effects of increasing crosswind on the transverse spread pattern of aerially applied superphosphate. They found that an increase in crosswind

will widen the swath width and reduce positive kurtosis. Although the distribution was displaced in the direction of wind, continued application at the swath width reduced variation. The study used three rows of 25 funnel shaped collectors. With a crosswind of 1.6 km h^{-1}, Macfarlane et al. (1987) found that the application rate ranged between 4 kg ha^{-1} and 270 kg ha^{-1}. A crosswind of 2.4 m s^{-1} and 3.5 m s^{-1} yielded a fertiliser application rate of 66 – 163 kg ha^{-1} and 48 – 181 kg ha^{-1}, respectively. The intended average application rate for the experiments was 100 kg ha^{-1}. Gillingham et al. (1985) showed that the greater the crosswind, the greater the spread pattern displacement in an unmodified fixed wing aircraft. It was concluded that this could be beneficial, since fertiliser would be applied more evenly. However, wind has a negative effect near boundaries as there is an increased likelihood of off-target application if wind is not considered during the flight. Although this has been identified as an issue, it is not well addressed in previous studies, because the flight path is at the discretion of the pilot.

It is difficult to minimise the effect of wind since there are a limited number of days in a year for an aircraft to be able to service all the farms. This is because farmers prefer to apply fertiliser in spring and autumn when it can dissolve into the soil. Single superphosphate has low levels of fluorine, which can be toxic to stock if consumed during grazing (Chok et al., 2014). The likelihood of ideal weather, in New Zealand, for the majority of spring and autumn is slim. Therefore, some applications will be done under unfavourable wind conditions. This has a significant impact on the accuracy and precision of the ground fertiliser distribution.

1.4.4. Altitude

Fixed wing aircraft fly 15 – 60 m above ground. Lower altitudes have a negative effect on the transverse spread pattern, because fertiliser particles have insufficient time to reach their terminal velocity and spread laterally. Trayford and Tremayne (1966) found that the swath width increased and the centre peak of a transverse spread pattern decreased with increasing altitude. They reasoned that the increased altitude gave the particles more time to travel laterally. Scott (1970) showed there was a significant difference in the swath width as the aircraft altitude increased for applications rates of 112 kg ha^{-1} or below. It was also observed that aerial superphosphate application experienced an increase in swath width with increasing altitude (23 m – 122 m), while there was no effect on homogenous granulated superphosphate. However, a disadvantage of operating at higher altitudes is that there is a greater chance of off-target application due to wind drift. Pilots have to consider both of these issues, as well as their safety, when selecting what altitude they will apply at.

1.4.5. Topography

Aerial application over challenging topography, such as steep or irregular terrain, adds to the on-ground variability in the spread pattern. Variable topography increases the difficulty of applying fertiliser, since pilots have to avoid obstacles. Aircraft experience leeward low pressure and uplift on the windward side of a hill, which could result in a rapid loss of altitude if not accounted for by the pilot. In the worst case scenario, the pilot will lose control of the aircraft and crash. Another consideration with hill country's variable elevation is that the aircraft altitude above ground will vary. At points where the aircraft and ground are closer together, the transverse spread pattern will have a narrower swath width, because there is insufficient time for the material to travel laterally. Akesson and Yates (1964) found that aerial application at 9 m did not produce a narrow lateral distribution compared to an altitude of 3 m. Although an aerial spreader is unlikely to apply at an altitude of 3 m, Akesson and Yates (1964) demonstrated that altitude has an effect on the spread pattern.

1.4.6. Aircraft Velocity

Aircraft velocity can be described in two ways. True airspeed is the speed the aircraft is moving through the air, while groundspeed is the true airspeed corrected for wind. It was not possible to measure groundspeed until the integration of GPS into aircraft navigation systems. Aircraft velocity affects the application rate. For a constant flow rate out of the hopper (measured in kg s^{-1}), an increase in aircraft velocity would decrease the application rate (kg ha^{-1}), since a larger area is covered in the same amount of time. To maintain the target application rate, the flow rate would have to increase. A case study by Murray and Yule (2006) showed that large variations in groundspeed may have a significant impact on the flow rate out of the hopper. Additionally, Murray (2007) found that minor fluctuations in groundspeed (average 56 m s^{-1} and standard deviation 2.5 m s^{-1}) have little effect on the fertiliser flow rate.

1.4.7. Spreaders

Ram air or venturi type spreaders were developed to achieve wider swath widths and reduce positive kurtosis of the transverse spread pattern. This improves CV and decreases the application time (NZFQC, 2016b). Spreaders have a multitude of designs but those discussed here are fish tail shaped spreaders with 9 or 11 ducts. Ducts are separated by vanes which curve out in the transverse direction (Figure 1.5). R. K. Bansal et al. (1998a) found, through simulation of an 11 duct spreader, that the air velocity within the ducts is greater than aircraft ground speed velocity by 1.04 – 1.14 times. The average air velocity in the centre duct was lower than the sides because it has the shortest length.



Figure 1.5: Port side image of an 11 duct spreader that is attached to the hopper door on an aircraft.

Ram air spreaders are designed for application rates less than 200 kg ha^{-1}. At higher application rates, fertiliser can clog the spreader ducts resulting in the spreader detaching from the aircraft (Charlton et al., 1983). Another disadvantage of spreaders is that it limits aircraft speed due to increased shear forces (Gillingham et al., 1985). A typical stainless steel spreader can weigh approximately 80 kg, and increase the drag forces on the aircraft.

A few settings can be adjusted on a spreader to optimise performance. These are the installation angle of the spreader, its distance from the hopper door and the amount of fertiliser that travels through each duct. The fertiliser flow rate through each duct is set by widening or narrowing the duct's entrance. This is a coarse adjustment, which could result in large flow rate variations through each duct. Therefore adjustments should be checked in the field to ensure an appropriate transverse spread pattern is achieved.

1.4.8. Swath width

A pilot will select the swath width based on their experience and their Spreadmark certification. The selected swath width is usually set at an optimistic swath width for a fertiliser type to maximise aircraft efficiency. Wide swath widths will decrease the amount of time required to complete a job, since fewer flights will be required to cover the application area. However, a pilot's first priority is to ensure an appropriate swath width is chosen so that the correct application rate is applied (NZFQC, 2016b). Although a pilot can set a swath width, it may not be the optimal field swath width because of changes in wind conditions, aircraft operation or fertiliser properties. Akesson and Yates (1964) found that increasing the fertiliser flow out of the hopper will decrease the swath width when applied with a Stearman aircraft. Striping can occur in this instance, where there is a visible difference in pasture/crop growth because the majority of fertiliser is applied along the centre of the flight path and insufficient fertiliser reached the edge. Therefore, the set swath width results in poor overlap between

flight lines. This could occur in situations where pilots maximise the set swath width in order to minimise the application time and therefore costs.

Before the introduction of GPS for aerial application, applicators relied on landmarks to determine the swath width and identify farm boundaries. This led to uneven swath widths, which was used to explain variability in aerial topdressing in several studies (Ballard and Will, 1971; Hedderwick and Will, 1982). Methods to reduce uneven applications included ground staff with flags, helium balloons and flares (Barker, 1979). Hedderwick and Will (1982) introduced a radar guidance system on to New Zealand helicopters for fertiliser application in forestry, which required multiple ground receiving stations. In recent years, operators have adopted DGPS (Differential Global Positioning Systems). DGPS is an improvement on uncorrected Global Positioning Systems, as it uses ground based reference stations to correct between GPS and the known fixed positions. VRAT uses the farm boundaries with their GPS co-ordinates, and the DPGS position of the aircraft in real time to improve the accuracy at which pilots can fly parallel swath widths (Murray, 2007).

1.5. Variable Rate Application Technology

Nutrient availability in pasture is spatially variable over a farm (During and Mountier, 1967; Gillingham and During, 1973; Morton et al., 2000). Therefore, blanket fertiliser application is not an efficient use of fertiliser. Variable rate application allows for different rates to be applied over a farm. The technology is established in truck fertiliser applications and irrigation. It has also been developed for variable rate aerial spraying of crops. However, only 3% of New Zealand agricultural land is cropped, while more than 50% is grazed (Hedley, 2014). Therefore, aerial application of granular fertiliser for pasture is the major use of agricultural aircraft in New Zealand, and utilising VRAT may increase the efficiency of fertiliser use on hill country.

A desktop economic study of a variable aerial application by Gillingham et al. (1999) showed that the benefit of the technology is dependent on the specific needs of the farm and the stock carrying capacity. However, it illustrated that the correct application of variable rate technology will achieve greater pasture and animal production. A more recent economic analysis by Murray and Yule (2010) found that a full variable rate application can increase a farm's cash surplus by 26% per hectare under optimum pasture growth conditions for a specific case study. Introduction of GPS technology alone is thought to increase farm efficiency by 5 – 10%, as it reduces overlaps and gaps, and prevents off-target application (Hedley, 2014). By reducing the number of overlaps and gaps, uneven application will decrease.

Grafton et al. (2012) showed that conventional applications using a pilot operated hopper door could yield a CV as high as 70%. This could be reduced to 43% with a GPS controlled hopper door, which is a 27% improvement in CV. This trial was carried out at application rates of 125 kg ha^{-1} and 250 kg ha^{-1} for pilot operated, and 250 kg ha^{-1} and 750 kg ha^{-1} for the automated system. The pilot completed each application zone individually. After the area was flown, the samples were collected before the collectors were moved to the next trial area. This sampling procedure was undertaken because the number of collectors was limited. The trial is not considered a variable rate application trial, because two application rates were not measured simultaneously and the variability at the boundaries was not captured. The most recent aerial variable rate application study was completed by Morton et al. (2016), but measurements of accuracy, precision and capability were not specified. They focussed on the initial development of a variable rate application system, and the field trials consisted of calibration, and flight observations.

Figure 1.6 and Figure 1.7 are simulated comparisons of an aerial application between a pilot operated and automated hopper door, respectively (Murray, 2007). It illustrates that an automated door can reduce off-target fertiliser application (Figure 1.7). In the simulation, the automated system only applied 6% of the total fertiliser outside of the application area compared to 16% in the pilot operated system. This constituted a saving of 10%. To model this, it was assumed that the hopper door closed on the boundary. Therefore, the majority of off-target application in the variable rate simulation was due to the forward motion of particles. Murray (2007) did complete a field trial with a target application rate of 150 kg ha^{-1} of superphosphate using a six duct non-air ram spreader. The pilot had a Satloc M3 navigation system for flight track guidance, but the hopper was pilot operated.

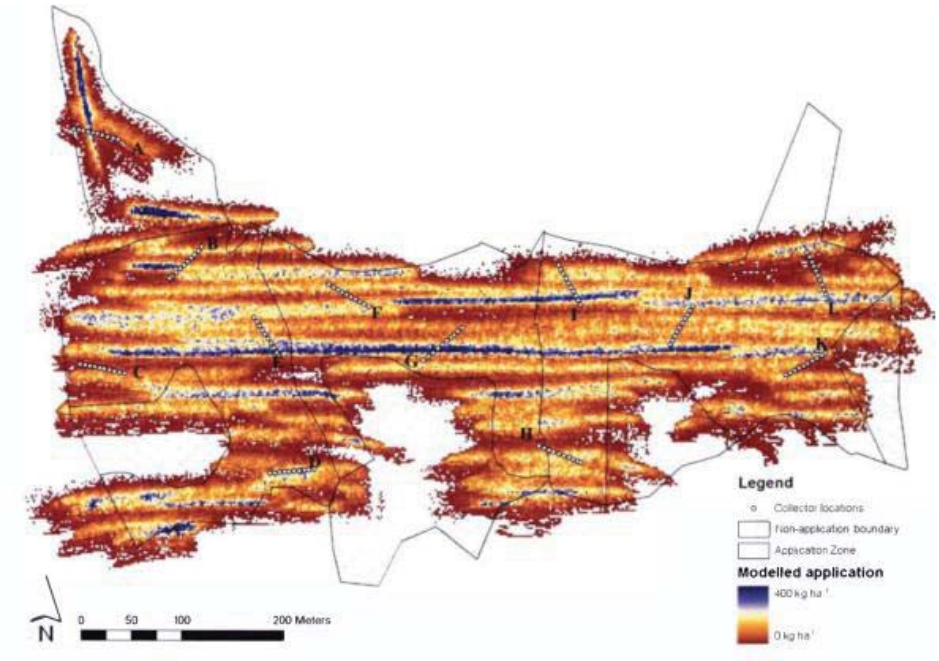


Figure 1.6: Predicted field scale application on a 25 ha site where the hopper door is pilot operated and there is no GPS guidance (Murray, 2007). The application rates were modelled using Jones et al. (2008) and recorded aircraft data.

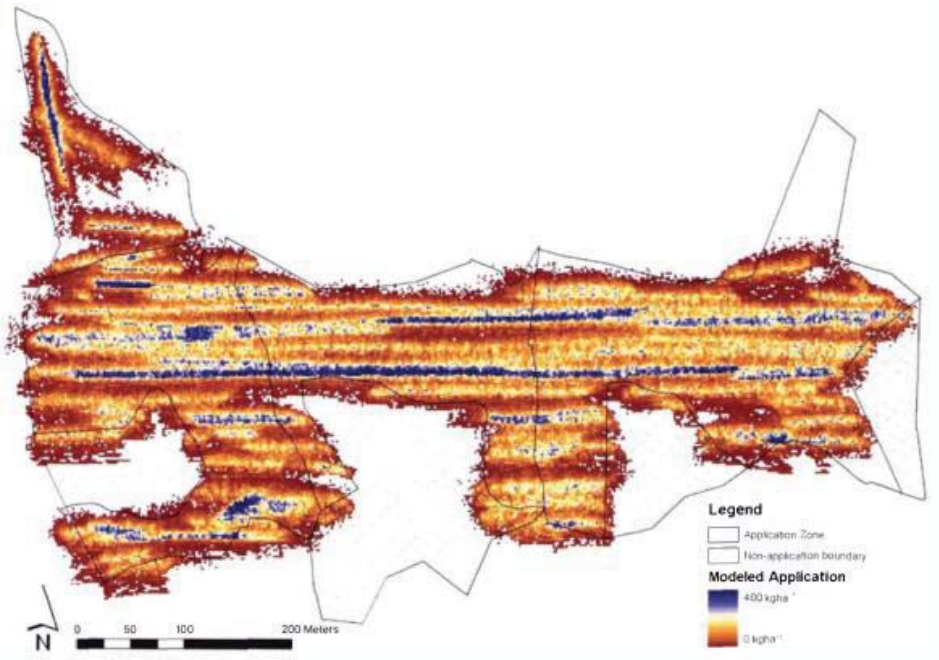


Figure 1.7: Predicted field scale application using an automated GPS guided hopper door. Murray (2007) produced this image from Figure 1.6 by removing all points outside the application area except when it was within 45 m of an application area.

A fully automated fertiliser delivery system will improve pilot safety. Between 2003 and 2012 there were 19 fatalities, 12 serious injuries and 8 minor injuries that were connected with aerial topdressing. A Civil Aviation Authority report on fixed wing accidents stated pilot fatigue

and inattention to surroundings as contributing factors to agricultural accidents (Wackrow, 2005). Grafton et al. (2012) estimated that a topdressing aircraft may land and take off 150 times a day. In a conventional application, the pilot will operate the hopper door at least four times per load. This equates to approximately 600 openings and closings of the hopper door. On a fine summer's day, a modern turbine Cresco could apply 300 tonnes of fertiliser per day (Grafton et al., 2009). However, this is usually not achieved because of farm storage limitations. The variable rate system will reduce the workload on pilots and allow them to be more aware of dangers in the surrounding area (i.e. power lines, hill top, other aircraft). It allows them to concentrate on where they are flying rather than the position of the hopper door. However, there are potential risks with automated systems that should be considered. Ultimately the pilot should be able to override the VRAT system in case there are any issues.

Prescription maps are used in variable rate application jobs to delineate the application rate in an area. Geographical information systems (GIS), such as ArcGIS and Mapstar, are used to produce these maps. Prescription maps also allow for the exclusion of sensitive areas, such as retired paddocks, eroded hill faces, water ways and native bush. Slope and aspect can be used to assign an application rate to a zone (Morton et al., 2016). Steeper slopes would receive less fertiliser than flat areas, and north facing aspects can receive a higher application rate because they receive more sunlight. Land Information New Zealand (LINZ) provides an 8 m and 15 m resolution digital elevation map (DEM), which is used to produce prescription maps based on slope and aspect. However, there are limitations. At the local level, elevation models are predicted poorly, especially for river valleys (Barringer et al., 2002). Although the national DEM does meet international accuracy standards, it may not be suitable for creating fertiliser application prescription maps. This depends on the accuracy required for aerial topdressing and the capability of the variable rate system to deliver.

Another method of assigning an application rate to a zone is site specific management. A farm can be split in to zones that account for within farm variability. These zones can be delineated by topography, soil fertility, plant species, soil moisture or a combination of these parameters. Combining these digital information layers and analysing them over time will allow informed decisions to be made to improve farm management, and therefore yield. Prescription maps created for these management zones can then be deployed in a variable rate application. If the prescription maps are executed correctly, it can reduce farm expenditure by 10 – 20% (Hedley, 2014). Diacono et al. (2012) found that nitrogen management based on real time sensing and fertilisation, on a tractor for wheat, returned larger profits than undifferentiated applications.

However, it is important to consider the spatial resolution of the management zone especially for aerial spreading.

The VRAT system's limitations are dependent on multiple factors. Automating the hopper door and controlling it with a prescription map relies on the GPS. The GPS receiver has a Hertz (Hz) rating, which indicates the number of times the receiver is able to record the aircraft's position per second. For example, a 5 Hz receiver calculates the aircraft's position five times per second. An aircraft travelling at 55 m s^{-1} would register a GPS point every 11 m. If the aircraft crosses a boundary in the 11 m gap, it would result in an application error. It is possible to have GPS receivers with 20 Hz (GPS point every 2.75 m when the aircraft is travelling at 55 m s^{-1}), but this requires more processing power and data storage. An additional limitation is the response time for the automated hydraulic hopper door system. When the variable rate system detects a change in the hopper door opening, the actuator uses a pressurised hydraulic fluid to drive the change in the hopper door position. This can represent a significant time delay. For example, a delay of 0.4 s when an aircraft is travelling 55.6 m s^{-1} is 22 m. Not accounting for these limitations may result in off-target application.

Navigation, machinery and prescription mapping are other errors associated with variable rate application that was discussed by Chan et al. (2004). Prescription maps are usually created based on a shapefile of the farm boundaries. The farm boundaries may not be accurately represented, which could result in off-target application. Also if the site specific management approach is used, it combines data layers from several sources, which may have different resolutions or GPS accuracy. GPS positional errors can occur for a number of reasons, such as the quality and connection of the GPS receiver, the strength of the GPS signal, and signal latency. Another source of error is mechanical, where the hopper door opens to the incorrect position or outside an application zone. This occurs when the prescription map is incorrectly prepared, and the system does not know what position the hopper door should be in for an application zone.

1.6. Ballistics Modelling for Aerial Topdressing

With the variable rate application system, the release point of fertiliser particles, from the aircraft, is known. However, the landing point is unknown but could be estimated using a granular fertiliser ballistics model. An ideal ballistics model would identify important factors in aerial topdressing, provide guidelines to optimise fertiliser application, and predict how changes/variations in initial conditions could affect a fertiliser's landing position.

Initial model development was based on aerial spraying (Craig et al., 1998; Koch et al., 2005; Walklate, 1992). AgDISP was developed over a 20 year period to predict the motion of spray material in the air after it leaves the nozzle from either an aerial or ground applicator (Bilanin et al., 1989). It uses a Lagrangian trajectory modelling approach, and accounts for local wind conditions, evaporation and the aircraft's wake effects. AgDRIFT is a Microsoft Windows-based tool in which an improved version of AgDISP is used. The tool focuses on assessing and evaluating the effect of different drift conditions in hopes of preventing off-target application of pesticides. Its expansions include input variable libraries for droplet size, aircraft characteristics and tank mix specifications (Hewitt et al., 2001). The tool also has algorithms to account for droplet evaporation. AgDRIFT has several improvements, including better approximations of aircraft and helicopter wake vortices, inclusion of smaller droplet sizes (less than 10 μm) and a solution to speed increases where an exact solution is calculated for the equations of motion at each step (Teske et al., 2002). These improvements increase modelling speed and accuracy.

Bird et al. (2002) carried out comprehensive validation of AgDISP/AgDRIFT. One hundred and eighty trials were used to validate the model, which were collected by the Spray Drift Task Force (Hewitt et al., 2002). Validation was completed for a variety of aircraft (i.e. Cessna AgHusky 188, Air Tractor AT-502, Aerodyne Wasp), spray tank mixes, nozzle types and meteorological conditions. Results showed that stochastic variability in each of the 180 trials limited the model's ability to be evaluated generally. However AgDRIFT was found to predict the average field deposition well over a range of application conditions. The model does have a tendency to over-predict at distances far from the release point and under-predict at near distances (Bird et al., 2002).

Several aerial granular spreading models have since been developed (R. Bansal et al., 1998; Grift, 2001; Jones et al., 2008; Walker and Gardisser, 1989; Walker et al., 1997). Single particle models are most common. Walker and Gardisser (1989) adapted AgDISP for granular fertiliser deposition, which considered material properties and environmental conditions. However validation was not completed on a spreading device. R. Bansal et al. (1998) used FLUENT, a computational fluid dynamics program, to determine air and particle flow through an 11 duct spreader. They encountered discrepancies between the modelled and actual velocities, and a correction factor was included to correct the difference. It was hypothesised that these differences were due to the model assumption that all fertiliser particles were spherical in shape. Teske et al. (2007) showed that the assumption of spherical particles could lead to a significant error of 26% in model predictions. It is therefore necessary to fully characterise the

material being modelled. R. Bansal et al. (1998) also produced a transverse spread pattern, using FLUENT, but the resulting distribution was M-shaped rather than the expected normal distribution. They theorised that this may have been caused by the assumption that flow through each spreader duct was equal (R. K. Bansal et al., 1998a). In addition, Walker et al. (1997) developed a single particle model that could accurately predict the fall time of a spherical or near-spherical particle. However, the model assumes a constant drag coefficient (i.e. turbulent model), and therefore fails to predict appropriate fall times for non-spherical material.

Jones et al. (2008) formulated a model predicting the landing position of a single granular fertiliser particle, using force balance equations. The model includes velocity-dependent drag, height dependent wind, aircraft attitude and propeller wash, which are extensions of previous work done in this area. The variable drag coefficient equation for non-spherical particles, by Haider and Levenspiel (1989), was used to account for changes in air flow. The Jones et al. (2008) model requires extensive inputs to produce an accurate prediction. Aircraft characteristic inputs include planform area, propeller length, distance between the hopper door and the propeller hub, and the aircraft drag coefficient. In terms of the material being applied, the particle size distribution, particle density and sphericity is needed. The aircraft altitude, groundspeed and heading are used for modelling. The wind velocity and direction are the only atmospheric inputs required in the model. Wind speed is extrapolated using the power law, height of the particle above ground and wind speed at a measured height (Equation 1.2).

$$v_2 = v_1 \left(\frac{z_2}{z_1}\right)^{\alpha} \tag{1.2}$$

where v_1 is the measured wind velocity at height z_1, and v_2 is the wind velocity at height z_2. The coefficient, α, is dependent on the stability of the atmosphere. Other initial conditions required by the ballistics model include particle discharge velocity, initial discharge position and initial discharge angle. R. K. Bansal et al. (1998a) pointed out that one of the limitations faced by all previous modellers was the lack of understanding in the initial trajectory of the fertiliser granule, which will significantly dictate where it will land. However, it is difficult to measure the exact discharge conditions for each particle. Therefore, Murray (2007) built a Visual Basic Application of Jones et al. (2008) single particle model that would consider constrained input ranges. This would allow random number generators to vary the input variables and produce a transverse spread pattern. The model can also be used to determine the distance particles travel in the longitudinal direction, in relation to the aircraft's heading.

Jones et al. (2008) carried out a simulated validation of the model on a Gippsland Aeronautics GA200C fixed wing aircraft. The results from the single particle model were compared to those from AgDISP 8.15 and the model created by R. K. Bansal et al. (1998b). Jones et al. (2008) model results showed similar trends to AgDISP 8.15. However, it is noted that there are distinct differences between the two models. One of which is AgDISP 8.15 has the ability to consider fluctuating propeller components. Assessment of the Jones et al. (2008) and R. K. Bansal et al. (1998b) model also showed similar results. A direct comparison could not be made because the respective models used different initial conditions and assumptions (i.e. the aircraft model and drag coefficients). Jones et al. (2008) also pointed out that there are unresolved errors in R. K. Bansal et al. (1998b), which over predict the lateral position of large particles. Jones et al. (2008) recommended that a field validation of the 2008 model should be carried out. They were not able to complete validation because of time and resource constraints.

1.6.1. Mass Flow Prediction

One of the major uncertainties in accurate ballistics modelling is the flow rate out of the hopper door opening. If the aircraft was applying the correct application rate, the mass flow rate out of the hopper can be calculated using the application rate and swath width. However, due to the variability in aerial spreading this can be challenging. There has been limited research in this area. Grift (2001) formulated a model to determine the mass flow of granular material through a spreader for aerial granular application. They assumed that granular particles travelled through spreader ducts as a sequence of cluster passage events. Data used to validate this model was collected under laboratory conditions with an optical sensor developed by Grift and Hofstee (1997). The model was not validated in the field as it was difficult to collect validation data from the spreader outlet during an aerial fertiliser application.

Grift and Crespi (2008b) studied the ability of Poisson driven arrival processes to predict the flow rate of fertiliser using an optical single interruption plane sensor (OptoSchmitt, SDP8601, Honeywell, Scotland, UK). In a lab environment, 4000 identical spherical particles with a diameter of 4.5 mm were dropped through a tube. The diameter of the tube was unspecified. The method was able to estimate that there were 4000 particles with a standard deviation of 44, using 30 datasets. Additionally, the Poisson driven arrival process was used to predict the mean particle diameter of free falling granular particles (Grift and Crespi, 2008a). The same experimental methodology was used, as Grift and Crespi (2008b). From 30 experiments, the method estimated a mean particle diameter of 4.5 mm with a standard deviation of 0.044 mm.

Both studies tested particles with a homogenous diameter (4.5 mm). However the authors noted that the method should be effective with any particle size distribution. A limitation of the Poisson driven arrival process is that the flow density should be lower than 167 particles per meter. Therefore the optical sensor needs to be placed a sufficient distance from the release point. If this was used in a field trial, the sensor would be placed at the exit of a spreader. Another measurement method would be required for high application rates. This method needs to be field validated.

A generic equation may be just as effective as a model. Beverloo equation (Equation 1.3) was formulated to determine the mass flow rate of free flowing material through an orifice (Beverloo et al., 1961).

$$M = C\rho g^{\frac{1}{2}}(B - kd)^{\frac{5}{2}} \quad (1.3)$$

where M is the mass flow rate, ρ is the bulk density, g is the acceleration due to gravity, d is the particle diameter, B is the orifice diameter of a circular opening, and C and k are empirical discharge and shape coefficients. The equation is known to be robust for different free flowing profiles (i.e. funnel flow, mixed flow). It is able to predict granular flow rates independent of their packing fraction, density, surface properties and particle shape, when the hopper diameter is much greater than the particle diameter. Although the equation has been successfully deployed for various situations, the coefficients C and k still need to be determined experimentally for every product. Beverloo et al. (1961) found that the discharge coefficient, C, is related to the bulk density and should be between 0.55 and 0.65. On the other hand, the shape factor, k, is believed to be dependent on the particle shape and hopper design (Grafton et al., 2011). Beverloo equation is normally applied to static industrial silos and hoppers. Grafton et al. (2011) used this equation to predict the flow rate of lime out of a topdressing aircraft. Its accuracy was validated by measuring the flow out of an indoor static hopper system and comparing the results. Regression analysis was used to find the values for the C and k constant. The equation was not validated in the field.

Since the Beverloo equation has not been used to predict the mass flow rate from a topdressing aircraft, it may not consider the interaction between air flow, the aircraft and the fertiliser granules. A factor could be included in to the Beverloo equation to account for air interactions. Several researchers have included factors to the equation to improve its accuracy for specific conditions (Gundogdu, 2004; Humby et al., 1998; Mankoc et al., 2007). For example, Mankoc et al. (2007) proposed a modification that could predict the mass flow of

grains for all orifice sizes. The modification allowed the orifice to be 1.5 to 100 times the particle size and eliminated the need for k. No correlations have been developed for the deposition of granule material from a hopper in an operating aircraft.

1.7. Sampling Methods

A variety of collectors have been used in previous studies to determine the transverse spread pattern. Ground based Spreadmark tests use square trays (0.25 m^2) for ground spreader certification. These are only 150 mm in height, which is an insufficient height for measuring aerial systems, since it will not prevent particles rebounding out of the collector. Ballard and Will (1971) used 7.5 L plastic buckets with a surface area of 0.04 m^2, while Scott and Grig (1970) used water filled jars to collect spread patterns. Scott and Grig (1970) found that their collectors were not suitable in accurately determining the phosphate concentration because the fine particulates did not dissolve in water. However, they were used to determine the relative concentrations. The advantage of using plastic jars and buckets as collectors is that they are relatively cheap, lightweight, and easy to obtain. However, the quantities collected are small. Precise scales and strict analysis protocols are necessary to avoid measurement errors. This is particularly important if there is a high fines percentage in the particle size distribution. Extra care would be required, during collection and analysis, to ensure the whole sample is measured.

Lockett (1998) designed a collapsible collector made of fibreglass rods on which a lightweight spinnaker cloth is draped (Figure 1.8). The goals of the design was to make portable collectors that were easy and quick to set up, and were large enough so that the sample collected did not require sensitive scales for in-field measurement. A field test of the collectors found that some material bounced out so a 200 mm extension was added. The New Zealand Agricultural Aviation Association (NZAAA) has 0.25 m^2 collectors that are held up with y posts (Figure 1.9). The collectors consist of a circular metal ring that supports a flexible plastic funnel that narrows to a short PVC pipe, where a collection bag can be attached.



Figure 1.8: Collector developed by Laslett (1994).



Figure 1.9: Collectors used by the New Zealand Agricultural Aviation Association.

In a Spreadmark test, only one transverse distribution is collected, but it assumes that subsequent swath widths will produce the same transverse spread pattern. This is unrealistic since there are changes in flight conditions with time. When applied at an altitude of 35 m, these slight differences can significantly impact the ground fertiliser distribution in subsequent flights. A different experimental set up is required to measure the variation in swath widths over large areas (Ballard and Will, 1971; Scott and Grig, 1970).

There are two levels of variation measured in an aerial topdressing trial assessing swath width. These are:

1. Variation between swath widths.
2. Variation within a swath width. This refers to the transverse spread pattern.

Scott and Grig (1970) had sufficient collectors to set up six grids, each with 336 collectors. This allowed them to study six flight lines. Ballard and Will (1971) set up a line of 75 collectors at 2.75 m intervals perpendicular to the flight path to determine the distribution of successive flights. In their study, they set the swath width to 10 m. However, the results of their study

showed that the swath width and application rate in each flight line could differ significantly. Both Scott and Grig (1970), and Ballard and Will (1971) completed their research before GPS was installed on topdressing aircraft.

Since 1970 – 1980, aerial topdressing trials of granular fertiliser have been extremely limited. This is because aerial topdressing trials are time and labour intensive. They are also costly, and there has been a lack of investment in aerial spreading in New Zealand. Recent trials include Murray (2007), who carried out a trial over 25 ha using a pilot operated hopper system on a Gippsland Aeronautics GA200C aircraft. Collectors were set up in groups of ten with each collector 5 m apart in a straight line. Each line was not orientated in the same direction. In total 12 groups of collectors were set out. The intended application rate was 150 kg ha^{-1} at a swath width of 12 m. A non-air ram six duct hopper was used in the trial. Grafton et al. (2012) used three rows of 20 collectors set out 20 m apart with each collector spaced at 2 m. There were 12 sample sites with three sites placed in each application zone. Grafton et al. (2012) stated that this method proved logistically challenging because it was labour and time intensive.

1.7.1. Geo-statistics

Geo-statistics allows the user to make spatial predictions from a small number of samples. This makes them useful in the interpolation and presentation of spatial data. Kriging or Gaussian process regression is a geo-statistical tool that interpolates discrete spatial data to produce a continuous layer. Kriging was originally used to estimate the distribution of gold in a mine based on a limited number of borehole samples (Krige, 1951). The concept was further developed by Matheron (1963). It has since been applied to various fields including soil science (Burgess and Webster, 1980), hydrology (Earls and Dixon, 2007) and real estate (Kuntz and Helbich, 2014).

Geo-statistics allows for the analysis of variance through a semi-variogram. This graphical representation quantifies the spatial correlation between collected data points to improve the accuracy of the interpolation (Montero et al., 2015). The semi-variance is described as

$$\gamma(h) = \frac{1}{2}\frac{1}{n(h)}\sum_{i=1}^{n(h)}\big(z(x_i + h) - z(x_i)\big)^2 \quad (1.4)$$

where $z(x_i)$ is the observed value at point x_i. n(h) is the number of observed pairs at distance h, and ϒ(h) is the semi-variance between samples h. The semi-variance is plotted against the lag distance, which is the average squared difference of values separated by the distance (Figure

1.10). It is assumed that the data is normally distributed, has a constant mean and reaches second order stationarity.

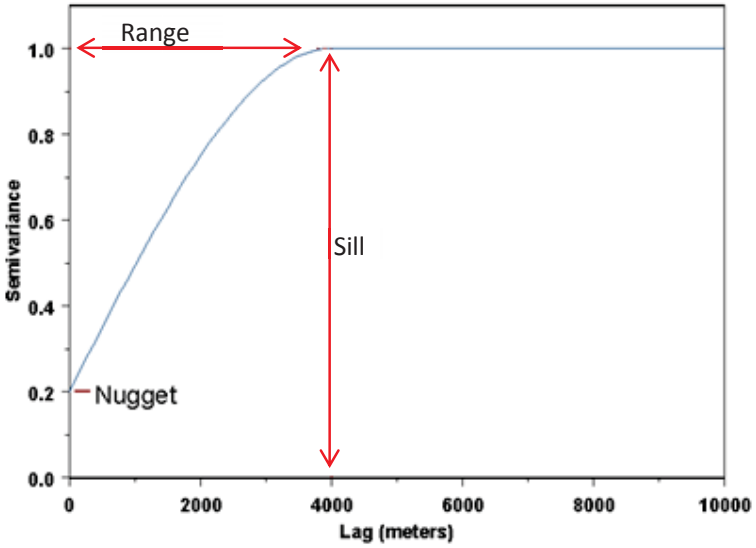


Figure 1.10: Example of a semi-variogram adapted from Bohling (2005).

A model is fitted to the data points so that an equation can be produced to interpolate an output layer. Models include circular, penta-spherical, Gaussian and exponential. The model fitting process is subjective, though many geo-statistical platforms (e.g. ArcGIS) have an option to optimise the fit of a model. Figure 1.10 is an example of a fitted semi-variogram. The sloped section indicates that a relationship exists between two points at the lag distance. This means they are spatially auto-correlated (Bohling, 2005). To get a well-represented output layer, it is important to sample sufficiently at distances along this slope. Stationarity is the section of the semi-variogram where there is no change in the semi-variance with the lag distance. This is called the sill. The distance needed to reach the sill is called the range, and the y-intercept is the nugget effect. It represents background variation that could not be quantified due to measurement and/or stochastic error. Once a suitable model is fitted to the semi-variogram, the geo-statistical platform will apply the model using the collected data to the surrounding area. The semi-variance is used to determine the effect of a collected data point on an estimated point, using the principle that data points close to the estimated intermediary point have more weight than those far away.

Kriging utilises stochastic processes in making predictions, which has been criticised as being limiting. Laslett (1994) stated that the main argument against kriging is that localised trends in the data set may be regarded as spatial correlations. It is, therefore, necessary to consider whether kriging is a suitable interpolation method for the data set. In the same paper, Laslett

(1994) made an empirical comparison between kriging and splines, a popular deterministic spatial predictor. Generally, the results showed little difference in the predictions made by the two methods. However, in areas with clustered data points kriging performed better.

Setianto and Triandini (2015) compared the accuracy between Ordinary Kriging (OK) and Inverse Distance Weighted (IDW), another geo-statistical method. The study found that kriging continuously outperformed IDW at all levels for complex data sets. However, if a qualitative discrete (nominal) data set is studied, both methods were found to perform the same. In cases such as these, it would be easier to use IDW as it has fewer steps. On the other hand, Yakowitz and Szidarovszky (1985) made a comparison between kriging and Kernel regression. Non-parametric regression (NPR) analysis uses information derived from the data to form a prediction equation. Yakowitz and Szidarovszky (1985) found that there was a greater risk of incorrect prediction using kriging when the data set is an intrinsic random function. These functions are processes that have stationarity that are not clearly defined as second order stationarity. Also, a good model has to be fitted to the semi-variance to achieve accurate predictions. Therefore they concluded that Kernel regression is more robust.

The advantage of kriging is that it only requires a limited data set. With successive samplings over time, a semi-variogram can dictate the number of samples required to ensure good predictions are made. This could result in fewer samples, which reduces costs. For kriging, the sampling regime is the most important factor in determining the accuracy of predictions (Laslett, 1994). Initial samples should be taken at short and long range distances to ensure a suitable semi-variance is fitted. Lack of samples at the short range will result in extrapolation of the semi-variogram towards the origin. Laslett (1994) therefore suggests that a basic grid is not a sufficient sampling regime. Instead samples should be taken at a variety of distances. Another advantage of kriging is that it compensates for data clustering so that a group of closely sampled points are not given more weight than individual points (Bohling, 2005). This prevents bias.

The use of geo-statistics in predicting fertiliser application patterns is limited. Studies involving geo-statistics in soil science are generally used to determine the plant yield or soil nutrient concentration in an area so that an appropriate fertiliser application plan can be developed (López-Granados et al., 2004; Schumann, 2006). They are also used to estimate the effect of a fertiliser application on nutrient leaching and plant response (Leopold et al., 2006; Verhagen, 1997). Goense (1997) used semi-variograms as a method of determining the spatial variability of site specific fertiliser application in ground spreaders. In particular, Goense (1997) compared

the variance between the applied and required application rates at different bout widths and for different three dimensional spread patterns (i.e. square pyramid distribution, square flat distribution, cone shape distribution). Spread patterns used in the analysis were both modelled and collected in the field. The data was collected at the resolution of the GPS equipment, and the spread pattern was assumed to be repeated in the following swath width. The semi-variograms showed that a square pyramid distribution gave the smallest variance between the applied and required rate. Kriged output layers were not produced.

1.8. Main Points

From the literature review, these points are emphasised.

- Wind has a significant impact on the transverse spread pattern, and therefore the field application rate and swath width. Wind can be highly variable throughout a day. Hill country topography effects air flow dynamics, which will affect the spread pattern.
- Spreaders increase the swath width and decrease positive kurtosis, but can only be used if the application rate is below 200 kg ha^{-1}.
- Variable rate application technology can improve the field CV and reduce off-target application of fertiliser. It has been established in ground based fertiliser application, and initial results from aerial application indicate promise.
- Assumptions exist around the flow of material from the hopper that has been untested. The majority of the work has focussed on the Beverloo equation as a means to predict the hopper door aperture required to achieve the desired application rate. However, this does not determine the flow consistency from the hopper, which has been assumed to be constant. Previous work has also not considered the interaction between airflow, the hopper door opening and the hopper flow regimes, and its effects on the flow pattern out of the hopper door.
- An aerial variable rate application trial has not been undertaken before, where multiple application zones are flown in one fertiliser load. Most trials have collected a single swath width and assumed that subsequent swath widths will produce the same spread pattern.
- Most of the work completed to date has not been validated in the field. This is because field trials are challenging and expensive. The field performance of these systems still needs to be tested and the suitable systems implemented.
- Field collectors are assumed to be 100% effective, but have not been previously tested. Appropriate collector placement is still to be determined, as well as methods to accurately calculate the application rate from spread data.

1.9. Structure of Thesis

The chapters in this thesis are organised in to three distinct topics.

Chapter 1 – *Introduction* begins the thesis with a literature review covering relevant background information and research. The chapter also states the specific objectives of the study.

Chapter 2 – *Ballistics Modelling for Aerial Topdressing of Granular Fertiliser* will cover the validation of a single particle ballistics model for single superphosphate, di-ammonium phosphate, urea and a superphosphate/Flexi-N fertiliser blend. The chapter will also describe the development of a Geographical Information System (GIS) tool, and a look up table that shows the number of meters a polygon should be shifted to minimise the amount of fertiliser applied outside of a boundary.

Chapter 3 – *Methods and Evaluation of Sampling for Aerial Topdressing Performance Trials* addresses the sampling techniques used in the trials presented in the thesis. The chapter will discuss the issues with particle bounce out of the collectors, and the process of finding a solution.

Chapter 4 – *Performance of an Aerial Variable Rate Application System* will discuss the results of the performance trials that were used to determine the accuracy, precision, level of off-target application, and capability of a variable rate system. The chapter will also cover kriging, bench testing and static hopper flow trials.

Chapter 5 – *Variability in Aerial Topdressing* will discuss the factors that influenced the trial results presented in this study, improvements to the research methodology and future areas of research.

Chapter 6 – *Summary* will include a summary of the results and discussion covered in this study. It will also include where the knowledge in the thesis was shared.

Chapter 2 - Ballistics Modelling for Aerial Topdressing of Granular Fertiliser

2.1. Introduction

This chapter covers the validation of the single particle ballistics model formulated by Jones et al. (2008) for fixed wing aircraft. The validation is completed for three common New Zealand fertilisers (superphosphate, urea and di-ammonium phosphate (DAP)) and a fertiliser blend. The fertiliser blend consists of 70% superphosphate and 30% Flexi-N (urea coated with magnesium oxide). The model was previously validated using AgDISP 8.15 (Bilanin et al., 1989), as a comparison, and also in a field trial using New Zealand single superphosphate applied from a Gippsland Aeronautics GA200C aircraft (Jones et al., 2008; Murray, 2007). Full validation has not occurred because of time and resource constraints. Model validation is important if the model is to be utilised in a commercial environment.

Ravensdown Limited is interested in using the Jones et al. (2008) model to estimate the effect of wind velocity and direction on an application area. Once known, that information can be incorporated in to the fertiliser application planning process. The objective of the model is to maximise the fertiliser applied within the farm boundaries, and reduce off-target application in to neighbouring farms and water ways. The predominant aircraft employed by Ravensdown Limited is the Pacific Aerospace Cresco (PAC) 600 (Figure 2.1). Therefore the model will only be validated for this aircraft.



Figure 2.1: Pacific Aerospace Cresco 600.

Jones et al. (2008) single granular particle ballistics model uses standard force balance equations. It considers the sum of gravity, buoyancy and drag forces to predict particle motion. Points of difference between this model and others are its consideration of velocity-dependent

drag, height dependent wind, aircraft attitude and propeller wash. A variable drag coefficient equation for non-spherical particles, by Haider and Levenspiel (1989), determines the velocity-dependent drag coefficient. Height dependent wind is estimated using the power law. Aircraft attitude is the orientation of the aircraft in relation to the horizon. Propeller wash is the disturbed tunnel of air produced by the aircraft's propeller, which may affect a particle's motion in its initial moments.

The model is able to reliably predict the landing position of fertiliser particles with a diameter greater than 0.5 mm. Particles below this threshold (defined as the fines fraction) have different aerodynamic properties. The model tracks the position of the particle to landing in a XYZ co-ordinate system in relation to its release point. However, this output does not show the overall spread pattern. To produce a model transverse spread pattern, the single particle model was modified in Visual Basic (VB) to generate a probability distribution by repeating the single particle model several thousand times (Murray, 2007). The VB program uses random number generators and constrained input ranges to ensure sufficient initial conditions are generated for a representative spread pattern. The inputs that are linked to the random number generators are particle size, particle sphericity, discharge angle, lateral discharge distance and discharge velocity.

Some of these inputs can only be measured discretely, but are continuous variables. For example, particle size distribution is determined by sieving, which categorises the particles in to sieve ranges. However, particle sizes will range within each sieve range. It is important to represent the particle size distribution in ballistics modelling, because particle diameter is used to determine the drag coefficient, and therefore the particle's terminal velocity. To model the sieve range distribution and other discrete variables, Murray (2007) selected normally distributed random generators. This is because the lateral distribution is normally distributed. A mean and standard deviation is required, which Murray (2007) approximated from published literature and laboratory measurements. However, some inputs were not determined and had to be estimated.

The model validation process, completed in this thesis, includes determining model inputs, which will reduce the number of unknown and estimated variables. Poor input selection limits the model's ability to accurately predict the particle's landing position. Flow rate out of the hopper door, initial discharge angle, and discharge velocity cannot be measured during topdressing. They are sensitive to changes in operating conditions, but are known to significantly influence the transverse spread pattern (R. Bansal et al., 1998; Walker and

Gardisser, 1988). This is further complicated by spreaders, which are utilised in aerial topdressing to widen the swath width and improve field fertiliser distribution. However they are only used when the application rate is less than 200 kg ha^{-1}. Spreaders studied in this thesis have 9 or 11 ducts. Accurately measuring the dimensions of a spreader is difficult since the vanes (walls separating the ducts) curve along their length. Vanes are equally spaced near the hopper door, but expand laterally towards the back of the aircraft. Minor adjustments can be made to the front vanes to change the flow rate into each duct. The ducts widen and have greater curvature the further they are from the centre of the spreader. Therefore, finding an appropriate method to measure the spreader is difficult, but it is beneficial to determine them as it reduces inaccuracies in the model results. To ensure an adequate number of particles are generated, the program interpolates between two aircraft GPS co-ordinates, which is set by the modeller. Further information about the model and its conversion to a VB program can be found at Jones et al. (2008) and Murray (2007).

This chapter will present the methodology and results of the validation for Jones et al. (2008)'s single particle ballistics model for superphosphate, DAP, urea and a superphosphate/Flexi-N blend. Two pilots were used in the trials, and each pilot operated their own PAC aircraft. They will be denoted as Pilot A and Pilot B. The aircraft and hopper design of both PAC aircrafts were similar. The chapter will also describe the development of the model in to the wind displacement calculator tool for Ravensdown Limited.

2.2. Method

Validation was completed in three trials carried out over a three year period. Each trial is summarised below.

2.2.1. Validation Trial 1

Trial 1 collected initial validation data for superphosphate, DAP and urea. It was carried out in May 2014 at a coastal sheep and beef farm named Longview, which is approximately 30 min from the township of Whanganui, North Island, New Zealand. The trial area was a flat paddock adjacent to the airfield. The collectors used in the trial will be referred to as NZCPA collectors. They are composed of three parts: stand, cone and collar. The metal stand is a ring held up by three spiked poles, which are driven in to the ground for stability. A cone fits into the ring and the collar sits on top of the cone. The cone funnels fertiliser to the bottom of the collector where a plastic sample bag is attached with a rubber band. Collars were introduced to reduce particle bounce out of the collector. NZCPA collectors have a diameter of 0.8 m at its widest point and are 0.9 m in total height. A single collector covers 0.5 m^2.

The sampling configuration used was based on Spreadmark tests, where collectors are set out in rows to collect the swath width. ArcGIS 10.1 was used to spatially visualise the sampling configuration and a Leica RTK-GPS (Real Time Kinematic Global Positioning System) was used to locate the position of each collector in the field (Figure 2.2). Nine rows of 20 collectors were set out with each row 20 m apart (Figure 2.3). Collectors in each row were 3 m apart; therefore, a row was 57 m in length. A line of six collectors was placed perpendicular to the centre of the rows for flight guidance.

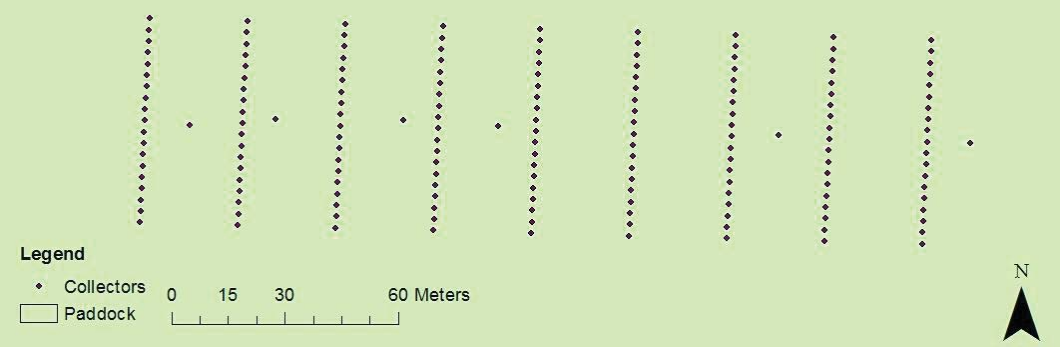


Figure 2.2: Pre-determined location of collectors for Trial 1 in ArcGIS 10.1.



Figure 2.3: Trial 1 set up.

A PAC 600 aircraft, fitted with variable rate application technology (VRAT), was operated by an experienced agricultural pilot (Pilot A). Pilot A flew over the collectors in a single pass for each fertiliser type. Samples were collected in between each flight. Urea was applied first, followed by DAP then superphosphate. The weather conditions for Trial 1 were sunny with light southerly winds. An anemometer recorded wind velocity and direction in relation to North every 30 s (Figure 2.4). It was mounted on a fence post approximately 2 m above the ground. The average wind velocity was 0.44 m s^{-1} with a range of 0.02 – 0.98 m s^{-1}, and the wind direction ranged between 67.38 – 227.4° with an average of 158.18° (Figure 2.5). An 11 duct Transland air ram spreader was used during the application of DAP and urea. A 2 kg fertiliser sample was collected from the on-site bulk storage pile to determine particle density and

particle size distribution, using the sampling guidelines set by the New Zealand Fertiliser Quality Council (NZFQC, 2016a).



Figure 2.4: Wind anemometer that records wind velocity and direction.

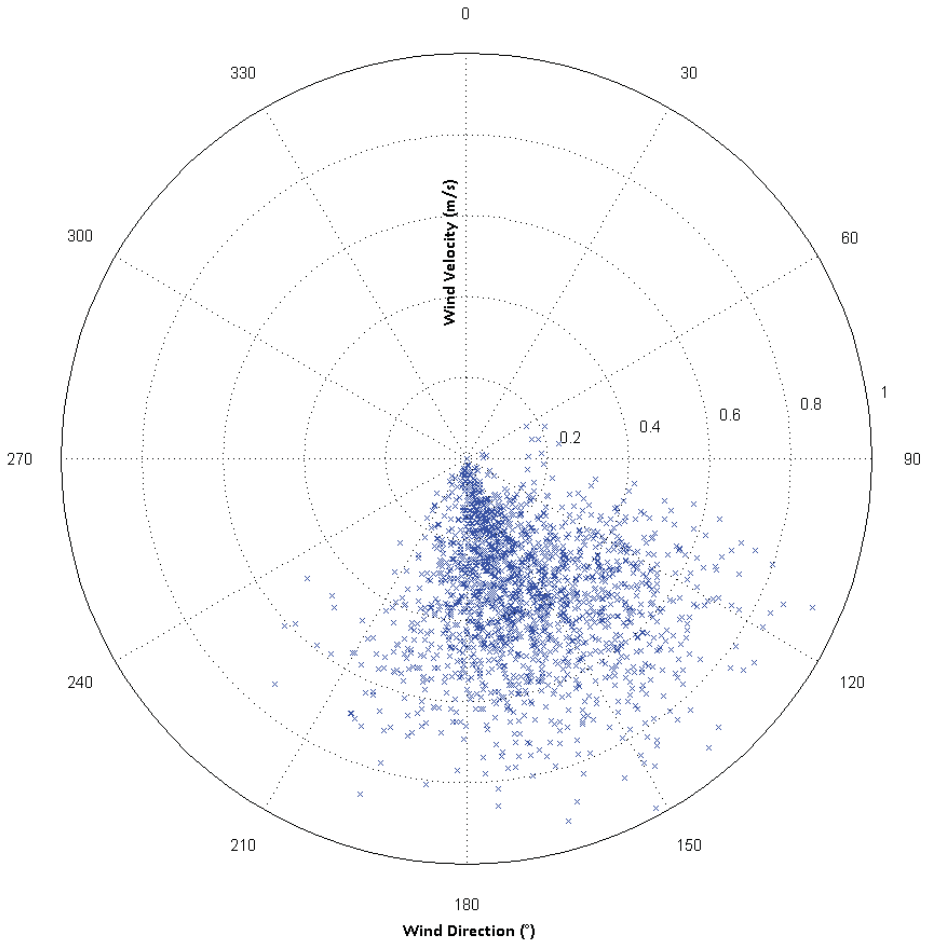


Figure 2.5: The wind velocity and direction over the trial period in Trial 1. True north is denoted by 0 degrees.

Prescription maps were uploaded to the aircraft before the trial. A prescription map designates the area of interest, average aircraft velocity with speed adjustment settings, and the gate openings. The speed adjustment setting enables the VRAT system to adjust the hopper door aperture to compensate for changes in groundspeed. The standard adjustment is 1.6 mm for a change in aircraft velocity of 5 m s^{-1}. This is necessary to ensure a uniform application rate is maintained in case the aircraft velocity changes significantly. Pilot A set the swath width, and was able to manually adjust the hopper door opening and aircraft speed to achieve the desired application rate. The application rate, pilot set swath width and speed adjusted hopper door opening are shown in Table 2.1 for Trial 1. The VRAT system (Satloc Intelligate G4 unit) installed on the aircraft recorded aircraft data every 0.2 s. This system allows for multiple application rates to be applied over an application area.

Table 2.1: Target application rate, swath width and hopper door opening for Trial 1.

Fertiliser Type	Target Application Rate (kg ha^{-1})	Set Swath Width (m)	Hopper Door Opening (mm)
Urea	73	22	33.3
DAP	115	22	36.5
Superphosphate	270	15	42.9

2.2.2. Validation Trial 2

The purpose of Trial 2 was to independently validate changes made to the model after Trial 1, to ensure the model was correctly validated and not over fitted. Transverse spread patterns for superphosphate, DAP and urea were collected. The trial was completed at Longview in November 2014. Six rows of 25 NZCPA collectors were set up (Figure 2.6 and Figure 2.7), with each row placed 70 meters apart. Collectors were placed 1 m apart at/near the centre of the row and 3 m apart at the edges. This was used to determine if there was noticeable variation in the centre of the distribution or whether the distribution was a smooth curve.

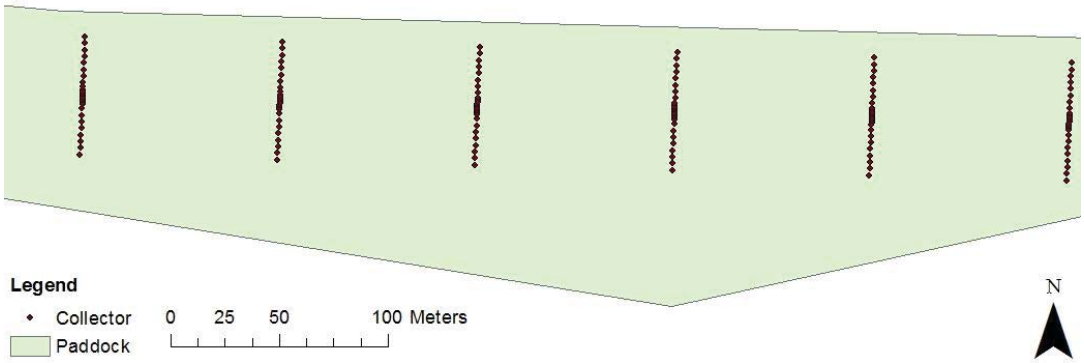


Figure 2.6: Pre-determined location of collectors for Trial 2 in ArcGIS 10.1.



Figure 2.7: Trial 2 set up.

Trial 2 was completed on a cloudy day with strong easterly winds. Wind measurements were recorded every 10 s using the anemometer. The average wind velocity, on the day, was 2.33 m s^{-1} but ranged between 1.22 – 3.75 m s^{-1}. The average wind direction was 93.82° with a range of 42.11 – 148.45° (Figure 2.8). Pilot A and his aircraft carried out the application. Each fertiliser type was applied once over the collectors in the order of urea, DAP then superphosphate. A spreader was not used on the day. A 2 kg sample of each fertiliser type was taken from the on farm bulk storage pile. Table 2.2 shows the prescription map settings completed by the aircraft.

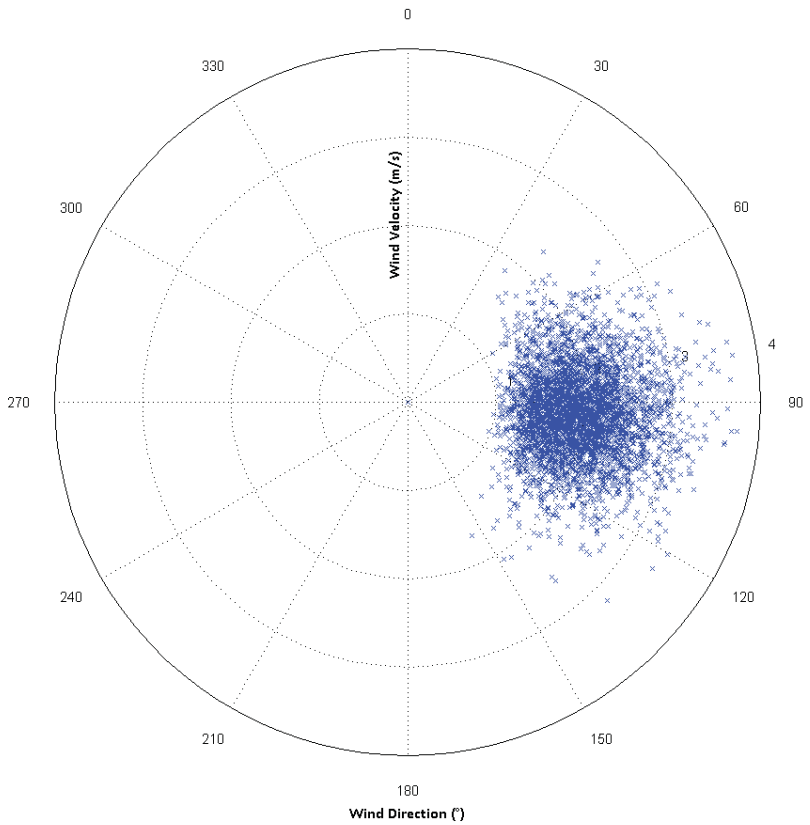


Figure 2.8: The wind velocity and direction over the trial period in Trial 2. True north is denoted by 0 degrees.

Table 2.2: Target application rate, swath width and hopper door opening for Trial 2.

Fertiliser Type	Target Application Rate (kg ha^{-1})	Set Swath Width (m)	Hopper Door Opening (mm)
Urea	90	22	50.8
DAP	140	22	49.2
Superphosphate	250	15	39.7

2.2.3. Validation Trial 3

Trial 3 was used to validate the single particle ballistics model for a 70% superphosphate and 30% Flexi-N blend. The trial was completed at Mairedale, a Central North Island sheep and beef farm in September 2016. The trial area was flat and was located next to the farm's airfield. Collectors from the New Zealand Agricultural Aviation Association (NZAAA) were used in this trial, because there was a perceived issue with the NZCPA collector. This is discussed in Chapter 3. The NZAAA collectors are composed of two parts: a y-post/waratah and a funnel shaped collector made of medium rigidity plastic with a metal rim, as described in Figure 1.8. The y-posts were rammed in to the ground so that they could support themselves and the collector. A sample bag was attached to the bottom of the funnel with a rubber band. The NZAAA collectors have an area of 0.25 m^2.



Figure 2.9: Trial 3 set up.

The NZAAA collectors were set up in three rows of 20 collectors (Figure 2.9). Each row was 10 m apart and the collectors in the row were 3 m apart. Two NZCPA collectors were placed perpendicular to the centre NZAAA collector for flight guidance. Wind measurements were logged every 15 s with the anemometer. The average wind speed was 0.46 m s^{-1} ranging from 0.09 – 1.28 m s^{-1}. The average wind direction was 175.11° with a range of 18.92 – 200.30° (Figure 2.10). Pilot B completed two flyovers without a spreader. The sample bags were collected at the end of each flyover.

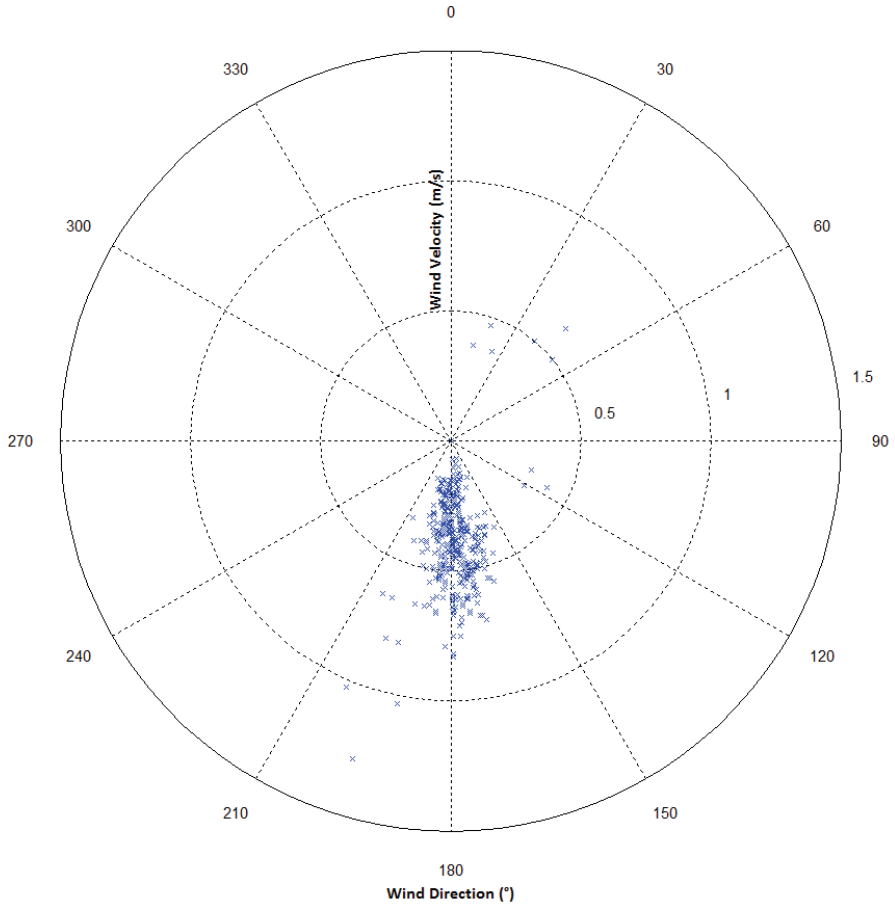


Figure 2.10: The wind velocity and direction over the trial period in Trial 3. True north is denoted by 0 degrees.

Both flights had the same prescription map and were trying to achieve similar transverse spread patterns. The intended application rate was 250 kg ha^{-1} with a swath width of 8 m and a hopper door opening of 34.9 mm. A fertiliser sample was taken from the bulk pile to determine the particle size distribution and particle density.

2.2.4. Pre – Processing

2.2.4.1. Laboratory

The 2 kg bulk fertiliser sample was divided into 500 g batches, using a riffler (Figure 2.11). An Electrolab electromagnetic sieve shaker sieved a 500 g sample at a power setting of 10 for 10 min. The sieve sizes were 4.75, 3.55, 2.36, 1.70 and 1.18 mm as per BSI (2013). Particle density was determined using the immersion method, where a known mass of fertiliser is placed in a known volume of kerosene and the displaced fluid is measured. This method was repeated three times for each fertiliser type, and the average particle density was used. A measuring cylinder and scale were used in the immersion method. Fertiliser samples, from the collectors,

were weighed to determine the lateral distribution in each row. Table 2.3, Table 2.4, Table 2.5 and Table 2.6 show the attributes of the bulk fertiliser material used in Trial 1 and Trial 2.



Figure 2.11: A riffler used to equally divide a fertiliser sample.

Table 2.3: Particle size distribution from the bulk pile for Trial 1.

Sieve range (mm)	Amount of material (%)		
	Superphosphate	DAP	Urea
> 4.75	27.54	0.13	0.19
4.75 – 3.35	34.51	39.97	58.21
3.55 – 2.36	16.15	43.69	37.17
2.36 – 1.7	10.81	14.10	4.33
1.7 – 1.18	4.79	1.69	0.09
< 1.18	6.21	0.42	0.01

Table 2.4: Particle density, size guide number (SGN) and uniformity index (UI) of particles from the bulk pile of Trial 1.

	Superphosphate	DAP	Urea
Particle density (kg m^{-3})	1757	1563	1183
SGN	336	273	303
UI	17	41	52

Table 2.5: Particle size distribution from the bulk pile for Trial 2.

Sieve range (mm)	Amount of material (wt. %)		
	Superphosphate	DAP	Urea
> 4.75	30.32	0.33	0.48
4.75 – 3.35	38.57	34.44	42.66
3.55 – 2.36	19.66	56.61	47.04
2.36 – 1.7	6.26	7.32	8.68
1.7 – 1.18	2.13	0.44	0.65
< 1.18	3.04	0.82	0.58

Table 2.6: Particle density, size guide number (SGN) and uniformity index (UI) of particles from the bulk pile of Trial 2.

	Superphosphate	DAP	Urea
Particle density (kg m^{-3})	1797	1288	963
SGN	363	273	282
UI	27	46	44

Table 2.7 shows the particle size distribution found in Trial 3. Particle density was determined using a specific gravity flask. This method is similar to the immersion method except the volume is determined with greater accuracy. Two particle density tests were completed, and the average result was 1832 kg m^{-3}. The SGN value for the distribution was 337 and the UI was 28.

Table 2.7: Particle size distribution from the bulk pile for Trial 3.

Sieve range (mm)	Amount of material (wt. %)
	Superphosphate/Flexi-N
> 4.75	20.15
4.75 – 3.35	41.14
3.35 – 2.36	27.02
2.36 – 1.7	6.42
1.7 – 1.18	1.79
< 1.18	3.49

2.2.4.2. Geographical Information Systems (GIS)

Information on GPS position, aircraft velocity, aircraft heading, altitude, and hopper door opening can be exported from the aircraft as log files into a supporting GIS platform called MapStar 8 (Hemisphere GPS, Phoenix, Arizona) (Figure 2.12). Mapstar is a bridging program that allows log files to be read and reformatted for use in other GIS Programs. ArcGIS 10.1 (ESRI, Redlands, California) processed the log files. The default co-ordinate system output from the aircraft was WGS 1984, which was converted to New Zealand Transverse Mercator (NZTM) 2000 format for model purposes.

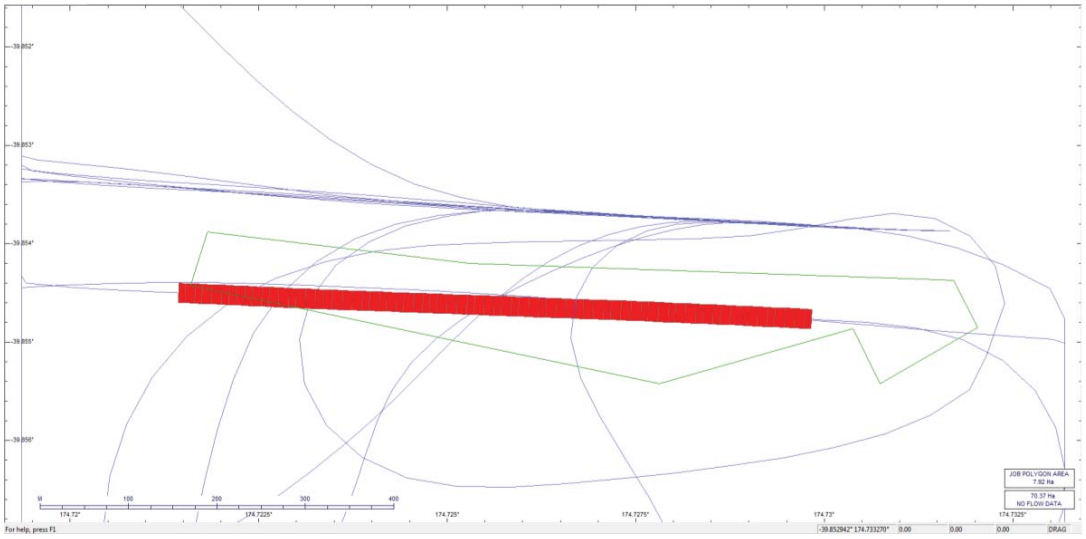


Figure 2.12: Example of Mapstar 8 output for Trial 2. The green outline represents the application area. Blue lines are flight lines, where the hopper is closed, and the red rectangles are the flight lines where the hopper door is open. The width of each individual rectangle represents the set swath width.

Altitude, exported from the aircraft, was recorded at above sea level. However, the model requires the aircraft's height above ground. Land Information New Zealand (LINZ)'s 25 m digital elevation map (DEM) was used to make the appropriate adjustments. It would have been beneficial to use a Real Time Kinetic (RTK) GPS system to get the exact height above ground for the trial area for a more accurate altitude.

The hopper door opening was converted to the flow rate out of the hopper door, using the Beverloo equation (Beverloo et al., 1961). This conversion was based on work previously completed by Grafton (2010). The Beverloo equation outputs the mass flow rate (M) in kg s^{-1} (Equation 2.1). A description of the inputs can be found in Table 2.8. These inputs were derived from Grafton (2010), except for mean particle diameter, which is sample specific.

$$M = K\rho g^{\frac{1}{2}} L(B - kd)^{\frac{3}{2}} \quad (2.1)$$

Table 2.8: Inputs for the Beverloo equation.

Nomenclature	Name	Value	Units
g	Acceleration due to gravity	9.83	m s^{-2}
p	Bulk density	740 – 1160	kg m^{-3}
d	Mean particle diameter	Sample Specific	m
K	Discharge coefficient	0.58	-
k	Shape coefficient	1.5 – 1.7	-
L	Hopper length	1.048	m

The Beverloo equation is also used to determine the hopper door opening required in the prescription map. The model is therefore highly reliant on the Beverloo equation, and it is important to ensure that the equation is accurate. Part of the validation process is to check the equation's accuracy in predicting the flow rate, and how the prediction compares with the intended application rate.

The model requires a comma-separated value (CSV) file with the aircraft's heading and velocity, the wind direction and speed, aircraft altitude, flow out of the hopper door, and GPS co-ordinates in NZTM format. Multiple rows of data can be included so that a whole area is modelled. Selection of the wind velocity and direction is difficult since wind conditions were not measured at 0.2 s (VRAT's recording time interval). Therefore, the wind direction and velocity around the time of the flight was used. In some cases, wind conditions were highly variable, and it was necessary to average wind conditions around the flight time. The particle size distribution, spreader parameters (if required), particle density, sphericity, GPS logging rate and the interpolation distance are also required. The GPS logging rate is the number of GPS points recorded by the aircraft in a second. In this case it was 5 Hz. The interpolation distance is the distance the plane travels per modelling event.

For all the single particle runs completed by the VB program, it returns a raw data file containing the particle size, sphericity, spreader duct number, particle position in the X, Y and Z direction, the mass that landed in that position, the X and Y co-ordinates of the landing position in NZTM 2000 format, and the time it took for the particle to reach the ground. Other variables could be returned in the raw file, if required. Additionally, a summary file is produced that summarises the particles at 1 m intervals in the transverse direction to produce the spread pattern.

2.3. Initial Model Program Set Up

2.3.1. Particle Size Distribution

A single sample was used to determine the particle size distribution of the bulk pile. These samples were taken at one third the height of the bulk pile, and may not be representative of the fertiliser distribution in the bulk pile or applied in the field. Fertiliser storage and transportation can create a heterogeneous particle size distribution, which can affect the ground transverse spread pattern.

Particle image analysis was used to determine if there was a significant difference between the bulk and collected particle size distribution. This was completed for Trial 1 and 2. Each collector sample was spread out on a matte black surface under fluorescent light, which

maximised the contrast between the particles and the background. Particles were separated to ensure each individual particle was distinguishable. An image of the particles was taken using a compact digital camera (14 Megapixel Panasonic DMC-FH2) mounted on several retort stands (Figure 2.13). A New Zealand 50 cent coin was used as a size reference (24.75 mm diameter). Several superphosphate samples were sieved before the image was taken to exclude the fines fraction (< 0.8 mm diameter). It would have been difficult to separate the fine particles from each other.



Figure 2.13: Image analysis of a collected DAP sample using a New Zealand 50 cent coin as a size reference.

Matlab R2013a (MathWorks, Natick, Massachusetts) was used to analyse the JPEG formatted images. The regionprops function determined the axis length of each particle in the image. It measured the major and minor axis in pixels, which were averaged to find the diameter. The pixel number was converted to a metric unit using the size reference. The diameters were then sorted in to the same sieve range that characterised the bulk pile (Table 2.9). To ensure the particle diameter predictions were accurate, the particle volume and mass were calculated, and compared with field observations. To simplify the analysis, each particle was assumed to be a perfect sphere, even though superphosphate and DAP are not. The image analysed and bulk particle size distributions were tested in the model to determine which produced the most similar distribution to the field transverse spread pattern.

Table 2.9: Image analysed particle size distribution from Trial 1 for DAP and urea.

Sieve range (mm)	Amount of material (wt. %)	
	DAP	Urea
> 4.75	14.05	18.61
4.75 - 3.55	49.04	54.82
3.55 - 2.36	34.11	24.28
2.36 – 1.7	2.35	1.5
1.7 – 1.18	0.35	0.46
< 1.18	0.06	0.21

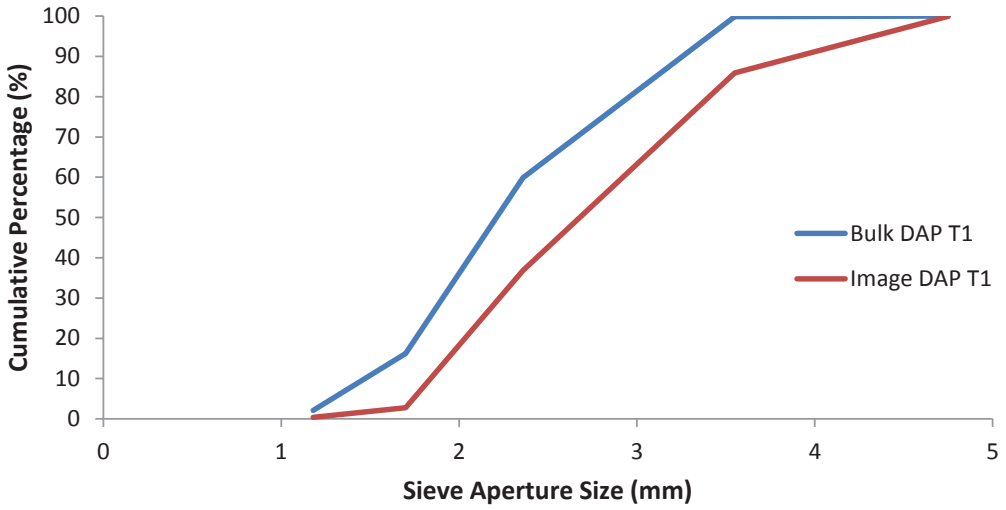


Figure 2.14: Cumulative particle size distribution of bulk and collected samples for DAP in Trial 1.

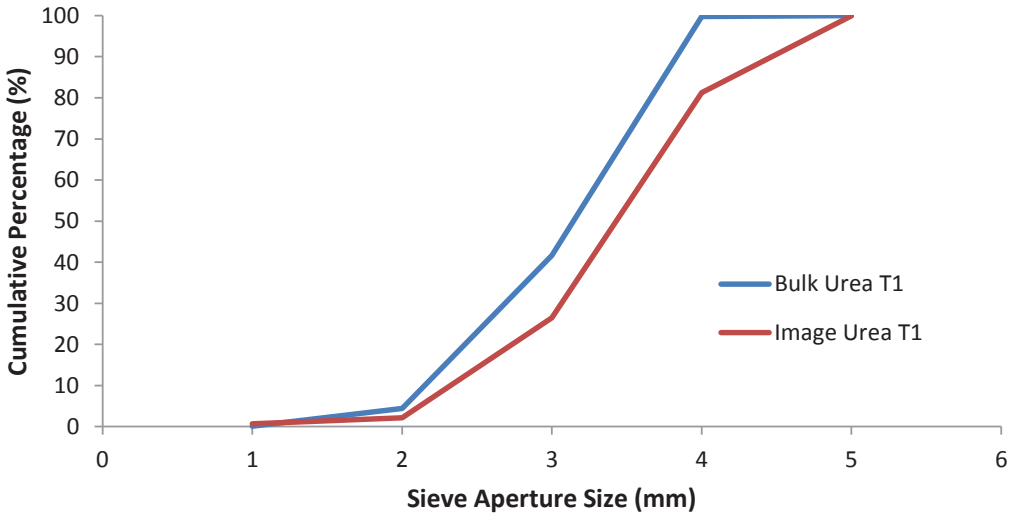


Figure 2.15: Cumulative particle size distribution of bulk and collected samples for urea in Trial 1.

There was a difference between the bulk and image analysed particle size distribution (Figure 2.14 and Figure 2.15). This occurred because fertiliser particles range in sphericity, but was

assumed to be spherical for analysis. Additionally, shadowing and reflection in the images impacted the quality of the analysis. Shadows occur when the light source is not placed directly above the particles. A shadow increases a particle's diameter because it obscures the particle's boundary, which will increase the particle's mass. Reflection captured by the camera over-exposes the image; also making it difficult to differentiate the particle's boundary. This error only affected some images.

The image analysed particle distribution had a higher fraction of large particle sizes compared with the bulk distribution, which produced wider swath widths in the modelled transverse spread pattern. This improved the modelled transverse spread patterns for DAP and urea. If shadowing and reflection were significant issues, the majority of particles would experience an increase in diameter and the particle size distribution would be unchanged. Since this is not observed, the image analysed distribution may indicate that a representative sample of the collected field particle size distribution collected in the field was not collected in the bulk pile sample.

To determine if the image analysed distribution is accurate, the transverse spread pattern of the image analysed distribution could be compared to the field collected distribution. This was not completed in this study but could be included in future research. Completing this analysis will also enable the comparison of the particle size fraction in each collector, which could be used to determine the effect of wind conditions on particle size.

2.3.2. Wind Power Law

The power law assumes wind speed and direction is uniform at a given height (Manwell et al., 2010). Several inputs are required in the power law equation. The equation has an exponent, n, which significantly impact the modelled transverse spread pattern. Previous studies indicate this exponent is between 0 and 1 (Chen et al., 1998; Spera and Richards, 1979). The exponent's value is based on height, wind velocity and surface roughness of the ground. Manwell et al. (2010) also found it depended on the time of day, temperature, season, and thermal and mechanical mixing. Counihan (1975) proposed Equation 2.2 as a method to determine n from surface roughness (z_0) for 0.001 m < z_0 < 10 m.

$$n = 0.096\, log_{10}\, z_0 + 0.016(log_{10}\, z_0)^2 + 0.24 \qquad (2.2)$$

Surface roughness is a difficult variable to quantify because it considers topography, other structures (i.e. buildings, trees) and their density (i.e. how many are they and how are they packed), and surface material. For example, rough pasture has a surface roughness of 8, while

crops are rated at 50. Justus et al. (1978) derived n using the reference wind velocity (v_{ref}) and height (h_{ref}) (Equation 2.3), which are both measureable and will, therefore, reduce uncertainty when determining n. However, Equation 2.3 may be an over simplification. Since n is site-specific, it will need to be considered prior to future modelling. The farms, Longview and Mairedale, were assigned an n value of 0.38, which were determined through trial and error.

$$n = \frac{0.37 - 0.88 \ln(v_{ref})}{1 - 0.88 \ln\left(\frac{h_{ref}}{10}\right)} \quad (2.3)$$

2.3.3. Particle Sphericity

Particle sphericity is used to calculate the drag coefficient, which affects a particle's motion through air and the landing position. The samples obtained from validation trials were not analysed to determine the sphericity. Murray (2007) calculated the sphericity of superphosphate by analysing a 38 g sample that was partitioned into sieve ranges (8.0 mm, 5.0 mm, 4.0 mm, 3.35 mm, 2.8 mm, 2.0 mm, 1.0 mm and 0.4 mm). He found a sphericity coefficient of 0.73 for superphosphate, which was used in the model. No sphericity values are available for DAP or urea particles, but they are more spherical in shape. DAP and urea was assigned an estimated sphericity of 0.85 and 0.9, respectively. Since fertiliser does not have a uniform sphericity, a standard deviation of 0.1 was included. Range constraints were included so that sphericity ranged 0.65 – 0.95 for superphosphate, 0.75 – 0.95 for DAP and 0.85 – 1 for urea.

2.3.4. Initial Discharge Variables

Initial particle discharge variables include velocity, angle and release point in relation to the hopper door. The initial discharge velocity is an important parameter in ballistics modelling and is dependent on aircraft velocity. R. K. Bansal et al. (1998b) carried out simulation studies of urea and found smaller particles are ejected with a velocity 30% higher than larger particles.

Ravensdown Aerowork completed an experiment to determine the air velocity at the hopper door and through a nine duct air ram FarmAir spreader. Pitot tubes were mounted at the exit of each spreader duct and at the hopper door. The plane then flew with no load at a variety of groundspeeds. Readings were manually recorded by a passenger when the aircraft reached a stable velocity. There is some variation in the values because it is difficult to maintain a constant aircraft velocity and the openings, where air enters the spreader, are not the same size. Results showed that air velocity through the centre ducts was lower than at the edges, and this was more significant when the hopper door was open (Table 2.10). Measurements were only taken for the closed position and for an application rate of 200 – 250 kg ha^{-1}.

Table 2.10: Air velocity in a nine duct spreader at an aircraft velocity of 62 m s^{-1}.

	Velocity in m s^{-1}										
Hopper Position	Ground Speed	Spreader Front	1	2	3	4	5	6	7	8	9
Closed	62	59	72	62	51	54	51	64	69	69	72
Open	62	51	54	36	44	44	44	44	41	41	57

R. Bansal et al. (1998) found from experiments that urea's particle discharge velocity is linearly related to the input duct air velocity. Particle discharge velocity is less than or half of the input duct air velocity. To obtain the same air velocities in their FLUENT model, as the laboratory tests, they included a 9% correction factor. R. Bansal et al. (1998) also carried out an analysis of variance (ANOVA) test which showed that particle velocities are dependent on their geometric mean diameters. Therefore, correction factors should be adjusted for changes in particle shape and size.

Jones et al. (2008) included a propeller wash component which required aircraft measurements, such as propeller length, aircraft drag coefficient and planform area (Table 2.11). These are constant inputs specific to an aircraft.

Table 2.11: Pacific Aerospace Cresco 600 aircraft parameters.

Name	**Value**	**Units**
Distance from propeller centre to spreader	0.91	m
Aircraft drag coefficient	0.0457	-
Propeller radius	1.41	m
Planform area of aircraft	27.97	m^2

Measurements of the hopper door were included in the model for fertiliser application without a spreader (Table 2.12). The angle range was estimated based on the swath widths achieved in Trial 1. Velocity reduction was calculated using Table 2.10, where the spreader front velocity was divided by groundspeed and then halved.

Table 2.12: Input values for the hopper door when a spreader is not attached for the application.

	Hopper Door
Lateral distance (m)	0
Distance range (m)	0.52
Inside angle (°)	0
Angle range (°)	66
Flow (%)	100
Velocity reduction	0.35

Ravensdown Limited utilises an 11 duct Transland ram air spreader and 9 duct FarmAir ram air spreader to apply fertiliser at low rates. Table 2.13 and Table 2.14 show the model parameters for these spreaders. The inside angle of each duct was used as the angle of interest. Percentage flow through each duct was determined by the distance between each vane in the front of the spreader divided by the whole length of the spreader. The model assumes that the fertiliser will flow out of the hopper uniformly across the width of the hopper door. Velocity reduction was calculated by dividing the results in Table 2.10, for an open hopper door, by the aircraft speed and then by two to account for particle velocity (R. Bansal et al., 1998). The values for duct 2 and 10 in the Transland spreader were interpolated from Table 2.10.

Table 2.13: Input values for a Transland spreader.

Duct Number	**1**	**2**	**3**	**4**	**5**	**6**	**7**	**8**	**9**	**10**	**11**
Lateral distance (m)	-1.45	-0.96	-0.72	-0.50	-0.28	0.0	0.28	0.51	0.93	0.97	1.43
Distance range (m)	0.45	0.24	0.22	0.22	0.20	0.08	0.20	0.22	0.23	0.24	0.46
Inside angle (°)	234	223	214	207	197	180	163	157	146	139	127
Angle range (°)	15.6	12.3	13.3	16.9	16.5	16.5	16.4	16.7	14.0	15.0	18.5
% Flow per duct	10.8	9.3	8.5	8.7	8.7	8.7	8.0	8.4	8.5	9.0	11.4
Velocity reduction	0.58	0.47	0.39	0.40	0.40	0.42	0.42	0.41	0.46	0.51	0.56

Table 2.14: Input values for a FarmAir spreader.

Duct Number	**1**	**2**	**3**	**4**	**5**	**6**	**7**	**8**	**9**
Lateral distance (m)	-0.96	-0.80	-0.59	-0.39	0.0	0.35	0.55	0.76	0.92
Distance range (m)	0.162	0.206	0.202	0.246	0.144	0.208	0.198	0.209	0.162
Inside angle (°)	214.3	206.8	201.2	193.7	178.0	166.3	160.8	151.0	143.7
Angle range (°)	6.1	8.5	9.3	12.5	9.7	11.5	8.2	9.0	8.4
% Flow per duct	11.8	11.0	10.8	10.8	11.2	10.9	10.8	11.0	11.7
Velocity reduction	0.72	0.61	0.51	0.52	0.50	0.53	0.53	0.64	0.66

Each spreader duct varies in length, angle and discharge velocity. The original VB program created by Murray (2007) did not constrain the values for differences between ducts in discharge angle, discharge distance, or particle velocity. Ranges were included when it became apparent the model overestimated some initial conditions, and did not produce the expected transverse spread pattern for the spreaders tested. Literature provided evidence that these variables need to be constrained and are significant (R. K. Bansal et al., 1998a, 1998b; Grift et al., 2001).

2.4. Validation Results and Discussion

Although the model was originally validated using the VB program, the results presented here were produced using Python as the programming language. The programming language does have an effect on the transverse spread pattern (i.e. random number generators). Since the

model will be run in a Python environment when it is commercially deployed, validation was completed again using the Python program. Information on the Python program can be found in Section 2.5.1.

After the completion of Trial 1 and 2, it was discovered that a significant percentage of fertiliser bounced out of the collectors. Therefore, Trial 1 and 2 data sets were corrected using coefficients found in Trial 6. The results for superphosphate, DAP and urea were increased by 5%, 35% and 16%, respectively. This will be discussed further in Chapter 3.

2.4.1. Trial 1

The field transverse spread distributions collected from Trial 1 were similar (Figure 2.16 – Figure 2.18), which was due to stable weather conditions on the day. Also the distance between each row was 20 m so it took the aircraft 2.3 s to transverse the collectors, which reduced the possibility of variability. The masses from the nine rows were averaged and compared to the modelled spread pattern. Table 2.15 shows the application rate and swath width for each row, which were calculated using Spreadmark V17 (NZFQC, Wellington, New Zealand). The calculated application rates coincided with the values in the averaged row, and swath widths were similar, which suggests that it is appropriate to use an averaged value in the model. Note the average swath width is calculated by averaging the swath width from rows 1 to 9, while the average row swath width was determined using Spreadmark V17.

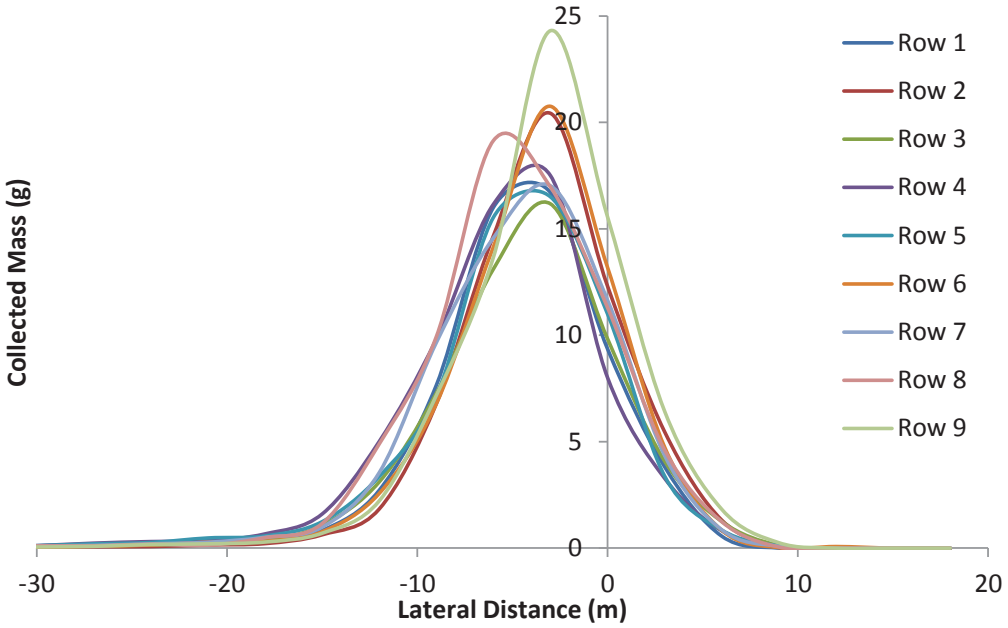


Figure 2.16: Trial 1 spread patterns collected from the nine rows for superphosphate.

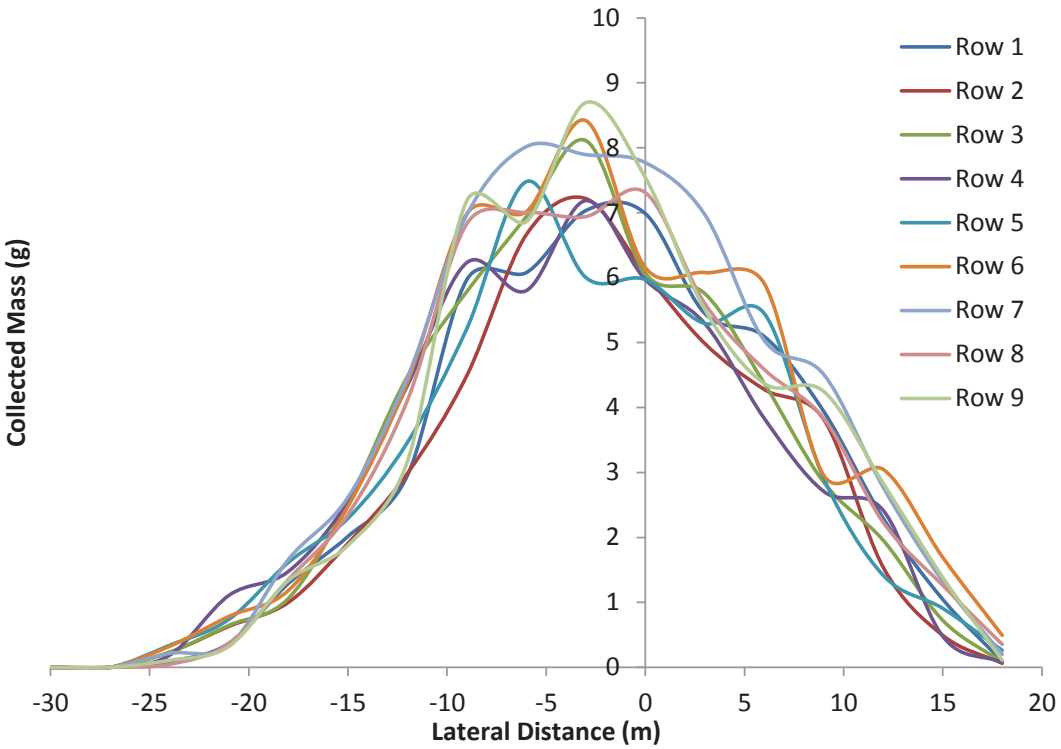


Figure 2.17: Trial 1 spread patterns collected from the nine rows for DAP.

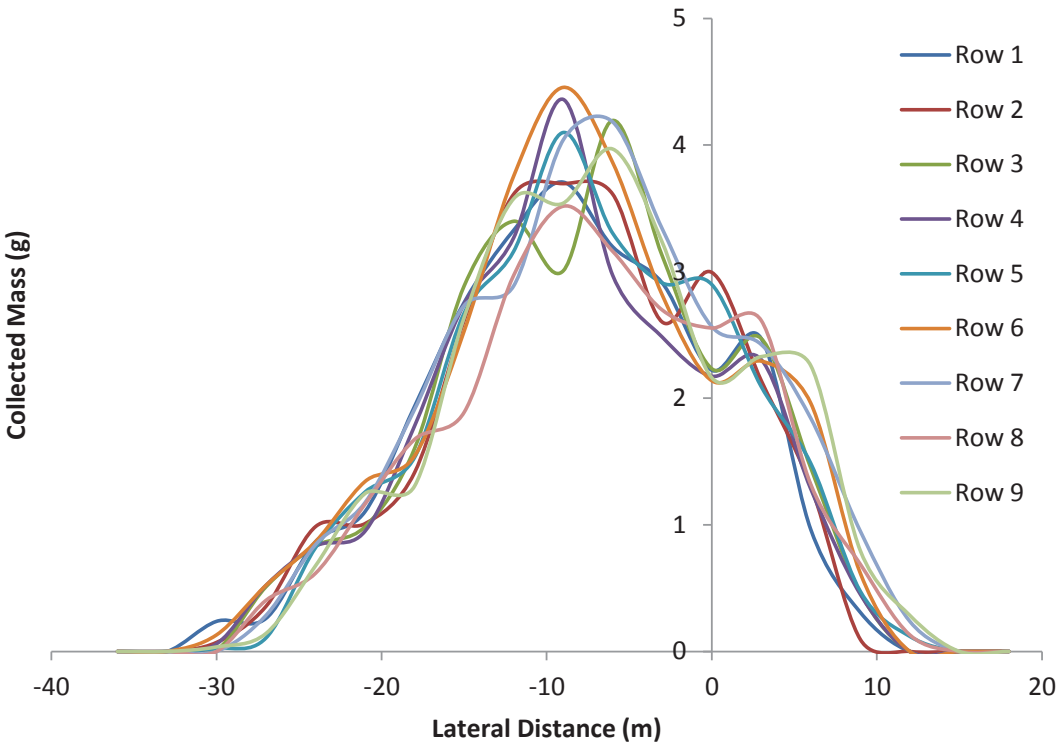


Figure 2.18: Trial 1 spread patterns collected from the nine rows for urea.

Table 2.15: Application rates and swath widths from Trial 1 for each collector row.

	Application Rate (kg ha^{-1})			Swath Width (m)		
Row	Superphosphate	DAP	Urea	Superphosphate	DAP	Urea
1	232	139	72	12	24	24
2	259	127	73	12	22	24
3	227	141	75	12	24	24
4	251	137	72	12	25	24
5	242	134	74	12	24	24
6	261	158	79	12	24	24
7	256	166	81	14	25	25
8	276	148	69	13.5	24	24
9	297	152	77	10.5	20	24
Average	256	145	75	12	24	24
Standard Deviation	21.7	12.4	3.8	1.0	1.6	0.3
Average Row (Spreadmark)	256	145	75	12	25	25

Superphosphate was the first fertiliser type to be modelled because its application did not involve a spreader, which reduced the number of discharge inputs. The field spread patterns for superphosphate were normally distributed, had positive kurtosis and a narrow swath width, which occurs when a spreader is not used. Figure 2.19 shows there are significant differences between the modelled and average superphosphate field spread pattern. The initial model predicted a distribution that was centred to the left of the aircraft flight path, with a skewed distribution. Since a spreader was not used in the application, the error is from a failure within the model rather than poorly characterised initial conditions. The displacement to the left suggests the error is caused by the propeller wash component.

The propeller on a PAC 600 rotates in a clockwise direction, which displaces particles towards the negative lateral direction (port side). This influences the landing position of a single particle. Larger particles are less affected than smaller particles, which can explain the shape of the displaced distribution. Particles flow out of the hopper door in a mass flow and, depending on the strength of the propeller wash, the mass flow of particles may not separate until they have fallen through the propeller wash. Therefore, individual particles would be shielded limiting the effect of the propeller wash. Another effect of mass flow is that the clustering of particles increases their inertia, which reduces their time in the propeller wash. Therefore, in the initial time steps, the assumption that particles are singular is incorrect. Validation was only completed on a PAC 600 so it cannot be concluded that the propeller wash component is ineffective for other topdressing aircraft. An aircraft with a more powerful engine may produce the modelled skewed distribution with its propeller wash.

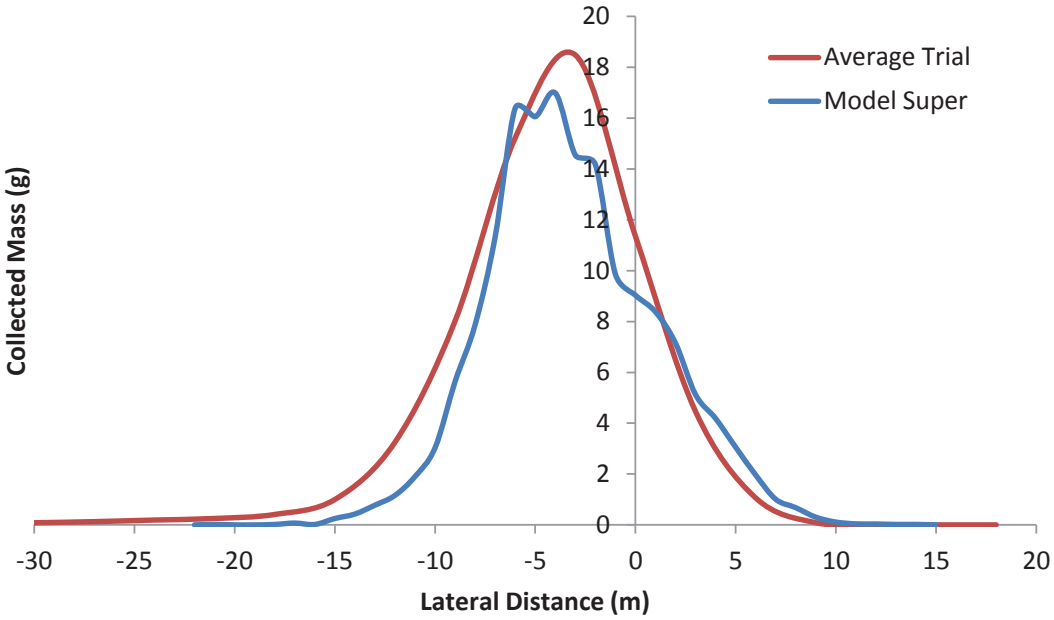


Figure 2.19: Comparison of Murray (2007) model and Trial 1 spread patterns for superphosphate. For this spread pattern, the aircraft was travelling at a heading of 92°, aircraft velocity of 69 m s^{-1} and an altitude of 34.2 m. The wind direction was 158.62° and wind speed was 0.1 m s^{-1}. The modelled flow rate of superphosphate out of the hopper was 1261 kg min^{-1}.

Removing the propeller wash component improved the overlap between the model and field results (Figure 2.20). It reduced the model's complexity for a PAC 600 aircraft and removed the model's dependence on the aircraft's design. However, the aircraft's aerodynamics still needs to be considered as it is relevant to discharge parameters.

Modelled spread patterns without the propeller wash still showed small, but observable differences between the modelled and average field distributions, especially for urea and DAP. The error bars in Figure 2.20 – Figure 2.22 represent the standard deviation of masses collected at that transverse distance in the field, which were obtained by collating Figure 2.16 – Figure 2.18. It shows that a wide range of values is possible and future users of the model should take this in to account when the modelled distribution differs from field observations.

In some cases, the modelled spread pattern did not produce a swath as wide as the field spread pattern. Errors in the bulk particle size distribution over-represented the percentage of small particles. Therefore, the particle size distribution from image analysis was used to achieve better results for DAP and urea (Figure 2.21 and Figure 2.22).

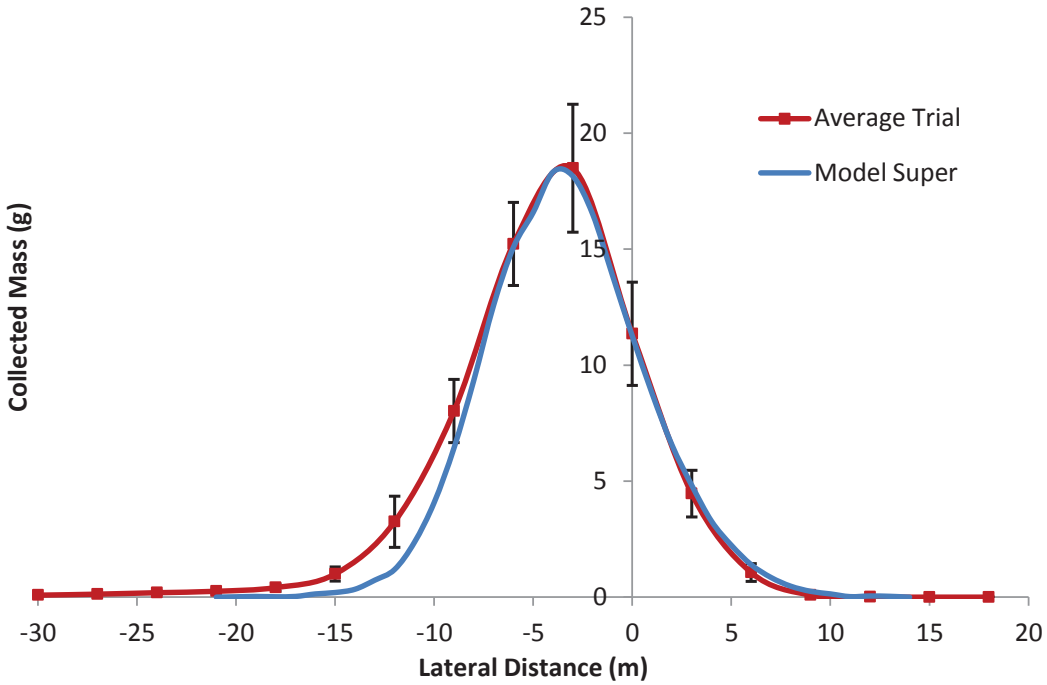


Figure 2.20: Comparison of model and Trial 1 spread patterns for superphosphate. For this spread pattern, the aircraft was travelling at a heading of 92°, aircraft velocity of 69 m s^{-1} and an altitude of 34.2 m. The wind direction was 158.62° and wind speed was 0.1 m s^{-1}. The modelled flow rate of superphosphate out of the hopper was 1261 kg min^{-1}.

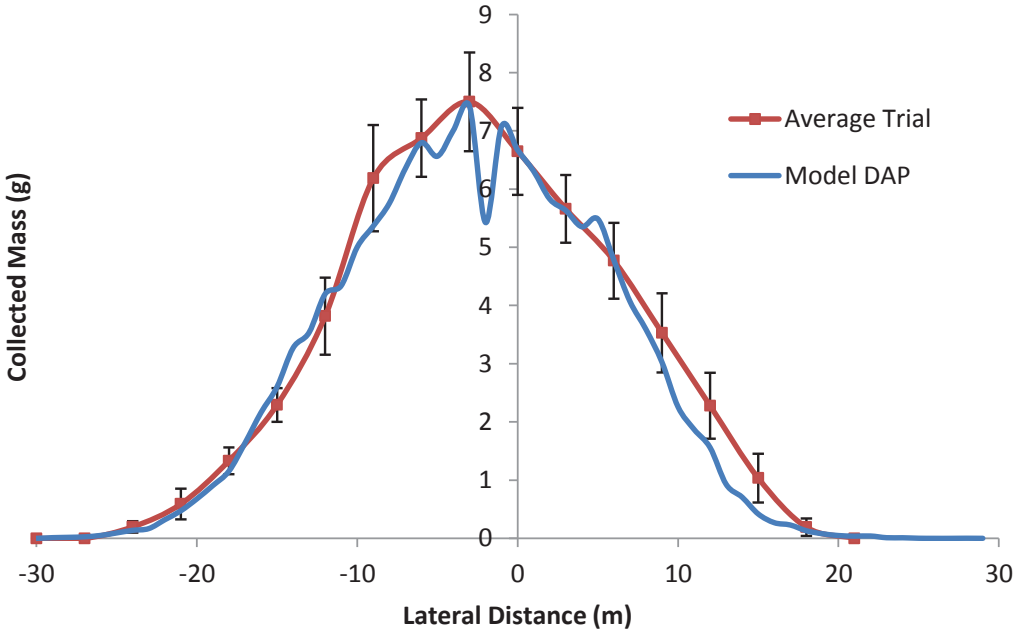


Figure 2.21: Comparison of model and Trial 1 spread patterns for DAP. For this spread pattern, the aircraft was travelling at a heading of 92°, aircraft velocity of 62 m s^{-1} and an altitude of 32.5 m. The wind direction was 149.15° and wind velocity was 0.214 m s^{-1}. The modelled flow of DAP out of the hopper was 1300 kg min^{-1}.

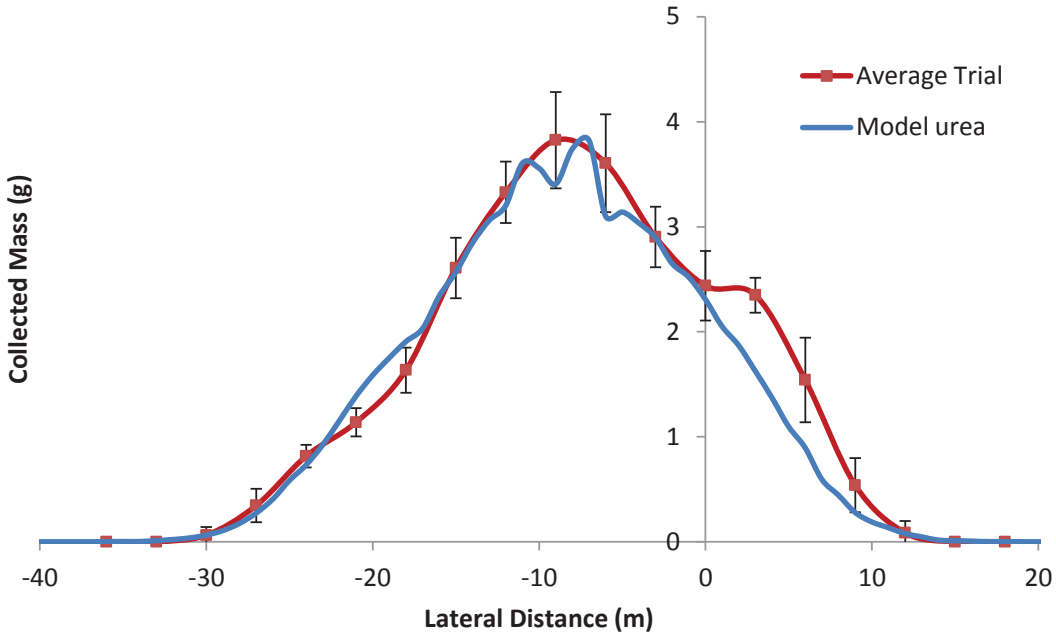


Figure 2.22: Comparison of model and Trial 1 spread patterns for urea. For this spread pattern, the aircraft was travelling at a heading of 92°, aircraft velocity of 65 m s^{-1} and an altitude of 34.4 m. The wind direction was 178° and wind speed was 0.58 m s^{-1}. The modelled flow rate of urea out of the hopper was 551 kg min^{-1}.

None of the modelled spread patterns were completely within the error bars of the average field spread patterns. The lateral distribution is sensitive to many parameters, and flight conditions are highly variable. Although the model was developed as a single particle model, it would take too much time to model all particles individually. Therefore, the VB program divides the total flow rate (kg s^{-1}) into categories of size, position and velocity to simplify the modelling process. This limits the number of inputs, and reduces the required modelling time. The modelling time is dependent on the number of runs required. This is dictated by whether a spreader is used, the number of sieve ranges in the particle size distribution, and the interpolation distance. For a single aircraft GPS co-ordinate, using a Transland spreader and an interpolation distance of 0.5 m, the modelling process will take approximately 40 min. A better overlap with the field data may be achieved with a smaller interpolation distance and more sieve ranges. However, this will increase the number of runs and the modelling time.

The modelled spread patterns of DAP and urea differed more from their trial counterparts. This is likely due to the Transland spreader. Since the spreader ducts curve, the range of discharge angles, discharge speeds and discharge positions are difficult to measure. Discharge velocity is influenced by wind speed and direction, groundspeed and the hopper gate opening. These variables are not recorded at the same time interval, so the model may not encounter the exact set of initial conditions to produce the trial's lateral distribution. However, this model

does not require 100% accuracy, because its end use is for predicting the effect of average wind conditions on the transverse spread pattern. Wind is the most significant factor in aerial topdressing so using the average wind conditions will introduce error. The average wind condition is a logical input because it is not currently feasible to model the spread pattern every minute. Since the field transverse spread pattern can change significantly, the random number generators will allow the model to introduce stochastic variability in the initial conditions. Therefore, the modelled average spread pattern is sufficient for the purpose.

2.4.2. Trial 2

The field distributions and masses varied significantly in Trial 2 because there were significant variations in environmental conditions on the day (Figure 2.23 - Figure 2.25), and rows were set 70 m apart. The row spacing meant the aircraft took approximately 6 s to transverse the trial area, and in that time wind conditions could change significantly. The average of these six rows was compared to the model. Since wind conditions were variable on the day, flexibility was allowed on the selection of wind velocity and direction for the model. The wind velocity and direction used for each fertiliser type was selected from around the time of their flight.

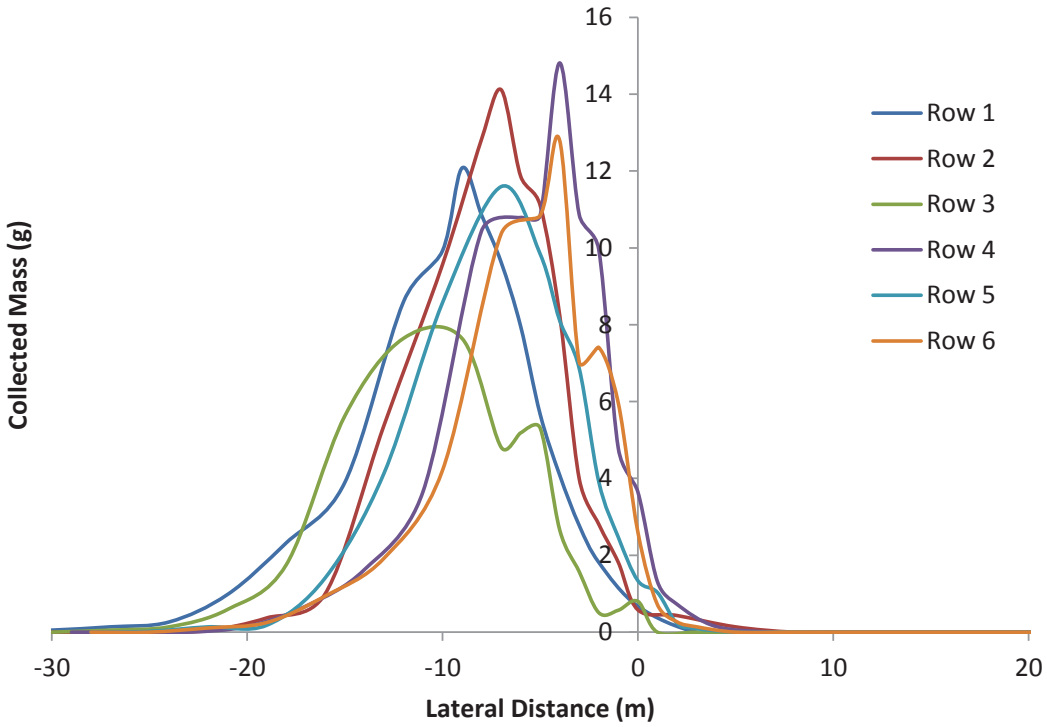


Figure 2.23: Trial 2 spread patterns collected from six rows for superphosphate.

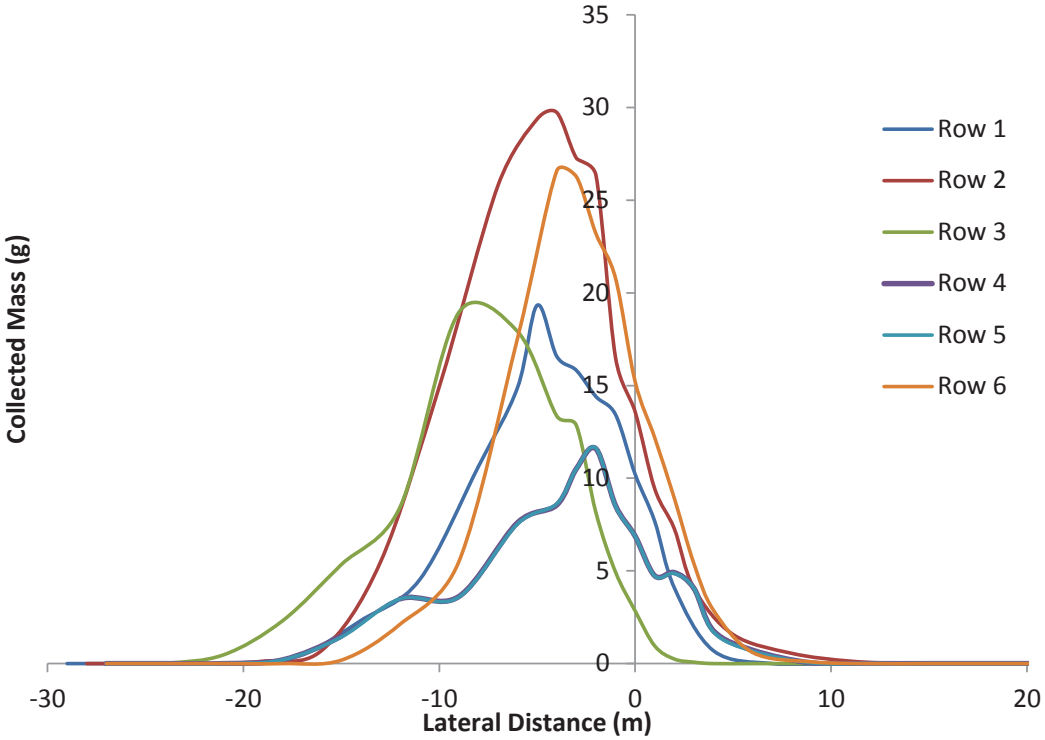


Figure 2.24: Trial 2 spread patterns collected from six rows for DAP.

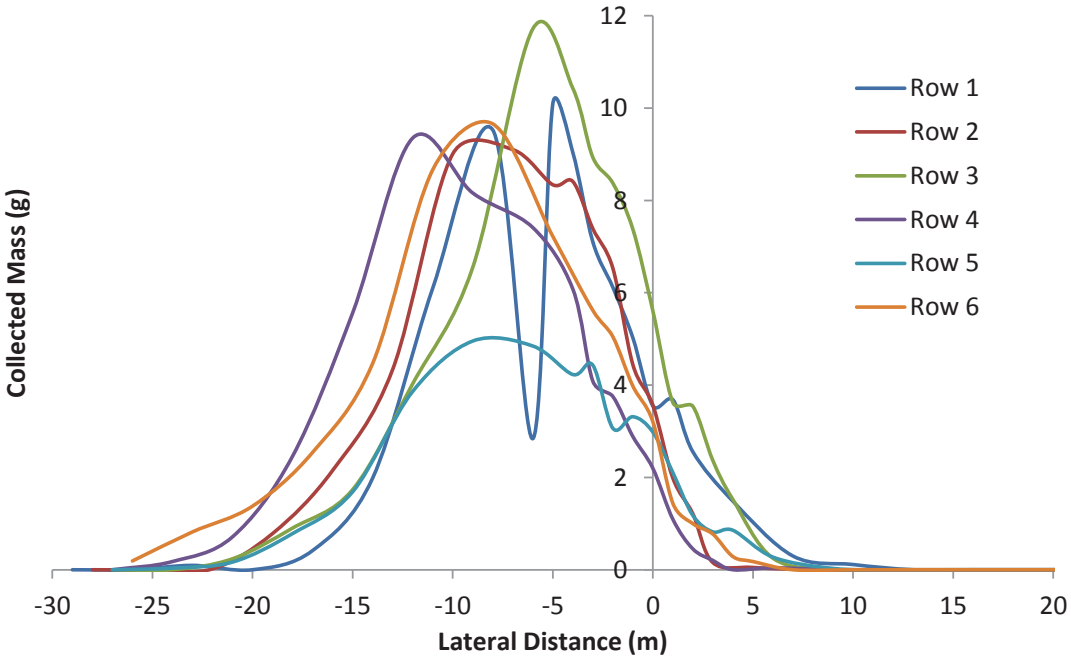


Figure 2.25: Trial 2 spread patterns collected from six rows for urea.

When modelling for spread patterns collected in Trial 2, the propeller wash was omitted. All other settings and initial inputs remained the same. This was important to ensure that the model was not over-fitted. A spreader was not used in this trial. Table 2.16 shows the application rate and swath width for the three fertiliser types as calculated by Spreadmark V17

based on Figure 2.23 - Figure 2.25. The application rates for each row were similar to the averaged row, but the swath width for urea varied. The averaged row swath width, calculated in Spreadmark V17, was higher than the average swath width, which was calculated by averaging the six rows. This occurred because the resulting shape of the averaged row was more evenly distributed than each individual row, which improved its maximum swath width.

Table 2.16: Application rates and swath widths from Trial 2 for each collector row.

	Application Rate (kg ha^{-1})			**Swath Width (m)**		
Row	Superphosphate	DAP	Urea	Superphosphate	DAP	Urea
1	157	161	107	10	9	12
2	158	273	106	10	11	12
3	126	185	113	14	9	12
4	148	105	110	10	10	12
5	155	104	68	12	10	15
6	157	196	112	10	8.5	12
Average	150.2	170.7	102.7	11.0	9.6	12.5
Standard Deviation	12.4	63.5	17.2	1.67	0.92	1.22
Average Row (Spreadmark)	150	172	104	12	10	15

The model was not able to predict all the oscillations of the field distribution, but could reliably predict the peak mass and swath width. There was sufficient overlap between the field and model distributions (Figure 2.26, Figure 2.27 and Figure 2.29). Again, the model represented superphosphate the best. An explanation for this is that the model was originally developed and validated for superphosphate. It has a wider particle size range than DAP or urea, and the sphericity was previously characterised by Murray (2007), so it has fewer estimated inputs. This gave it the best chance to be accurately modelled. There are several differences between superphosphate, DAP and urea, which would affect how each are modelled. DAP and urea is applied at wider swath widths because their average particle size is greater than superphosphate's. They have a lower fines fraction and greater particle strength. DAP has the greatest particle strength, while urea is the most spherical followed by DAP then superphosphate (Chok et al., 2014). These particle characteristics contribute to the fertiliser's particle motion and will, therefore, affect how they are modelled.

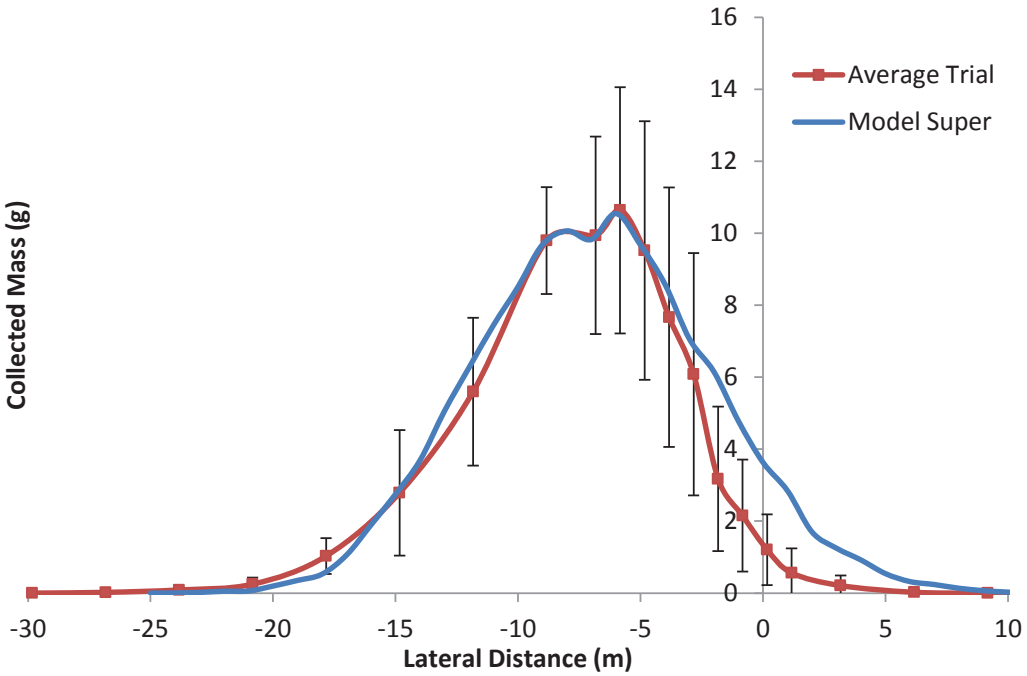


Figure 2.26: Comparison of model and Trial 2 spread patterns for superphosphate. For this spread pattern, the aircraft was travelling at a heading of 273°, aircraft velocity of 59 m s^{-1} and altitude of 33.3 m. The wind direction was 77° and wind speed was 1.6 m s^{-1}. The modelled flow rate of superphosphate out of the hopper was 982 kg min^{-1}.

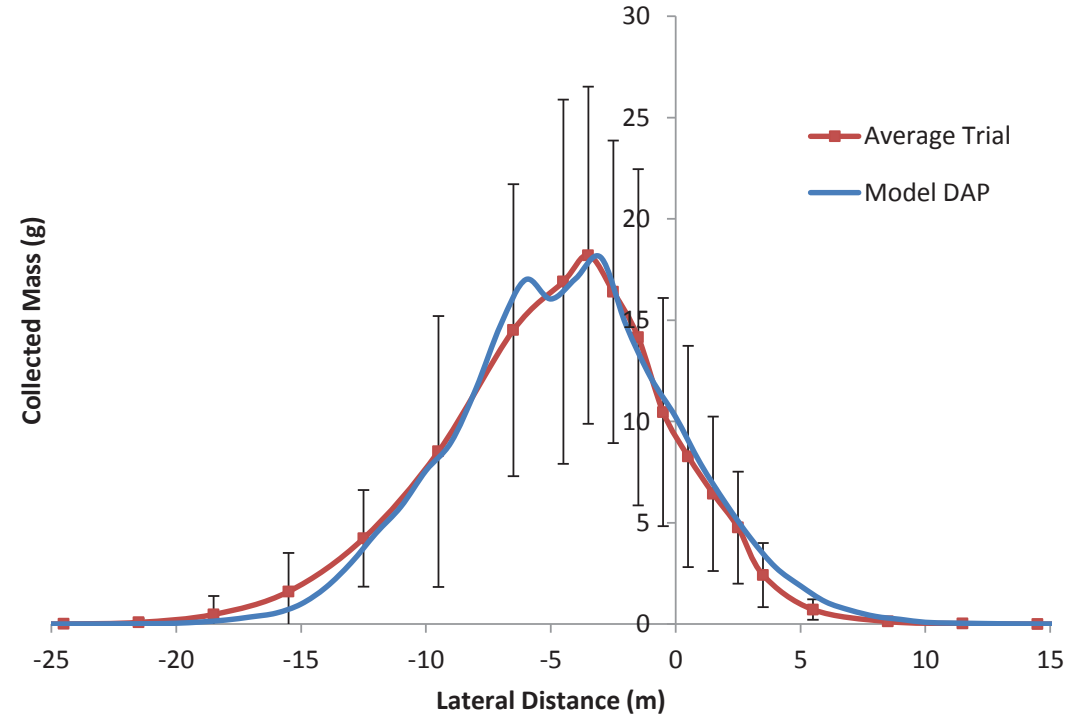


Figure 2.27: Comparison of model and Trial 2 spread patterns for DAP. For this spread pattern, the aircraft was travelling at a heading of 273°, aircraft velocity of 58 m s^{-1} and altitude of 32.5 m. The wind direction was 81° and wind velocity was 1.44 m s^{-1}. The modelled flow rate of DAP out of the hopper was 1490 kg min^{-1}.

The modelled spread pattern for urea resulted in a narrower swath width compared to the field spread pattern. Therefore, the image analysed particle size distribution was utilised in the model to give a more accurate result (Table 2.17 and Figure 2.28). The percentage of large particle sizes increased, which meant that the modelled spread pattern for urea achieved a similar swath width, and mass was well distributed (Figure 2.29).

Table 2.17: Image analysed particle size distribution from Trial 2 for urea.

Sieve range (mm)	Amount of material (wt. %)
	Urea
> 4.75	7.15
4.75 - 3.55	50.64
3.55 - 2.36	40.21
2.36 – 1.7	1.94
1.7 – 1.18	0.06
< 1.18	0.82

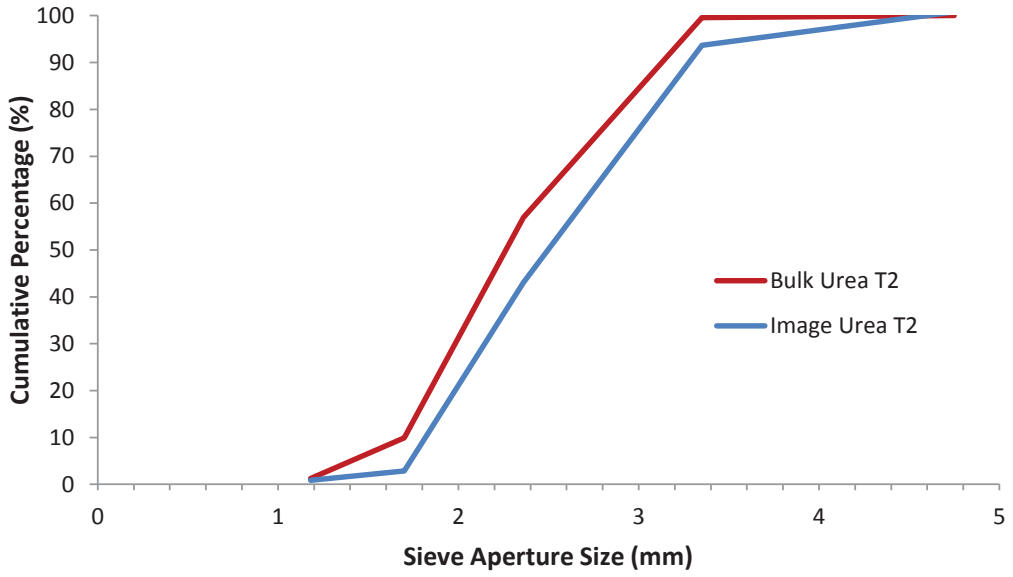


Figure 2.28: Cumulative particle size distribution of bulk and collected samples for urea in Trial 2.

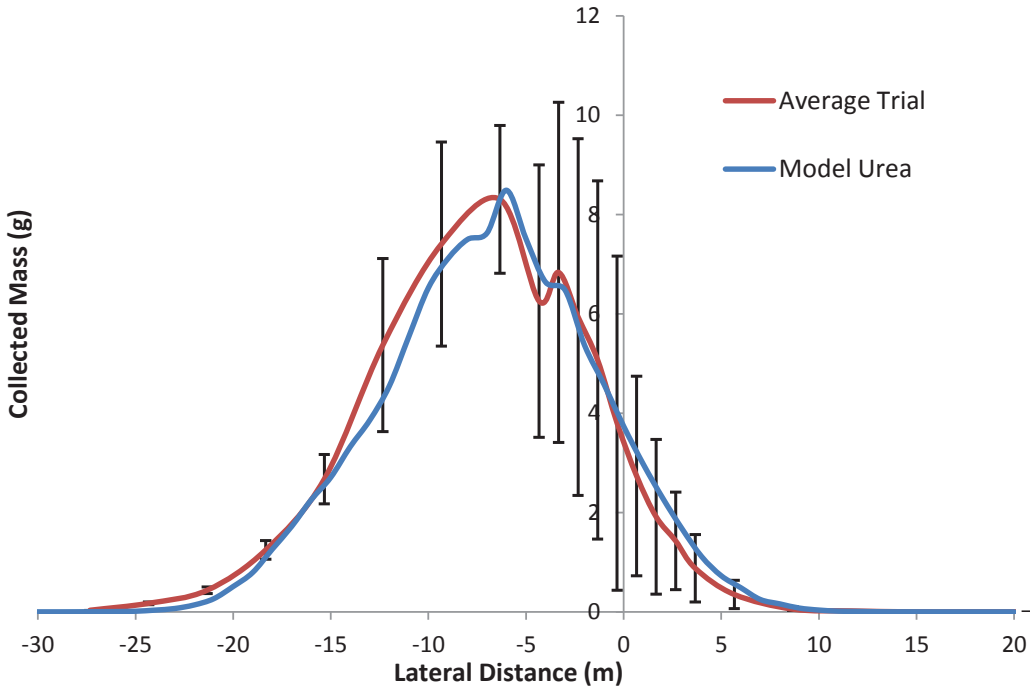


Figure 2.29: Comparison of model and Trial 2 spread patterns for urea. For this spread pattern, the aircraft was travelling at a heading of 273°, aircraft velocity of 63 m s^{-1} and altitude of 41.8 m. The wind direction was 85° and wind velocity was 2.57 m s^{-1}. The modelled flow rate of urea out of the hopper was 845 kg min^{-1}.

2.4.3. Trial 3

A spreader was not used in Trial 3. The collected spread patterns did not vary significantly because wind conditions were stable (Figure 2.30 and Figure 2.31). Table 2.18 compares the Spreadmark calculated application rates and swath widths for the three rows in each flight to an averaged row. The application rates and swath widths of the averaged rows were similar to the values found in the flight rows. The swath width was calculated using a CV of 15% because nitrogen is a major component of Flexi-N.

Table 2.18: Application rates and swath widths from Trial 3 for each collector row.

	Application Rate (kg ha^{-1})		**Swath Width (m)**	
Row	Flight 1	Flight 2	Flight 1	Flight 2
1	214	206	5	4
2	211	214	4	6
3	220	200	4	4
Average	215	207	4	5
Standard Deviation	4.6	7.0	0.6	1.2
Average Row (Spreadmark)	215	207	4	4

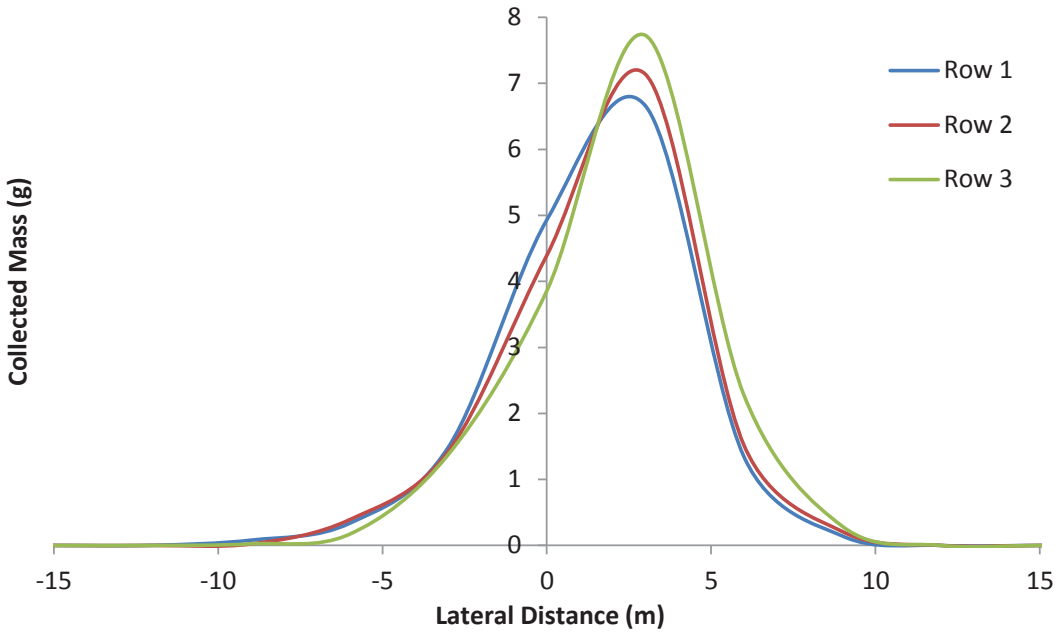


Figure 2.30: Trial 3 spread patterns collected from Flight 1 for the 70% superphosphate/30% Flexi-N blend.

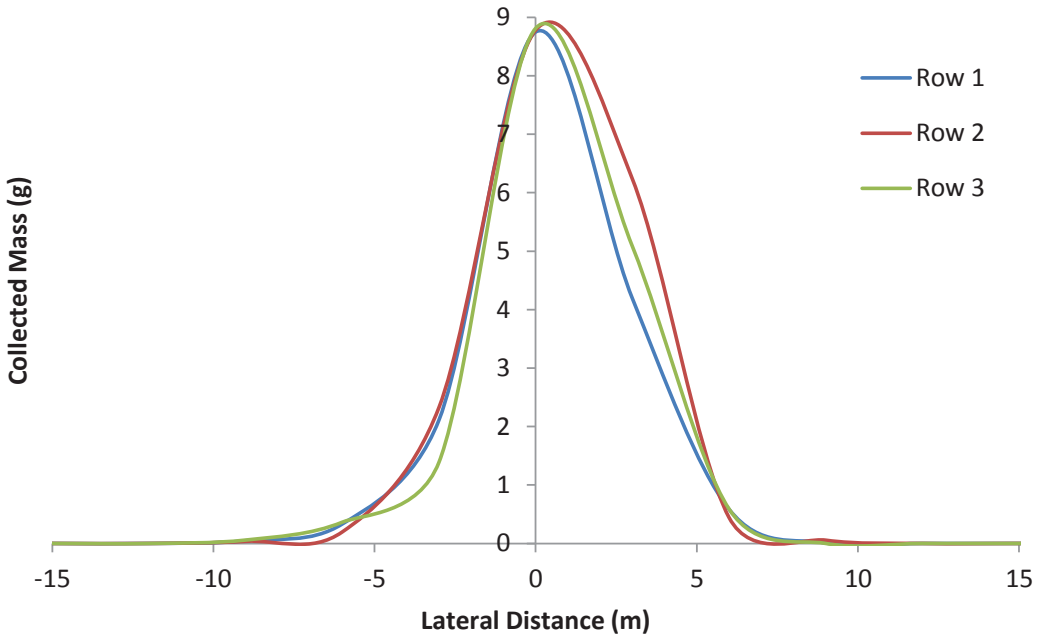


Figure 2.31: Trial 3 spread patterns collected from Flight 2 for the 70% superphosphate/30% Flexi-N blend.

The NZAAA collectors had a collection area of 0.25 m^2, so the modelled masses were divided by two for comparability to the field collected masses; the model was formulated for the NZCPA collectors (area of 0.5 m^2). Initial modelling of the first flight produced model transverse spread patterns with wider swath widths than field distributions. A possible cause is the altitude of the aircraft above ground. The PAC 600 flew at an altitude of 11 – 19 m, which is

the lowest altitude that has been flown in a trial. Past trials had altitudes of 30 – 45 m. To determine if altitude has an effect, it was modelled at 1 m, 3 m, 5 m, 8 m, 10 m, 25 m and 50 m in still conditions. Below 5 m, the modelled spread pattern had a narrow swath width and a greater peak mass than the field distribution, which occurred because the particles had less time to travel laterally. At altitudes greater than 5 m, there was little change in the model distribution. This was also demonstrated, in field trials, by Akesson and Yates (1964), and Scott (1970). Therefore altitude does not explain the difference in the two distributions.

Light wind conditions could be a contributing factor for the narrow swath width. Previous studies have shown that wind tends to widen the swath width. However, in Trial 1 for superphosphate the wind velocity was 0.1 m s^{-1}. This is less than the wind speed during Flight 1 in this trial, so wind was excluded as the main contributor. A high coefficient of restitution between superphosphate and Flexi-N could be an explanation. The collisions between the two fertiliser types may reduce their discharge velocity. Adjusting the particle discharge velocity out of the hopper door from 0.35 to 0.25 resulted in the narrower swath width observed in the field patterns (Figure 2.32 and Figure 2.33). This achieved sufficient overlap of the distributions. Although this was a model fitting exercise, the adjustment value found during validation of Flight 1 was independently validated in Flight 2.

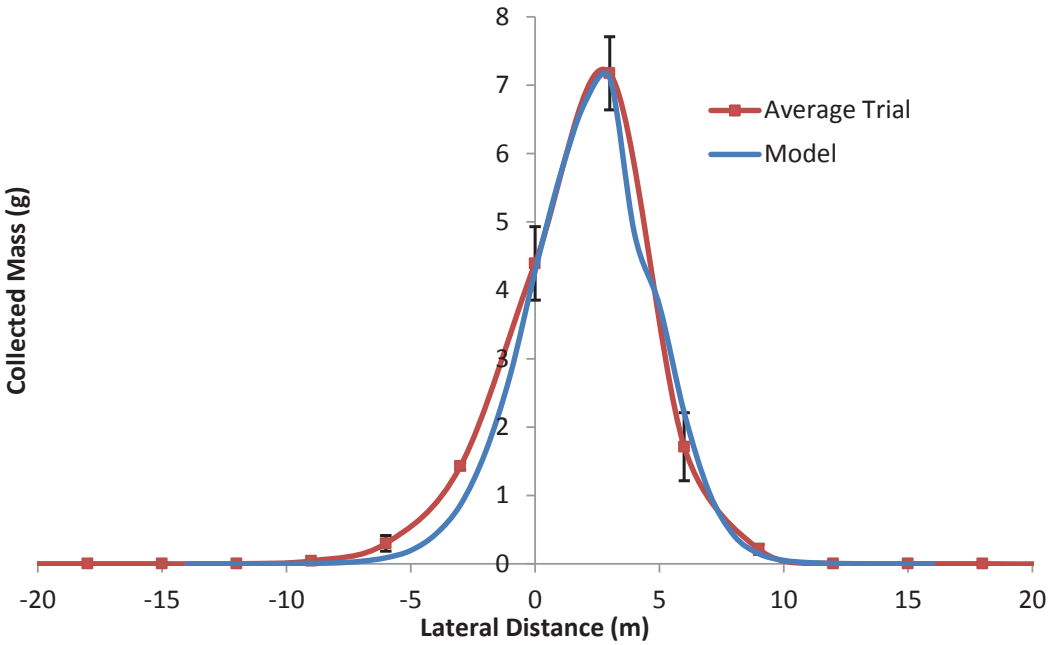


Figure 2.32: Comparison of model and Trial 3 spread pattern for Flight 1. For this spread pattern, the aircraft was travelling at a heading of 251°, aircraft velocity of 67 m s^{-1} and altitude of 18.6 m. The wind direction was 185° and wind speed was 0.4 m s^{-1}. The flow rate of the blend out of the hopper was 684 kg min^{-1}.

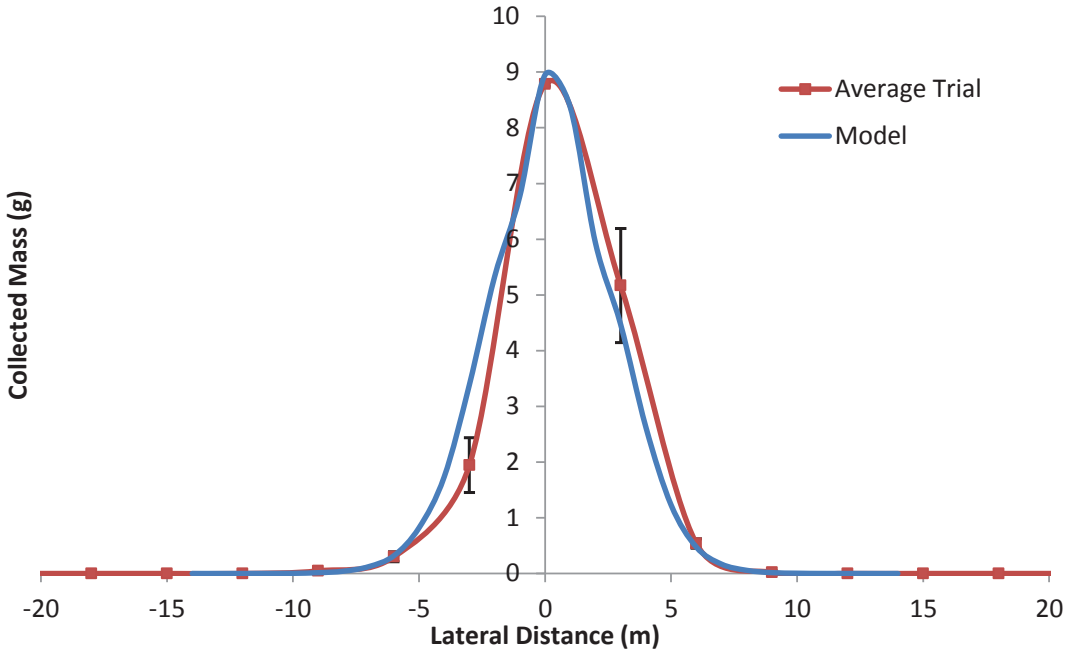


Figure 2.33: Comparison of model and Trial 3 spread pattern for Flight 2. For this spread pattern, the aircraft was travelling at a heading of 251°, aircraft velocity of 69 m s^{-1} and altitude of 11.6 m. The wind direction was 184° and wind velocity was 0.215 m s^{-1}. The flow rate of the blend out of the hopper was 822 kg min^{-1}.

2.4.4. Model Accuracy

The model will be applied commercially, therefore it is important to characterise its level of accuracy and limitations. The cumulative mass, which is the area under the curve, of the modelled and field distribution was compared in Table 2.19. In the model, the cumulative mass is dependent on the flow rate of fertiliser out of the hopper door. This is difficult to measure during the trial; therefore the Beverloo equation is used to estimate the value.

Table 2.19: Comparison of ballistics model and Beverloo flow rates for Trial 1 and 2.

Fertiliser Type	Superphosphate	DAP	Urea
Trial 1			
Beverloo Flow Rate (kg min^{-1})	954	755	421
Model Flow Rate (kg min^{-1})	1261	1300	551
Difference (%)	24.3	41.9	23.6
Trial 2			
Beverloo Flow Rate (kg min^{-1})	747	1055	789
Model Flow Rate (kg min^{-1})	982	1490	845
Difference (%)	23.9	29.2	6.6

For all validation trials, the Beverloo equation under-estimates the flow rate out of the hopper required by the model to produce the field spread pattern (Table 2.19 and Table 2.20). There is no clear relationship between the fertiliser type and percentage difference, and the sample size is too small to make any final conclusions. Therefore, a correction factor was not found.

However, the model flow rate is not a perfect indication of the actual flow rate. For example, the model flow rate for Trial 2 superphosphate (Figure 2.26) produced a transverse spread pattern that over-estimated the mass at some distances, in particular the starboard side. In this case, the model flow rate was too high, but was required to achieve the peak collected mass.

Table 2.20: Comparison of ballistics model and Beverloo flow rates for Trial 3.

	Flight 1 (kg min^{-1})	**Flight 2 (kg min^{-1})**
Beverloo's Flow Rate (kg min^{-1})	572	572
Model Flow Rate (kg min^{-1})	684	822
Difference (%)	19.6	43.7

The relationship between the application rate and Beverloo equation requires validation before it can be utilised commercially. The equation is used to determine the door opening settings for the prescription map and the resulting flow rate used in modelling. This circular reference prevents the validation of the Beverloo equation. Measuring the flow rate out of the hopper during an application would be valuable in validating the model and the Beverloo equation. This is difficult to achieve, because of significant shear forces at the hopper door, which would affect the measuring device. Another method of determining the flow rate out of the hopper is to measure it in the laboratory using a replica aircraft hopper. This is explored in Chapter 4.

Spreadmark V17 was used to calculate the application rate and swath width for both the modelled and field transverse spread pattern, so that they could be compared to the intended application rate. Spreadmark V17 calculated the field and model application rate from the set swath width. The field and model swath width was based on when the swath width exceeds a coefficient of variation (CV) of 15% or 25%, depending on the fertiliser type. Table 2.21 shows the differences between the intended and field results. On the other hand, the field and model results were similar, especially for the swath widths. Differences between the trial and model application rates were between an underestimation of 11.7% to an overestimation of 17.3%, with an average under-estimation of 3.3%.

Table 2.21: Comparison of intended, trial and model application rate and swath width for Trial 1-3. The difference (%) is between the trial and model application rate.

	Application Rate (kg ha^{-1})				Swath Width (m)		
Trial	Intended	Trial	Model	Difference (%)	Intended	Trial	Model
Super T1	270	256	226	-11.7	15	12	12
DAP T1	115	145	135	-6.9	22	25	24
Urea T1	73	75	67	-10.7	22	25	25
Super T2	250	150	176	17.3	15	12	15
DAP T2	140	172	178	3.5	22	10	12
Urea T2	90	104	100	-3.8	22	15	15
Super/Flexi-N F1	250	215	206	-4.2	8	4	4
Super/Flexi-N F2	250	207	228	-10.1	8	4	6

The two sample Kolmogorov-Smirnov (K-S) test was used to determine the accuracy of the model. It is a non-parametric test, which compares two distributions and determines whether they are similar (null hypothesis) or different (alternative hypothesis). The K-S test calculates the maximum likelihood distance between the cumulative distributions and compares it to a critical value (D_{crit}).

$$D > c(\alpha)\sqrt{\frac{n+m}{nm}} \tag{2.4}$$

Where n and m are the sample sizes of the two distributions and c(α) is the critical value at the significance level (α). If D is greater than D_{crit}, the null hypothesis that the two distributions are similar can be rejected.

A 90% confidence interval was proposed as the accuracy limit. P-values greater than 0.1 indicate there is insufficient evidence to reject the null hypothesis. The test was carried out using Matlab R2013a. Table 2.22 and Table 2.23 show the p-values, D and D_{crit} values for Trial 1 and 2. All the p-values were greater than the 0.1 significance level and D was less than D_{crit}, which indicates the null hypothesis, that the distributions are similar, cannot be rejected.

Table 2.22: P and D values from the Kolmogorov-Smirnov test for Trial 1 and 2.

Fertiliser Type	**Trial 1**			**Trial 2**		
	P-Value	**D**	**D_{crit}**	**P-Value**	**D**	**D_{crit}**
Superphosphate	0.5794	0.2834	0.4721	0.9847	0.1433	0.4013
DAP	0.4828	0.2778	0.4265	0.8527	0.1818	0.3821
Urea	0.4231	0.2877	0.4214	0.8417	0.1818	0.3769

Table 2.23: P and D values from the Kolmogorov-Smirnov test for Trial 3 for a 70% Superphosphate and 30% Flexi-N fertiliser blend.

	P-Value	D	D_{crit}
Flight 1	0.7475	0.2889	0.5606
Flight 2	0.3155	0.4444	0.6148

The advantages of the K-S test are that it can be used with small samples and is a more powerful test than the chi-square test for any sample size. However it has limitations. The distribution must be fully specified and none of its parameters can be estimated. It is only applicable to continuous distributions. It also tends to be more sensitive near the centre of the distribution than at the tails, because it uses a cumulative distribution function, and the majority of the mass is centred.

Additional modelling was completed to determine the flexibility of the model. The results from Trial 2 showed that a single flight could produce significantly different transverse spread patterns. For the DAP field results in Trial 2, each row was modelled to determine the change in wind angle, wind velocity and flow out of the hopper door required to produce the collected pattern. Figure 2.34 is an example of the modelled transverse spread pattern produced for row 6 for DAP. To produce the transverse spread patterns in Trial 2 DAP, the wind angle would need to have ranged 80.5° - 91°, wind velocity of 1.8 – 2.88 m s^{-1}, and flow of 390 – 1490 kg min^{-1} (Table 2.24). The range of wind velocities and angles required were recorded in the field on the day with the wind anemometer. The two sample Kolmogorov-Smirnov test showed there is insufficient evidence to reject the null hypothesis that the model and collected distributions differed (Table 2.24). Therefore the model is flexible, and future iterations of the model can include a wind vector component that predicts multiple or the distribution of transverse spread patterns based on a range of wind conditions.

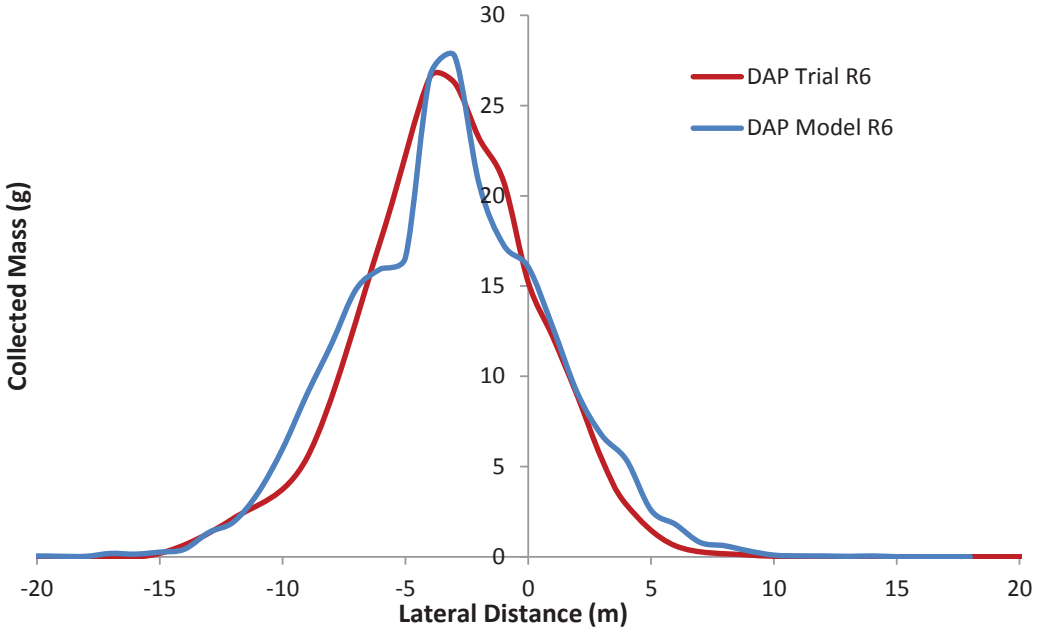


Figure 2.34: Comparison of model and Trial 2 row 6 spread pattern for DAP. For this spread pattern, the aircraft was travelling at a heading of 273°, aircraft velocity of 58 m s^{-1} and altitude of 32.5 m. The wind direction was 88.2° and wind speed was 1.8 m s^{-1}. The modelled flow rate of superphosphate out of the hopper was 1090 kg min^{-1}.

Table 2.24: The wind velocity, wind angle and flow required to produce a transverse spread pattern for DAP in Trial 2 that rejected the null hypothesis when tested with the K-S test.

Row	Wind Angle (°)	Wind Velocity (m/s)	Flow (kg/min)	P-Value	D	D_{Crit}
1	88.2	2.5	790	0.2755	0.3286	0.4251
2	87.68	2.88	1490	0.554	0.2465	0.3980
3	80.5	1.8	840	0.9155	0.1825	0.4214
4	91	1.82	390	0.5285	0.2639	0.4192
5	90	1.9	490	0.3896	0.2875	0.4092
6	88.2	1.8	1090	0.9011	0.1889	0.4265

2.5. Wind Displacement Calculator

Off-target application is both wasteful and environmentally harmful, and is a concern to both the farmer and the applicator. Although the model has many uses, Ravensdown Limited's objective is for the model to predict how average wind conditions can affect the transverse spread pattern. The wind displacement calculator will be implemented as a GIS tool to predict the shift in the transverse spread pattern due to wind conditions. Ravensdown Limited also has an interest in the swath width of the modelled transverse spread pattern, which will be included in the tool. The average wind conditions will be measured before the fertiliser application, and the modelled result will be uploaded to the aircraft in the prescription map. The following section will explain the development of the wind displacement calculator tool.

2.5.1. Python script

Ravensdown Limited utilises ArcGIS as their GIS platform. Tools can be written for ArcGIS if it is in the Python language format. PyCharm Community Edition 4.5.1 was the Integrated Development Environment (IDE) used to code the model into Python. The model is written in three Python script files and three text files. One Python script file has the ballistics model, the other has the code necessary for the model to be deployed in ArcGIS, and the last outputs the swath width for the modelled transverse spread pattern. The text files consist of fertiliser, aircraft and spreader inputs.

Swath width was calculated using the same principles as Spreadmark V17. The CV was calculated for swath widths between 4 m and 30 m. The maximum swath width is assigned by fertiliser type. If urea or DAP is modelled, the swath width returned is the maximum swath width when the CV is below 15%. For superphosphate, it is the maximum swath width below a CV of 25%. A comparison of the swath widths outputted by the Python script and Spreadmark V17 showed they were similar.

Several adjustments were made to the VB program code to improve the modelling process and result. The number of model inputs required from the user was reduced. The particle size distribution was obtained from Ravensdown's manufacturing sites. Particle density was averaged from Trial 1 and 2. An option of spreader type was included. The user only needs to input the CSV file with aircraft data and wind conditions for the application, the fertiliser type from a choice of superphosphate, DAP, urea or superphosphate/Flexi-N blend, and whether a spreader was used and how many ducts it had (9 or 11 ducts).

Python has functions that can complete actions more efficiently than VB. This meant some VB code was deleted and simplified to decrease modelling time. If a spreader is not used, the modelling time is now less than 5 min per scenario, compared with 40 – 50 min using the VB program. Once the modifications were completed, the resulting modelled transverse spread patterns were re-validated to ensure the model still performed correctly.

2.5.2. GIS Tool

ArcGIS has a python library called ArcPy which allows existing ArcGIS tools to be used in Python. In the wind displacement calculator tool, ArcPy was used to retrieve parameters from an ArcGIS dialog box (GetParameter), copy the application area (CopyFeatures_management) and shift the copied application area based on a distance in the X and Y direction (UpdateCursor). The tool inputs are average wind velocity and direction, fertiliser type, flow rate, spreader usage and if one is used, is it nine or eleven ducts, and the shape file of the

application zone. There is the option to include the aircraft's altitude or else a default of 25 m is included. Aircraft velocity can be set by the user or at 62.5 m s^{-1}, and aircraft heading had a default of 0°. A file with the aircraft co-ordinates also needs to be uploaded.

The Python script was uploaded to an ArcGIS toolbox, where the inputs are linked to a parameter input dialog box. When the tool is chosen, the user will enter the required inputs and run the model. The output from the model is the distance the transverse spread pattern's centre peak is displaced by average wind conditions, and the swath width of the modelled spread pattern. If this distance is negative, the spread pattern was displaced to the left of the flight centreline and if it is positive, the spread pattern is centred to the right of the aircraft.

Equations 2.5 and 2.6 are used to calculate the distance the application area should be shifted in the X and Y direction to counter average wind conditions. The equations use the model output value (d_y) and the aircraft heading (h).

$$X = d_y \cos(180 - h) \quad (2.5)$$

$$Y = d_y \sin(180 - h) \quad (2.6)$$

Figure 2.35 is an example of how the wind offset and subsequent X and Y co-ordinates are calculated. DAP was applied using the Transland spreader. The model output was 15 m for a wind speed of 0.75 m s^{-1} and wind direction of 300°. X and Y resulted in -14.77 m and -2.60 m, respectively.

The output is a shape file with the shifted application zone (Figure 2.36). Wind conditions can vary significantly throughout the day. Therefore multiple prescription maps should be prepared to allow the pilot to fly the offset most suitable for the conditions at the time. However, a limitation of this is the modelling time required to be able to predict all the wind conditions.

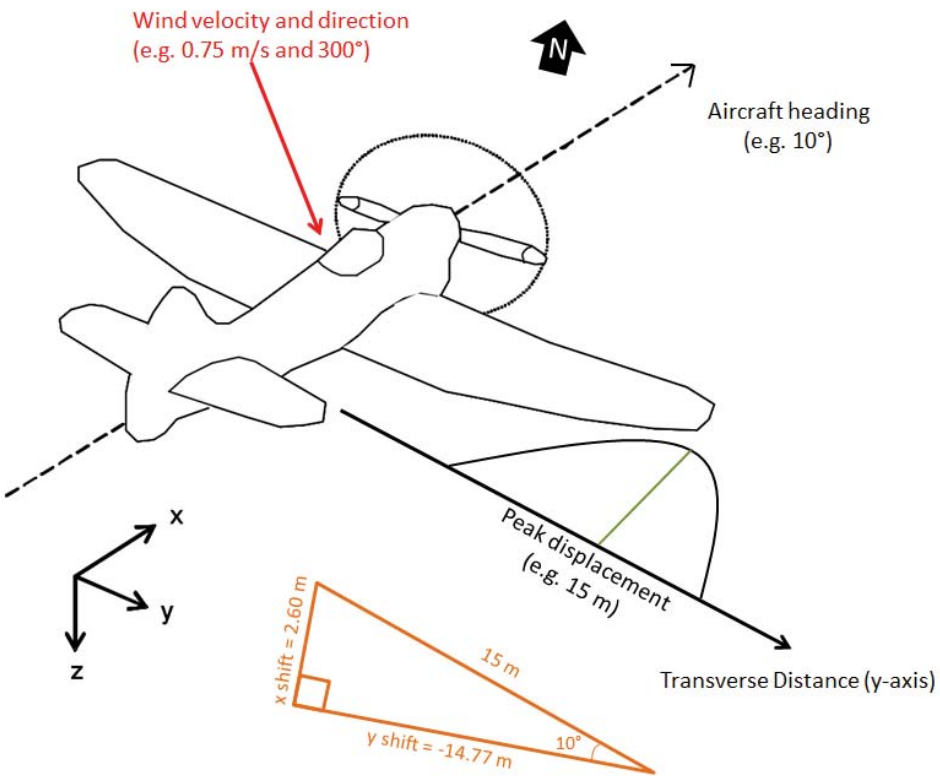


Figure 2.35: Example vector diagram of the wind offset calculated for a wind speed of 0.75 m s^{-1} at 300°.

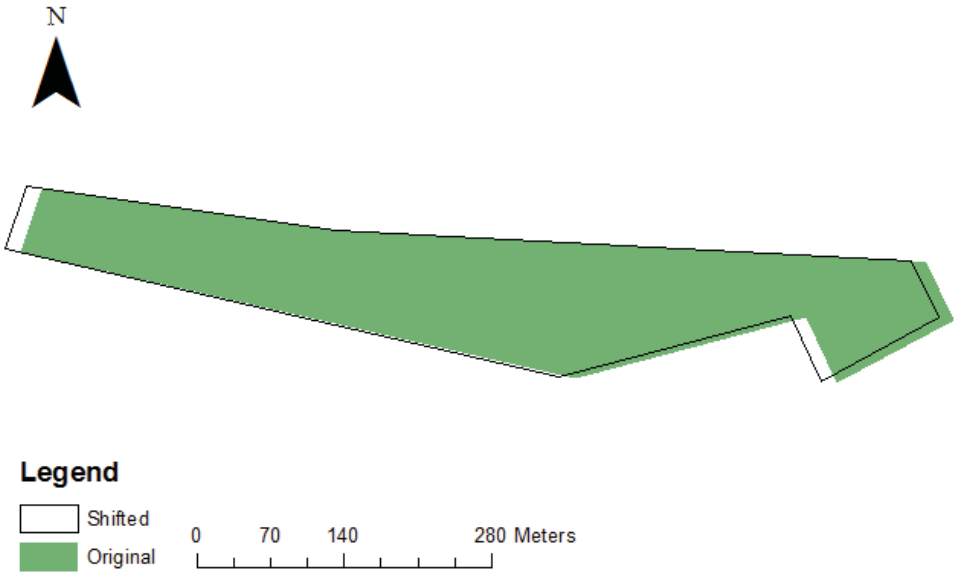


Figure 2.36: Example of application area and its offset when the average wind speed is 0.75 m s^{-1}, wind direction is 300° and aircraft heading is 10°. This was modelled for superphosphate.

2.5.3. Wind Displacement Look Up Tables

Wind displacement look up tables were completed for superphosphate, DAP and urea to reduce modelling time. Wind speed between 0 m s^{-1} and 4 m s^{-1} were tested at 0.1 m s^{-1} intervals. These wind speeds are assumed to be measured at a height of 2 m. The model uses the power law to extrapolate to the release point height. Wind direction was tested at 10° intervals. To complete the table, the model was required to run 1440 times per fertiliser type, which would take 120 hours at 5 min per run without a spreader. With a spreader, a run takes 40 – 50 min. The Python code was modified so that the 1440 runs would run automatically, and multiple computers were used to reduce the number of runs each computer had to complete. To be able to achieve this, all inputs were standardised except for wind velocity and direction. The wind displacement look up table consists of the peak offset value for a wind velocity and direction, and the swath width of that transverse spread pattern.

Including a spreader was found to not have an effect on the location of the maximum peak so initial runs were carried out without a spreader. The application rate was set at 400 kg ha^{-1} with a set swath width of 14 m, which gave a hopper flow rate of 2200 kg min^{-1}. The aircraft velocity was set at 62.5 m s^{-1}, the aircraft heading was 0°, and the altitude was 35 m. A check of the input variables showed that standardising flow rate and aircraft velocity has an insignificant effect on the placement of the peak mass. The typical standard deviation of the peak mass displacement was in the range of 0.66 – 1.08 m. However, altitude has a significant effect because it will dictate the particle fall time. The longer a particle's fall time, the further it will be displaced; therefore, if the altitude is known prior to an application it should be modelled. The input file for this Python program consisted of a list of wind speed and direction combinations. The output file contained the offset value and swath width for each wind combination modelled.

Another set of look up tables were completed for DAP and urea with a 9 duct spreader and an 11 duct spreader. This was required because the swath widths produced from spreaders are wider and would differ to spread patterns without spreaders. The level of error observed in these tables is higher because of the presence of the spreaders, which are not perfectly characterised. There are still uncertainties around the particle velocity through the spreaders, the angle range of each duct, and the flow rate through each duct. In some cases, the shape of the transverse spread pattern is M shaped rather than normally distributed, which results in two peaks, but only the maximum peak is returned. This means some peak values are offset when there is no offset in the spread pattern (i.e. wind direction 180°). Since this error occurred in wind conditions that have not been measured in the field, it is not possible to

discount the M shaped distribution. Therefore extra care should be taken when using the wind displacement look up tables for spreaders.

The wind displacement look up tables with no spreader show that the maximum peak mass displacement occurs when there is a high crosswind (wind angle 90° or 270°). The peak mass displacement is 70 – 80 m (Figure 2.37), which occurs because the ballistics model predicts particles can take 4 – 10 s to fall 35 m. Smaller particles have longer fall times and are more affected by the wind velocity (Gillingham et al., 1985). At a height of 35 m, wind velocity was predicted to be greater than 4 m s^{-1}, due to the power law wind equation, so a peak displacement of 80 m is possible. Swath width also increases with wind velocity and direction (Figure 2.38). The swath width cannot exceed 30 m because the wind displacement calculator was developed to only calculate the CV up to this swath. These trends are expected and have been demonstrated in previous studies (Macfarlane et al., 1987; NZFQC, 2016b). The modelled transverse spread patterns show that wind spreads the distribution wider and reduces the peak mass. This results in a reduced application rate; therefore, the pilot will need to adjust the hopper door opening and set swath width to ensure the intended application rate is still achieved.

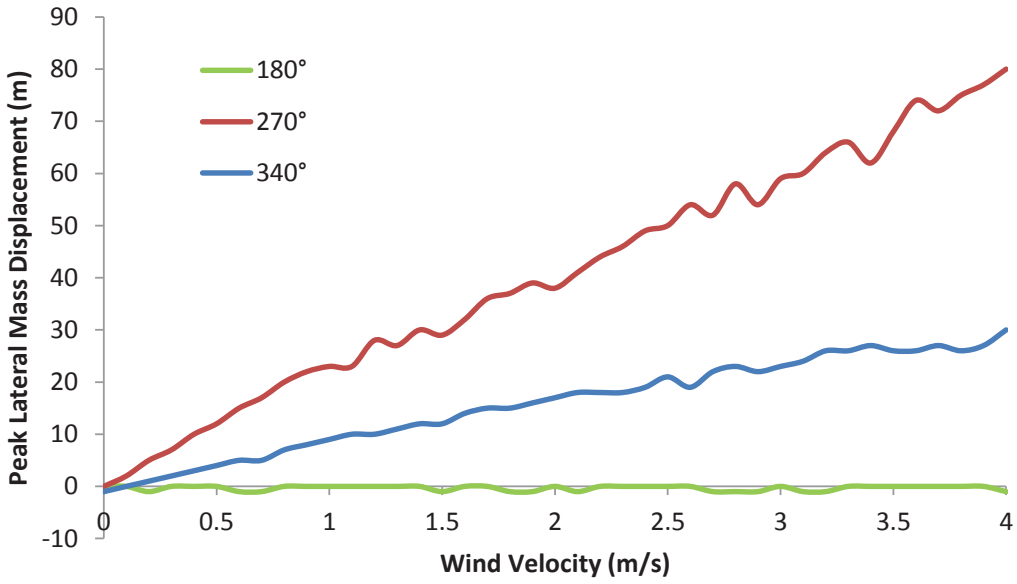


Figure 2.37: Peak lateral mass displacement for wind direction of 180°, 270° and 340°, and wind velocity for superphosphate with no spreader.

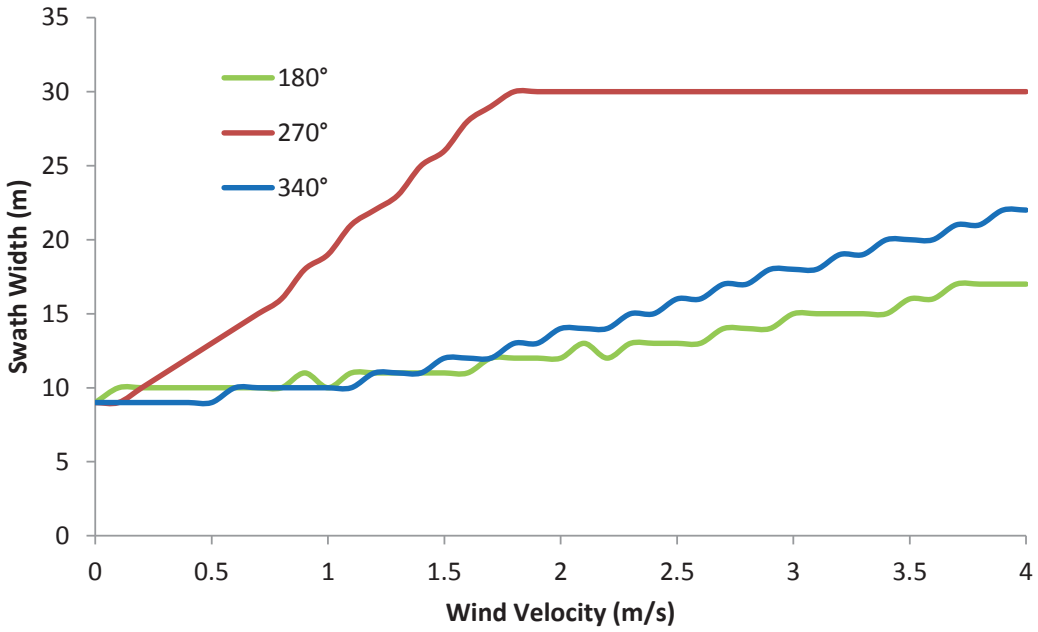


Figure 2.38: Swath width for wind direction of 180°, 270° and 340°, and wind velocity for superphosphate with no spreader.

With the spreader, the trends are similar. M shaped distributions are observed for wind velocities above 3 m s^{-1} and 180° wind angle. These spread patterns are still centred at 0 m, but the two peaks (in this case -5 m and 9 m) produce an offset (Figure 2.39). This occurs because the model predicts that the initial motion of a small particle will be angular due to the spreader. However, as it reaches its terminal velocity, wind will have greater effect causing the M shaped distribution. Another difference is the narrowing of the swath width for wind angles ± 20° from centre (i.e. 0° and 180°) (Figure 2.40). This occurs for all fertiliser types when applied with a spreader. The modelled distributions from these angles were not normally distributed, which reduced the maximum swath width. The distributions may be a model error or a true representation of the distribution. Field trials with a spreader at these wind velocities and angles are required to form a conclusion.

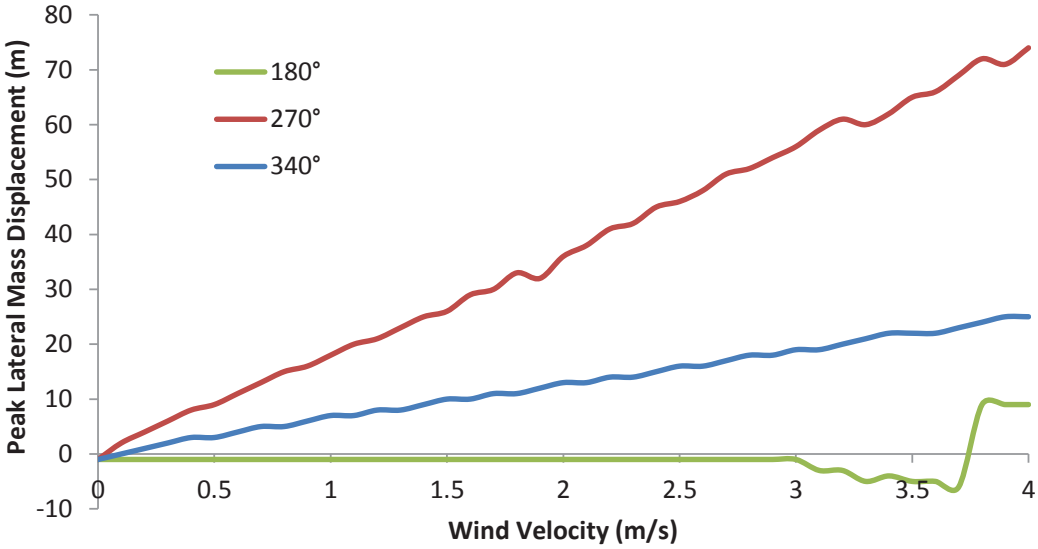


Figure 2.39: Peak lateral mass displacement for wind direction of 180°, 270° and 340°, and wind velocity for urea with an 11 duct spreader.

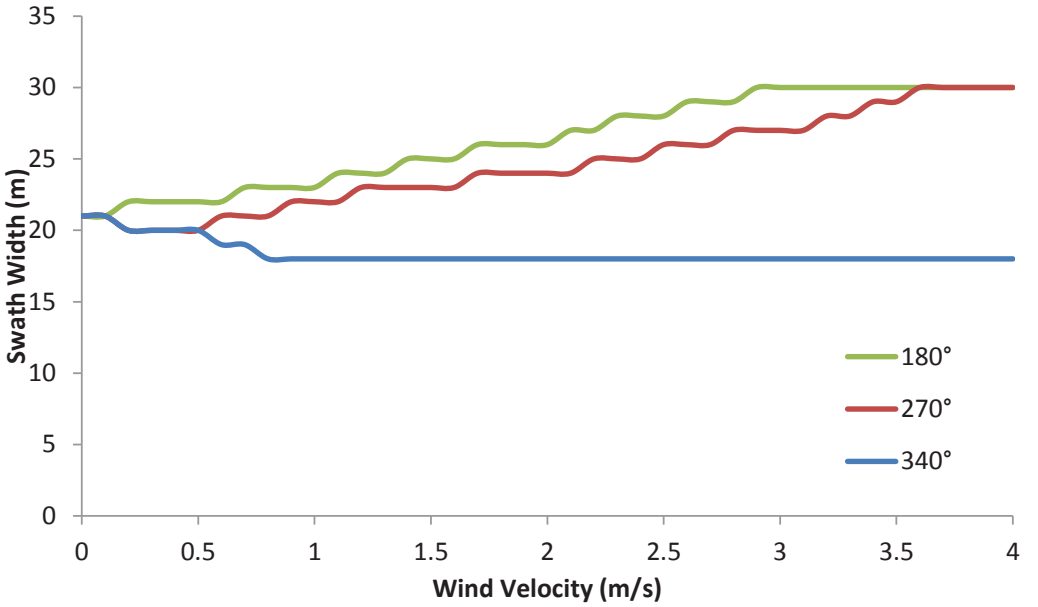


Figure 2.40: Swath width for wind direction of 180°, 270° and 340°, and wind velocity for urea with an 11 duct spreader.

If the aircraft heading is not 0°, wind direction and speed need to be adjusted so that it is in relation to the aircraft's heading rather than true north. The corrected wind direction is calculated by subtracting the wind direction from the aircraft heading. Equation 2.7 shows how the corrected cross wind velocity (w_c) is calculated. The absolute value of w_c is taken.

$$w_c = \frac{\cos H}{w} \tag{2.7}$$

Where H is the aircraft heading and w is the wind velocity (m s^{-1}) in relation to north.

The look up tables only indicate the wind offset. Equations 2.5 and 2.6 are used to calculate the distance the application area should be shifted in the X and Y co-ordinate. These were included in the look up tables for ease of use. For the example shown in Figure 2.35, the look up table outputted 15 m with an X and Y offset of -14.77 m and 2.60 m, respectively. This is the same result as the wind displacement tool. The wind displacement look up tables can be found in the Appendix.

2.6. Conclusion

The single particle ballistics model by Jones et al. (2008) was validated for the coarse fraction (> 0.5 mm) of single superphosphate, urea, DAP and a 70% superphosphate/30% Flexi-N blend for a PAC 600 aircraft. Validation was completed by comparing field and model application rates and swath widths, using the K-S test. The field and model application rates and swath widths were found to be similar. The two sample K-S test calculated p-values that were statistically insignificant for a 90% confidence interval. Therefore, there is insufficient evidence to indicate that the field and model distributions are different. The accuracy of the Beverloo equation and the flow rate out of the hopper door continues to be an issue, which is further discussed in Chapter 4.

To achieve model validation, the propeller wash component was removed as it skewed the transverse spread pattern to the left of the aircraft. It was hypothesised that fertiliser particles exited the hopper in a mass flow rather than as single particles. Therefore, propeller wash would have less influence on the particles because they would be shielded. Removing the propeller wash component succeeded in improving the overlap between the model and field transverse spread patterns. There is still some variability and differences between the two distributions, but that is expected since aerial topdressing is complex and occurs in highly variable conditions. The model and validation trials indicate that wind was the most significant factor in determining the landing position of a fertiliser particle.

The validated model can be used to determine the forward motion of particles (longitudinal distribution), the effect of new spreader designs, and offer explanations for variability in the transverse spread pattern. However, Ravensdown Limited would initially like to deploy the model as a GIS tool to predict the offset required to counter the effect of wind conditions in the field. This is to ensure that the majority of fertiliser will land within an application zone. A wind displacement tool was created with Python and ArcGIS to achieve this. To further simplify the tool and reduce modelling time, wind displacement look up tables were created for superphosphate, urea and DAP. All inputs were standardised, except for wind velocity and

direction. Sensitivity analysis showed that the standard deviation in the distance the peak mass shifts were low when standardising aircraft velocity and flow rate (0.66 – 1.08 m). However, altitude significantly affected the peak mass offset. Errors were higher for the 9 and 11 duct spreader look up tables. These results may be sufficient for estimating the effect of average wind conditions, but the user should be aware that the model's performance will improve if representative inputs are used.

It should be noted that the model does not guarantee that off-target application will not occur. Instead it adjusts an application area to reduce the risk of fertiliser being applied into sensitive areas. Additionally, the application rate will reduce with increasing wind conditions, due to a reduced peak mass. Therefore, the pilot needs to compensate for the decreased application rate by widening the hopper door opening and selecting a suitable swath width. Lastly, the granular ballistics model does not consider the fines fraction (< 0.5 mm), which is an issue since fines travel further in wind than larger particles. This requires further investigation. Compensating for wind conditions in aerial topdressing has not been previously completed, and the work completed in this study is seen as a valuable step in improving granular fertiliser application in hill country.

Chapter 3 - Methods and Evaluation of Sampling for Aerial Topdressing Performance Trials

3.1. Introduction

Ravensdown Limited is investing in variable rate application technology (VRAT) for aerial topdressing. The system's performance is assessed against the required standards set by Spreadmark (NZFQC, 2016). There are four main requirements that the VRAT system will be evaluated for. The first is its ability to recognise application zone boundaries, which aims to reduce off-target application, especially into sensitive areas. The second is the ability of the VRAT system to deliver the target application rate. As defined by Spreadmark (NZFQC, 2016), the field application rate should be within 30% of the target rate. Thirdly is precision, which is the ability of the system to spread fertiliser evenly across an area. In this study, the coefficient of variation (CV) is used to quantify precision. It is the standard deviation of the application over the average field application rate. The last requirement is the capability of the VRAT system to apply at two different application rates. This is assessed by statistically comparing the application rates and variances between two application zones, using a one way Analysis of Variance (ANOVA) test.

Ground truth trials were used to collect field data to assess the VRAT system. These trials are direct observations of the field application rate, which makes it more accurate than modelling because the information is not inferred and there are fewer assumptions. Therefore, they are a more realistic indicator of the VRAT system's performance. The majority of aerial topdressing trials were completed over 30 years ago (Macfarlane et al., 1987; Scott and Grig, 1970). Recent trials were completed by Murray (2007), Grafton et al. (2012) and Morton et al. (2016). Each study carried out different sampling configurations and collected different results (i.e. transverse spread pattern, swath width and application rate). In general, ground truth trials are not completed frequently because they are time and resource intensive; therefore expensive to complete. Performance trials, such as Trial 8, cost approximately $18,500 for labour, equipment transportation and vehicle hire. This does not include the cost of the aircraft and fertiliser, which was supplied by Ravensdown Limited.

The validation trials discussed in Chapter 2 are a form of ground truth trials. It is similar to the sampling configuration used by Spreadmark to assess the accuracy and precision of an aerial topdressing aircraft. However, Spreadmark assumes that the swath width and transverse spread pattern of subsequent flights are similar, which is not be the case, because environmental conditions and aircraft operation significantly affect field results. Another

disadvantage of this sampling configuration is that it does not determine the capability of an aerial topdressing system, because the collectors do not cover a large area. Since aerial application can occur over hundreds of hectares, the placement of collectors in an area less than one hectare does not provide a representative sample of the application. The solution may be to place collectors over a large area, but this is dependent on the number of available collectors, costs, and the level of accuracy required. The sampling configuration is important and needs to be carefully considered. A representative sample of the application is required to ensure that the correct conclusions are made. Various sampling configurations were undertaken to evaluate the VRAT system, which will be discussed in this chapter.

Accurate data collection is pivotal to any sampling trial, and the type of collector used in the trials must be capable of collecting a complete sample. Studies have been published on the development of collectors, but few focus on their collection efficiency (Lockett, 1998; Scott and Grig, 1970). Most studies assume the collectors are able to catch all the material. However this may not be the case. This chapter investigates the New Zealand Centre of Precision Agriculture (NZCPA) collectors to determine their efficiency. This is important because the true accuracy, precision and capability of the VRAT system cannot be assessed without knowing the margin of error in the ground collection method. If it is a significant measurement error and is not corrected, it will decrease the value of the results. Therefore, this chapter discusses collectors used in the trials, methods of evaluating their efficiency, and the results of the evaluation.

The objective of this chapter is to explain the collection methods used to evaluate the performance of the VRAT system, and discuss their advantages and disadvantages. Collection methods include both the sampling configuration and the collector's efficiency. These have a significant effect on the efficacy of the results and have not been well studied in the past. Factors that increase the variation in aerial topdressing results, such as aircraft velocity, hopper door opening and swath width, will also be investigated. The trials are presented in chronological order to show the progression of ideas.

3.2. Trial 4 – Grid Sampling

A performance trial was carried out at Limestone Downs, Port Waikato, New Zealand in February 2014. Limestone Downs is a 3,200 hectare coastal sheep, beef and dairy farm with large variations in topography. The trial plan was determined before the PhD started; therefore this researcher did not have input in to the plan but was present during the trial. The

trial set up was completed over 3 days by 3 – 4 people and on the trial day, approximately 30 people took part in data collection and packing up.

The planned sampling configuration for this trial was an 11 by 11 grid of NZCPA collectors placed 70 m apart. Five of the collectors in the grid had four additional collectors placed 5 m from them, which were meant to determine spatial variance. In total 141 collectors were expected to be utilised. However, the grid size was reduced due to cattle in a paddock during the set up phase. The cattle tipped over the collectors they had access to. These collectors were disregarded and the sample points were shifted to new locations within the grid. Other collectors were shifted because their position was on a steep slope, which could not be reached safely. Figure 3.1 shows the collectors arranged in an incomplete grid configuration. An additional two groups of five collectors were placed randomly in the grid along with three additional collectors. The total trial area was 61 ha. Collector locations were found using a handheld Trimble Juno 5 Series, which is accurate to approximately 5 m so there are differences between the position of points presented in Figure 3.1 and in the field.

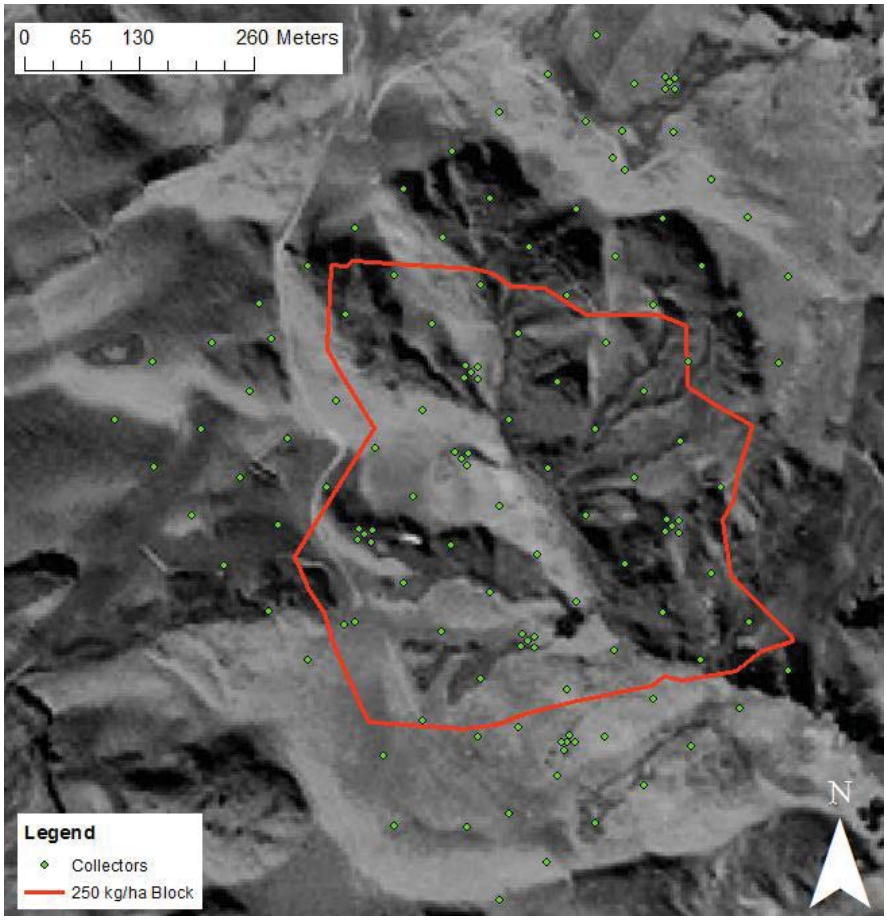


Figure 3.1: Sampling configuration for Trial 4.

Wind conditions were not measured on the day; however there was a noticeable westerly wind that intensified through the day. Single superphosphate was applied at 250 kg ha^{-1} inside the outlined block and 500 kg ha^{-1} outside of it (Figure 3.1). This trial was completed within a larger aerial topdressing job, which covered half of the farm area. Variable rate application only occurred within this area. In the remaining farm area, 500 kg ha^{-1} of superphosphate was applied.

The aircraft used in the trial was a Pacific Aerospace Cresco (PAC) 600 operated by Pilot A (see Chapter 2). The variable rate application system was a Satloc Intelligate G4 system. An automated hydraulic hopper door controlled by the G4 was installed in the aircraft. The pilot took approximately 4 hours to complete application of this area as the grid was not overflown separately. Instead it was part of the topdressing job, as if no sampling was being undertaken. The area was flown in a racecourse configuration, where the aircraft travels the area in large loops that are shifted across a swath width for the following flight track. A log file was downloaded from the VRAT system at the end of the job for analysis.

During collection, some sample bags were found wet and others had holes in them. Sample bags were set out the previous day, because it was the only option with four people available to set up. Water in the sample bags was due to overnight condensation, a light drizzle and morning dew over some of the area. The holes were most likely created by wild turkeys feeding on black crickets in the area. In total, 26 collectors were affected, five of which were unrecoverable. The wet samples were oven dried overnight at 80 °C. Some losses from the oven drying were expected because of left-over residue and evaporation. It may have been more beneficial to dry all the fertiliser samples so the moisture contents were similar and the samples could be compared.

Grid sampling is a common statistical sampling method that is simple to design. The most important consideration of grid sampling is the sampling density, which depends on the size of the sampling area and the response being sampled. In Trial 4, a low sampling density was used to maximise the area under study, so that a large representation of the system's performance could be assessed. Grid sampling can also assess the capability of the VRAT system using simple statistical analysis.

There are several disadvantages to grid sampling. One issue is that grid sampling does not indicate the spatial variance of aerial topdressing. Understanding spatial variation is important when trying to determine precision and carrying out geo-statistical analysis. The original purpose of this trial did not involve geo-statistical analysis, but when it was included the data

could not be adapted for kriging. Geo-statistical analysis is useful for making continuous predictions over large areas, but the grid sampling configuration lacked variance information between 5 m and 70 m. This is a significant section of the semi-variogram. The field swath width was also not measured using this sampling method, which could have explained variation in precision and accuracy. Another issue is that the pilot may have inadvertently used the collectors for guidance by aligning to the grid lines, which meant that it was no longer a random trial.

3.3. Trial 5 – Nested Grid Sampling

A nested grid sampling configuration was undertaken at Longview, Waitotara, New Zealand in April 2015. This sampling technique combines two sampling configurations; a grid is used as a frame for nested sampling. Nested sampling was undertaken by Oliver and Webster (1986) as a method to collect data, so that the Kriged layer could describe and analyse variation in the system, which in their case was the top soil layer. Longview is a 3,049 hectare coastal sheep, beef and dairy farm that is predominantly flat, with grassed sand dunes, as the main topographical variation. Collectors were placed at varying distances from each other to determine the spatial variation in aerial topdressing:

- Between two application zones. This was desired because it tested the capability of the VRAT system to vary the application rate between two application zones.
- Between two flight paths/swath width. Ballard and Will (1971) found a non-GPS aircraft was more likely to double apply or miss areas when pilots relied on physical landmarks to reference their flight path. In contrast, VRAT records and displays the aircraft's position and accounts for the swath width, which simplifies the pilot's job.
- Within a swath width. This is the variability within a transverse spread pattern. Variability at this level is attributed to fertiliser properties, changes in wind conditions and aircraft operation (e.g. aircraft speed, altitude, pitch).

One hundred and sixty-five collectors were placed over a 30 ha site. Collectors were placed 5, 25, 50 and 150 m from each other in a branching configuration. The configuration was achieved by laying out a 3 x 3 collector grid over the trial site, with each collector 150 m apart. From each of these, two collectors were placed 50 m away and so on. The direction of the collector's placement was determined using a random number generator. A Leica RTK-GPS, which is accurate to a centimeter, was used to mark out the configuration. Four people set up the trial area over two days; conducting the trial and packing up was completed in one day by six people.

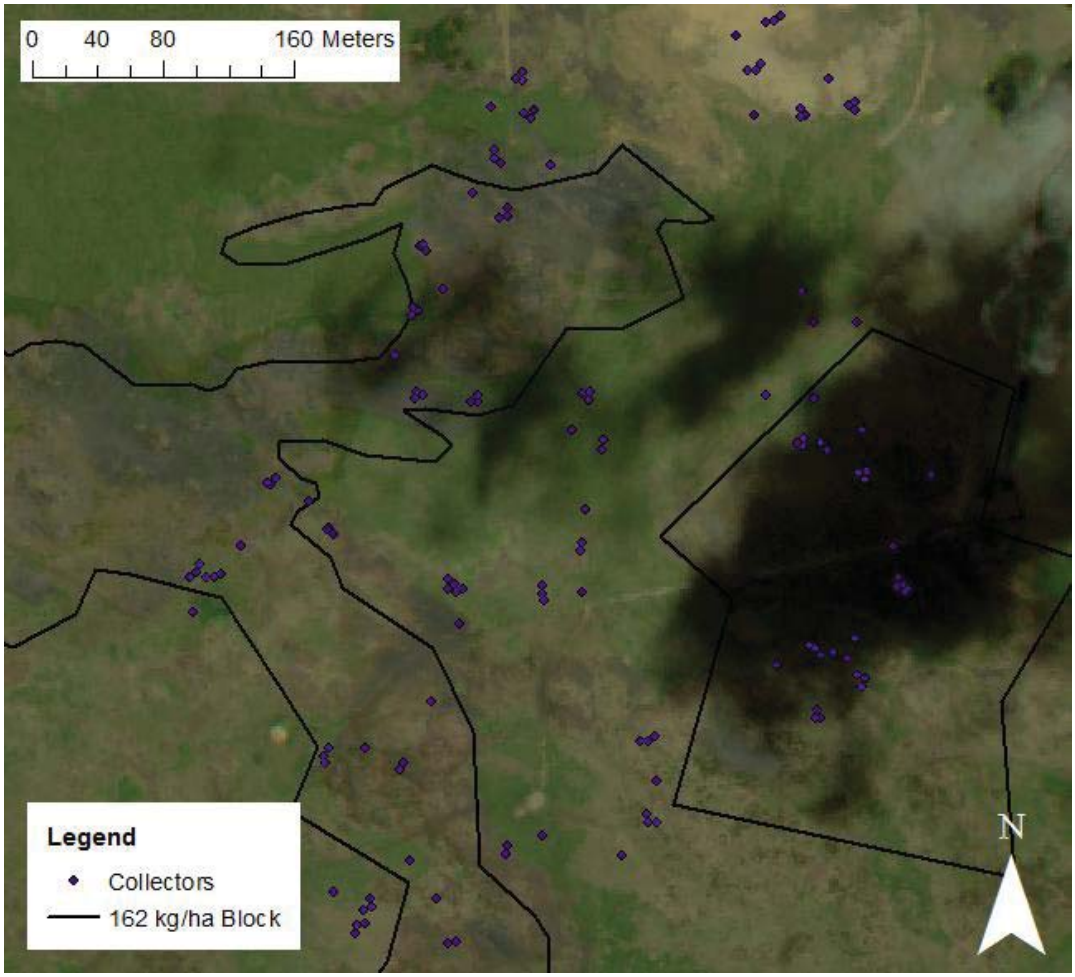


Figure 3.2: Sampling configuration for Trial 5.

A fertiliser blend, consisting of 59% superphosphate, 17% Flexi-N, 13% Maxi Sulphur Super (single superphosphate with additional sulphur injected in the granule), 11% potassium chloride, and other trace elements, was applied. This blend was formulated specifically for Longview and its ballistic properties were not previously tested. The target rate was 284 kg ha^{-1} outside the blocks and 162 kg ha^{-1} within the blocks, which predominantly consisted of sand dunes (Figure 3.2). A lower application rate was used on the sand dunes because they are less productive and over fertilisation is not cost effective. Pilot A completed the flight in approximately 2 hours. Wind speed and direction was measured every 30 s using an anemometer. Wind speed averaged 0.9 m s^{-1} with a range of 0.17 m s^{-1} to 1.97 m s^{-1} (Figure 3.3). The average wind direction was 38° with a range of 342.16° - 96.86°. Twenty three collectors had to be excluded because there was precipitation on the collector. These were not fully dried before the sample bag was attached. They could not be recovered through oven drying because the fertiliser mix is reactive when exposed to moisture.

An advantage of this sampling configuration is that the apparently random placement of collectors prevents the pilot from aligning directly above collectors and therefore biasing the results. The spatial variance of aerial topdressing is captured in this configuration, since samples were collected at a variety of distances. The disadvantages of the configuration are that it requires a slightly more complex statistical analysis method than grid sampling. This is because distance between collectors is now a factor of variability. Also the swath width was not collected with this sampling method, which again made it difficult to determine the cause of the variability in the results.

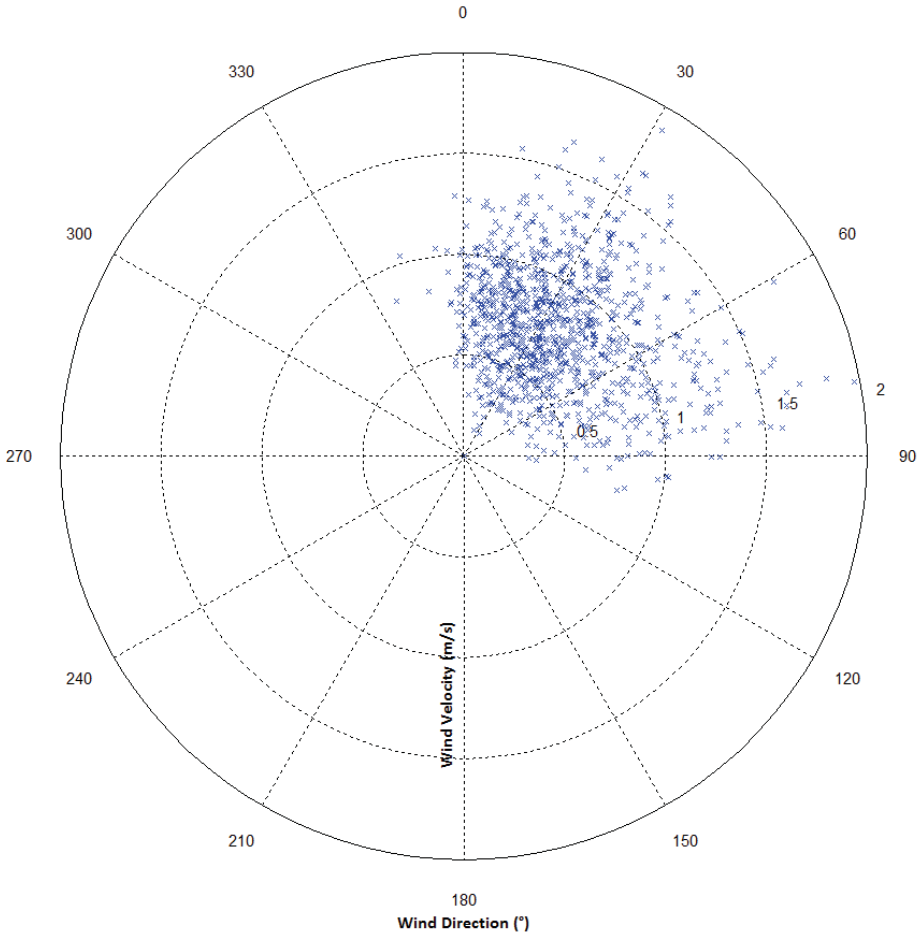


Figure 3.3: Wind velocity and direction over the trial period in Trial 5. True north is denoted by 0 degrees.

3.4. Trial 6 – Pickwick Trial

Trial 6 was carried out at Pickwick Farm, a dairy/sheep and beef farm located at the edge of Whanganui, a coastal town in the southwest of New Zealand's North Island. It was carried out in November 2015. This trial was added to the original sampling plan and had multiple objectives. The objectives were to:

1. Quantify the relationship between intended application rates, aircraft speed and swath width, and the field application rate found in the collectors. The trial is applicable to aerial topdressing in general and is not focused on the VRAT system. This objective was included because of the significant variability observed in the field application rates of previous trials, which is unexplained.
2. Determine if the Beverloo equation is an appropriate method for setting the hopper door opening. The Beverloo equation is used to determine the flow rate out of the hopper for prescription maps and in ballistics modelling. However, it was originally developed for static hoppers. Further work was required to determine how well the equation predicts the flow rate from an operating aircraft.
3. Determine the optimum setting for 'edge on'/'edge off' timings. The VRAT system automates the opening and closing of the hopper door as the aircraft enters and leaves an application zone. To prevent application over boundaries, the forward motion of fertiliser particles from its release point was measured in this trial.
4. Determine the collection efficiency of the NZCPA collectors. The collectors are integral in this study since all field data has been collected with them. It is therefore important to determine if any fertiliser particles bounce out, and correct previous results.

To fulfill the objectives, multiple sample sites and sampling configurations were set up, which will be discussed in each section. It took one day to set up and one day to carry out the trial with a team of 10 people. Pilot B completed the trial. An anemometer was used to measure wind conditions on the day every 30 seconds. Wind speed and direction varied significantly (Figure 3.4). Wind speed ranged between 0.08 – 2.37 m s^{-1} with an average of 1.25 m s^{-1}. Wind direction was 47.03° - 274.08° with an average of 168.64°. The anemometer ran out of battery and did not record data for the last three flights of the day.

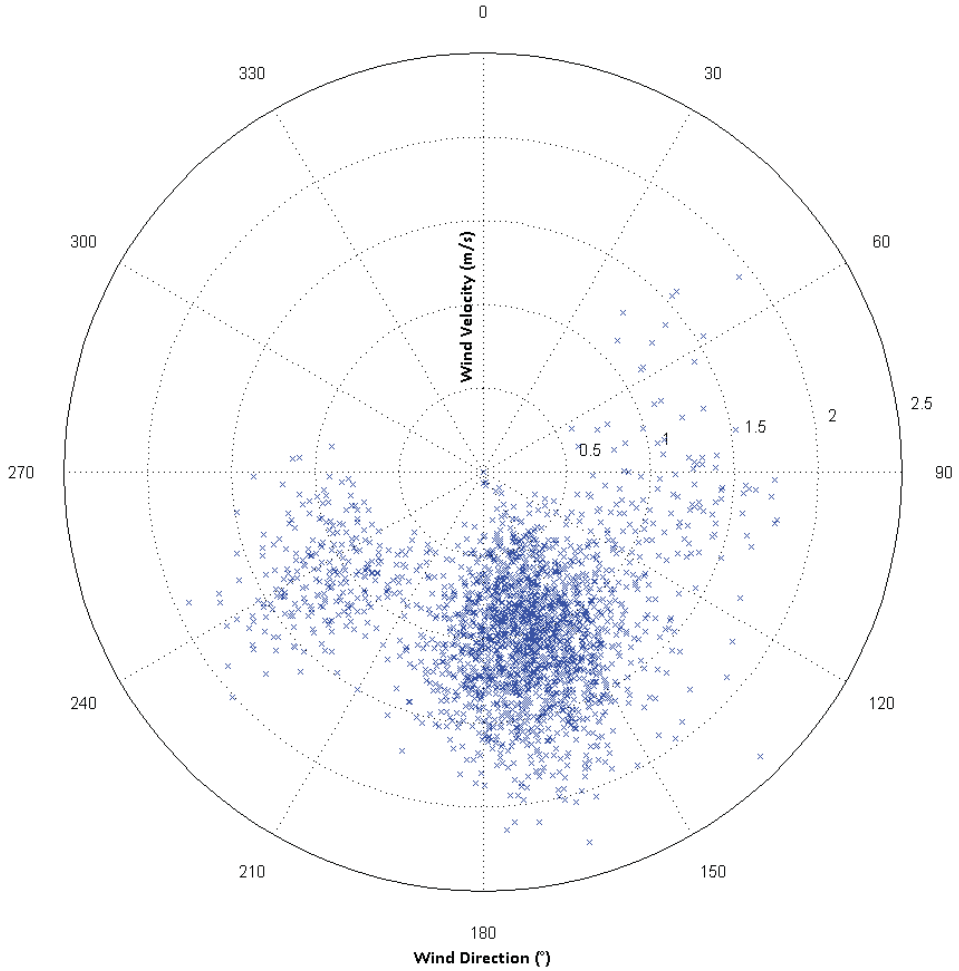


Figure 3.4: Wind velocity and direction over the trial period in Trial 6. True north is denoted by 0 degrees.

3.4.1. Objective 1

A three factor two level factorial design trial was carried out for superphosphate, urea and di-ammonium phosphate (DAP). The three factors tested were swath width, intended application rate and aircraft ground speed, and the response (what is measured) was the field application rate (Table 3.1). The swath width and intended application rate are set by the hopper door opening. Each factor has two levels; a high and low level. A factorial design involves varying one factor and keeping the other two constant so for a full data set, eight tests were required. Two of the tests were replicated twice, which meant that 12 tests were completed for each fertiliser type and 36 tests were done in total. Replication was important to determine the level of variance in the data set. A factorial test was thought to be the best method of investigating the variability in aerial topdressing, because multiple variables and their interactions can be analysed.

Table 3.1: Level settings for swath width, intended application rate and aircraft groundspeed for Trial 6.

Fertiliser	Level	Swath (m)	Application Rate (kg ha^{-1})	Aircraft Groundspeed (m s^{-1})
Super	High	16	300	69
	Low	12	240	62.5
DAP	High	22	160	67
	Low	18	120	60
Urea	High	24	110	69
	Low	20	70	62.5

To reduce trial time, three areas were set up with collectors (Figure 3.5). Each area had three rows of nine collectors placed 6 m apart with each row placed 10 m apart (Figure 3.6). For a complete factorial design, each fertiliser type consisted of four flights with 12 flights in total. Each flight completed three tests. The runs were ordered randomly using a random number generator, for each fertiliser type, to isolate the factor of interest. To help guide the flight path of the aircraft, two collectors were aligned with the centreline collector, perpendicular to the three rows. Sample bags were not attached to these collectors. A 9 duct Farm Air spreader was used to apply DAP and urea. Raw data from all three areas for the fertilisers' tested can be found in the Appendix.



Figure 3.5: Sample areas for Trial 6.



Figure 3.6: Trial set up in Area 3 in Trial 6.

The transverse spread patterns collected were analysed in Spreadmark V17 to determine the field application rate. An unforeseen problem was that Spreadmark V17 dictates that the minimum distance between each collector had to be 3 m. The trial collectors were 6 m apart, so the missing collectors had to be interpolated. This is a source of measurement error since the peak mass/application rate may not have been collected. Another measurement error was that fertiliser bounced out of the collectors, which will be discussed in Objective 4. The following data has been corrected with collector bounce coefficients found in 3.4.4. Objective 4.

N-Way ANOVA tests were completed on the field application rates, using Matlab R2013a. Table 3.2 shows the p-values (Prob > F) of the ANOVA and interaction test for application rate, swath width and aircraft velocity for urea yielded no statistical significance. Superphosphate and DAP had similar results. The lack of relationship between the three factors and the field application rate is counter-intuitive; an increase in the intended application rate causes a widening of the hopper door, which should result in an increase in the field application rate. The false negative was caused by high variance in the field application rates, due to variable conditions on the trial day. Factorial trials require all factors, except the factor being tested, to remain constant. However, the variability in the aircraft velocity, hopper door opening and wind conditions resulted in poor results from the ANOVA test and the factorial trial.

Table 3.2: ANOVA and interaction test results for urea in Trial 6.

Source	Sum of Square	Degrees of Freedom	Mean Square	F	Prob > F
rate	8791.2	1	8791.2	3.25	0.132
speed	6200.1	1	6200.1	2.29	0.191
swath	4264.2	1	4264.2	1.57	0.265
rate*speed	3713.1	1	3713.1	1.37	0.294
rate*swath	3808.1	1	3808.1	1.41	0.289
speed*swath	96.3	1	96.3	0.04	0.858
Error	13539.7	5	2708.0		
Total	62785.7	11			

The data set's high variance makes it difficult to determine the significance of individual factors and interactions. The variability in the results is a reflection of the complexity of aerial topdressing. Variability will occur in aerial spreading, to varying degrees, because it is dependent on and sensitive to multiple previously mentioned factors. The hopper door opened to the intended setting 11 out of 12 times so the VRAT system does work, but the field application rate varied significantly as expressed through individual collector measurements. Therefore, factorial trials are not appropriate for aerial topdressing because there are too many factors to control. It is difficult to isolate the factor of interest and analyse its effect. There was also significant uncertainty around the Beverloo equation and collector efficiency. If there was no relationship between Beverloo equation and the flow rate out of the hopper door, or the variance in the collector efficiency was significant, the results of the factorial trial would be unusable. It would have been beneficial to determine objective (2) and (4) before completing the factorial trial.

3.4.1.1. Application rate

When creating prescription maps for Trial 6, the Beverloo equation was used to estimate the hopper door opening required to achieve the intended application rate. Aircraft velocity and swath width was also used. It was expected that as the hopper door openings widened, the application rate will increase. Linear regression shows a positive relationship between hopper door position and the field application rate for all three fertiliser types (Figure 3.7 - Figure 3.9). There was significant variance in superphosphate's field application rate, which resulted in a weak linear relationship. An explanation is that superphosphate had large door openings, compared to DAP and urea, and a spreader was not attached; therefore it had a narrower swath width and was more sensitive to changes in wind and flight operation. The first DAP flight over Area 3 yielded an outlier, which was removed. This improved DAP's R-Squared from 0.35 to 0.72.

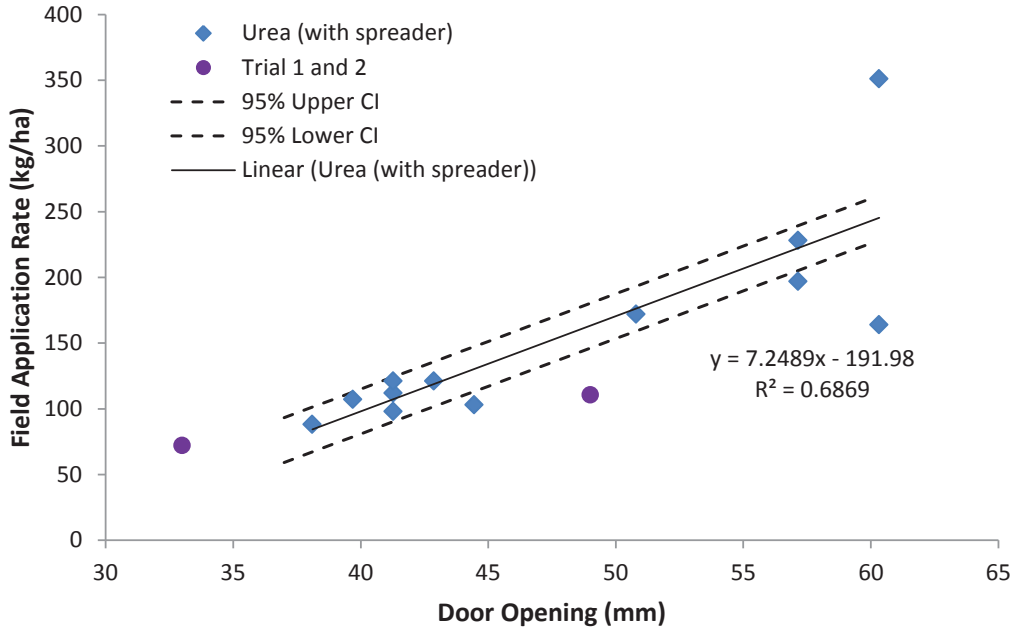


Figure 3.7: The relationship between the measured field application rate and hopper door opening for urea in Trial 6. The dashed lines are the confidence interval (CI) of the linear equation.

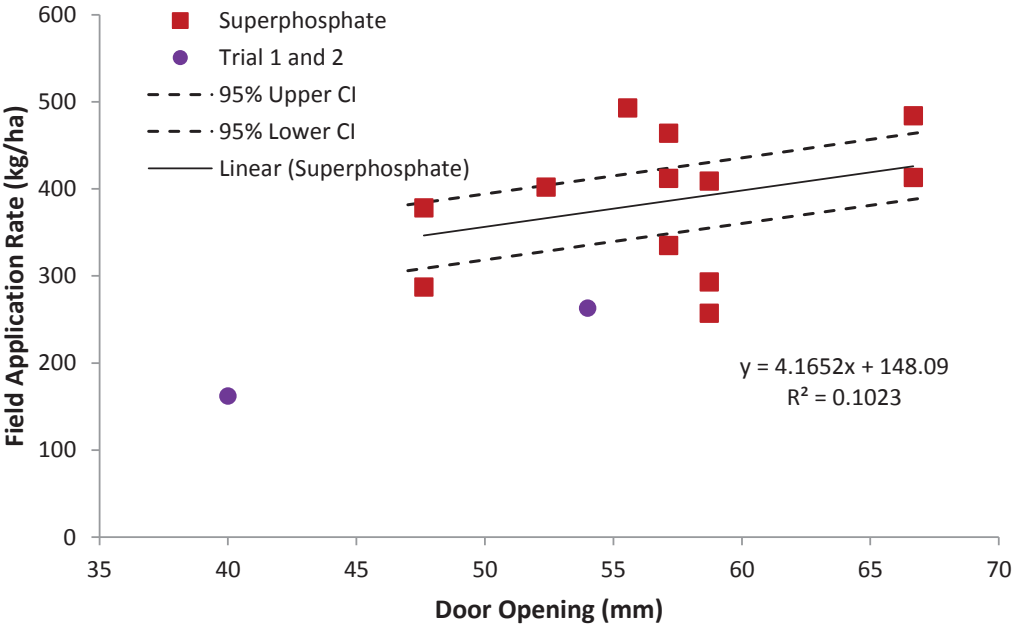


Figure 3.8: The relationship between the measured field application rate and hopper door opening for superphosphate in Trial 6. The dashed lines are the confidence interval (CI) of the linear equation.

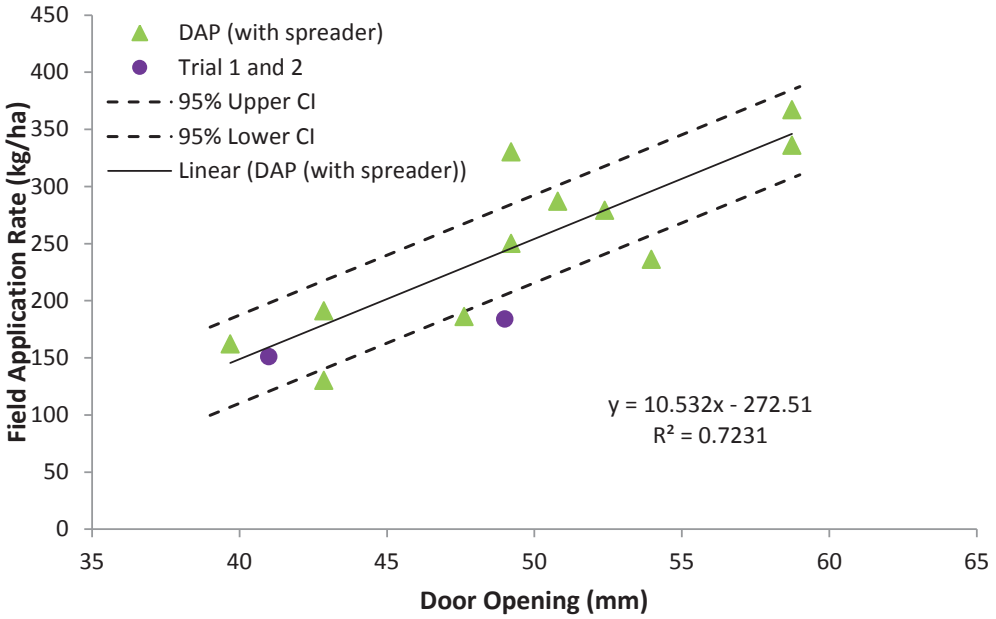


Figure 3.9: The relationship between the measured field application rate and hopper door opening for DAP in Trial 6. The dashed lines are the confidence interval (CI) of the linear equation.

Using the initial prescription map settings from Trial 1 and 2, application rates were calculated from the linear equations in Figure 3.7 - Figure 3.9 to determine if the linear equations could predict the field application rate. Table 3.3 shows that the linear equations did not make accurate predictions. On average, the predicted application rates are larger than the Spreadmark field application rates from Trial 1 and 2. However, Trial 1 and Trial 2 were completed under different conditions. For example, urea and DAP were applied with an 11 duct spreader in Trial 1 and no spreader in Trial 2. The results of Table 3.3 are, therefore, inconclusive. Plotting the Spreadmark values from Table 3.3 on to Figure 3.7, Figure 3.8, and Figure 3.9 shows only one point was within the 95% confidence interval (CI) for the linear equation. This means these linear flow rate equations should not be used to predict the application rate from the hopper door opening without further investigation.

Table 3.3: Using Figure 3.7, Figure 3.8 and Figure 3.9 equations to predict field application rate from Longview validation trials (Trial 1 and 2).

Fertiliser Type	Trial	Gate Opening (mm)	Equation (kg ha^{-1})	Spreadmark (kg ha^{-1})	Difference (%)
Urea	Trial 2	49	163.22	110.5	-48
Urea (11 duct)	Trial 1	33	47.23	72	34
DAP	Trial 2	49	243.56	184	-32
DAP (11 duct)	Trial 1	41	159.30	151	-5
Superphosphate	Trial 2	40	315.70	162	-95
Superphosphate	Trial 1	54	373.01	263	-42

Figure 3.10 illustrates that, on average, the field application rate was greater than the intended application rate. This will be discussed further in Objective 2 on the Beverloo equation. A possible explanation for the range of field application rates is that since the aircraft groundspeed was not constant, the intended application rate changed because the VRAT system tried to compensate for changes in velocity. The VRAT velocity compensation setting has not been calibrated or studied, so it is uncertain how aircraft velocity will affect the application rate. Currently it is assumed that the relationship between aircraft velocity and application rate is linear and of the same magnitude, which may be false. The compensation setting is available on the Satloc G4 system and can be manipulated through the prescription maps.

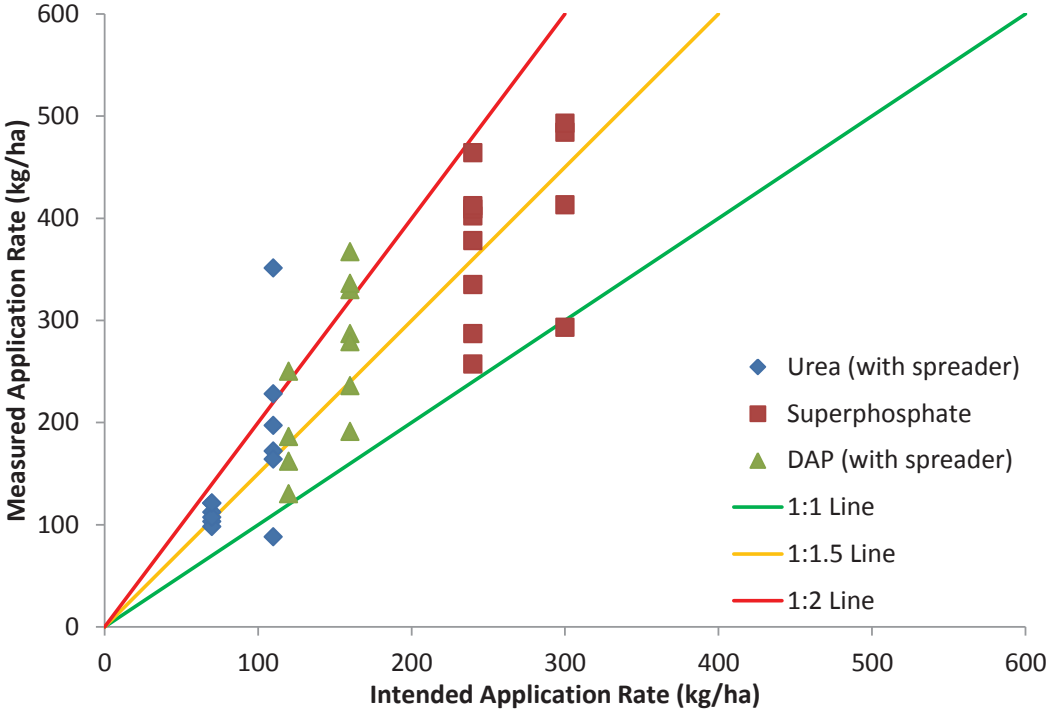


Figure 3.10: Relationship between intended and measured field application rate in Trial 6. Lines representing 1:1, 1:1.5 and 1:2 are included to illustrate the magnitude of difference between the two application rates.

3.4.1.2. Swath width

There was a strong negative relationship between the field application rate and the field swath width for urea and DAP (Figure 3.11 and Figure 3.13). This means the higher the application rate, the narrower the field swath width, which was discussed by Scott and Grig (1970), and Akesson and Yates (1964). They found from their own experiments that the swath width narrows with increased application rate. Neither articles discussed the reason this occurs. It is

likely that the higher flow rate causes particles to cluster, which prevents outward spread of the particles. Clusters are heavier and will fall faster. Therefore the fast moving flow of air at the hopper door cannot spread the fertiliser laterally, and the particles will fall as clumps creating a narrower swath width.

Superphosphate's linear relationship had an R-Squared less than 0.01, which suggests that there is no relationship between its field application rate and the measured swath width (Figure 3.12). However, this is unlikely. Variability in superphosphate's field application rate could be caused by having no spreader or another reason may have concealed any relationship. Although the VRAT system allows a specific bout width to be set, the resulting ground swath width is highly dependent on environmental conditions, aircraft operation, and the fertiliser's ballistic properties.

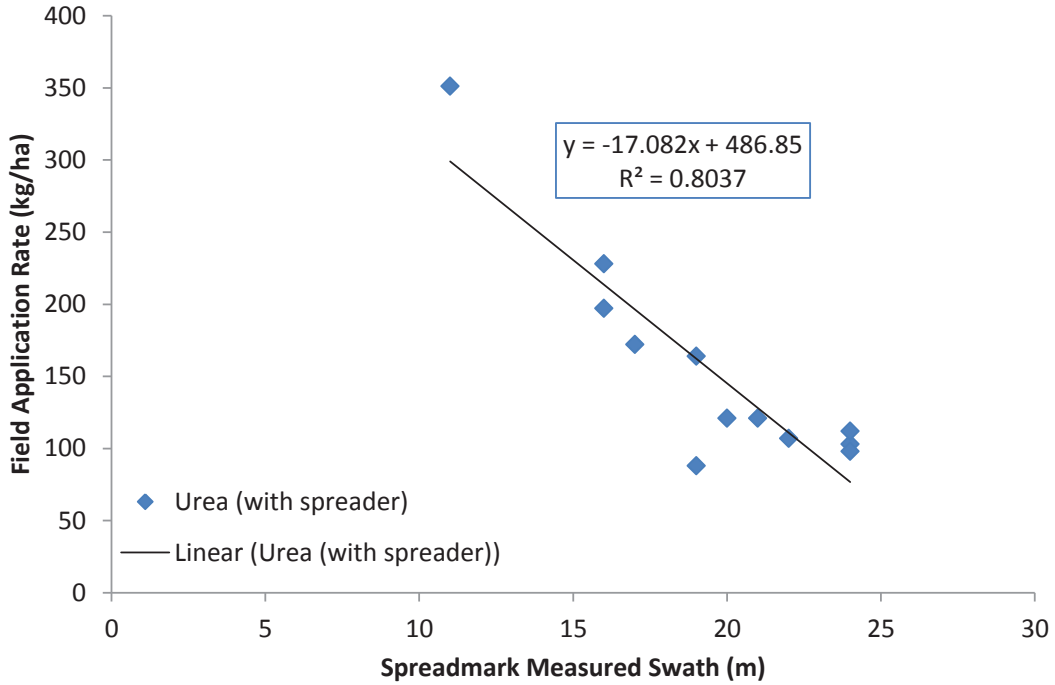


Figure 3.11: The relationship between the measured field application rate and swath width for urea in Trial 6.

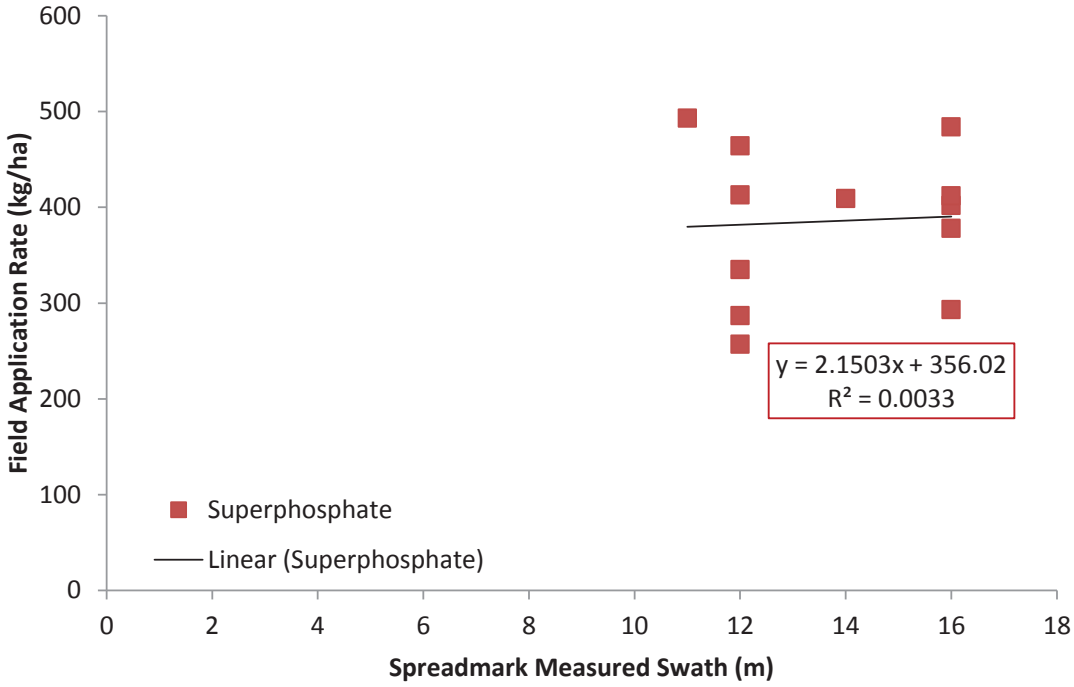


Figure 3.12: The relationship between the measured field application rate and swath width for superphosphate in Trial 6.

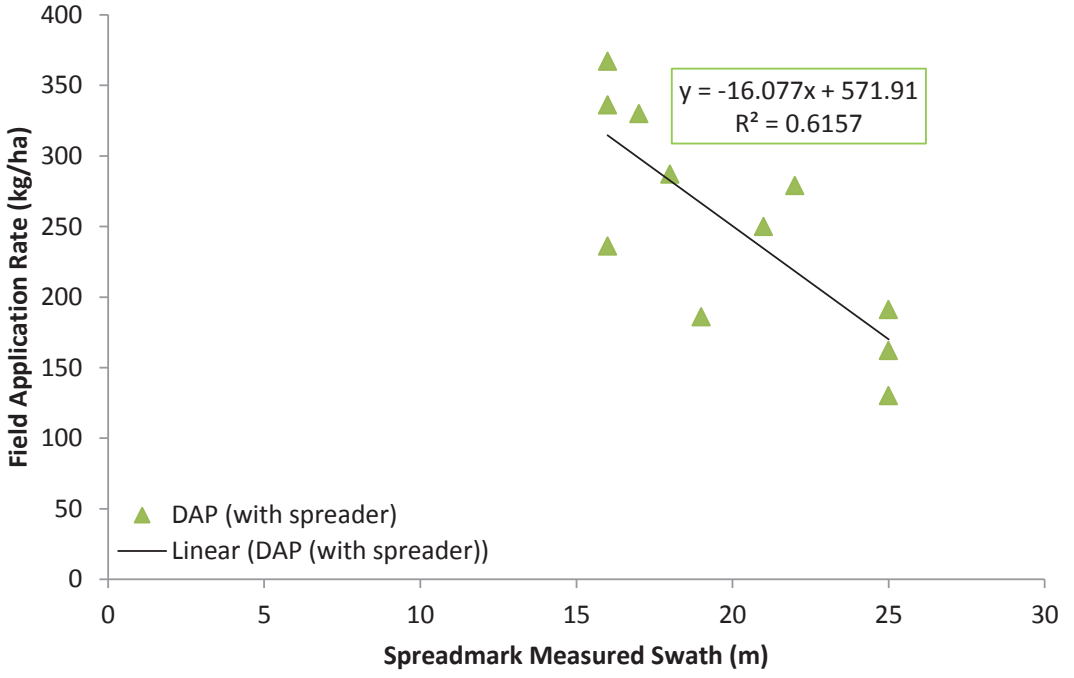


Figure 3.13: The relationship between the measured field application rate and swath width for DAP in Trial 6.

3.4.1.3. Aircraft velocity

The time required for the aircraft to complete application to one hectare depends on the aircraft velocity and set swath width. Since aircraft velocity can vary, the velocity compensation setting was used to adjust the hopper door opening so that the application rate

would remain constant. In this trial, the setting varied depending on the set of factors. Aircraft velocity was expected to significantly impact the field application rate (Murray, 2007). However, this was not observed in the results. Urea had the strongest linear relationship between aircraft velocity and the field application rate with an R-Squared of 0.36 (Figure 3.14). DAP and superphosphate had no relationship; the points were highly variable (Figure 3.15 and Figure 3.16). The reason strong relationships may not be observed is because the velocity compensation setting adjusted the hopper door to consider aircraft velocity. The large variation in the data indicates that the setting is incorrect. It would be beneficial to carry out field trials without using the velocity compensation setting to determine how significantly aircraft velocity contributes to the variance in the field distribution.

Another reason could be experimental errors, such as placing collectors 6 m apart, and using collectors with low collection efficiency. These errors could have masked relationships between application rate and aircraft velocity. However, if a strong relationship exists between aircraft velocity and field application rate, it would have been observed in DAP as well, since the trial found relationships for DAP in swath width and application rate. Since a relationship was not observed and the R-Squared for urea was small, it could indicate that a small change in the aircraft's velocity (7 m s^{-1}) will not significantly affect the field application rate because other factors, such as a change in the hopper door opening or wind, have a greater and more noticeable effect. Therefore, when creating a prescription map, the velocity compensation setting in the prescription map could be large (i.e. 8 m s^{-1}). This will give the pilot a large velocity range to operate in, which may yield less variable field application rates.

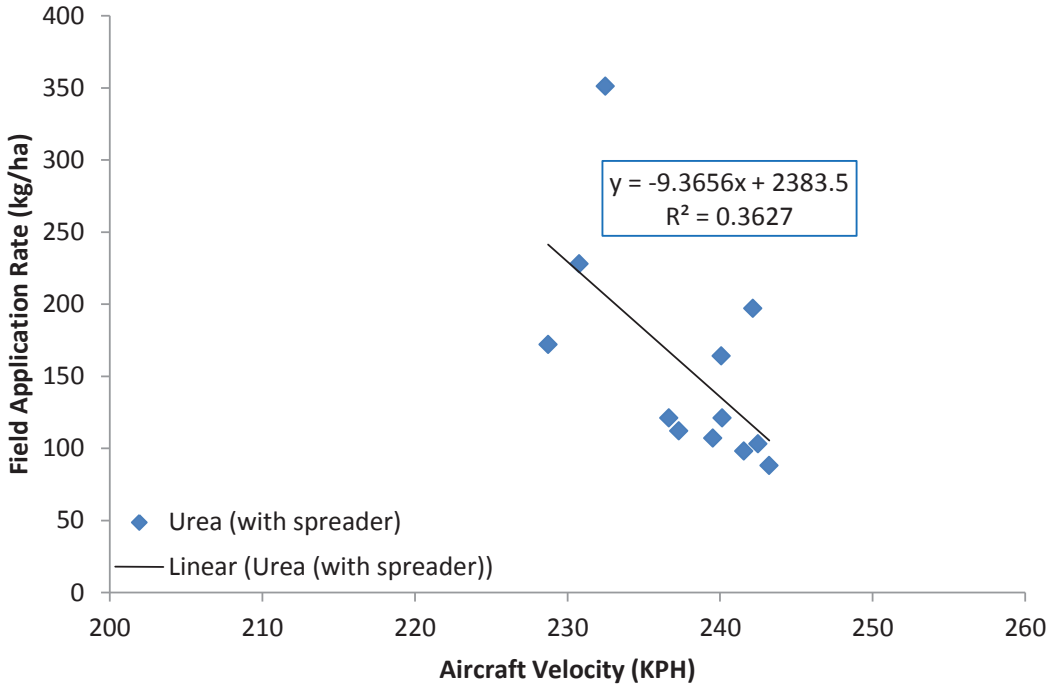


Figure 3.14: Relationship between the measured field application rate and the recorded aircraft velocity for urea in Trial 6.

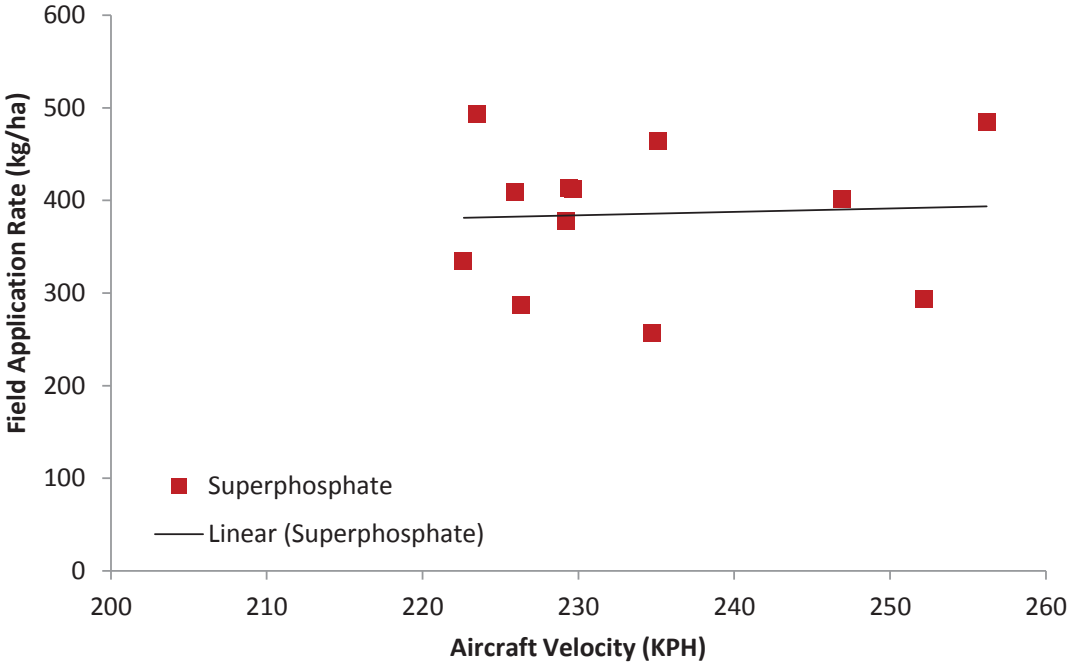


Figure 3.15: Relationship between the measured field application rate and the recorded aircraft velocity for superphosphate in Trial 6.

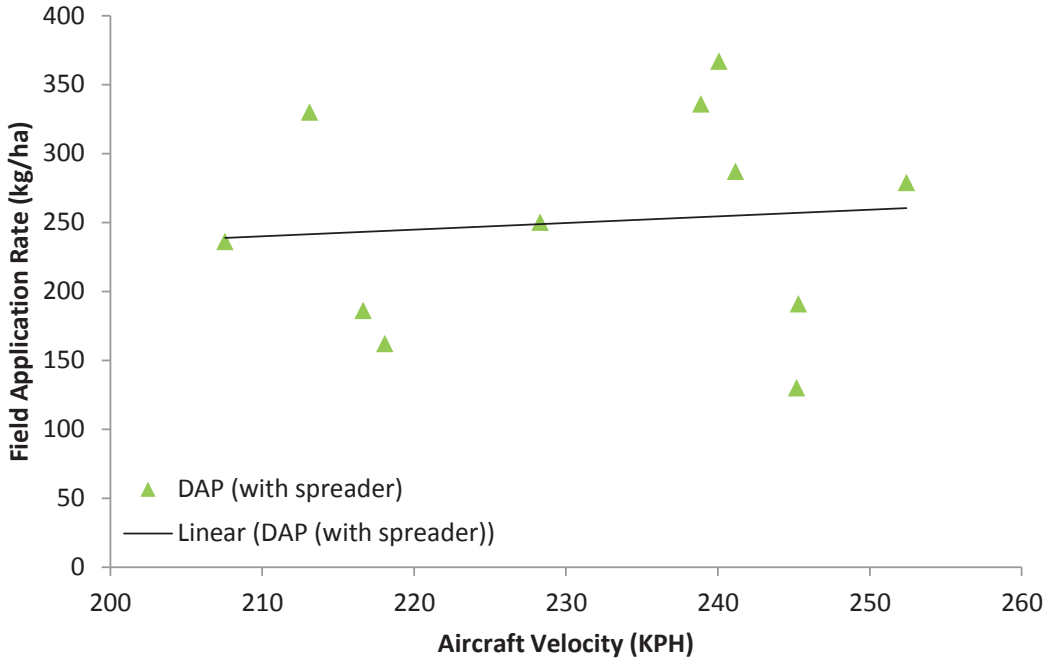


Figure 3.16: Relationship between the measured field application rate and the recorded aircraft velocity for DAP in Trial 6.

3.4.2. Objective 2

Beverloo equation was used to calculate the application rate from the field hopper door opening on the trial day, which was recorded in the aircraft's log files. This was compared to the field application rates. Results show that the field application rate was, on average, greater than the rate calculated by Beverloo (Figure 3.17).

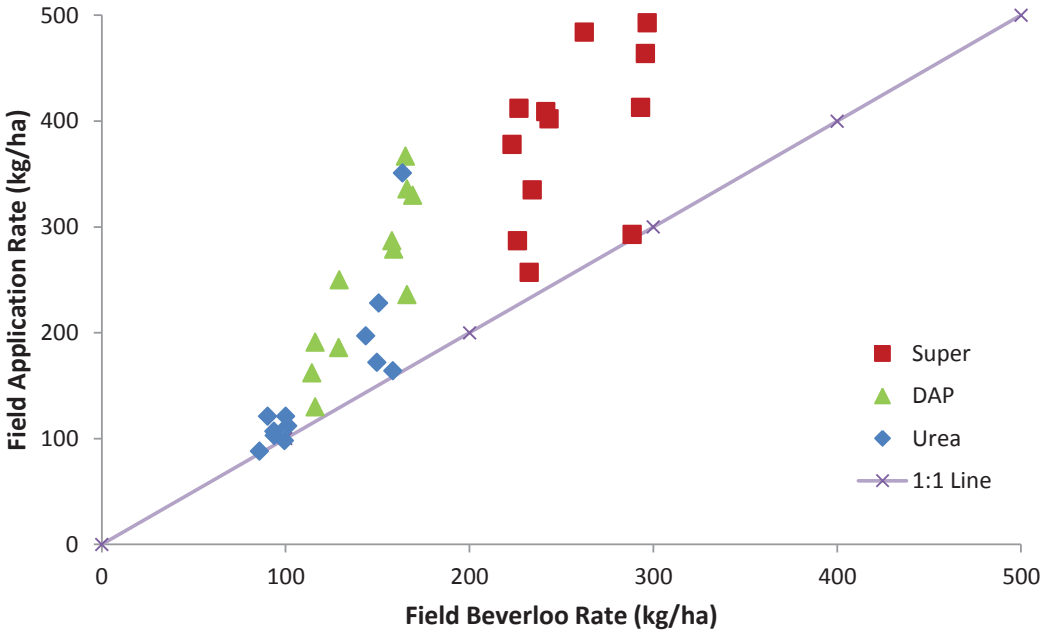


Figure 3.17: Comparison of the field application rate and the field Beverloo equation for Trial 6.

At Trial 4, the Beverloo equation was used to calculate the required hopper door opening to achieve an application rate of 500 and 250 kg ha^{-1}. During the application, the pilot estimated that the flow out of the hopper door was 21% greater than expected. This was based on measuring how long it took to empty the hopper and the distance travelled in that time. The pilot's observation suggests that the interaction between air flow and the hopper door causes an increase flow rate out of the hopper. The variability in Trial 6's results suggests the increase is not constant. If the increase is due to air flow interactions then the variability could be explained by changing flight conditions on the trial day. It would be beneficial to carry out trials with no wind present to determine an accurate correction factor for the Beverloo equation.

3.4.3. Objective 3

An additional trial was completed at Pickwick farm to determine the 'edge on' and 'edge off' time setting. 'Edge on' is when the aircraft is entering an application zone and 'edge off' is when it is exiting. The hopper door should open on the boundary line as the aircraft enters, and close before the exit boundary because fertiliser particles tend to travel forward of the aircraft. To achieve this, the settings must account for the delay in the VRAT system. The 'edge on' setting should register the boundary before the aircraft enters the application area so that it can prepare to open the hopper door. If the hopper door opens too early, fertiliser will be applied outside the application zone.

To determine the correct settings, collectors were set up 2 m apart in a line that intersected the entry and exit boundary of Area 2. In total 50 collectors were used, 25 at each boundary line. Twelve trials were completed. Depending on where the first/last fertiliser particle was found, the timing would be adjusted. An 'edge on' setting of 0.5 s was used throughout the trial. Figure 3.18 illustrates the variation in the distance a fertiliser particle will travel for the same 'edge on' timing. This variation can be explained by slight differences in the VRAT system response time, wind conditions, particle size distribution, and aircraft operation. On average, particles landed 1.3 m inside the boundary with a standard deviation of 5.3 m. The large standard deviation was attributed to the different conditions during individual flights. An 'edge off' timing of 1.3 s yielded particles that landed, on average, 13 m from the boundary, which is a good safety buffer. The standard deviation was 4.2 m. Therefore, the recommended 'edge on' timing is 0.4 s to ensure that particles are released inside of the boundary and the 'edge off' timing is 1.3 s.

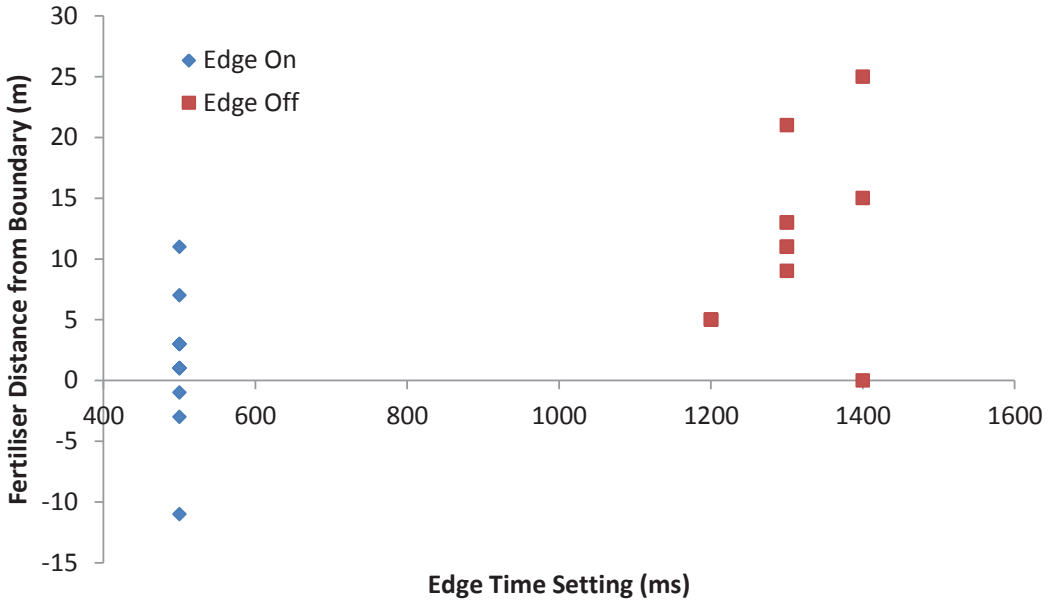


Figure 3.18: Distance fertiliser particles were found from the boundary for different edge time settings in Trial 6. A positive distance from the boundary indicates the particle landed within the application area and vice versa.

3.4.4. Objective 4

High speed video was taken of fertiliser particles falling into a NZCPA collector. The camera was set up in Area 2 on a flight guidance collector. A rigid black board was placed behind the collector to provide colour contrast. The samples from the collector were not collected. Although there were four flights per fertiliser type, only three videos were analysed because one flight was required for calibration. The number of fertiliser particles that bounced out was measured manually by counting each fertiliser particle that entered and exited the collector (Figure 3.19). Results showed that the harder the particle, the higher the percentage that bounces out (Table 3.4). The percentage is based on the proportion of particles that bounced out, not the weight. This assumes that particles of all sizes bounced out equally. Average percentage losses were used to correct the transverse distributions in Trial 6 and all previous trials (i.e. validation, performance). The accuracy of the percentage is limited because only three videos were analysed for each fertiliser type. However, the benefit of doing this work is that the issue of particles bouncing out of the collectors has been identified and needs to be addressed.



Figure 3.19: Image still of a video taken at 500 frames per second recorded at Pickwick farm of superphosphate taken at Trial 6.

Table 3.4: Percentage of particles bouncing out of a collector and their average particle strength.

	Percentage of Particles Bouncing Out (%)				Particle
Fertiliser Type	Video 1	Video 2	Video 3	**Average**	**Strength (N)**
Urea	12.50	26.98	8.00	15.83	2.72
Superphosphate	8.56	4.08	4.55	5.73	1.91
DAP	41.62	40.63	22.81	35.02	6.13

3.5. Collector Improvement

Collectors are an important component of experimental field work. The results from Trial 6 indicate that the NZCPA collectors require significant improvement. This section examines the NZCPA and alternate collectors, and their collection efficiency.

3.5.1. Initial Collector Study

An initial study was completed to find an alternate collector. The criteria for the new collector were minimal cost, ease of use and improved collection efficiency. Several materials, such as polyester and cotton fabrics, plastics of different thickness, garbage bags and bubble wrap, were tested. The NZCPA collector stand was used as a frame to hold up the new collector to minimise cost. A set of 60 collectors were also borrowed from the New Zealand Agricultural Aviation Association (NZAAA). These collectors are used to carry out Aerial Spreadmark tests. Therefore their collection efficiency is important in order to ensure that the testing regime is accurate, but it has not been previously studied.

An initial investigation was completed on the fire stairwell of a three storey building, which was 9 m high. A high speed camera was used to ensure that fertiliser particles of different sizes reached their terminal velocity at the 9 m height (Figure 3.20). To ensure that terminal velocity is reached, calculations were completed for the three fertiliser types for particle sizes between 1 – 6 mm (Table 3.5). Terminal velocity was calculated using Haider and Levenspiel (1989)'s

non-spherical particle equation. The sphericity for all three fertiliser types was assumed to be 0.9. To validate these terminal velocity calculations, superphosphate, DAP and urea was separated into the sieve ranges used in Chapter 2, and was dropped from the top of the stairwell. The terminal velocities calculated from the high speed imagery were compared with values found using Haider and Levenspiel (1989) (Figure 3.21 – Figure 3.23). There was good agreement, so 9 m is a sufficient height for all three fertiliser types to reach terminal velocity.



Figure 3.20: Set up for terminal velocity of 9 m height.

Table 3.5: Height required to reach terminal velocity for three fertiliser types.

	Calculated Height to Reach Terminal Velocity (m)	
Particle Size	**1 mm**	**6 mm**
Superphosphate	1.3	8.2
DAP	1.2	7
Urea	0.8	5.2

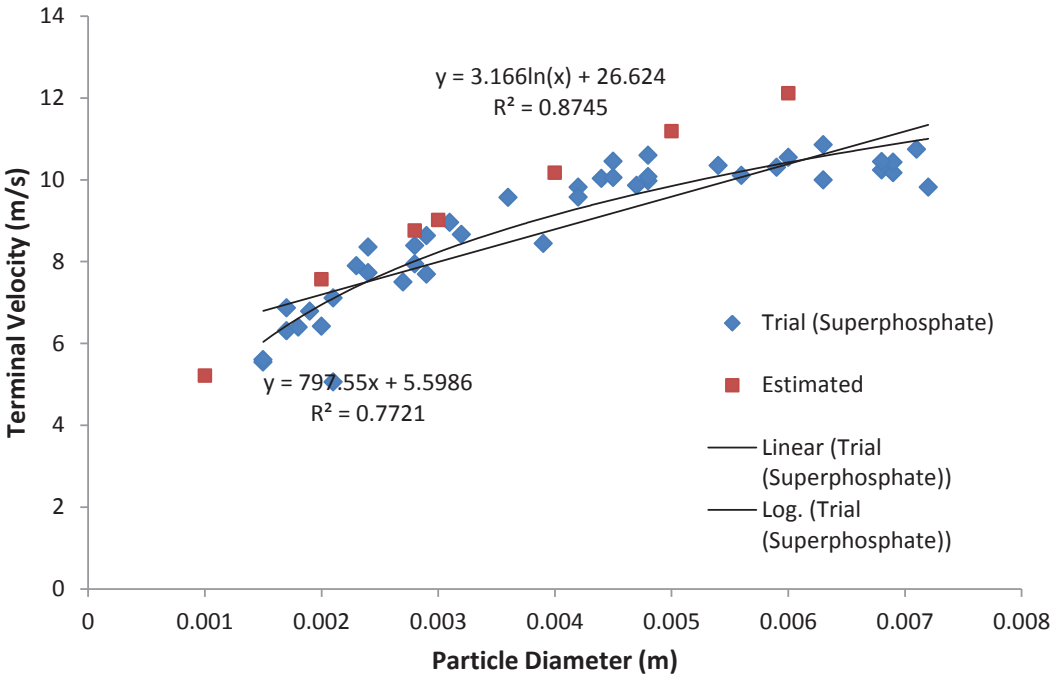


Figure 3.21: Comparison of calculated and measured terminal velocities for various superphosphate particle sizes. Calculations were made using Haider and Levenspiel (1989).

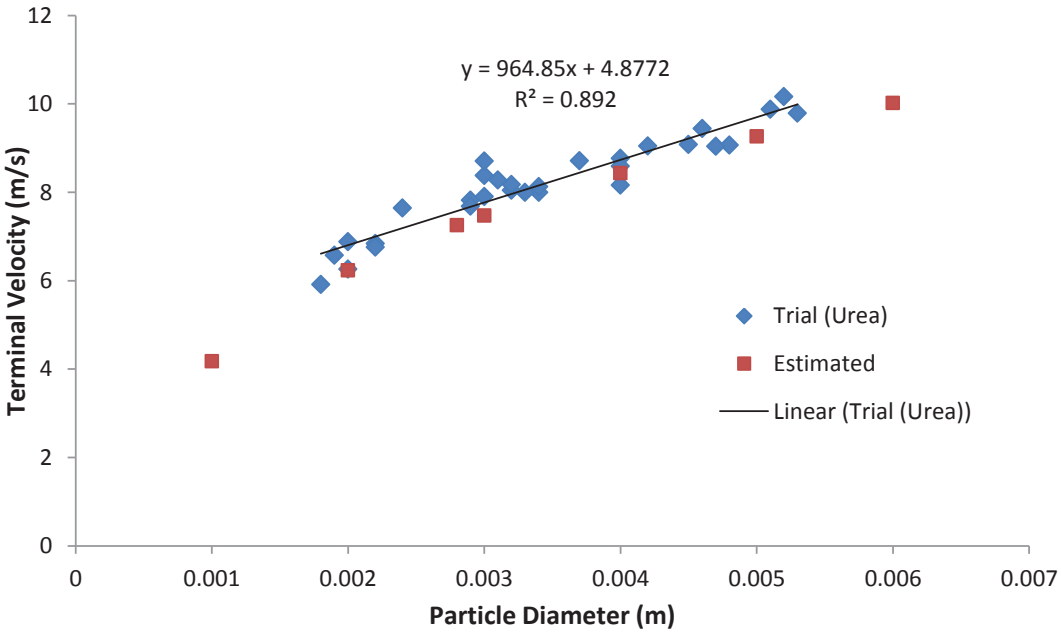


Figure 3.22: Comparison of calculated and measured terminal velocities for various urea particle sizes. Calculations were made using Haider and Levenspiel (1989).

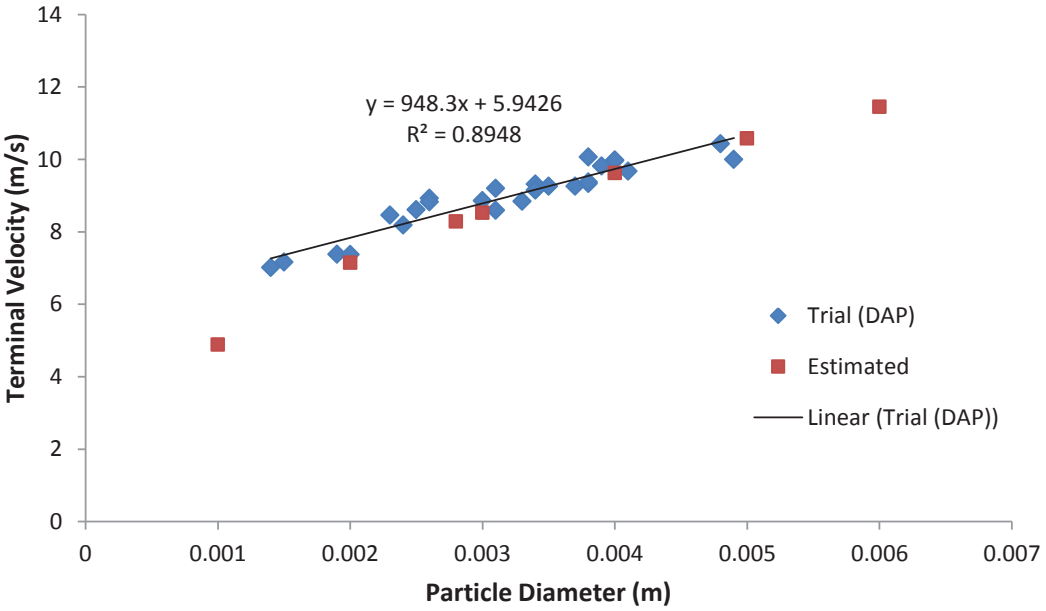


Figure 3.23: Comparison of calculated and measured terminal velocities for various DAP particle sizes. Calculations were made using Haider and Levenspiel (1989).

The first test was to determine which collectors were capable of collecting the material. Different collector designs were placed below the fertiliser release point and an observer stood by the collector to make subjective observations about the collection efficiency. This was not a scientific process, but a cheap method to acquire information on feasibility. Adjustments to the release point were required because of changes in the wind conditions. Fabric and plastic bags did not improve the collection efficiency of fertiliser particles. The material easily distorts in wind and creases in the material decrease the collection efficiency. Collectors lined with bubble wrap seemed to capture superphosphate and DAP at greater efficiency, but a significant amount of urea was observed to bounce out. This was likely due to its low particle density. The NZAAA collector improved the collection efficiency of all three fertiliser types.

The NZCPA, NZAAA and NZCPA collector with bubble wrap was tested in the field. One of each collector was set up at a small sheep and beef farm located 30 km east of Hunterville, Central North Island, New Zealand. A high speed camera capturing images at 500 fps was set up perpendicular to the flight path. A black background was set up behind the collector for increased contrast. The trial was completed in conjunction with an aerial topdressing job where 500 kg ha^{-1} of superphosphate was applied at a swath width of 15 m. A different pilot (Pilot C) with a PAC 600 was utilised. The pilot's aircraft did not have a VRAT system installed; therefore a log file was not available.

The camera was set up between 2 – 20 m away from the collector. A constant distance could not be maintained because the flight path was constantly moving at the swath width distance. Each flight took approximately 3 min, which was a short time to reset the vehicle and camera. The issue was the camera's computer was sensitive and was not built for fieldwork. This meant that the computer needed to be switched off when it was moved. To save time, the computer was only shifted after every second flight. However, this meant that in some videos individual particles could not be identified, because there was significant noise from other fertiliser particles applied in the 20 m interval.

In-field observations and high speed videos showed that fertiliser particles bounced out of all the collector types. However the collection efficiency varied. The NZCPA collector was subjectively observed to have the lowest collection efficiency while the addition of a bubble wrap layer was the most efficient.

3.5.2. Trial 7 – Collector Trial

The initial collector study does not provide sufficient statistical evidence that the NZCPA collector lined with bubble wrap has the highest collection efficiency of the three collector types. Therefore a statistical trial was carried out. Trial 7 was completed at Mairedale Farm, a sheep and beef farm located in Rangiwahia, a town in the Central North Island. Three collector types were tested: NZCPA (control), NZAAA and NZCPA with a bubble wrap layer. Thirty of each collector type was used. This was a sufficient sample size to carry out robust statistical analysis. In total, 90 collectors were set up in a line with each collector 1 m apart (Figure 3.24). The collectors were set up in an alternating sequence to decrease sampling error (Figure 3.25). Pilot B used this 90 m line of collectors as the flight line. Three rows of 20 collectors were placed perpendicular to the 90 m collector line. Each row was a different collector type, which was used to collect the transverse spread pattern. Collectors in these rows were 3 m apart.

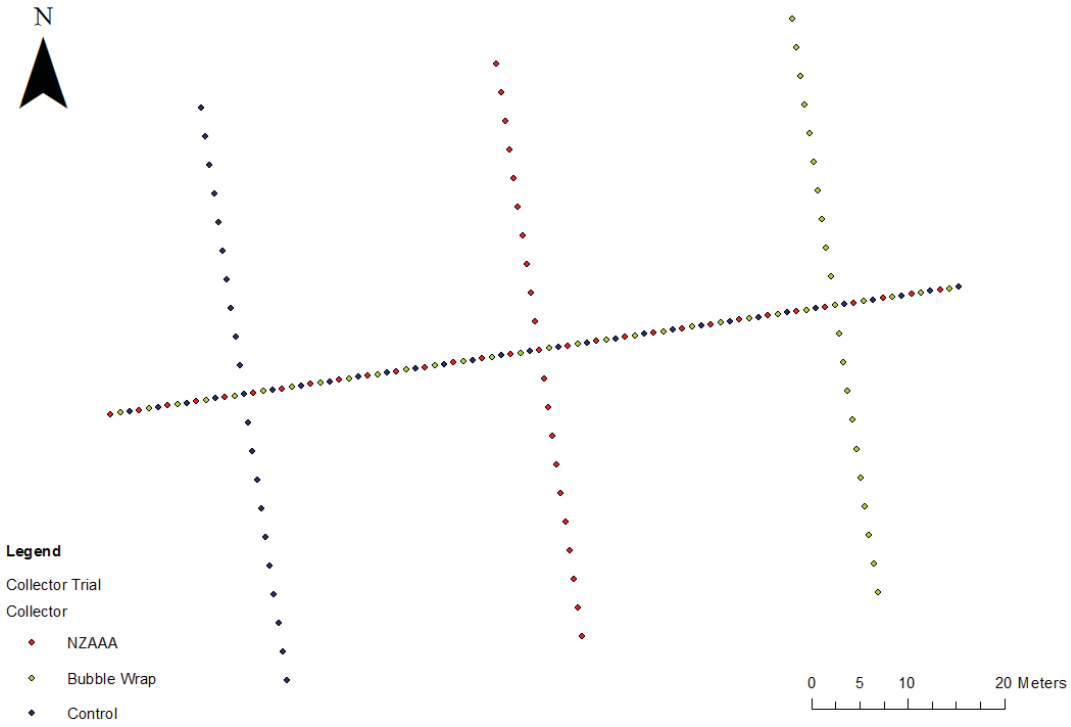


Figure 3.24: Sampling configuration for Trial 7.



Figure 3.25: Collector set up for Trial 7 on trial day.

The trial took half a day to set up with five people, and a day to complete and pack up with 10 people. Pilot B applied superphosphate over the area at an application rate of 400 kg ha^{-1}. The VRAT system had technical issues on the day, which meant that Pilot B flew without the prescription map and a log file was not available. Two flights were completed. Weather conditions were overcast and there was light rain for the majority of the day. The average wind

velocity was 0.38 m s^{-1} with a range of 0 – 1.02 m s^{-1} (Figure 3.26). Average wind direction was 76.15° ranging from 315.84° to 128.79°.

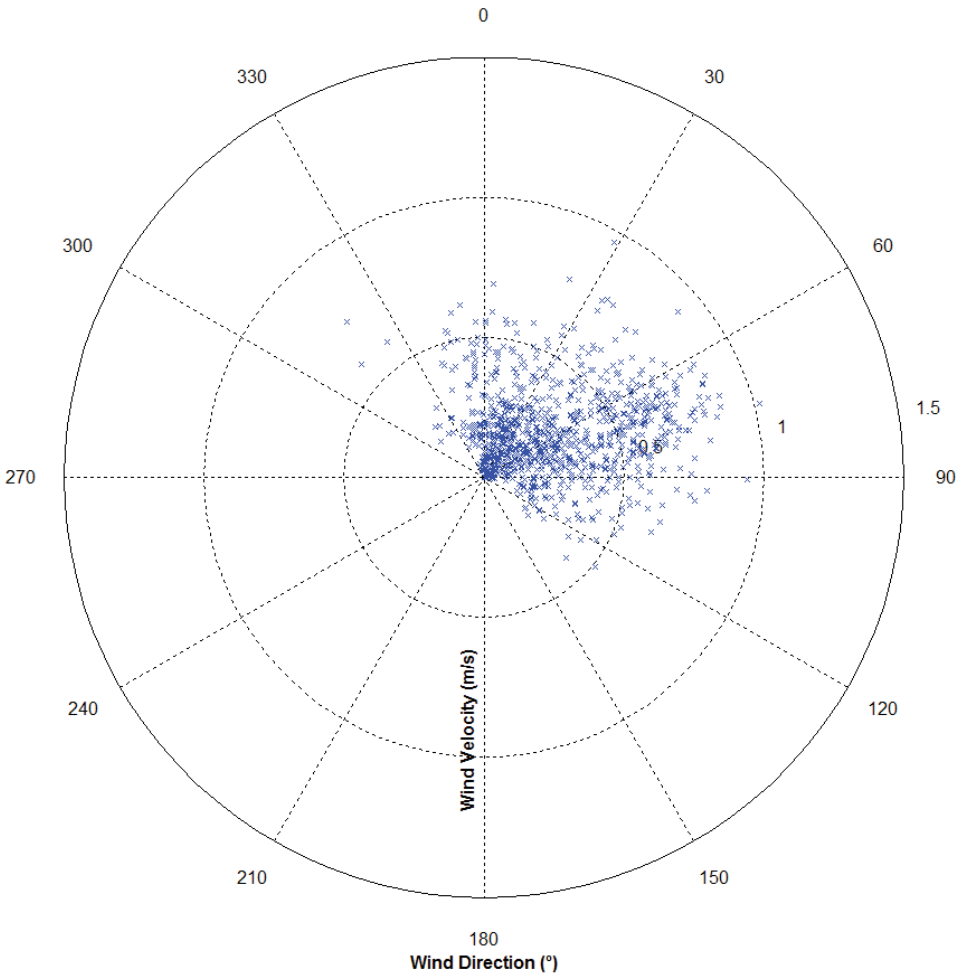


Figure 3.26: Wind velocity and direction over the trial period in Trial 7. True north is denoted by 0 degrees.

Flight 1 had some light rain, which meant only 18 samples of the NZAAA collectors were recovered. A complete data set was collected for the two NZCPA collectors. There was significant rain after the second flight, which meant only 12 samples of the NZAAA collectors and 21 samples of the NZCPA collector were recovered. The NZAAA collectors were affected by rain because of the collector's smooth plastic surface. Samples got wet due to the order in which they were collected, with those collected last being the wettest. The NZCPA collector with a bubble wrap liner was not greatly affected by rain because the bubbles prevented the flow of water. However, this meant that the fertiliser particles trapped in the bubble wrap were not collected to prevent moisture getting into the sample bags.

The Trial 7 results show the NZCPA with bubble wrap liner collected the most amount of fertiliser (Table 3.6). In terms of percentage, the NZCPA with bubble wrap collected 38% more than the NZCPA collector (Table 3.7). A single factor Analysis of Variance (ANOVA) test was carried out on the data set at a 5% significance level. This was to confirm there was a significant difference in the averages and distributions of the three collector types. P-values from both flights were much smaller than the significance level ($P < 0.001$), which indicates that there is a highly significant difference in the averages between the collector types.

Table 3.6: Average masses collected from the three fertiliser collectors in Trial 7.

	Flight 1		Flight 2	
Collector Type	Average (g)	Standard Deviation (g)	Average (g)	Standard Deviation (g)
NZAAA	13.86	1.98	20.40	2.42
NZCPA with Bubble Wrap	14.65	1.75	21.99	1.72
NZCPA	10.63	0.91	15.90	1.57

Table 3.7: Percentage difference in masses between collector types in Trial 7.

Percentage Difference	**Flight 1 (%)**	**Flight 2 (%)**
NZCPA Bubble Wrap-NZCPA	37.85	38.36
NZAAA-NZCPA	30.43	28.36
NZCPA Bubble Wrap-NZAAA	5.69	7.79

Although the NZCPA collectors with bubble wrap were experimentally shown to improve data collection compared to the other two options, it is likely that some particles are still bouncing out. This will reduce the measured field application rate. A possible method to quantify the true field application rate, using the NZCPA collectors, is to line the collector with bubble wrap and extend the collar by the maximum bounce distance. To reduce cost, the collar extension could be done with cardboard. This is not a practical solution for performance or validation trials, since cardboard is not a robust material. However, it could indicate the true field application rate. There are also other collector options, but it is important to test their efficiency before using them in the field (Lockett, 1998; Morton et al., 2016).

3.6. Trial 8 – Line Sampling

The objective of Trial 8 is to collect a complete data set of the system's accuracy, precision and capability without having the intention of kriging. This simplifies the sampling requirements for the trial. The sampling design completed by Ballard and Will (1971), where a single line of 75 collectors was placed perpendicular to the aircraft's flight path, was used as a blueprint for Trial 8. This method allows the collection of multiple transverse spread patterns, which can

indicate the three levels of spatial variation in aerial spreading and is able to assess the system's performance.

Trial 8 was completed at Mairedale Farm in February 2017 on hill country paddocks. This was the final trial used to determine the performance of the VRAT system. NZCPA collectors lined with bubble wrap were set up in a line that was 432 m long with each collector 3 m apart (Figure 3.27). One hundred and forty-five collectors were placed in the main line (Figure 3.28). Replicates, for some of the collectors, were placed 10 m parallel to the main line. There were six replicates with five collectors in each replicate. Three replicates were north of the centre line and the other three were south of the line. In total 175 collectors were planned for. However, the line crossed two marshes in the field, which meant that five collectors were excluded. Set up occurred over two days with four people. On the trial day, 10 people were involved in the final set up and pack up of the collectors.

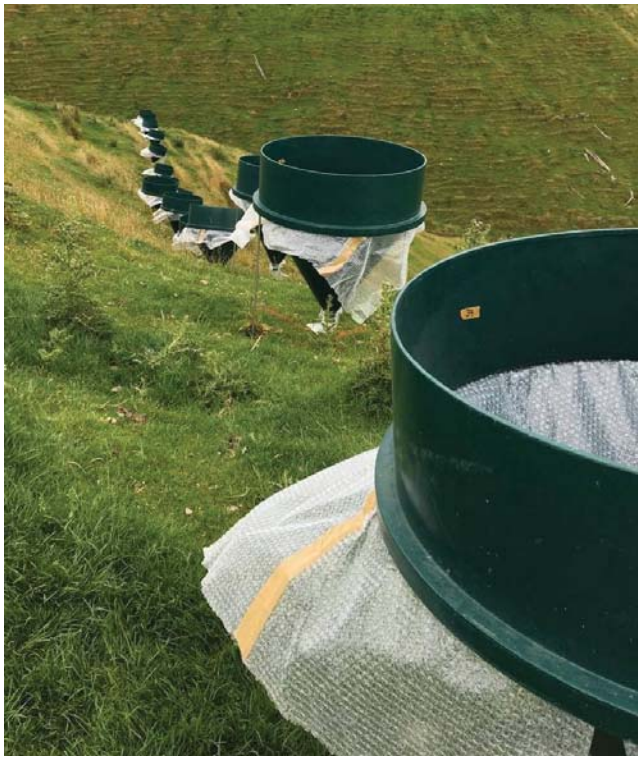


Figure 3.27: Collectors set up with the bubble wrap liner in Trial 8.

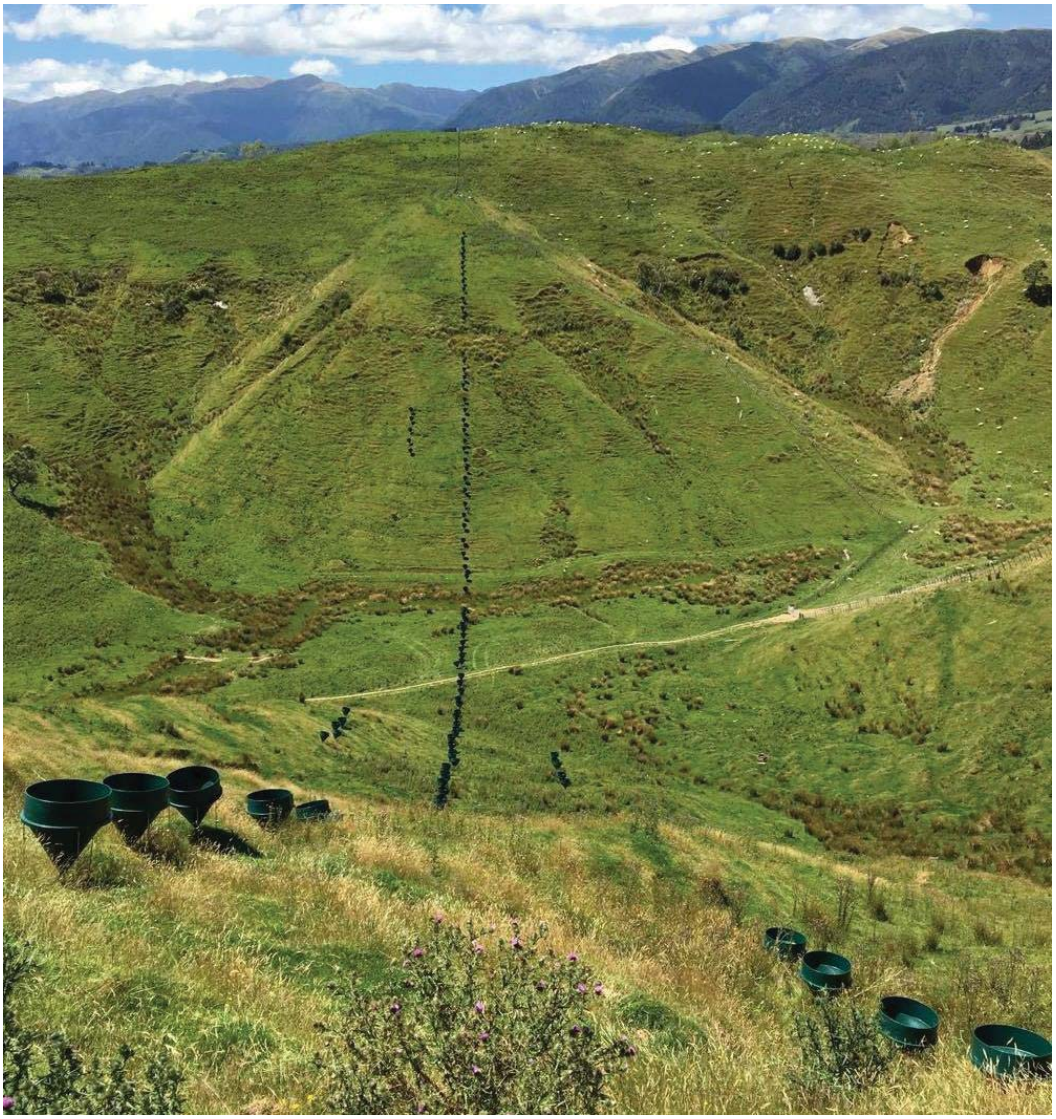


Figure 3.28: Collectors set up in a line with replicates in Trial 8. The collectors travel over one hill and up one hill.

The pilot was asked to fly perpendicular to the collector line, so that multiple transverse spread patterns could be collected. Eleven tonnes of superphosphate was applied over a 35 ha area at application rates of 250 kg ha^{-1}, 500 kg ha^{-1} or 0 kg ha^{-1}. The zero application rate zone was included to check the VRAT system's ability to not apply in a narrow sensitive zone. The application area consisted of three paddocks with variable topography. Figure 3.29 illustrates the application zones and was the foundation of the prescription map. The boundaries are oddly shaped to test the performance of the VRAT system at applying to different boundary lines. Some boundaries were defined by existing paddocks.

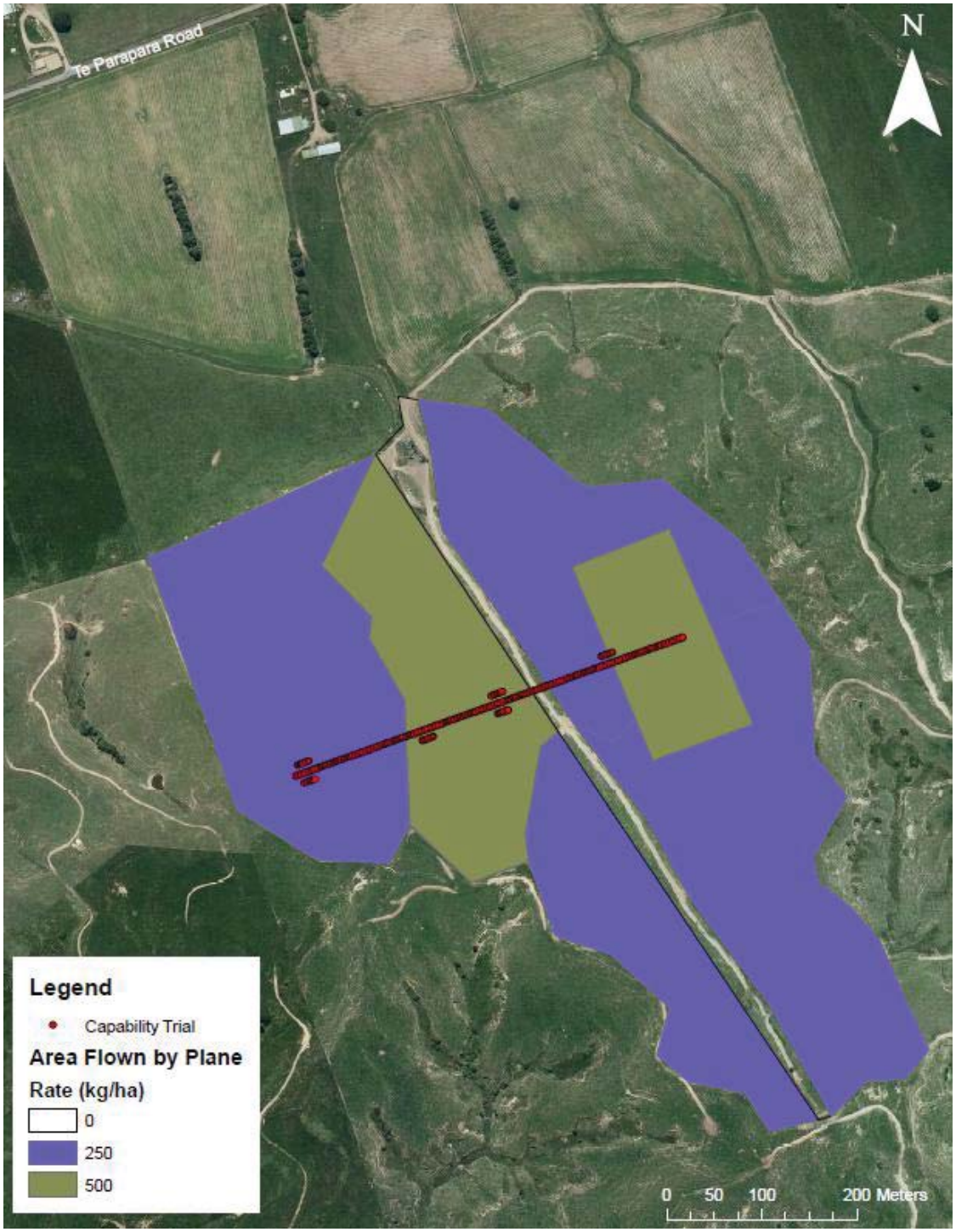


Figure 3.29: Sample configuration and application zones for Trial 8.

Wind measurements were taken using an anemometer that logged wind direction, wind velocity and time every 10 s. Average wind speed and direction was 0.34 m s^{-1} and 103.76°, respectively with a range of 0.01 – 1.38 m s^{-1} and 0.4° - 359.35° (Figure 3.30). Pilot B applied fertiliser at a swath width of 12 m and an average aircraft velocity of 59 m s^{-1}.

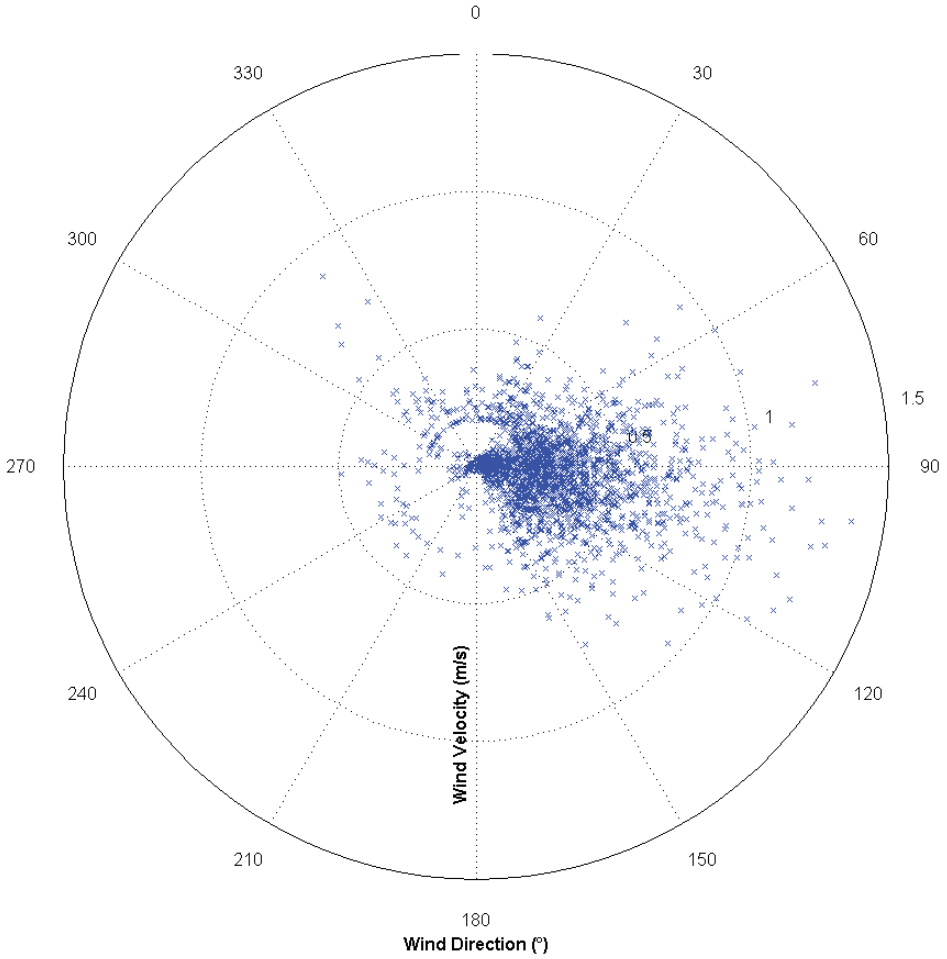


Figure 3.30: Wind velocity and direction over the trial period in Trial 8. True north is denoted by 0 degrees.

The advantage of setting out a line is that it is a proven sample configuration, since it has been utilised in previous aerial topdressing trials (Macfarlane et al., 1987). If correctly executed, information about the VRAT system's accuracy, precision and capability can be determined. It can also determine the field swath width, which could not be calculated in previous performance trials. Another advantage is that, compared to previous trials addressed in this chapter, this configuration requires less set up time and resources. A disadvantage of this method is that it does not provide sufficient information about the spatial variance for geo-statistical analysis, and should therefore not be used if kriging is required. There is also continued uncertainty about whether a representative sample of the application is collected. The application area is large compared to the collectors' surface area. If a representative sample of the application zone is not collected, then the results will be biased and unreliable.

3.7. Conclusion

Different sampling configurations were used for the three performance trials. Trial 4 carried out grid sampling, which is a simple sampling configuration. However, it is an unsuitable design for kriging. Since the collectors were placed 70 m apart, the grid is incompatible with the sources of variation in aerial topdressing. A nested grid sampling design was completed in Trial 5. The sampling method is appropriate in characterising the spatial variance for kriging, but it does not explain the variability within the trial. In Trial 8, kriging was not an objective. Instead the focus was on finding a sampling configuration that would collect data on accuracy, precision, level of off-target application, and the capability of the VRAT system. Line sampling has been used in previous studies and fulfilled all the requirements. However, there is still uncertainty about whether a representative sample of the application area is collected. The sampling configuration can significantly affect the validity of the collected data. Since performance trials are expensive and labour intensive, proper consideration is required to determine the level of variation in the system, and how that can be measured effectively, prior to a trial.

A factorial trial was completed in Trial 6, but the trial did not produce expected results because aerial topdressing is highly variable. It was not possible to limit aircraft velocity to a high and low level, and wind conditions were a significant factor on the day. Sources of variation, such as the flow rate out of the hopper door and wind conditions, could not be directly measured or controlled, which made it difficult to determine the impact of a single variable. Therefore a factorial trial should not be undertaken in aerial topdressing unless all variables can be controlled.

Trial 6 also found that fertiliser bounced out of the NZCPA collectors, and the percentage of particles that bounced out varied with fertiliser type. Initial experiments investigated alternate collectors. Trial 7 found that NZCPA collectors lined with bubble wrap improved superphosphate collection by 38% compared to the original NZCPA collector. Although this is a significant improvement, future users should be aware that the collection efficiency of the NZCPA collector lined with bubble wrap is not 100%. Previous validation and performance trials were corrected for particle bounce out of the collectors, using the correction factors found in Trial 6 and 7.

Chapter 4 - Performance of an Aerial Variable Rate Application System

4.1. Introduction

The objective of this chapter is to discuss the performance of the variable rate application system installed on two Pacific Aerospace Cresco (PAC) 600 aircraft. Performance trials, bench testing and static hopper flow trials were used to improve the system's performance. These were completed over a three year period. During that time, the variable rate application technology (VRAT) system was modified, updated and improved. Chapter 3 discussed the methodology, advantages and disadvantages of the performance trials, and the issue of fertiliser particles bouncing out of the collectors. The data in this chapter has been corrected for particle bounce. Trials applying single superphosphate had a correction factor of 38% that was added to the collected fertiliser mass. This correction factor was measured in Trial 7. Corrections from Trial 6 were used for urea and di-ammonium phosphate (DAP), which was an additional 16% and 35%, respectively. The Trial 6 corrections assume that the same amount, by percentage, bounces out of each collector. This assumption is false but was the best estimation of particle bounce for DAP and urea. Trial 5 applied a fertiliser mix that consisted of superphosphate, Flexi-N, Maxi Sulphur Super and trace elements. The bounce factors of the trace elements were not studied but superphosphate, Flexi-N (urea) and Maxi Sulphur Super (superphosphate) were adjusted using the correction factors. It is likely that the fertiliser bounce out of the collectors in Trial 5 was not fully corrected.

Previous studies did not test the performance of a variable rate application system, where two application rates are consecutively applied. Trial 4 (Limestone Downs), 5 (Longview) and 8 (Mairedale) were performance trials, where a VRAT system applying two rates was tested. The performance of the VRAT system is judged by its accuracy, precision, capability and the level of off-target application.

- Accuracy compared the field application rate to the intended application rate. Spreadmark (NZFQC, 2016b) states that if the field application rate is within 30% of the target application rate, the application is sufficiently accurate.
- Precision was assessed using the coefficient of variation (CV), which is the standard deviation of the application over the average field application rate. A low CV is desirable, but field CV begins at 15% or 25%, depending on the fertiliser type, not zero. This is because 15 – 25% is the maximum CV an aircraft is Spreadmark certified for.

- Off-target application in the field was assessed by placing collectors in exclusion zones and observing if fertiliser landed in them. If the system performs as expected, no fertiliser would be collected in the exclusion zone. However, since wind conditions are variable some fertiliser is expected.
- Capability is determined by how well the system responds to changes in the set application rate, especially near zero rate application zones. It is measured using a one way analysis of variance (ANOVA) test at a 95% confidence interval. Capability is the most important measurement parameter for VRAT, because the capability of the system to change application rates is new to aerial spreading and the main purpose for its installation.

Automation of the hopper door and GPS is expected to improve accuracy and precision. However, these requirements are limited by aerial spreading variables, such as fertiliser quality and wind conditions, which will negatively impact the results.

Kriging is used to visualise spatial data. It has not been previously employed to represent spatial data from aerial applications. Therefore, its ability to accurately represent the capability of the VRAT system is tested. Data for kriging was deduced from the collectors and the VRAT system log files. To ensure the data is suitably Kriged, a semi-variogram is produced. More data is available from the VRAT log files because information is recorded every 0.2 s. They produce proof of release maps that illustrate where fertiliser is released from the aircraft, but they do not account for wind conditions or particle motion. In comparison, collectors are placed some distance apart and only 180 collectors are available, but they represent the field application rate, so they produce proof of placement maps.

This chapter discusses the results of the performance trials, bench testing and kriging. It assesses the VRAT system and concludes whether the system improves fertiliser application.

4.2. Results and Discussion of Performance Trials

4.2.1. Accuracy

Table 4.1 shows that fertiliser was under applied at Trial 4 and 5 by between 9.7 – 19.6%, except for the 250 kg ha^{-1} application zone at Limestone Downs, where over application occurred. However, all the trial zones were within the 30% accuracy range stated in Spreadmark (NZFQC, 2016b). There are simple solutions for obtaining a more accurate application. Under/over application is due to poor calibration between the hopper door and the application rate, or environmental variability (e.g. wind conditions, topography).

Calibrating the hopper door opening to the target application rate would increase the accuracy. This could be carried out at the start of an application to help account for environmental factors and variation in fertiliser physical quality, which affects particle ballistics. Calibration is currently completed by pilots, but it tends to be a rough and ready calculation.

Table 4.1: Summary of collector data for Trial 4 (Limestone Downs) and Trial 5 (Longview).

	Trial 4		**Trial 5**	
Intended application rate (kg ha^{-1})	500	250	284	162
Average measured application rate (kg ha^{-1})	402	265	241	146
Difference between intended and measured average rate (%)	-19.6	6.1	-15.0	-9.7
Standard Deviation (kg/ha)	219	134	84	78
CV (%)	54.4	50.6	34.7	53.0

4.2.2. Precision

The standard deviations improved in Trial 5, when compared with Trial 4 (Table 4.1), which could be explained by the local topography. Trial 5 was carried out in a flat area while Trial 4 was in hill country. Grafton et al. (2012) found that pilot operated systems achieved a CV of 63 - 70%, but these trials had assumptions on the consistency of the swath width pattern and collection efficiency. These assumptions have never been tested and, one would suspect, are subject to the same patterns of variation as those measured in the automated system. These pilot-operated CV are likely to be under estimates of what could be measured in the field.

The VRAT system achieved lower field CV (CV = 35 - 55%). Although the field CV has improved over conventional blanket aerial application, Ravensdown Limited wants to consistently achieve CV between 30% and 35%. This could be attained by selecting suitable swath widths, ensuring parallel flight lines over the application area, and maintaining consistent flight operation (i.e. altitude, groundspeed). However, fertiliser applications on farm begin with a transverse CV of 15 – 25%, depending on the fertiliser type. It is the maximum CV pilots and their aircraft produced in Spreadmark tests for a specific swath width. Pilots apply at this swath width to decrease application time and cost. Therefore, the field CV is unlikely to achieve anything less than this, because during applications, localised topography and wind conditions increase variation. It is challenging for the pilot to consistently achieve a CV of 30 – 35%, but is possible if the effect of localised variables is reduced. This is achievable using the ballistics model discussed in Chapter 2.

An ANOVA test was used to determine the relationship between collector distance and application rate for Trial 5. Collectors at each distance (5 m, 25 m, 50 m and 150 m) were combined and tested against each other. Table 4.2 shows that the averages for each group were not significantly different ($P > 0.05$). Therefore, the variation of collectors of the same distance group is similar to the variation between the other distance groups, which suggests all groups experienced the same type of variability. The variation could be from collector error or changes in wind conditions. If it is assumed that all collectors experienced the same percentage of particle bounce, then the variation is due to wind changes that occurred between the aircraft's successive runs. Wind conditions are uncontrollable and difficult to model. Macfarlane *et al.* (1987) showed that cross wind speeds of 0.44 – 3.5 m s^{-1} resulted in application rates of 4 – 270 kg ha^{-1}. The intended mean application rate for their study was 100 kg ha^{-1}. Therefore, wind significantly impacts the transverse spread pattern, and likely contributed to differences in the intended and field application rates reported here.

Table 4.2: ANOVA test for collector distance and application rate from Trial 5.

Groups	*Count*	*Sum*	*Average*	*Variance*
5 m	76	14985.6	197.2	8349.9
25 m	37	6946.8	187.8	12429.5
50 m	19	3782.5	199.1	6755.9
150 m	10	1812.3	181.2	3632.9

ANOVA

Source of Variation	*SS*	*df*	*MS*	*F*	*P-value*	*F crit*
Between Groups	4330.1	3	1443.4	0.16	0.92	2.7
Within Groups	1228008	138	8898.6			
Total	1232338	141				

Fertiliser spreading in little or no wind can decrease the CV. However, it may also increase the CV; the wind displacement look up tables in Chapter 2 showed that in still conditions the modelled swath width was narrow (< 10 m), if a spreader is not attached. In little to no wind conditions, it would be necessary to apply fertiliser at narrower swath widths and hopper door openings to achieve the intended application rate.

Figure 4.1 and Figure 4.2 compares the field application rate with the distance of the collector to the nearest treatment boundary line for Trial 4 and 5, respectively. A positive distance indicates the collector was within the low application zone, and a negative distance means the collector was within the high application zone. A large variation in the field application rate is expected close to the treatment boundary line (x = 0), as the hopper door opening changes. When the collector is further away from the boundary line, the application rate should vary

around the new average. Less variance is observed in Figure 4.2 for Trial 5 than Figure 4.1. The field application rates in the 500 kg ha^{-1} application zone for Limestone Downs had the largest dispersion of points. This corresponds to the high standard deviation found in Trial 4.

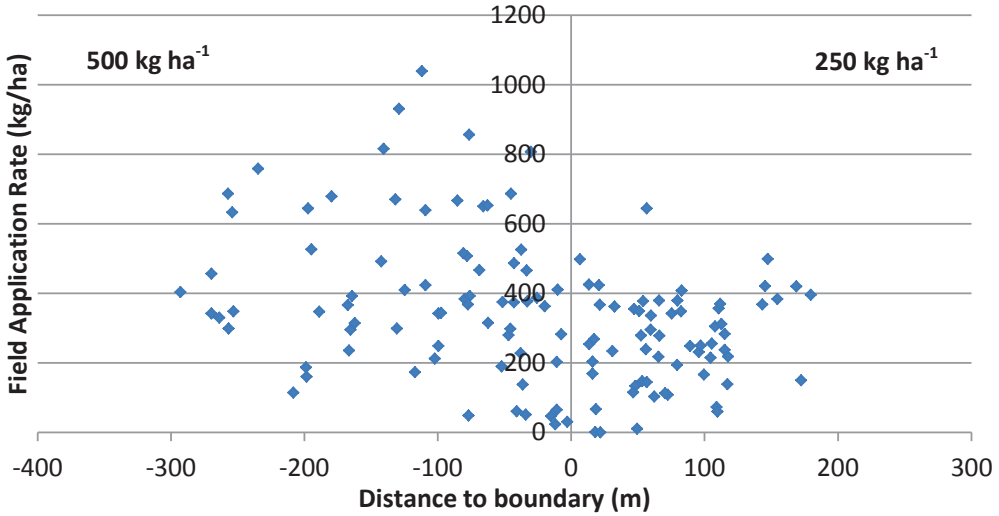


Figure 4.1: Comparison of application rate with the collector's proximity to the nearest treatment boundary line for Trial 4. A positive distance means the collector was in the 250 kg ha^{-1} application zone.

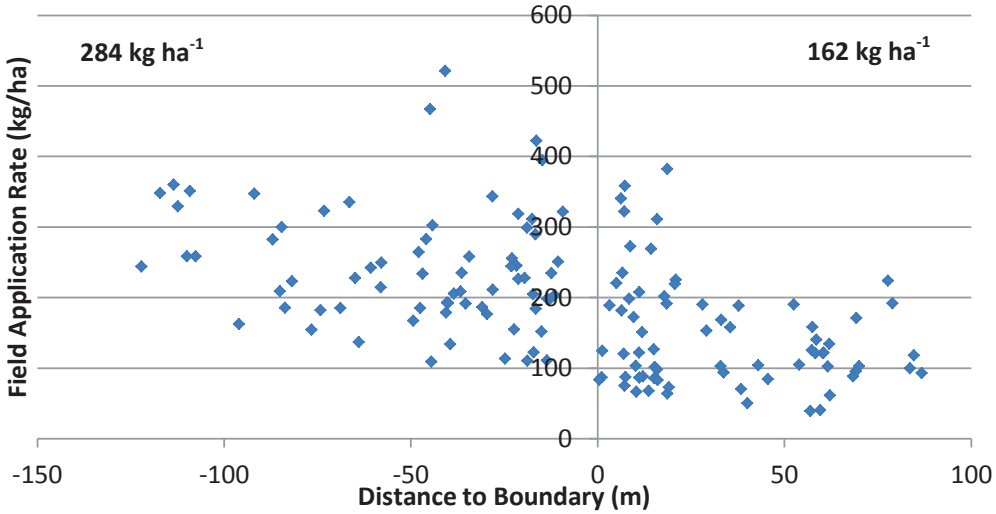


Figure 4.2: Comparison of application rate to the collector's proximity to the nearest treatment boundary line for Trial 5. A positive distance means the collector was in the 162 kg ha^{-1} application zone.

4.2.3. Capability

A one way ANOVA test of the collector data set was undertaken to determine if the averages of the two application zones differed for both trials. Trial 4 and 5 both achieved a highly significant result ($P < 0.001$), which indicates the variable rate system can recognise the treatment separation boundary line and adjust the hopper door opening to apply two rates.

Although there is a high level of variance between the application zones, this result shows the system performed as intended in the field trials.

Kriging can help to visualise the VRAT system's capability. Semi-variograms were produced for the aircraft and collector data in preparation for kriging (Figure 4.3 and Figure 4.4). The y-axis is the semi-variance (ϒ) and the x-axis is the lag distance (m). The exponents represent the magnitude of the semi-variance. The penta-spherical model was used by the four data sets because it provided the best fit. Trial 5's collector data set had to be log transformed to be normally distributed.

Ordinary Kriging (OK) was completed, which assumes a constant unknown mean over the area of interest. OK is the most widely used kriging method as it aims to reduce variance errors so that the mean residual is equal to zero (Kiš, 2016). Trial 4's collector semi-variogram has the largest nugget effect, which indicates that placing collectors 70 m apart is not suitable for kriging (Figure 4.4A). Aircraft data also has a significant nugget effect because the recorded flight points were a minimum of 14 m apart. It is likely that there are significant correlations at shorter distances (Figure 4.3). Compared to collector data, the semi-variogram for aircraft data is better modelled because more spatial information was available.

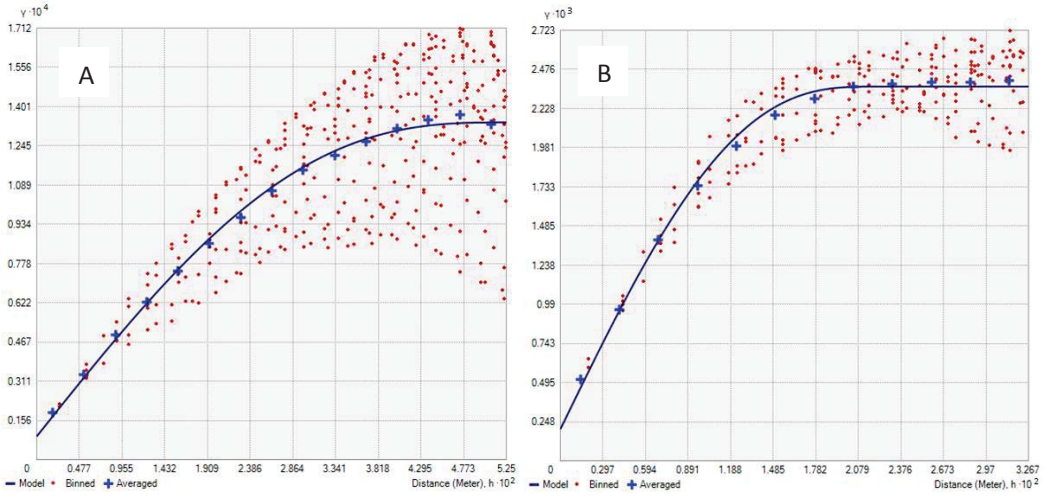


Figure 4.3: Semi-variogram of aircraft data from Trial 4 (A) and Trial 5 (B). The y-axis is the semi-variance and the x-axis is the lag distance (m).

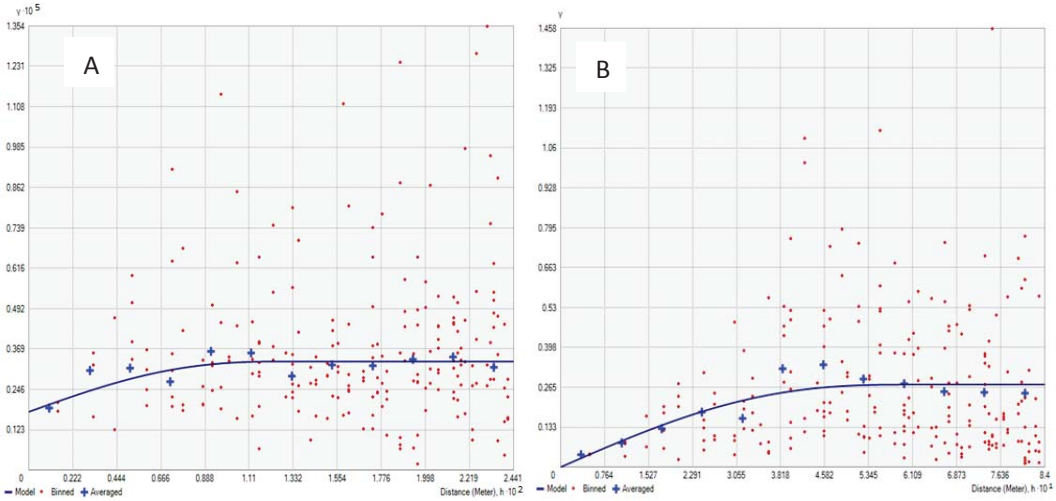


Figure 4.4: Semi-variogram of collector data from Trial 4 (A) and Trial 5 (B). The y-axis is the semi-variance and the x-axis is the lag distance (m).

The semi-variograms for collector data in Trial 4 and Trial 5 have a sinusoidal sill, which represents cyclicity in the data (Pyrcz and Deutsch, 2003). Applied fertiliser creates a normally distributed transverse spread pattern. Overlapping the flight paths, at the optimal swath width, should average the field application rate to the target rate. However, this is difficult to achieve with variability in wind conditions and aircraft operation; hence cyclicity occurs. It is also described as 'hole effect'.

Figure 4.5A and Figure 4.6A are proof of release maps for Trial 4 and Trial 5, respectively. The release maps display an identifiable change in application rate at the treatment separation boundaries. This indicates that the variable rate system made an adjustment in the hopper door as it approached and crossed the boundary. The flight direction can be observed in the high application rate zones since there are strips of different colours. On the other hand, the proof of placement maps do not show the treatment separation boundary (Figure 4.5B and Figure 4.6B). The placement of the collectors led to large areas of interpolation that do not capture the variation in aerial spreading. This is truer for Trial 4's placement map than Trial 5's, because Trial 5 occurred in a smaller area with an improved sampling technique for kriging.

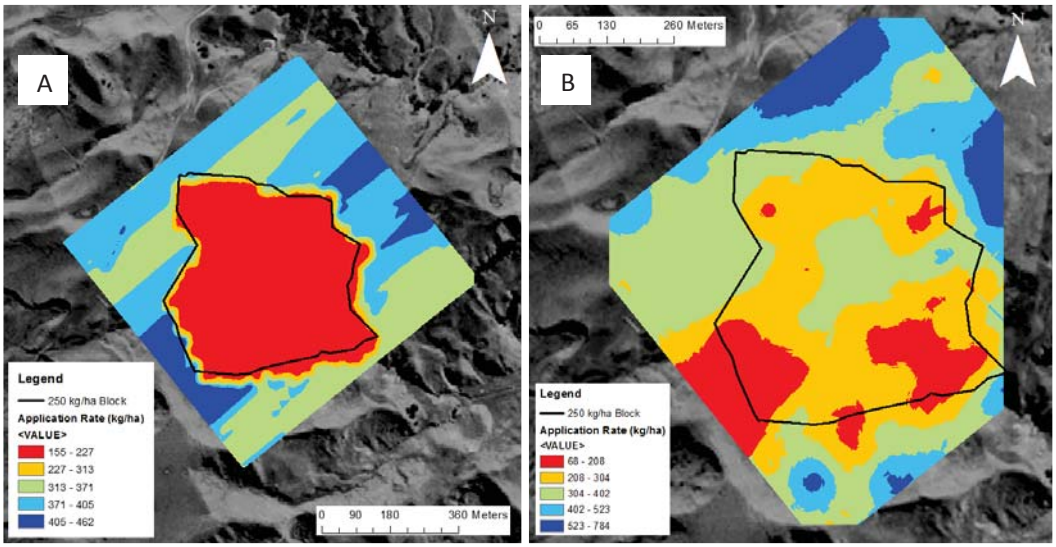


Figure 4.5: Proof of release (A) and placement (B) maps for Trial 4.

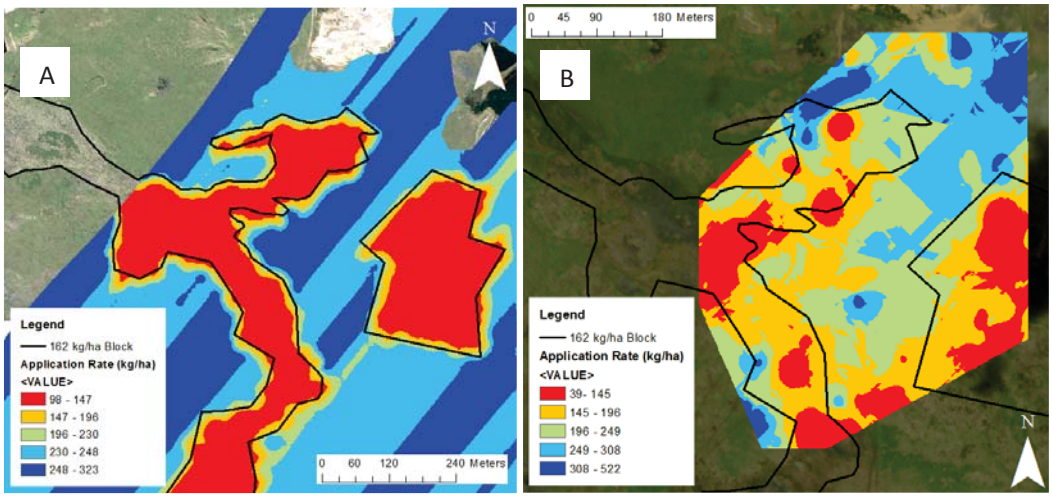


Figure 4.6: Proof of release (A) and placement (B) maps for Trial 5.

Figure 4.7 and Figure 4.8 are plots of the collected/recorded data against the predicted value. These are produced from cross-validation, where points are systematically removed and predicted (Johnston et al., 2001). There are two distinct areas in Figure 4.7 (proof of release), which represent the distribution in the two application zones. The majority of values from the proof of release maps fall along a 1:1 line, which means the predicted values are well correlated with the aircraft recorded application rate. Points that deviate from the 1:1 line are near the treatment separation boundary and are interpolation errors. Therefore, kriging does not predict the application rate well near the boundaries, because the hopper door changes instantaneously, but kriging attempts to produce a gradient in the application rate.

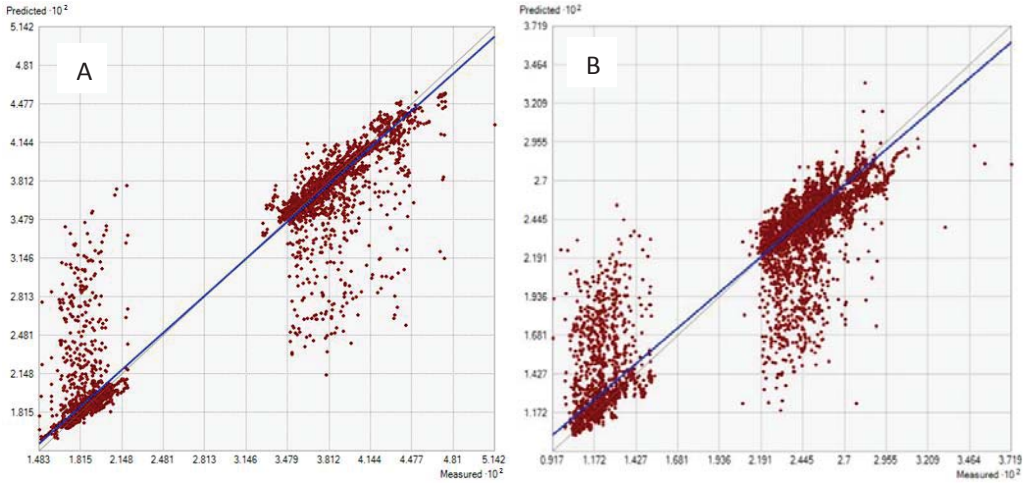


Figure 4.7: Error between predicted values and recorded aircraft values for Trial 4 (A) and Trial 5 (B). The y-axis is the predicted application rate (kg ha^{-1}) that was found using kriging, and the x-axis is the aircraft application rate (kg ha^{-1}).

There was a difference between the predicted and collected data for the proof of placement maps for Trial 4 (Figure 4.8A). For the proof of placement map in Trial 4, there was under prediction of the field application rates for the high rate zone and vice versa. The magnitude of under/over prediction in Trial 4 is significant and this continues to relate to the sampling configuration. Since the collectors were placed far apart, the semi-variogram did not have sufficient samples to make reliable predictions. Trial 5's data set was better correlated to the predicted values, because the sampling configuration captured the spatial variance.

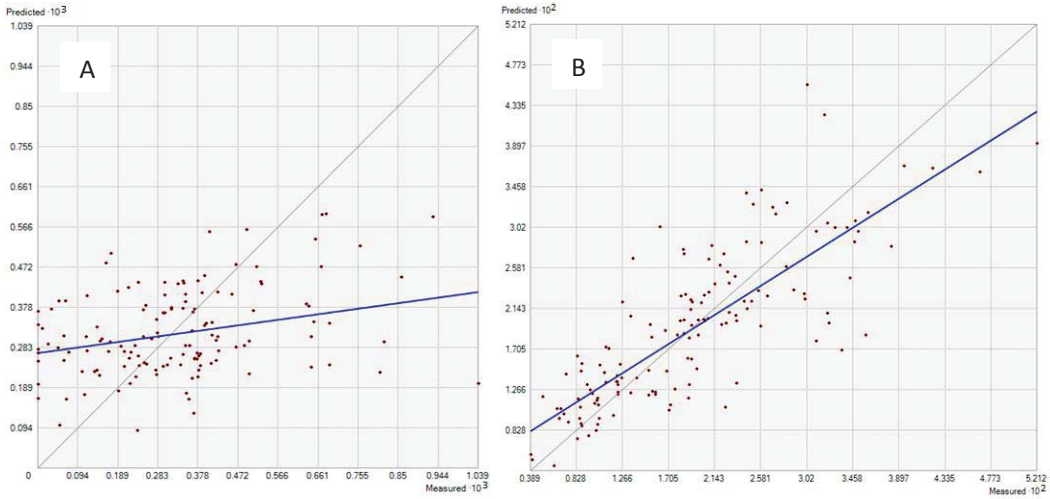


Figure 4.8: Error between predicted values and collector data for Trial 4 (A) and Trial 5 (B). The y-axis is the predicted application rate (kg ha^{-1}) that was found using kriging, and the x-axis is the field application rate (kg ha^{-1}).

Figure 4.9 shows the prediction standard error (PSE) for collectors in Trial 4 and 5. PSE is the square root of the prediction variance and indicates the uncertainty of an intermediary point

(Johnston et al., 2001). If the collected data is normally distributed, the true value of any prediction should be within two times of the standard error for 95% of the events. Figure 4.9 show predictions made far from the collected data have significant variances, which makes the overall map less reliable. Most of the area at Trial 4 had a PSE greater than 100, which means the predictions could be ± 200 kg ha^{-1}. This error is similar, in magnitude, to the low application rate (250 kg ha^{-1}), which means the estimated field application rate could be almost double the low application rate or near zero. Although, this has been observed in the field results in Trial 4, the level of variability makes it difficult to predict exact values using geo-statistical analysis. A significant area of Trial 5 also had a PSE over 100. Red areas in Figure 4.9 represent low PSE, which occur because of the high sampling frequency in that area.

High PSE could occur because of kriging error, collector error, changes in flow rate out of the hopper door, stochastic variability in aerial topdressing (noise), or a combination of these factors. Figure 4.9 does not indicate which of the factors contribute to the standard error. However, it does show that the maps produced by kriging are not suitable for aerial topdressing. There is too much variance to model, and kriging does not produce a good representation of the aerial performance trials. It might be possible to collect a representative sample size if there were more collectors, so that a more accurate placement map is produced. However, this will be prohibitively expensive.

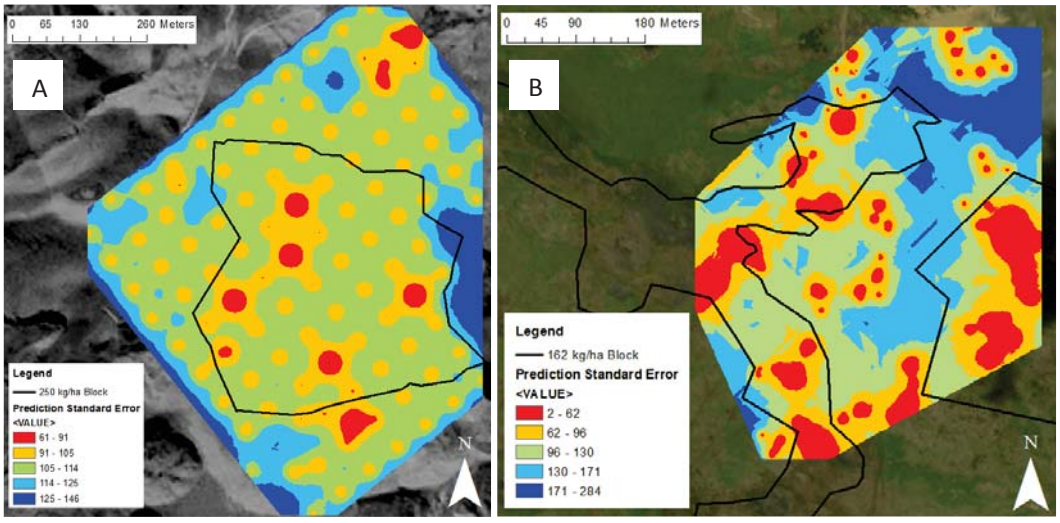


Figure 4.9: Prediction standard error maps for collector data for Trial 4 (A) and Trial 5 (B).

4.3. Bench Testing

Bench testing was used to test the electronic/mechanical/hydraulic response of the VRAT system under different settings. This method is cheaper and less time consuming than carrying out field trials. Bench testing also allows the electronic/mechanical/hydraulics' of the system

to be assessed without the uncertainty of field variability. Bench testing was completed intermittently over a year, using a fully operable G4 Satloc Intelligate variable rate system. The Satloc program has a simulated flight function, which allows an uploaded prescription map to be tested. It can be programmed to be in any geographical location. The simulation uses the co-ordinates of the application area in the prescription map; the user needs to input the initial co-ordinates of the aircraft. The aircraft's heading and velocity can be adjusted. A hydraulic hopper door was attached to the bench test VRAT unit. The Satloc system automatically adjusts the hopper door to the opening stated in the prescription map based on the simulated aircraft's location. Therefore the VRAT system could be assessed on how it responds to different scenarios.

Multiple scenarios were bench tested to determine the limitations of the VRAT system. The majority focussed on the system's response to application zone boundaries. The output measured from the log files was the distance it took the hopper door to respond to a boundary. If the response distance was negative, the hopper door opened/closed outside the application zone, and if the hopper door opened/closed inside the boundary, a positive value was assigned. Ideally, the response distance would be positive. The ruler tool in Mapstar 8 measured the response distances to one decimal point. In some scenarios, ANOVA was used to test statistical significance, which objectively determined whether a factor had an effect on the response distance.

4.3.1. Method

Prescription maps were prepared for bench testing, using ArcGIS 10.1 and Mapstar 8. The maps include the GPS points of the application zone vertices, application rates used in the prescription map, and the hopper door opening for each application rate. The application rates are used as labels to organise each zone. Hopper door openings are written in number of 1/16 inches (e.g. 33 is equivalent to 2.06 inches, which is 0.052 m) and ranged between 0 and 48. The hopper could have wider openings, but the bench test unit was not calibrated to do so. Figure 4.10 and Figure 4.11 show the automated hopper door at the closed (door opening 0) and open position (door opening 48), respectively. When initialising a prescription map, the location of the aircraft has to be shifted from its default location (USA). Figure 4.12 shows the bench test VRAT and hydraulic system. To ensure the log file is recorded and the hopper door responds, the whole system is activated. If it is not switched on, the simulated aircraft can fly over the application zones with no effect.



Figure 4.10: Aircraft hopper door in closed position.



Figure 4.11: Aircraft hopper door in the open position.



Figure 4.12: Mechanical set up of variable rate bench testing unit.

Figure 4.13 shows the pilot interface after a simulated flight of a prescription map was completed. The blue lines represent the hopper in the closed position and bold green lines are an open hopper door. The flight lines can be downloaded and re-projected in Mapstar 8. In Figure 4.13, the aircraft was flying at a velocity of 71.5 m s^{-1} and a heading of 0° and 180° in a to and fro pattern.



Figure 4.13: Satloc user interface with simulated flight example. Blues lines represent a closed hopper and bold green lines are an open hopper. The red square is the application area.

4.3.2. Results and Discussion

4.3.2.1. *Part 1*

The objective of Part 1 was to determine the response time of a single and dual accumulator. An accumulator is a pressure storage reservoir that holds a non-compressible fluid under pressure. A small external force is used to activate and release the potential energy from the pressurised fluid. The dual accumulator has two charging valves, while a single accumulator has one. The dual accumulator allows the hopper door to react faster, which is advantageous, but more expensive.

Twenty response times were recorded for each accumulator. Ten responses were measured for the aircraft's entry into an application zone and the other half were for the exit. On average, the dual accumulator performed twice as fast as the single accumulator for both the 'edge on' and 'edge off' setting. A single accumulator had a response time of 0.34 – 0.37 s, while the dual accumulator had a response time of 0.18 – 0.23 s. Therefore an aircraft travelling at 61 m s^{-1} with a dual accumulator will respond in 11 – 14 m, while single accumulator will take 21 – 23 m to fully open and close the hopper door.

4.3.2.2. *Part 2*

Part 2's objective was to determine the distance the hopper closes or opens in relation to the treatment separation line depending on the 'edge on' and 'edge off' settings on the VRAT system. 'Edge on' is the time the hopper door will open when approaching an application zone. While 'edge off' is the time the hopper should close before the aircraft leaves the application zone. Timings were tested at 0.05 s, 0.1 s and 0.1 s intervals to 1.1 s. The hopper gate position and aircraft velocity used in the tests were 33 m s^{-1} and 67 m s^{-1}, respectively. The application area was 1000 m by 1000 m (Figure 4.14).

The distance between the opening and closing of the hopper door to the boundary is plotted in Figure 4.15. The 'edge off' setting performed as expected. As the setting increased, the hopper door closed earlier within the application zone so the distance between the hopper door closing and the boundary increased. 'Edge on' operated to 0.5 s, where increasing the setting opened the door earlier. After 0.5 s, the distance the hopper door opens in relation to the boundary did not change significantly. Based on these results, an 'edge on' setting of 0.4 s and an 'edge off' setting of 0.7 s was found to be most appropriate for applying fertiliser within a boundary when using a dual accumulator. For a single accumulator, Trial 6 showed that a setting of 0.4 s for the 'edge on' and 1.3 s for the 'edge off' was sufficient.

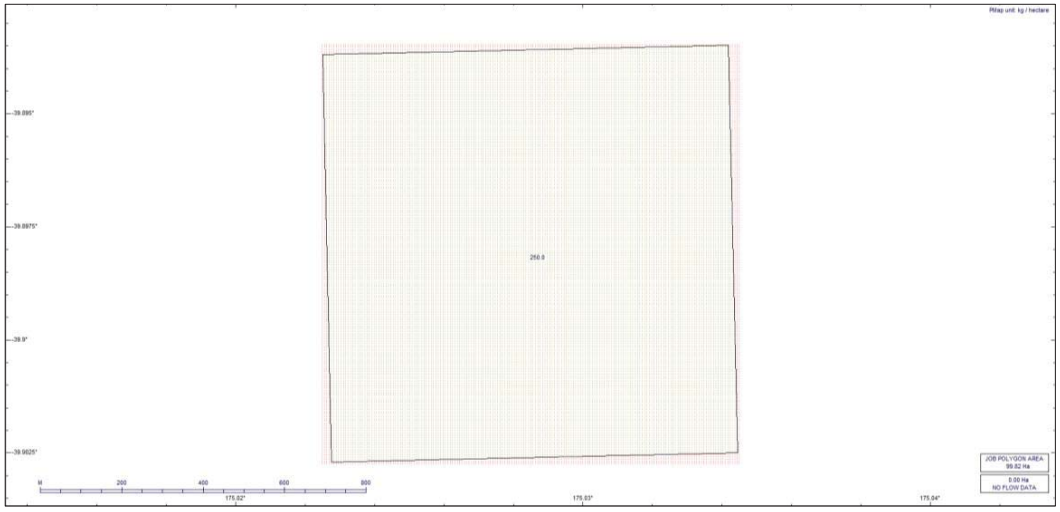


Figure 4.14: Example of 1000 m by 1000 m application zone displayed in Mapstar 8.

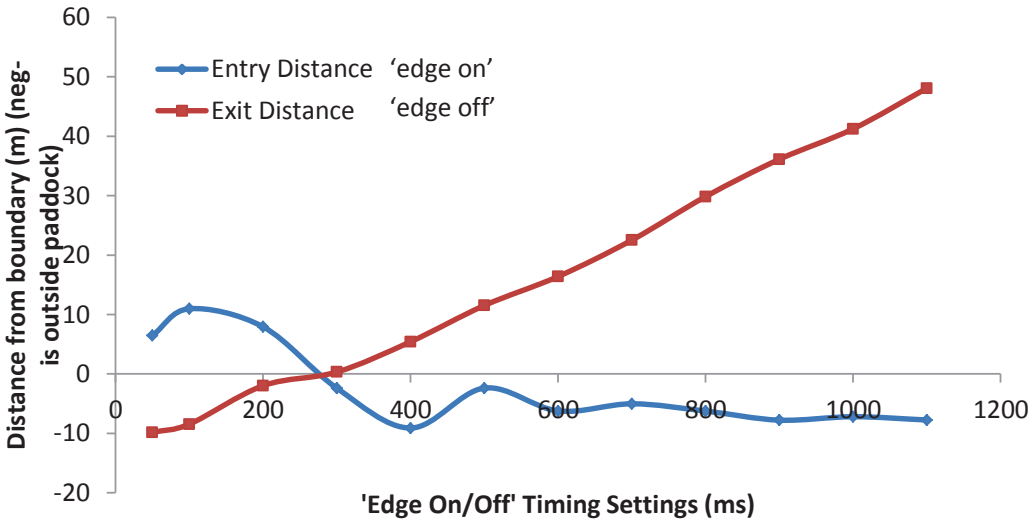


Figure 4.15: Distance to/from boundary against the edge on/off setting for a dual accumulator.

4.3.2.3. ***Part 3***

In Part 3, the simulated aircraft flew over two polygons separated by a zero application gap (Figure 4.16). The length of the gap varied between 10 m to 400 m. The objective of this test was to determine how a gap of varying length (10 – 400 m) affects the VRAT system. The standard hopper gate opening was 33 and the simulated aircraft velocity was 67 m s^{-1}. A dual accumulator was used, and the 'edge on' and 'edge off' setting was 0.5 s and 0.9 s, respectively. These settings were pre-set in the prescription maps before the results of Part 2 were known. This 'edge on'/'edge off' setting was used for Part 3 – 8.

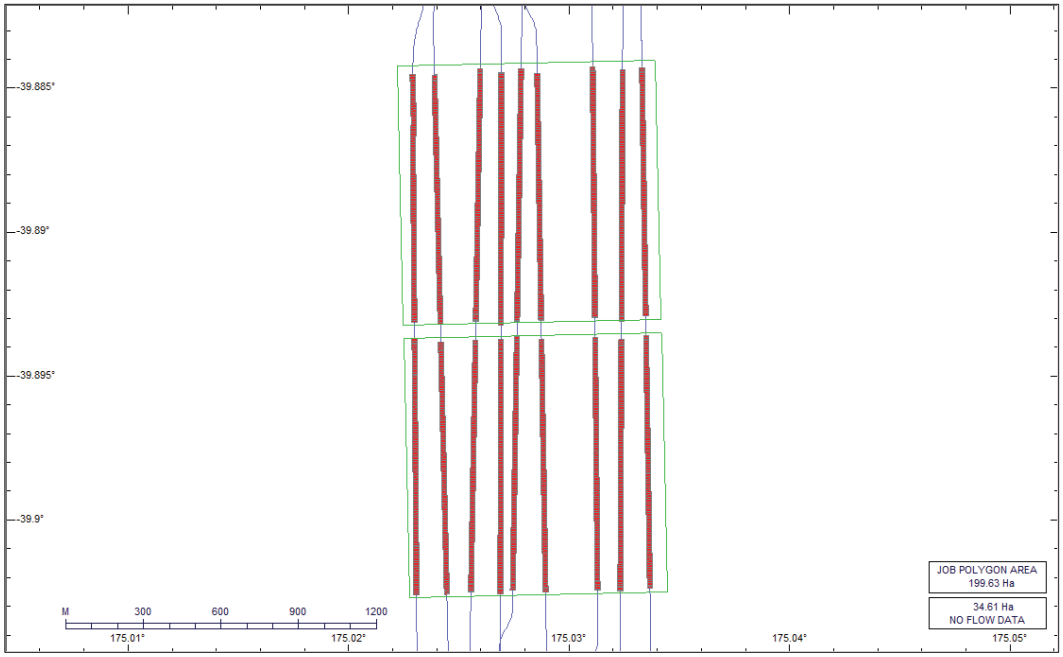


Figure 4.16: An example of a prescription map and flight lines for Part 3 displayed in Mapstar 8. This shows a 50 m gap. The green line represents the application area. Flight lines are represented by the blue (fully closed hopper) and red lines (open hopper).

The log files showed that when the gap was 15 m or less the hopper door would not fully shut for the gap before opening again. This occurred because the distance was too short for the velocity of the aircraft, the GPS log rate of the VRAT system, and for the response time of the accumulator. For an aircraft travelling at 67 m s^{-1}, data is logged every 13.4 meters. It is, therefore, difficult for the system to respond to changes in the hopper door opening that occur in less than 0.2 s. Additionally the system's lag will contribute to the delay in the response, and for a single accumulator, the system lag will be twice as long.

In general, an application zone should not be less than 15 m in the direction of flight for a dual accumulator. If the gap is an exclusion zone, a buffer is necessary to prevent off-target application. Buffers should be added to the excluded area so that the flight length of an exclusion zone is greater than 15 m. It is also important to consider the forward motion of particles, which would increase the buffer zone area. The buffer size can be determined using the ballistics model, discussed in Chapter 2, and the aircraft heading, because if the aircraft is travelling perpendicular to the exclusion zone, the buffer would be larger than if the aircraft travelled parallel.

4.3.2.4. ***Part 4***

This section investigates how the angle of the entry/exit boundary affects the hopper response distance. The VRAT system lacks the ability to recognise or compensate for angled boundaries,

so this test will determine the effect of flying at an angle into a boundary will have on off-target application. Boundaries varied between 10° − 80° and the simulated aircraft flew directly North and South in a to and fro direction (Figure 4.17). The gate opening was constant at 33 and the aircraft velocity was 67 m s^{-1}. The swath width was set at 19.8 m.

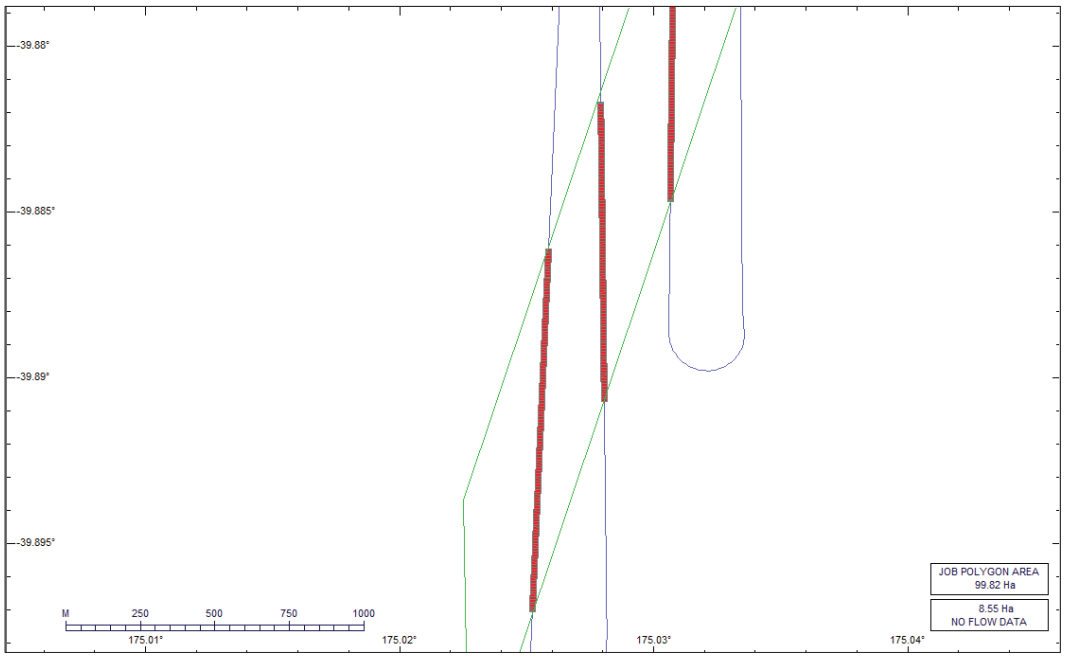


Figure 4.17: An example of a prescription map and flight lines from Part 4 displayed in Mapstar 8. This polygon is angled 20 degrees.

A one way ANOVA test was used to determine if there was a difference in the distance that the hopper door opens or closes in relation to the sloped treatment separation line. A difference was not observed. However, due to the angle of the boundary, an area of the swath was applied outside the application zone. This meant that as the boundary angle increased, more fertiliser was applied outside the boundary. If there is a sensitive zone along the treatment separation line, this would be an issue. To minimise fertiliser entering sensitive areas, it is recommended the pilot fly perpendicular to the entry boundary rather than at an angle.

4.3.2.5. ***Part 5***

The objective of Part 5 was to determine if the number of vertices in a prescription map will increase the response time as an application zone becomes more complex. The Satloc Intelligate G4 system states that the maximum number of vertices allowed for a single polygon in a prescription map is 250. This was assessed using ANOVA tests and determining whether the VRAT system made mistakes (i.e. wrong door opening). The test represents application jobs where a single rate is applied over a whole farm or a simple variable rate job (i.e. two large areas with different application rates on a farm). Prescription maps were set up where a

1000 m by 1000 m square was reshaped to create a polygon with 5, 10, 50, 100, 150, 200, and 250 vertices (Figure 4.18). Gate opening and aircraft velocity was set at 33 and 67 m s^{-1}, respectively. In some cases, Mapstar 8 did not include all the vertices created in ArcGIS 10.1. Mapstar 8 may not have identified them as vertices because they were not pronounced. A one way ANOVA test comparing the entry and exit response distance for the different number of vertices did not find any statistically significant relationship at a 95% confidence interval. This indicates the number of vertices for a single polygon is not an issue for the performance of the VRAT system.

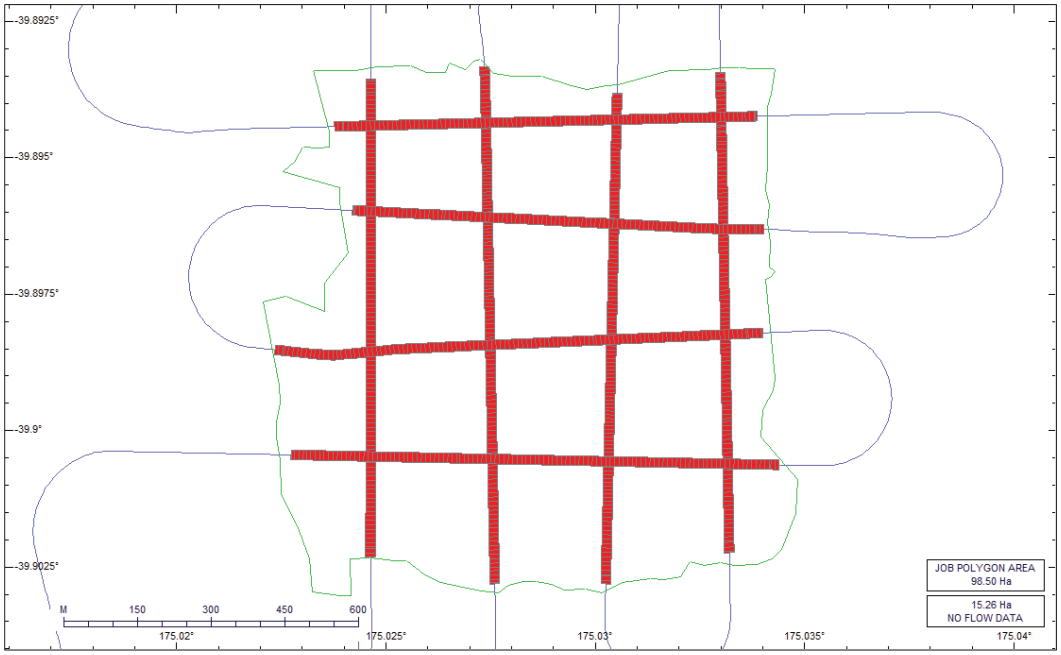


Figure 4.18: An example of a prescription map and flight lines for Part 5 displayed in Mapstar 8. This polygon has 100 vertices.

4.3.2.6. ***Part 6***

The objective of Part 6 was to determine if the file size and number of vertices had an effect on the VRAT system's performance. Accuracy was measured by the percentage the hopper door opened to the correct position. The Satloc system manual states it can process a maximum of 10,000 vertices in a single prescription map. Three prescription maps were tested with varying number of vertices. Each prescription map was a paddock map of a large New Zealand farm. The farms are named Farm 1, Farm 2, and Farm 3. Each paddock on the farms was randomly assigned an application rate of either 200 kg ha^{-1} or 350 kg ha^{-1}, and a hopper door opening of 33 and 46, respectively. Aircraft velocity varied between 51 and 77 m s^{-1}, and both the 'edge on' and 'edge off' setting was set at 0.5 s.

Table 4.3 shows there were incorrect hopper door openings over some areas of the application map. The results suggest prescription maps with more vertices are less accurate. Reasons for inaccurate hopper door openings include the lack of response from the VRAT system as the aircraft travelled between application zones, and a delayed system response. Errors could be explained by frequent changes in the hopper door position, and increased processing time required for large files, which delays the hopper door. This is a limitation that needs to be examined in future work, as it can significantly impact field application rate, CV and off-target application.

Table 4.3: Percentage of correct hopper door openings for bench tested prescription maps of different sizes.

		Correct Hopper Door Opening Percent (%)	
Farm	**Vertices**	**200 kg ha^{-1}**	**350 kg ha^{-1}**
Farm 1	4802	89.9	91.7
Farm 2	6188	82.38	78.33
Farm 3	7745	87.1	74.75

4.3.2.7. ***Part 7***

Part 7 is to determine the effect of hopper door opening and aircraft velocity on the response distance. Three gate openings (33, 38 and 43) were tested at each velocity increment (62, 67 and 72 m s^{-1}), so nine prescription maps were used. The simulated aircraft flew over a 1000 m by 1000 m application zone. Using a two factor ANOVA test, a comparison of the response distance based on velocity and gate opening was made (Table 4.4). At a 95% confidence interval, aircraft velocity was found to have no effect on the response distance ($P > 0.05$) but aircraft hopper door setting did ($P < 0.05$). This indicates that previous results and conclusions from bench testing will not be affected by changes in aircraft velocity, but a change in the aircraft hopper door opening will likely have an effect on the response distance.

Table 4.4: Two-way ANOVA test comparing hopper door opening and the aircraft velocity to the distance the hopper door closes in relation to the application zone boundary.

SUMMARY	28	38	48	Total		
Aircraft velocity (knots) = 120						
Count	4	4	4	12		
Sum	97.7	81	65.9	244.6		
Average	24.4	20.3	16.5	20.4		
Variance	29.4	0.96	12.8	23.3		
Aircraft velocity (knots) = 130						
Count	4	4	4	12		
Sum	98.1	95.1	75.6	268.8		
Average	24.5	23.8	18.9	22.4		
Variance	14.9	12.3	21.4	20.0		
Aircraft velocity (knots) = 140						
Count	4	4	4	12		
Sum	109.1	93	77	279.1		
Average	27.3	23.3	19.3	23.3		
Variance	7.8	24.7	3.4	21.5		
Total						
Count	12	12	12			
Sum	304.9	269.1	218.5			
Average	25.4	22.4	18.2			
Variance	16.1	130	11.9			
ANOVA						
Source of Variation	*SS*	*df*	*MS*	*F*	*P-value*	*F crit*
Sample (rows)	52.3	2	26.1	1.8	0.17	3.4
Columns	314.1	2	157.0	11.1	0.00031	3.4
Interaction	15.9	4	4.0	0.28	0.89	2.7
Within	382.6	27	14.2			
Total	764.8	35				

4.3.2.8. ***Part 8***

Combinations of application rates in different zones were tested in this part to determine if the VRAT system could respond accurately. Figure 4.19 is an example of a complex prescription map that was tested. The large square application zones were 500 m by 500 m. 'Edge on' and 'edge off' was set at 0.5 s and 1.6 s, respectively for the single accumulator. In general, the VRAT system operated as expected. However, when a zero application rate zone of 20 m and 50 m was introduced between two adjacent application zones (Figure 4.20), the VRAT system did not respond as intended (Figure 4.21). This occurred because the 'edge off' setting was too large for the zero rate zone. As a result, the hopper door could not fully close before opening for the next application zone. This was studied in Part 3 for a dual accumulator. With the single

accumulator, reducing the 'edge off' time to 0.9 s resolved the issue for the 50 m gap. A solution was not determined for the 20 m gap. To ensure this does not occur in the field, exclusion zones should be suitably sized to avoid off-target application.

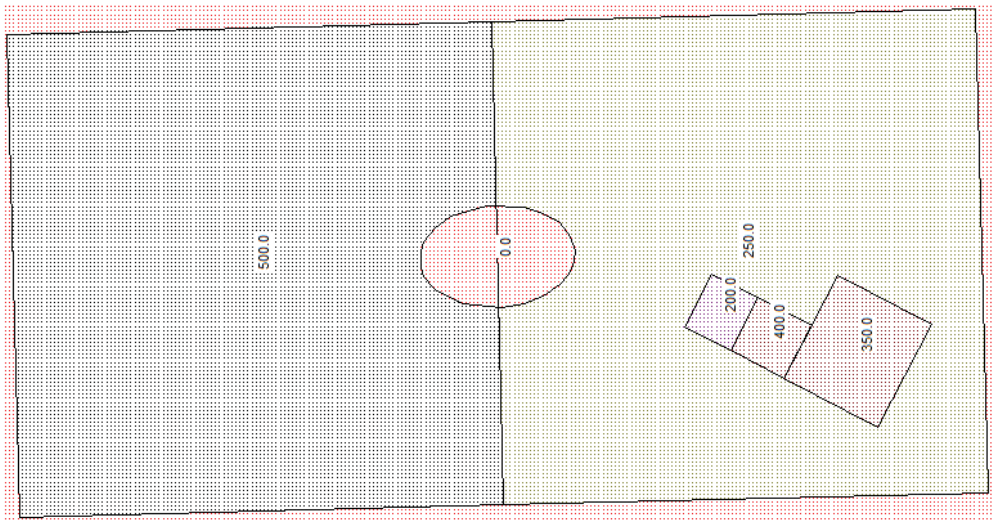


Figure 4.19: An example of a prescription map that consists of adjacent polygons (250 and 500 kg ha^{-1}), exclusion zones (0 kg ha^{-1}) and different application rates (200, 350, 400 kg ha^{-1}). This is displayed in Mapstar 8.

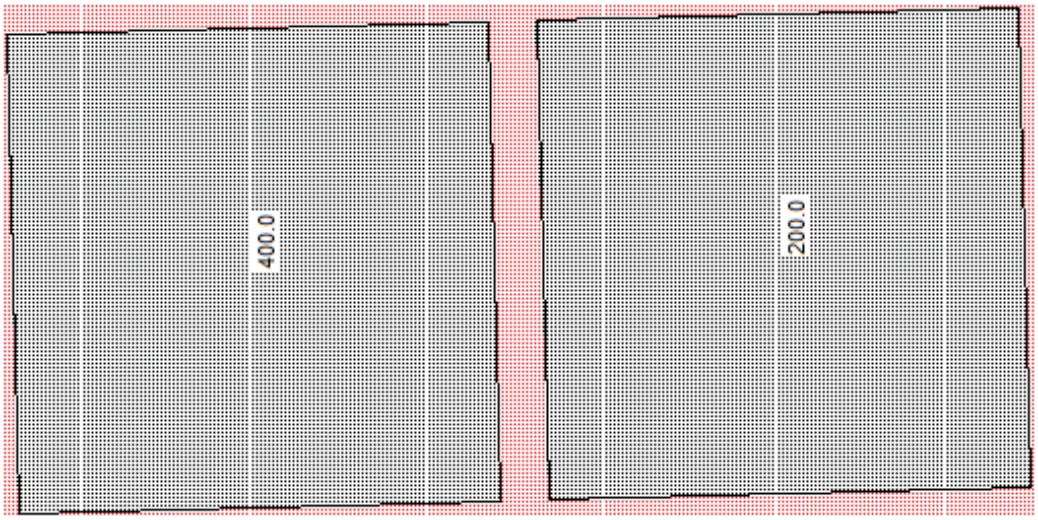


Figure 4.20: Two polygons separated by a gap of 50 m, where no application should occur. Application rates in the polygons are 200 and 400 kg ha^{-1}. This is displayed in Mapstar 8.

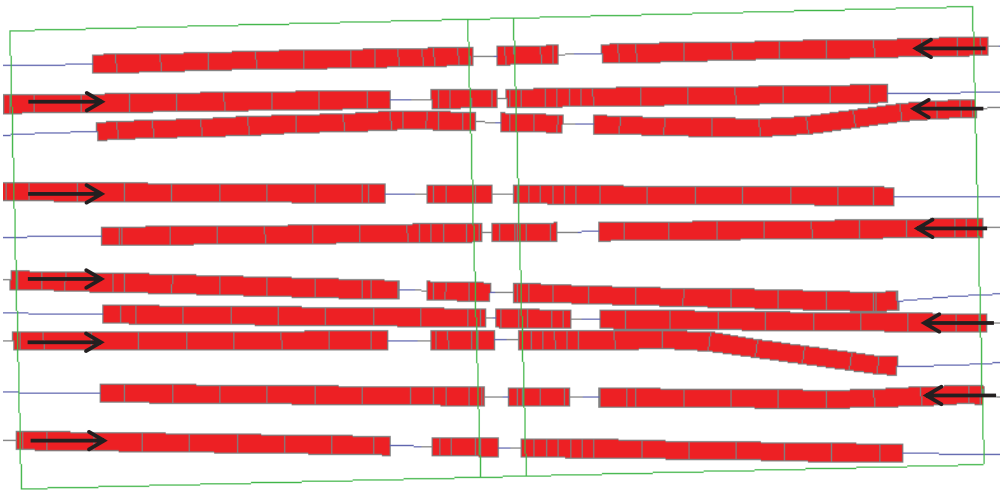


Figure 4.21: Simulated response of Figure 4.20 from the bench VRAT system in Mapstar 8 based on 'edge on' setting of 0.5 s and 'edge off' of 1.6 s. Entry into the application zone is denoted by the black arrows. The system did not react as intended.

4.3.2.9. ***Part 9***

Fertiliser application was completed on a large farm but there was an issue with the variable rate controller. Some fertiliser was applied to a waterway highlighted in Figure 4.22. In the prescription map, the waterway was not enclosed so it was considered a zero application area and treated the same as the area surrounding the application zone. This means 'edge on/off' timings were in effect. However on farm, the hopper door opened over the waterway. Bench testing was completed to determine why the variable rate system did not perform as intended and to find a solution.

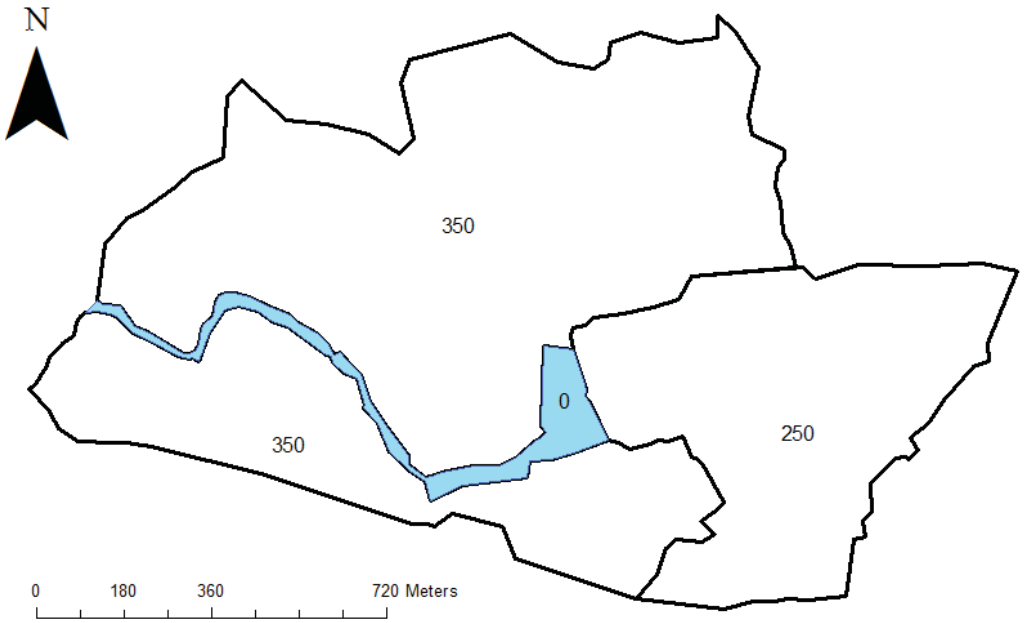


Figure 4.22: Large farm prescription map for variable rate application.

Bench testing found that the strip was too narrow for the 'edge on/off' time setting, which meant the hopper door did not have sufficient time to close before it had to reopen. The best solution was to create an enclosed polygon of the waterway, and assign a generic label (i.e. 50 kg ha^{-1}) in the prescription map with a door opening of 0. In an earlier attempt, the waterway zone was labelled 0 kg ha^{-1} with a zero door opening, but the VRAT system did not recognise it as an application zone and the hopper door did not perform accurately. The enclosed polygon method excluded most of the zone correctly (Figure 4.23). However, in some areas, the waterway was too narrow and the hopper door could not react accordingly. If the best solution is used, a buffer is required to account for the forward motion of fertiliser particles.

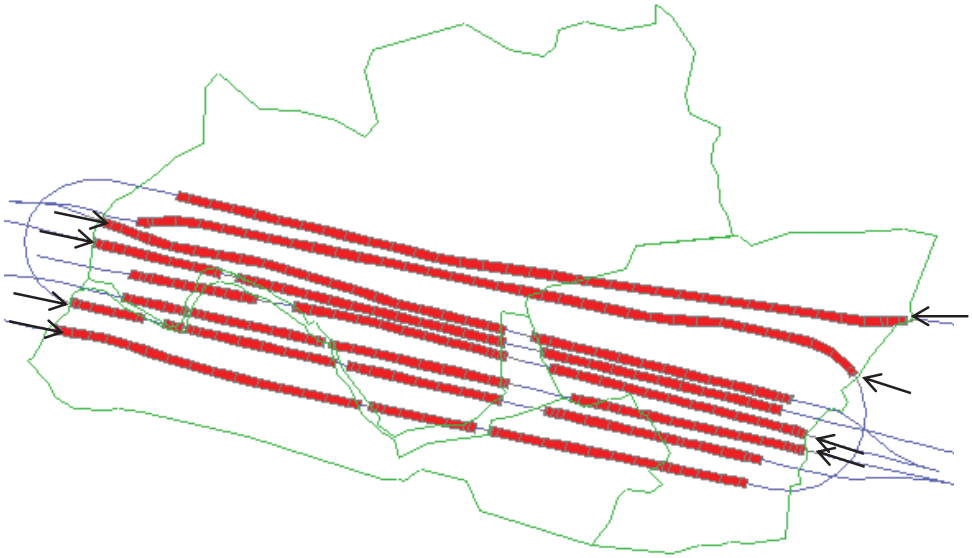


Figure 4.23: Response from creating an exclusion application zone displayed in Mapstar 8. Entry into the application area is denoted by black arrows. The red strips represent an open hopper door.

The purpose of a buffer zone is to minimise the amount of fertiliser that lands in an exclusion area. The size of a buffer zone is dependent on the wind conditions, size of the exclusion zone, direction of flight and the forward motion of particles. Ballistics modelling can be used to determine the forward motion of particles and the effect of wind. In no wind conditions, buffers should be 35 m on either side of the exclusion zone to account for the changes in the aircraft heading. This value was estimated using the ballistics model, which considers average conditions and particle sizes. Therefore the 35 m buffer may not prevent outlying particles from landing in a sensitive zone.

4.4. Static Hopper Flow Calibration

The objective of the static hopper flow calibration test was to determine the flow characteristics of superphosphate, DAP and urea from a typical PAC 600 hopper. This was so a

standardised method of determining the hopper door openings required for a flow rate could be formulated. On an automated system, where fertiliser is applied at different rates, the flow rate out of the hopper is controlled by the hopper door opening. Therefore, it is important to calculate the hopper door required to achieve an application rate. This has been difficult to determine in the past, because there are multiple variables to consider during aircraft operation that will affect the mass flow rate out of the hopper. Currently, the Beverloo equation is used to determine the required hopper door position, which may not be suitable in predicting flow rate from a topdressing aircraft hopper. The static hopper flow trial provides flow rate measurements for the hopper door, which could be used to validate the Beverloo equation, or provide an alternate means of determining hopper door openings. This would assure the pilot that the correct application rates are applied over the farm.

A PAC hopper was connected to two weigh cells linked to a weighing terminal (Mettler Toledo IND560). The terminal recorded the change in mass with respect to time as the hopper emptied of fertiliser. Weights were recorded every 2 s, while the hopper was suspended in the air, using a forklift. The hopper door was not automated; therefore, it could not be opened to specific settings. Instead, the hopper door was opened manually and once flow stopped, the opening was measured (in inches) using a calliper that was accurate to four decimal points (Figure 4.24). Flow was regulated by clam shell doors, which are no longer installed on aerial spreaders; instead cantilever doors are used. This may affect the final results, but in these initial tests only the clamshell door was available. After these tests and Trial 8 was completed, it was decided that further tests were necessary with a cantilever door, which will be discussed in Section 4.6.

The number of runs completed was not sufficient for good statistical analysis; six runs were undertaken for superphosphate, five for DAP and nine for urea. However, this is an initial investigation and further work will be done once the correct hopper door is installed. Replicates should also be completed for some hopper door openings to determine the variance in the flow rate. For the trial, the hopper was filled to its maximum capacity, which was 1400 – 1800 kg depending on the fertiliser type. It was filled using a spreading truck until fertiliser overflowed from the top of the hopper. The PAC hopper was asymmetrical and did not have a conventional hopper shape (Figure 4.25).



Figure 4.24: Hopper door was manually opened using the lever and, in this case, the flow rate of superphosphate was being measured.



Figure 4.25: Static PAC hopper with clamshell doors operated by a lever (on left). A Mettler Toledo display is fixed on the front (centre of picture).

As fertiliser exited the hopper door, funnel flow was observed for all three fertiliser types, where fertiliser from the top of the load exits before the bottom material (Figure 4.26). Approximately 15 – 30 kg of fertiliser remained on the hopper door, and this was more

noticeable with a narrow hopper door position. In the field, urea and DAP are applied at lower rates than superphosphate so small hopper door openings were tested in their runs. The particle size distribution was found by sieving a sample of each fertiliser type so that the average particle diameter could be determined for the Beverloo equation. The bulk density was supplied by the manufacturing plant, which measures it frequently to satisfy product quality standards.

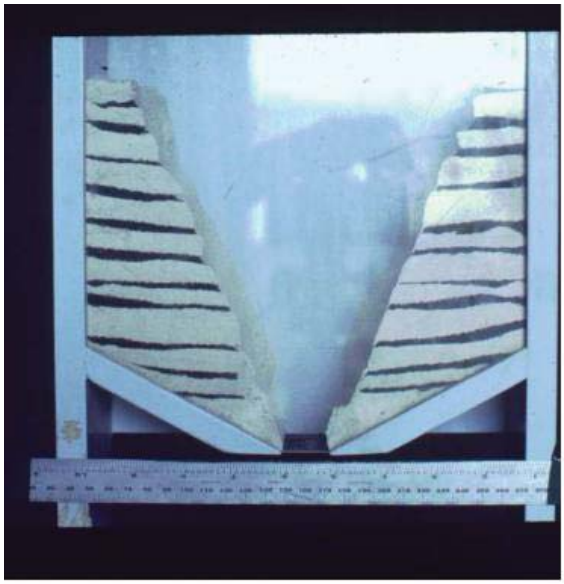


Figure 4.26: Example of funnel flow regime for a powder, courtesy of John Maber (Grafton, 2010). The angle of the standard PAC hopper allowed the hopper to empty and ratholing did not occur.

The flow profiles differ depending on the size of the door position. The initial flow out of the standard PAC hopper increased rapidly until it reached the peak flow rate, where it stabilised. After the peak rate, the flow rate decreased quickly. Small oscillations were also captured in the flow. During the experiment, the whole system juddered. This was likely caused by funnel flow dynamics, where fertiliser fell from the top of the hopper to the hopper door. Additionally, measurement error was likely, due to the sensitivity of the sensors. Preliminary results showed that for small hopper door openings, the flow rate was constant. For example, Figure 4.27 shows an almost constant flow rate for superphosphate at a 0.025 m door opening. For larger hopper door openings, the flow profile is hill shaped and there are several flow regimes present. From the static flow tests, hopper door positions greater than 0.046 m resulted in a hill shaped flow profile (Figure 4.27). The largest hopper door position tested was 0.075 m, where the flow rate did not remain at the peak rate for very long. Having different flow profiles made it difficult to predict the flow rate out of the hopper door at any one time.

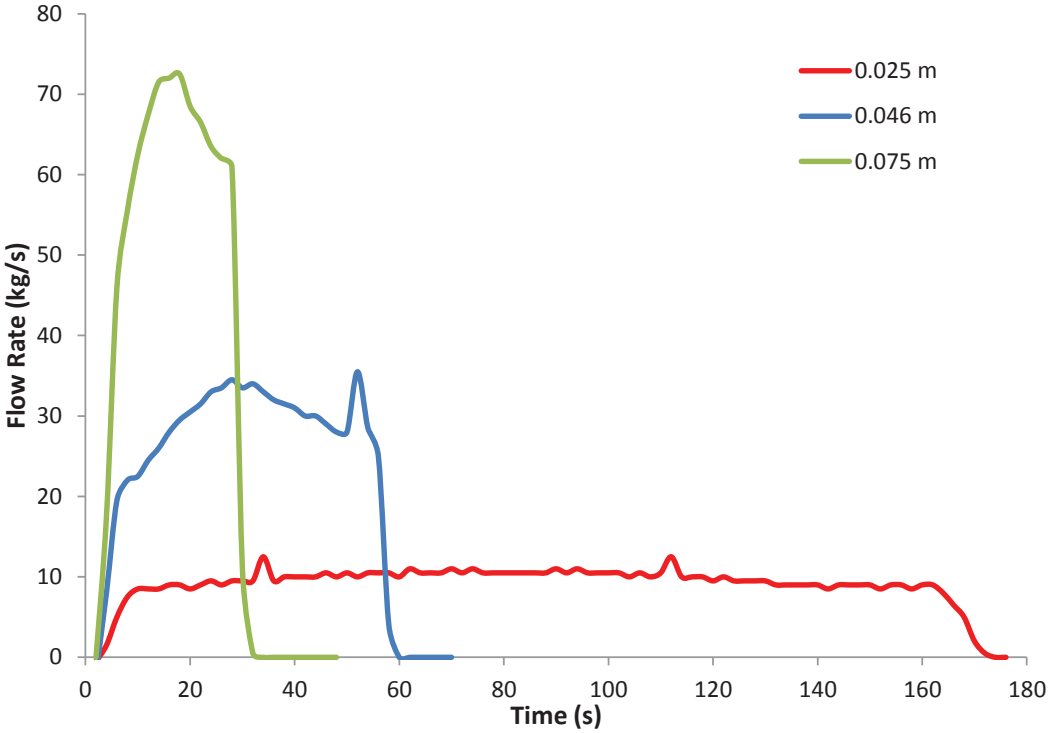


Figure 4.27: Flow rate out of the clamshell hopper door against time for three door openings (0.025 m, 0.046 m and 0.075 m).

The flow rates were averaged so that they could be plotted against the hopper door position. Each fertiliser type found a positive linear relationship between the hopper door opening and the flow rate out of the door (Figure 4.28 - Figure 4.30). R-Squared values for all three fertiliser types were above 0.98, which shows a strong linear relationship.

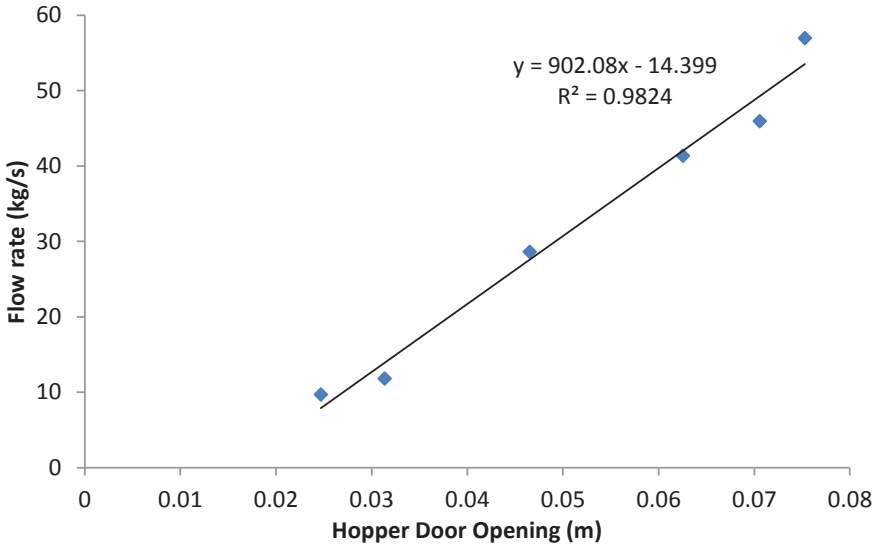


Figure 4.28: Relationship between flow rate and the clam shell hopper door opening with linear regression for superphosphate.

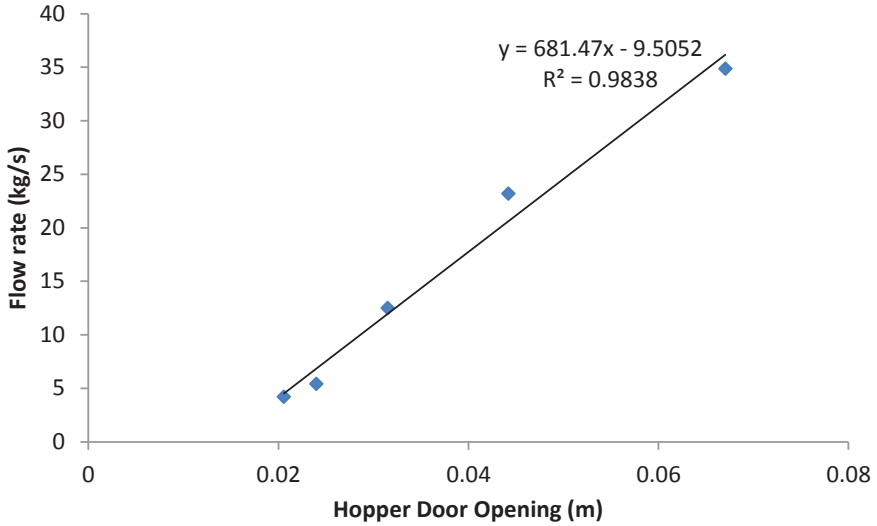


Figure 4.29: Relationship between flow rate and the clam shell hopper door opening with linear regression for DAP.

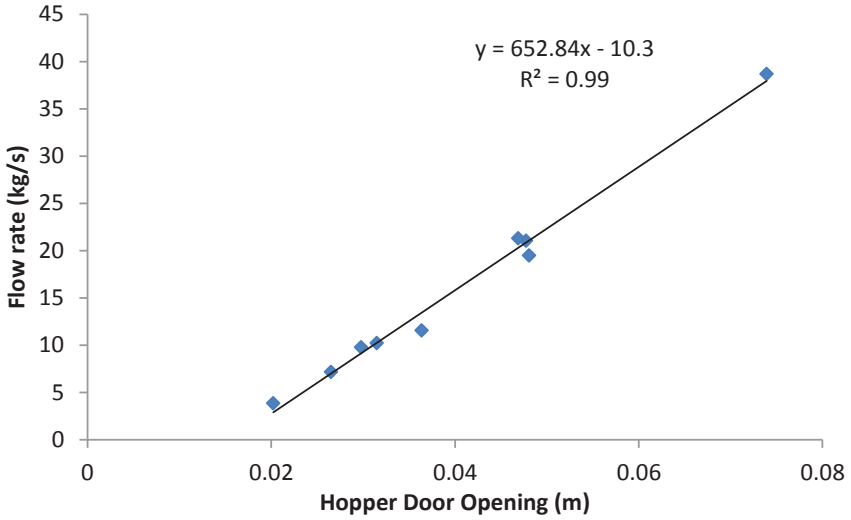


Figure 4.30: Relationship between flow rate and the clam shell hopper door opening with linear regression for urea.

The accuracy of the Beverloo equation was investigated. First, the coefficients K and k were determined for the Beverloo equation and compared to previous values. These coefficients are specific to the flow material and hopper design. To find the coefficients, the Beverloo equation was rearranged so that it is in the linear equation form $y = mx + c$, where m is the slope of the straight line and c is the y-intercept (Equation 4.1). The hopper door opening (B) is x and the mass flow rate (M) is y.

$$M^{\frac{2}{3}} = \left(K\rho g^{\frac{1}{2}}L\right)^{\frac{2}{3}} B - \left(K\rho g^{\frac{1}{2}}L\right)^{\frac{2}{3}} kd \qquad (4.1)$$

Flow rate to the two third power ($M^{2/3}$) was plotted against the hopper door opening (Figure 4.31 - Figure 4.33). The slope of the linear equation was used to determine K. Once K is known, it and the y-intercept were used to find k.

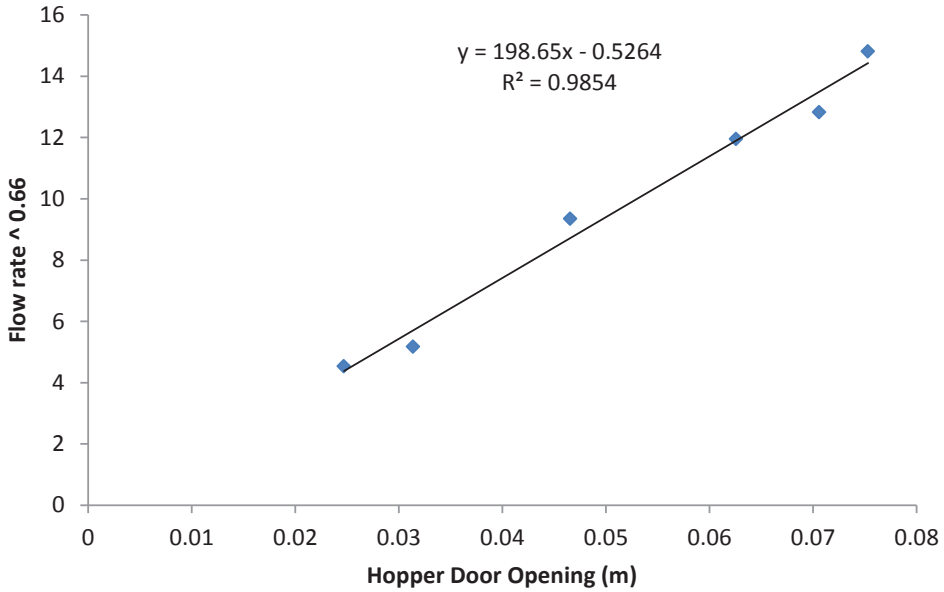


Figure 4.31: Relationship of flow rate to the 2/3 power and the clam shell hopper door opening with linear regression for superphosphate.

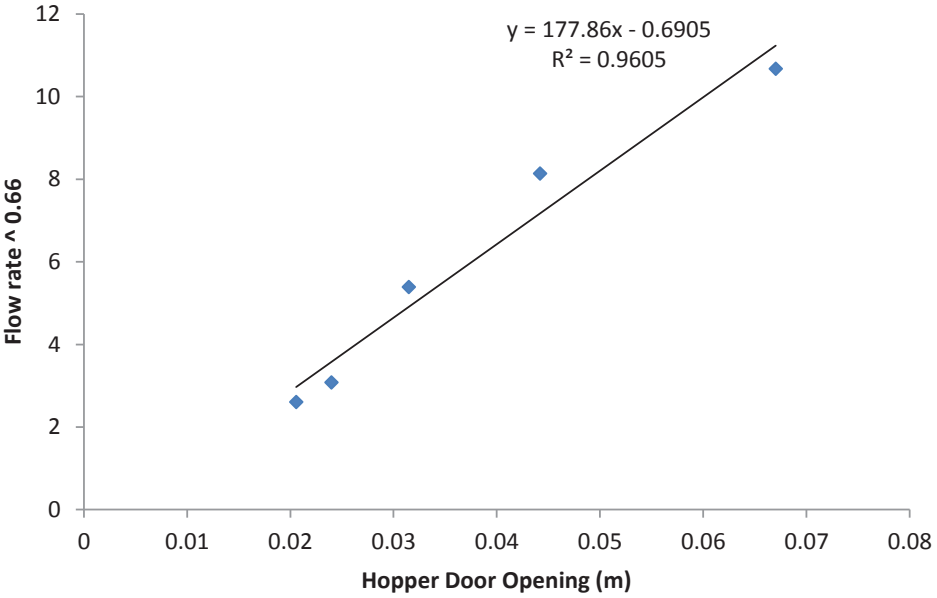


Figure 4.32: Relationship of flow rate to the 2/3 power and the clam shell hopper door opening with linear regression for DAP.

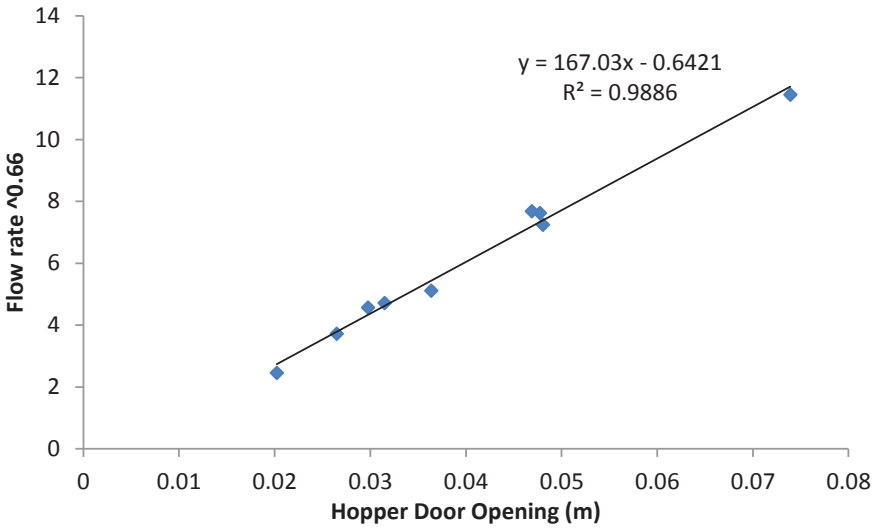


Figure 4.33: Relationship of flow rate to the 2/3 power and the clam shell hopper door opening with linear regression for urea.

Table 4.5 compares the original and new terms of the bulk density, average particle density, K and k. There were some differences in the K value. The original K values were constant for all three fertiliser types, but differed in the static hopper flow trials. Original K was also lower than the newly calculated K. The discrepancies occurred because the original values of the Beverloo equation were estimated and not based on the hopper design. There were also differences between the original and current bulk densities, and average particle sizes. To ensure more accurate Beverloo equation predictions, the particle characteristics should be updated frequently.

Table 4.5: Comparison of parameters determined by linear regression for Beverloo equation and original coefficients.

	Original			Static Hopper Test		
Parameters	**Super**	**DAP**	**Urea**	**Super**	**DAP**	**Urea**
Bulk density (kg m^{-3})	1039	947	679	1230	1010	755
Average particle size (m)	0.0033	0.00225	0.0026	0.00225	0.00188	0.00255
K	0.58	0.58	0.58	0.69	0.72	0.87
k	1.7	1.6	1.5	1.18	2.07	1.51

The results from the static hopper trial required validation. If the hopper flow rate is correct, the field and intended application rate will be within 30% of each other. The application rate can be determined by using the mass flow rate, swath width and aircraft velocity. Door openings found in previous field trials were compared to the door openings calculated using the original Beverloo equation, the improved Beverloo equation and the linear regression (Table 4.6). The linear regression and improved Beverloo equation door openings were similar. There were some similarities between these hopper door openings and the field's, but a

pattern or consensus was not observed. The hopper door openings from the field trials differed significantly sometimes for similar application rates and swath widths, which is due to environmental variability from trial to trial.

Table 4.6: Comparison of field results with calculated clam shell door openings. Linear and Beverloo equation application rates were calculated using an aircraft velocity of 59 m s^{-1}.

			Door Openings (mm)			
Fertiliser Type	**Field Swath Width (m)**	**Field Application Rate (kg ha^{-1})**	**Field**	**Linear**	**Beverloo**	**Original Beverloo**
Urea	22	75	39.69	30.66	31.11	42.27
DAP	22	200	52.39	51.97	53.11	62.71
Superphosphate	11	500	53.98	51.87	53.80	70.09
Superphosphate	12	500	66.68	55.13	56.85	73.94

Hopper door openings for Trial 8 were determined using the linear regression equation in Figure 4.28 rather than the Beverloo equation. From the results in Table 4.6, it was likely the selected equation will require adjustment. Therefore, the linear regression equation was selected because it had fewer variables so corrections would be simpler, and there was little divergence between the two methods (linear and Beverloo).

Beverloo et al. (1961) studied orifice areas between 0.049 cm^2 and 7.28 cm^2, and particle sizes below 1.6 mm. The authors showed that at the higher range of tested orifice areas, the discharge rate from the hopper has a linear relationship. The orifice area of a PAC 600 hopper is much larger than those tested by Beverloo et al. (1961), and superphosphate particles are 0 – 6.0 mm in diameter. Therefore, the linear equation is a sufficient substitute for the Beverloo equation, because the orifice areas of interest are large and are in the linear section of the Beverloo equation.

4.5. Trial 8

For the trial, the pilot made an effort to apply fertiliser with care and attention, ensuring that each flight line was aligned adjacent to the previous swath width. This can be observed in Figure 4.34. A conservative swath width of 12 m was used, which is a distance equivalent to four bubble wrap lined collectors. Wind conditions on the ground were light. However, the pilot mentioned that the wind velocity at the flight altitude was much stronger and increased as the trial progressed. The pilot flew in a racecourse configuration, and entry into the application area can be observed in Figure 4.34 where the points begin at the boundary. Gaps between the points and the boundary occurred because the ‘edge off’ setting considered the

forward motion of particles. From Figure 4.34, the hopper door closed 65 – 85 m before the edge of the boundary.



Figure 4.34: Flight points recorded every 0.2 s on VRAT system. Hopper door opening in 1/16th inches are labelled.

A variety of hopper door openings are shown in Figure 4.34 because the aircraft velocity changed to compensate for the variable topography, changes in wind conditions, and manual adjustments of the heading. Table 4.7 shows a summary of the results. The average application rate found in both zones, in the trial, was below the target application rate, although the 250 kg ha^{-1} zone was within the target application rate range of 175 – 325 kg ha^{-1}. The CV from the collectors was 47 – 51%, which is similar to the CV measured in previous performance trials. A narrower swath width would have increased the overall application rate and decreased the CV, but the trial was intended to replicate an actual fertiliser application. The standard deviation contributed to the high CV. Field application rates were highly variable, which can be observed in Figure 4.35. A one way ANOVA test comparing the two application zones resulted in a highly significant result ($P < 0.001$) for a 95% confidence interval (Table 4.8). This further illustrates that the system is capable of variable rate application.

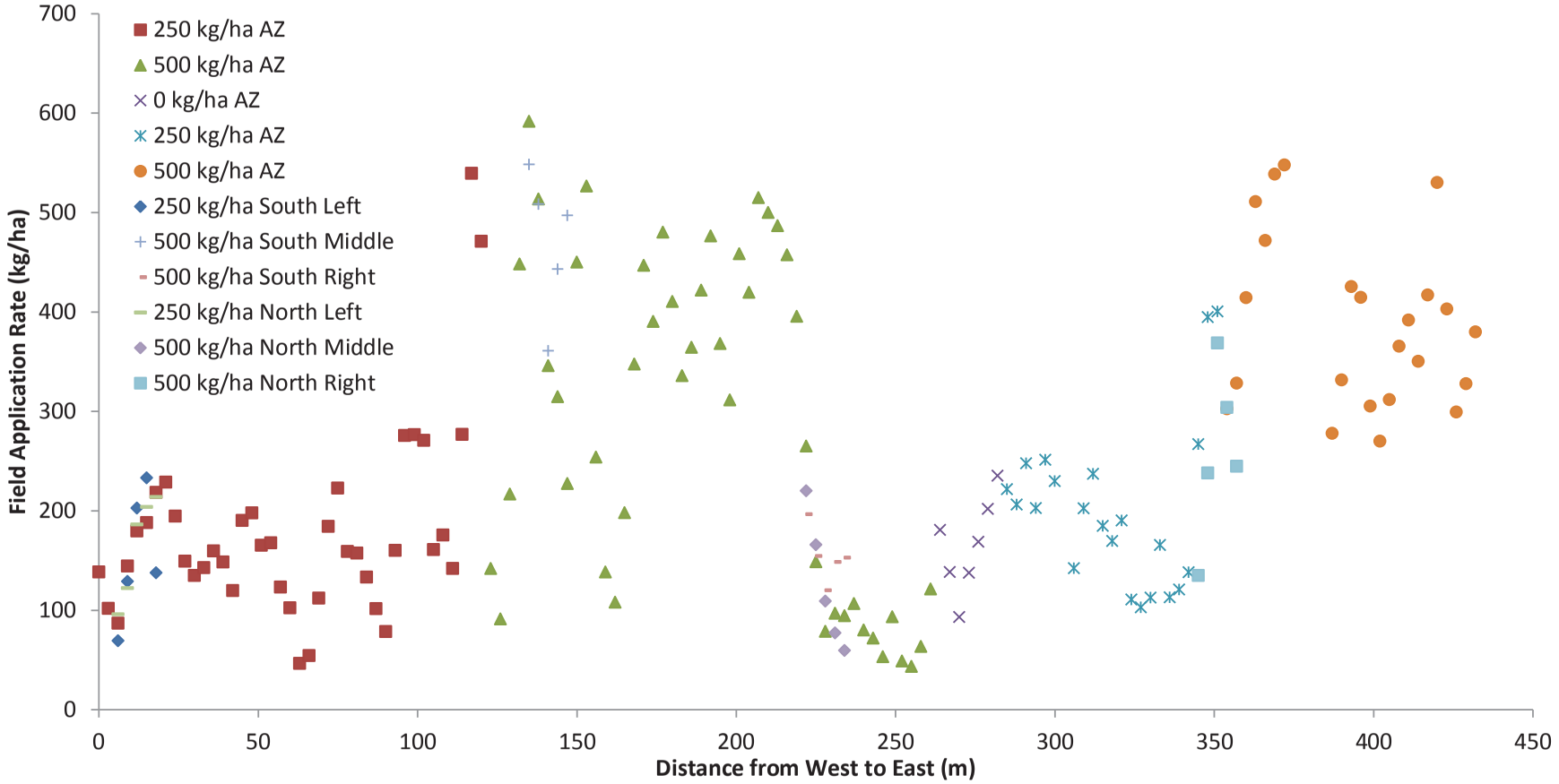


Figure 4.35: Field application rate across the line of bubble wrap lined collectors from the west to east direction. Replicate lines are included. The location of the replicate line is denoted in the legend as north or south of the main center line. AZ stands for application zone.

Table 4.7: Summary of collector data for Trial 8.

Target Application Rate	**250 kg ha^{-1}**	**500 kg ha^{-1}**
Field Application Rate (kg ha^{-1})	184.7	307.5
Difference in Application Rates (%)	-26.1	-38.5
Standard Deviation	87.4	156.5
Coefficient of Variation (%)	47.3	50.9

Table 4.8: One way ANOVA test comparing the applications rates in the 250 kg ha^{-1} and 500 kg ha^{-1} application zones at a 95% confidence interval.

Groups	*Count*	*Sum*	*Average*	*Variance*
250 kg/ha	76	14037.5	184.7	7636.7
500 kg/ha	87	26756.4	307.5	24504.0

ANOVA

Source of Variation	*SS*	*df*	*MS*	*F*	*P-value*	*F crit*
Between Groups	612112.7	1	612112.7	36.8	9.13E-09	3.9
Within Groups	2680093.8	161	16646.6			
Total	3292206.5	162				

Field application rates in the replicate groups were similar to the samples collected at the central line. Figure 4.36 shows the collectors with their application rate categorised into colour. Unusual application rates at the boundaries were caused by wind conditions, which blew fertiliser west (to the left). Fertiliser was collected in the zero application rate zone even though the hopper door closed over the area. The distance of the gap ranged between 50 – 70 meters, which gave the VRAT system time to act appropriately. However, the forward motion of the particles, and the wind conditions resulted in a noticeable quantity of fertiliser landing in this area. The solution for preventing unwanted fertiliser application is to create a larger buffer zone, which would result in large exclusion areas. Therefore, it is more efficient to fly parallel to exclusion zones.

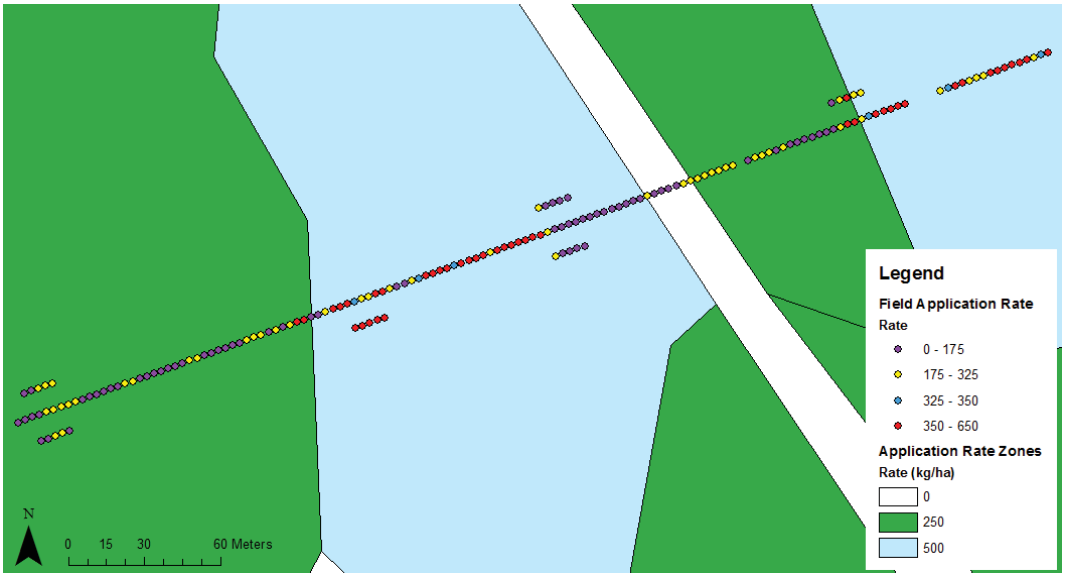


Figure 4.36: Categorised application rate from collectors at each location. Yellow coloured points represent the target application rate range for the 250 kg ha^{-1} zone and red is the target range of application rates for the 500 kg ha^{-1} zone.

The linear equation from Figure 4.28 applied at the target application rate, but this was not consistent. Forty-seven percent of the mass collected was below or above the target application rate range for their particular application zone. The shortages in the field application rate may have been caused by fertiliser bouncing out of the collectors. To test this theory, the fines fraction (< 1.18 mm) of the bulk fertiliser sample and the field samples were compared. Fine particulates are not expected to bounce out of the collectors; therefore a comparison of the fines content would indicate if the full sample was collected. The field sample is the combination of all the collector samples. Both the bulk and field samples were sieved. The field sample was found to have a higher fines content than the bulk sample (Figure 4.37). However, particle bounce was unlikely to be the main reason for under application, because the difference does not account for the 26 – 38% of losses observed in the field application rate.

There are two potential reasons for the difference in the particle size distributions in Figure 4.37. The sample in the field appears to have a similar pattern of distribution in the sieve sizes below 3.35 mm. The single bulk sample used for comparison could have been unrepresentative, or in the infield sample it was mainly the larger particles which bounced out. It could still be that there is attrition of these larger particles in terms of collection or that there has been some breakup of particles during the application process.

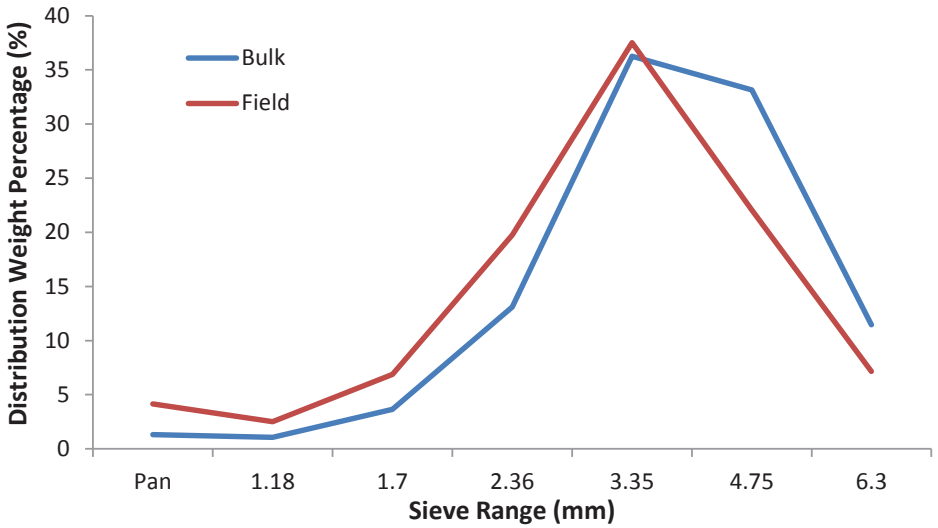


Figure 4.37: Particle size distribution comparison between the bulk and field samples for Trial 8.

It is difficult to produce a uniform application rate across all the collectors because the transverse spread pattern is normally distributed, and there is insufficient overlap between swath widths. To produce a field application rate closer to the target application rate, the hopper door position should be larger so that the field application rate varies above and below the target rate. This will produce a higher average. A 33% increase in the flow rate out of the hopper is an appropriate starting point. It was determined by averaging the difference in both application zones (Table 4.7). This trial provides one data point to determine the best coefficient to increase the flow rate, and was a good first step in determining a method to standardise hopper door openings. However, it is a starting point and future experiments are required to improve the correction factor. Equation 4.2 is an example of how the coefficient would be applied for superphosphate.

$$M = 0.66(902.08B - 14.399) \quad (4.2)$$

where M is the mass flow rate in kg s^{-1} and B is the hopper door opening in meters.

4.6. Static Hopper Flow Calibration Re-test

After Trial 8, a cantilever hopper door was installed on the static hopper. Superphosphate was re-tested to determine the effect of the hopper door design on the flow rate. Six hopper door openings were tested, with each door opening tested twice. An objective of the re-test was to reproduce the same hopper door openings as those in Figure 4.28. To achieve this, an automated hydraulic hopper door was attached, along with the Satloc Intelligate G4 system. These systems are the same as those installed in Ravensdown's VRAT aircraft. Additional tests were carried out where the hopper door was open-close-open to determine if the mass flow

rate was dependent on the remaining mass in the hopper. Three door openings were tested twice (31.75 mm, 44.45 mm and 73.03 mm). Weights were recorded at one second intervals.

On the test day, it was discovered that this particular automated system did not open the hopper door to the set door opening a majority of the time. This was due to a mechanical issue within the hydraulic unit that could not be fixed easily, but the measured hopper door position was usually close to the set value (Figure 4.38). This meant it was difficult to complete replicates of each hopper door opening used in the original tests. In two open-close-open tests, the hopper door did not return to the same aperture as the first opening, which resulted in different mass flow rates. The re-test was not perfect, but it provided an indication of the hopper's flow regime with a cantilever door.

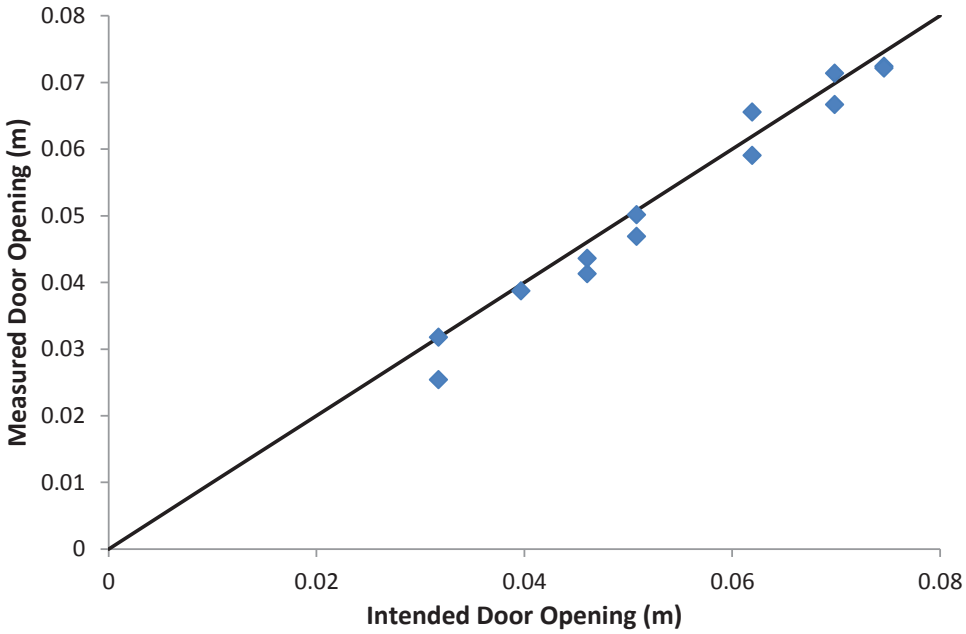


Figure 4.38: Comparison of the intended hopper door opening and the measured hopper door opening.

For the cantilever hopper door, flow rate was constant at all measured hopper door openings (Figure 4.39). This occurred because the cantilever door design creates three orifices when the aperture is sufficiently large. There is the main opening and two smaller orifices created behind the hopper doors as the doors hinge open (Figure 4.40). Figure 4.41 is a plot of the average flow rate against the measured hopper door opening. Average flow rates from the cantilever hopper door were higher than the clam shell hopper door at larger openings, due to the additional orifices. It was not possible to observe if the flow pattern from the hopper was mass or funnel flow.

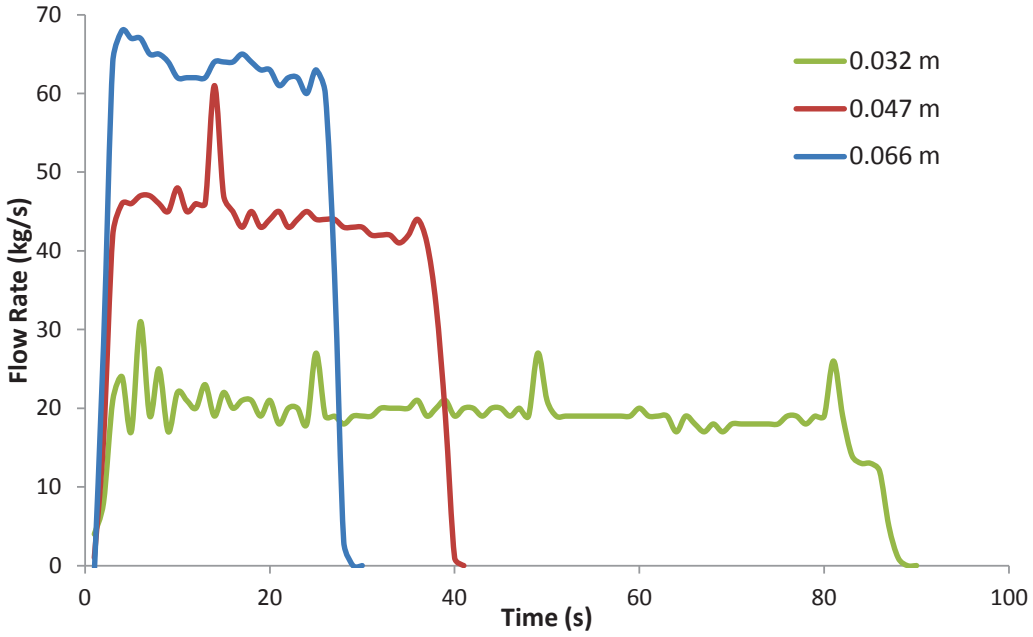


Figure 4.39: Flow rate out of the cantilever hopper door against time for three door openings (0.032 m, 0.047 m and 0.066 m).

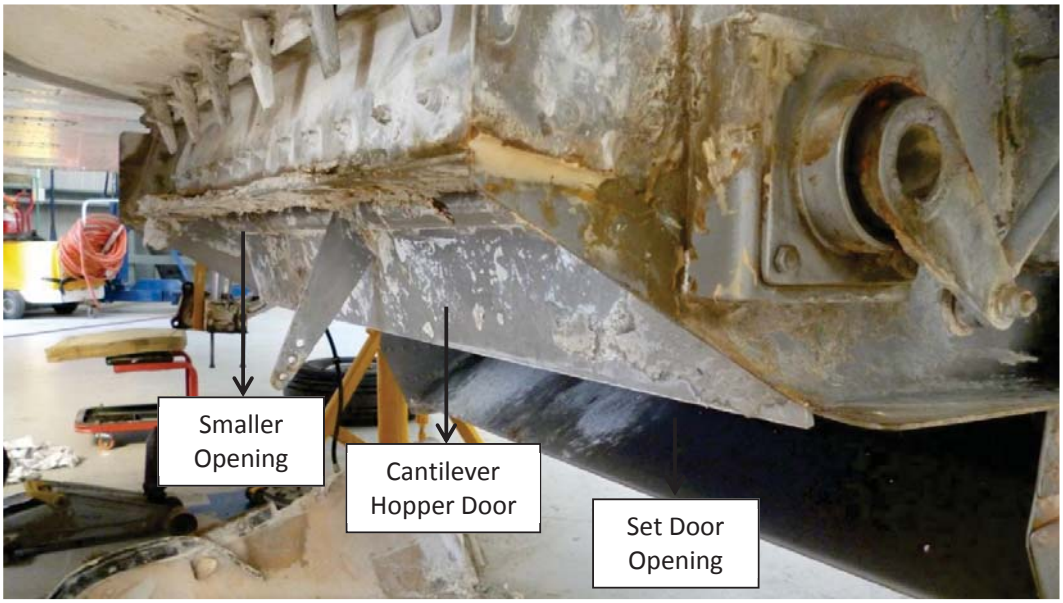


Figure 4.40: Open cantilever hopper door illustrating the main door opening and the smaller opening.

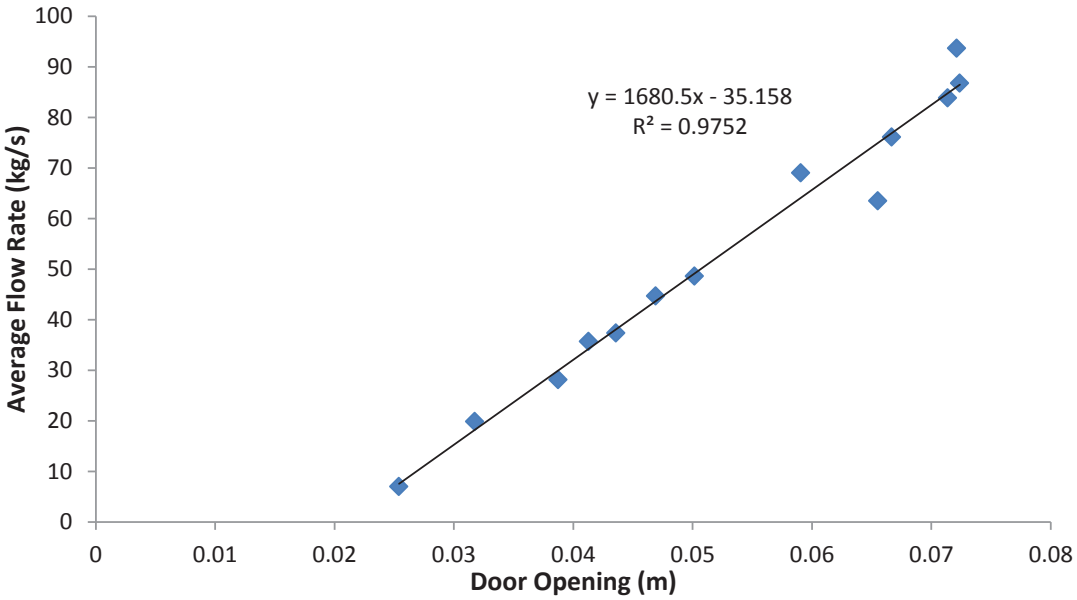


Figure 4.41: Relationship between average flow rate and the cantilever hopper door opening with linear regression for superphosphate.

Figure 4.39 demonstrates that the flow rate oscillated at each hopper door opening. Measurement error was likely to be the main cause since the oscillations were less pronounced than in the clamshell door trials (Figure 4.27). Therefore, the cantilever hopper door design was better at regulating flow. However a contributing factor to the high variance observed in the field results is the time it takes for the flow rate to reach the maximum/equilibrium. From the retests, the flow rate takes 2 – 3 s to reach the maximum flow rate. If the topdressing plane is travelling at 56 m s^{-1}, inconsistent flow will result in varied application rates for 112 – 168 m from where the hopper door opens. This is a significant area over an application and increases CV at the boundaries.

The constant coefficients for the Beverloo equation were recalculated using Figure 4.42. K was 1.39 and k was 4.12. These values are larger than those calculated for the clamshell hopper door (Table 4.5). Table 4.9 shows that the improved Beverloo and linear equation predicted similar values, but were below what was measured in the field. If these values were used to determine the hopper door openings for Trial 8, the collectors would have shown under application. Static hopper flow tests were thought to be a good indicator of the flow rate from the hopper door for an applying aircraft. However, the differences observed between the results of the static hopper flow tests and the performance trials indicate the delivery method is still not fully understood, and there are unknown factors affecting field results, which require further investigation.

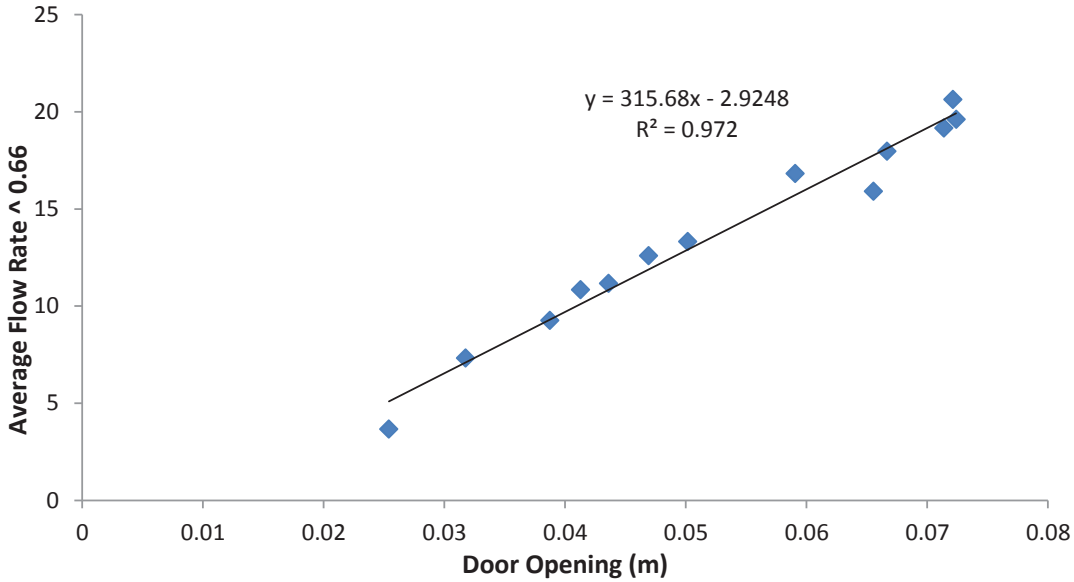


Figure 4.42: Relationship of flow rate to the 2/3 power and the cantilever hopper door opening with linear regression for superphosphate.

Table 4.9: Comparison of field results with calculated cantilever door openings for superphosphate. Linear and Beverloo equation application rates were calculated using an aircraft velocity of 59 m s^{-1}.

		Door Openings (mm)		
Field Swath Width (m)	**Field Application Rate (kg ha^{-1})**	**Field**	**Linear**	**Beverloo**
11	500	53.98	40.19	41.45
12	500	66.68	41.45	43.37

4.7. Conclusion

All three performance trials found the VRAT system improves the performance of aerial topdressing. VRAT decreases the CV when compared to conventional aerial application. The CV for each performance trial ranged between 45 – 55%, except for the 284 kg ha^{-1} application zone in Trial 5, which achieved 35%. VRAT also improves a pilot's capability to apply in consecutive straight flight lines, and the system has demonstrated its ability to apply fertiliser at different application rates. The application rates for Trial 4 and 5 were accurate, after compensating for fertiliser bounce.

Proof of placement maps, produced by kriging, are unsuitable for representing the ground fertiliser distribution. The sampling frequency was too small for the application areas. Proof of release maps are better representations because a large data set was available from the aircraft's log files. However, the nugget value was not zero because the logging rate is 5 Hz, which corresponds to approximately 14 m. A higher frequency logging rate would improve the nugget value. To ensure the accuracy of the proof of release maps, further work is required on

determining the flow rate out of the hopper based on the hopper door opening, and on understanding the flow dynamics.

The static hopper flow trials found that for clam shell hopper door positions over 0.046 m, the flow rate out of the hopper was not constant. Regression analysis found linear relationships between the clam shell hopper door opening, and the average mass flow rate for all three fertiliser types. Coefficients (K and k) for the Beverloo equation were also calculated for DAP, urea and superphosphate, using the standard PAC hopper. The linear and Beverloo equation hopper door openings were similar. However, the hopper door openings from field trials were significantly different to the linear/Beverloo equation. The static hopper flow trial was an initial investigation, and there were insufficient runs to make statistically sound conclusions. Re-tests were completed for superphosphate when the cantilever door was installed. The re-tests found the flow rates from the cantilever door were constant in the door aperture range tested (0.0254 m – 0.0762 m). Flow rate was also higher at wider door openings than for the clamshell hopper door; the cantilever door design creates two additional orifices so flow is less restricted.

Trial 8 was completed after the first static hopper flow test. The hopper door openings calculated for the prescription map used the clamshell hopper door linear equation for superphosphate, and the main objective of Trial 8 was to determine if the equation was an accurate predictor of flow rate out of the hopper door. The linear equation was used instead of the Beverloo equation because it was simpler to correct, if a correction factor was required. Under application occurred by 26 – 38% in Trial 8; therefore a correction factor of 33% is suggested in future trials. This was only one test of the linear equation and further testing is required.

Bench testing helped to improve aerial application without the high costs associated with trials. It enabled the assessment of the VRAT system, without having to consider environmental conditions and fertiliser flow dynamics from the hopper door. The main outputs from bench testing were the ‘edge on/off’ settings, and the importance of sufficiently sized buffers to prevent off-target application. Since software updates for the VRAT system is common, bench testing should be continued to avoid future issues with off-target application in the field.

A direct comparison between Trial 4, Trial 5 and Trial 8 cannot be made because there were significant differences in the objective, trial area, sampling configuration and environmental conditions on each farm. Collector efficiency and placement are also important to consider as

they will affect the validity of the results. An ideal study would complete replicates at each farm, but this is prohibitively expensive. However, the work completed in this thesis will be useful in improving future testing of aerial application.

Chapter 5 - Variability in Aerial Topdressing

5.1. Introduction

It is extremely difficult to fully assess the variable rate application technology (VRAT) system, as gathering sufficient performance data is time consuming and expensive. Previous studies have collected limited performance measurements, and either made assumptions around variability or ignored it completely. A few studies in the 1970 – 1980s sampled on a grid and line basis, with a high interval sampling rate over a small area (Macfarlane et al., 1987; Scott and Grig, 1970). The results of these studies were highly variable, with much of the variability attributed to wind conditions. The studies also expressed the difficulty and expense of the trials. Since these earlier studies, aerial topdressing trials have been simplified to single swath widths and fly overs, and modelling has been deployed as a method to minimise costs but with limited field validation (Grift, 2011). Assumptions are generally made about the reproducibility of the swath width, the efficiency of the collectors, the flow characteristics from the hopper door and the effect of wind conditions. Initially, similar assumptions were applied to the performance trials in this study. The results were similar to what has been initially shown; aerial topdressing is highly variable, and the level and origin of the variability is not fully explained.

Aerial topdressing is a complex process to measure and model. In this chapter, application of a granular fertiliser particle is considered in three parts. The first is the particle's release from the aircraft. This is influenced by aircraft operation and settings, such as airspeed, flow dynamics from the hopper door and spreader design. It also includes the particle's physical characteristics (i.e. particle size and sphericity), which will affect the particle's initial conditions and motion while it is falling. The VRAT system has electronic, hydraulic and mechanical limitations, which reduces the level of accuracy that the VRAT system can deliver. It is difficult to measure particle ballistics and flow rate while the aircraft is applying fertiliser, so assumptions were made regarding the consistency of fertiliser flow from the hopper door. This study found there was significant variability in the flow dynamics from the hopper door, which contributes to the variability captured in the field application rate of the performance trials.

The second part to consider is the ballistics of the particle as it falls from its release point. Previous studies have demonstrated the significance of wind velocity and direction on a particle's landing position, with topography also being shown to have an effect (Gillingham et al., 1985; Macfarlane et al., 1987; Scott, 1970). Ballistics modelling has been used to predict the transverse spread pattern of fertiliser applications with limited success, due to model

assumptions. Jones et al. (2008) formulated a single particle ballistics model for coarse granular fertiliser (> 0.5 mm). It has been used to create a wind displacement calculator, which predicts the effect of wind on a transverse spread pattern. However, the performance trials have shown that wind can vary significantly, especially in hill country, which limits the effectiveness of the calculator.

The third component is the placement of fertiliser on the ground and how this is measured. The performance trials have highlighted the importance of selecting an appropriate sampling configuration and collector. The sampling configuration can influence the field application rate and CV, and most trials are limited in the number of collectors they use, making it uncertain whether a representative sample is being captured. The eight trials completed within this study are summarised in Table 5.1, and were carried out over a period of three years. Each trial had different objectives, a different sampling configuration, and the collector type varied. The variation in the objectives, location, and sampling methodology means that care is needed when comparing the results of these trials to each other.

Table 5.1: Summary of trials undertaken in this study.

Trial	Farm	Trial Date	Purpose	Collector Type
1	Longview	May 2014	Model validation	NZCPA
2	Longview	November 2014	Model validation	NZCPA
3	Mairedale	September 2016	Model validation	NZAAA
4	Limestone Downs	February 2014	Performance and kriging	NZCPA
5	Longview	April 2015	Performance and kriging	NZCPA
6	Pickwick	November 2015	Understanding variability, calibration, collector efficiency	NZCPA
7	Mairedale	July 2016	Collector efficiency	NZCPA, NZAAA, NZCPA with bubble wrap
8	Mairedale	February 2017	Performance	NZCPA with bubble wrap

Previous studies simplified the sampling configuration, and determined the field application rate and coefficient of variation (CV) from a single swath width in a small area (< 1 ha) (NZFQC, 2016b). They assumed that the transverse variation (swath width) was repeatable and that longitudinal variation (i.e. along the flight line) was negligible. This study has shown that these assumptions are false. It has also been assumed that the collector efficiency for the New Zealand Centre for Precision Agriculture (NZCPA) collectors was 100%. However, Trial 6

showed that a significant percentage of fertiliser particles bounce out of the NZCPA collectors. Other styles of collectors are available, but at this stage their efficiencies are unknown.

The CV from the performance trials was lower than the CV in conventional application (reported at approximately 70%). Ravensdown Limited wanted the VRAT system to halve the CV of pilot operated applications, but this was not achieved in the performance trials. However, the pilot operated CV were based on the assumption that the swath width pattern was repeatable (Grafton et al., 2012). Pilot operated CV may actually be higher, which means that the VRAT system may have halved the CV. The trials completed in the 1970 – 1980s with conventional applications did not calculate field CV. Performance trials in this study have not been completed for aerial variable rate application. They differ from previous studies because data is collected from a fully operational aerial variable rate application system for granular fertiliser. The performance trials considered accuracy, precision, off-target application and capability together rather than individually, as was the case in previous work. Therefore, it is difficult to form final conclusions about the improvement in CV from a VRAT system.

Figure 5.1 summarises the factors that contribute to variability in aerial topdressing. It is not possible to rank, in magnitude, the factors that contribute to high variance as these will vary with the conditions on the application day. These factors also have variable temporal resolution. Some of the factors have short temporal resolution (i.e. during a single flight run) and others have long (i.e. over a farm). For example, wind velocity and direction changes significantly in a short time, and cannot be controlled or predicted. On the other hand, fertiliser characteristics, such as particle size and sphericity, are pre-determined before application and are less changeable on the day. However, particle characteristics can vary throughout an application due to their transportation and storage, and the raw materials used in production. Previous studies have attempted to isolate and test single factors from Figure 5.1 with limited success. This chapter seeks to explain the observed variance based on the trial results undertaken in this work and previous studies.

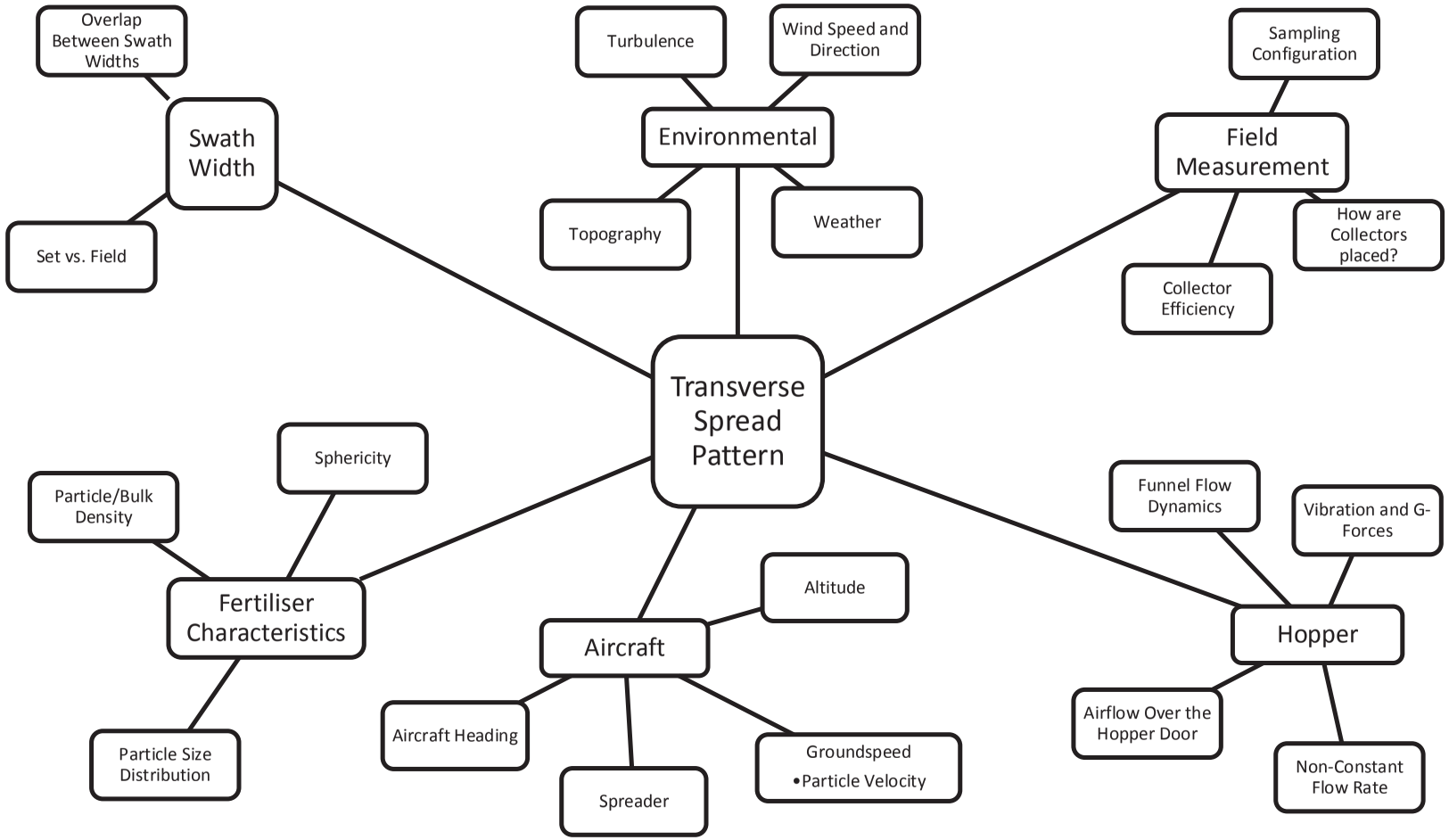


Figure 5.1: Factors that affect the transverse spread pattern in aerial granular fertiliser application.

5.2. Part 1: Release of Fertiliser Particle from Aircraft

5.2.1. Hopper Flow Characteristics

Ravensdown Limited has a standardised hopper design for the Pacific Aerospace Cresco (PAC) 600 aircraft. The hopper is asymmetrical with a rectangular opening (Figure 4.25). The maximum hopper door opening is 0.34 m. This door opening is only used in an emergency situation, where 80% of the fertiliser load is jettisoned in 5 s to reduce the weight of the aircraft so it can gain lift.

The static hopper flow retests for superphosphate indicate that there is a difference between the flow rates from static ground tests, and the amount collected in field trials. In the static flow tests for the cantilever hopper door, flow rate was constant between 0.0254 m and 0.0762 m. However, performance trials have shown there is a high level of variability between swath widths measured on the ground. A constant and higher flow rate was observed in the cantilever hopper door compared to the clamshell door because there were essentially three orifices, which allowed unrestricted flow from the hopper. The three orifices consist of the main opening and two smaller openings created by the design of the cantilever hopper doors. The cantilever door is not hinged along a side but rather 40% along the door (Figure 5.2); therefore, the larger the main hopper door opening, the larger the other two openings.



Figure 5.2: Top view of the cantilever hopper door with door hinges annotated.

Constant flow from the hopper should produce less variation in the field results. However, this was not observed in the performance trial results. The average field application rate in Trial 8 was below the intended and the CV was higher than the 30 – 35% desired by Ravensdown Limited. The difference in application rate between the static hopper flow retests and the field application rates could be due to air flow interactions at the hopper door that disrupt the flow of material out of the orifices. The front small orifice would be most affected due to shear

forces, which would restrict flow out of this orifice. Since the hopper door opens perpendicular to the air flow, a high pressure zone accumulates in front of the hopper door, and larger door openings will disrupt air flow more than smaller door openings. Air would be turbulent at the main hopper door opening, which could be a cause of variability in the flow pattern. In the pitot tube air velocity tests, described in Table 2.10, the air velocity through the spreader ducts changed with the opening of the hopper door, so the cantilever doors do have an effect on airflow. Additional investigation is required.

Vibration and g-forces could contribute to variability in the flow rate out of the hopper door. Slight vibrations were observed in the static hopper flow trials for small door openings. The recorded data showed a sinusoidal flow rate with small amplitude change (Figure 5.3), part of which was caused by the sensor's resolution (± 1 kg).

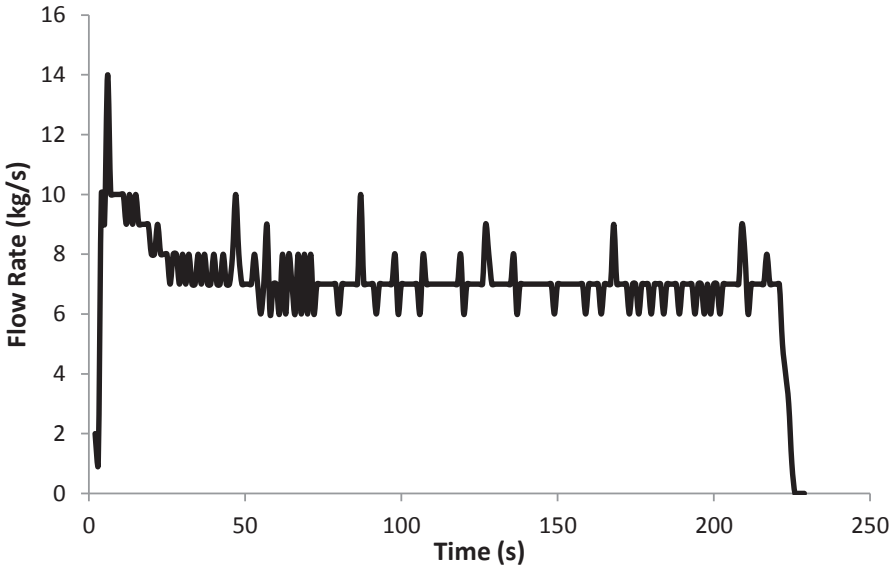


Figure 5.3: Flow rate out of a 0.0254 m cantilever hopper door opening against time for superphosphate.

Yule and Flemmer (2005) measured vibration, using an accelerometer (ACC 101), in three dimensions on a PAC hopper to assess whether it was a factor in bed consolidation. They found an increased level of vibration during application in all axes. Possible explanations for the vibration were the operation of the hopper door, sudden changes in mass during application, which affected the aircraft's momentum, and the aerodynamic turbulence of having the hopper door open. However, Yule and Flemmer (2005) compared the level of measured vibration to a standard Endicott sieve shaker at its lowest power setting (10%), and found that the shaker's vibration was twice the strength of the maximum value found during

aerial application. Therefore, it was concluded that vibration was unlikely to be a factor in bed consolidation due to the hopper's flexibility.

Aircraft vibrations may cause particle sizes to segregate, which will significantly impact the particle size distribution leaving the hopper door over time. Further work should be completed to determine if a load of fertiliser will segregate in the hopper. A container filled with fertiliser could be shaken at the intensity experienced by the aircraft during flight to determine if particle size segregation occurs. To determine the effect of vibration on the flow, a vibrator of the right magnitude and frequency could be attached to a hopper, and static hopper trials completed. These initial tests can give a preliminary indication of how vibration affects flow before attaching a camera to the aircraft to observe the hopper door. It is possible for these vibrations have a significant effect on flow characteristics from the hopper and may even aid flow from the hopper, but further investigation is required.

Field variance may also be affected when small hopper door openings are blocked by fertiliser agglomerations. DAP, used for the clamshell static hopper flow tests, had large clumps. When hopper door openings were small, these clumps impeded a significant proportion of the flow out of the door. If this occurred in the field, it would affect the field application rate and shape of the transverse spread pattern. Fertiliser particles agglomerate due to moisture introduced during storage. For example, superphosphate is hygroscopic and will conglomerate when stored in humid environments. The fertiliser mix used in Trial 5 was also prone to clumping in the presence of moisture, so the results of that trial may have been affected by agglomerations. However, at the end of each flight run, the hopper door is fully opened to ensure the hopper is not overloaded in the next run, which has the added benefit of removing any clumps.

5.2.2. Future Work

There are several areas that could be improved with further investigation. The relationship between the hopper door opening, the flow rate out of the hopper door, and the field application rate requires additional study. Due to time constraints, limited static hopper flow runs were completed using the PAC 600 hopper. Multiple runs should be completed at the same door position to determine the level of variance in the flow rate. Retests were done for superphosphate using the cantilever hopper door but should also be completed for urea and DAP. There is a discrepancy between flow out of the static hopper and what is found in performance trials. A way to control the flow rate from the hopper may be to install a flow monitoring device in the aircraft (such as weigh cells). This has been attempted in the past, by

Ravensdown Aerowork, but there were issues with the sensor's durability, since it is situated in a corrosive environment. More research should be carried out to find a suitable substitute. Cameras could also be attached to the underside of the aircraft to observe the flow dynamics of fertiliser out of the hopper door from different angles to capture what is happening with each orifice.

Further consideration should be given to the air flow over the cantilever hopper door and how it affects the flow rate out of the hopper. These doors create a low pressure zone at the hopper door opening because they open outwards and disturb the aerodynamics of the aircraft. The flow of fertiliser out of the hopper also creates a high pressure area as air encounters greater resistance. The magnitude of this effect may be related to the aircraft velocity. Currently, a linear relationship is assumed between aircraft velocity, swath width and the flow rate required out of the hopper door, and the field application rate. For example, the higher the velocity the higher the flow rate required to achieve the target application rate. However, it may be that the higher velocity will negatively impact the flow rate out of the hopper so a larger hopper door opening is required. Further study should be completed to explain the 33% difference in the field application rates recorded in Trial 8.

Once these uncertainties are known, discrete element modelling (DEM) can be used to determine the level of clustering that occurs out of the hopper door. DEM is able to model the interaction between particles and boundaries to predict the flow behaviour of these particles. It was speculated in Chapter 3 that particles clustered together at higher flow rates creating narrower swath widths. A discrete element model could aid in the understanding of why and how this is occurring. Another area that could be investigated is the interaction between two fertiliser types in a blend. In Trial 3, it was postulated that the narrow swath width occurred because there was a high coefficient of restitution. It is important that there is a greater understanding of the aerial topdressing process before DEM is undertaken as it requires high computational power.

The aircraft's design can affect the transverse spread pattern. Yule et al. (2005) partially validated the ballistics model for a Gippsland Aeronautics GA200C and this study has validated the model for a PAC 600. The original Jones et al. (2008) model had a propeller wash component that was not required for the PAC 600, but may be used for other aircraft that have stronger propeller washes. Therefore, it is beneficial to validate the model for different topdressing aircraft since it will improve the model and advance the understanding of variability in aerial topdressing.

There are still a few gaps in the granular fertiliser ballistics model. The look up tables indicate that the spreader ducts have not been fully characterised. This is observed in the narrowing of the maximum swath width for angles ± 20° of the plane's direction (Figure 2.40). As previously mentioned, the spreader ducts curve so it was difficult to measure the range of initial particle velocities, discharge angles and percentage of flow through each duct. FLUENT, a fluid dynamics software program, was used by R. Bansal et al. (1998) to model the flow dynamics of an 11 duct spreader with limited success. The model produced an M shaped distribution while the field data was normally distributed. The difference was attributed to the model assumption that the flow rate through each duct was the same. In this study, flow through the spreader ducts varied but at high wind velocities an M shaped distribution was modelled. Further experimentation is required to better understand what is occurring. Experiments could include attaching cameras in front of and behind the spreader to observe the flow dynamics during application, and measuring the air and particle flow rate through each duct. Future instrumentation may also allow the measurement of particle discharge angle and velocity from each duct. It would be useful to look into the distribution created by each duct, by blocking some ducts and collecting the distribution from the unblocked ducts. These tests should occur during application to truly understand the effect of changes in airflow and hopper door position.

5.3. Part 2: Fertiliser Particle Motion through Air

5.3.1. Wind and topography

Wind direction and velocity varies frequently over small time intervals. Since wind can significantly impact the transverse spread pattern and is usually the dominant parameter in predicting where fertiliser lands, ballistics modelling for an entire application zone is challenging. In hill country, wind conditions have additional spatial variability that needs to be considered. Air turbulence is a complication in a hilly environment as air must travel around and over topographical obstacles. The dynamics between sun radiation and hill slopes can cause updrafts and downdrafts, which will differ depending on the aspect of the hill and farm location. There are differences in the wind dynamics on a coastal farm compared to a farm based inland, with coastal farms subjected to coastal convergence. All of these issues have an effect on the transverse spread pattern and increase variability. This contributed to the high standard deviations found on the two hill country farms (Trial 4 and 8) compared with the farm in Trial 5, which was predominantly flat land.

Wind is a complex system and there is on-going research to improve wind models for local environments. While the research is there, this level of accuracy may be too high for ballistics modelling of fertiliser application at this time. The gains from on the go wind modelling may be small because the VRAT system is currently unable to deliver to that level of accuracy. Wind conditions at a specific moment and location cannot be predicted; therefore, the average wind speed and velocity is used in the wind displacement calculator. The complex dynamics of air flow in hill country is not considered, which certainly limits the reliability of the model's predictions. It is, therefore, important that the user recognise and disclose that the wind displacement calculator is only a method of improving and understanding aerial application of granular fertiliser in hill country. It does have limitations, and does not prevent unfavourable fertiliser distribution.

Aerial spreaders try to maintain a constant altitude above ground level and fly topographical contours for evenness of spread, which could be above the surrounding hill country. Ballistics modelling, as described in Chapter 2 and Akesson and Yates (1964), found that there is no significant difference in the transverse spread pattern when the fertiliser is applied from an altitude of 10 m or above in still conditions. However, wind significantly impacts where fertiliser particles land. Ground elevation can vary significantly in a hilly environment; therefore, the fall times of the fertiliser particles will also vary. Particles that have to travel further because the ground is further away from the release point will remain in the air for an extended time period. With prolonged fall times, these particles are exposed to the wind for a longer period of time, which will increase the variability within a swath width as they are blown off target.

The ballistics model predicts that a single particle can take 4 – 10 s to fall from a release altitude of 35 m. Small particles take longer to fall, and they are more affected by wind (Gillingham et al., 1985). Particles that are smaller than 0.5 mm are not modelled, because their aerodynamics differs from larger particles, and the model has not been developed to take these particles into account. The wind displacement calculator only predicts for one wind velocity and direction at a time. In 4 – 10 s, the wind conditions can change significantly if it is unstable (Figure 2.23 – Figure 2.25), so there are limitations to the calculator. The calculator also assumes the power law wind equation to model the wind velocity at a specified height from wind measurements taken at 2 m. This may not be representative of the actual wind velocities, but is difficult to test.

Additionally, a field transverse spread pattern may consist of multiple wind conditions, and a collector could have particles released at different points in the application (i.e. parallel flight, far behind or forward of the collector) that travelled there by wind. The ballistics model validated in this study is able to cope with additional wind measurements. However, the wind displacement calculator tool can only process one wind condition because the model was simplified to make it a user friendly tool.

5.3.2. Future Work

Wind dynamics are variable and have an effect on the variability of the field application rate. This will continue to be an issue in aerial topdressing. On the go ballistics modelling could improve fertiliser placement in the field, but this is dependent on the processing power of the installed aircraft computer. PAC 600 is basic in design and the cockpit already has plenty of instruments. However, the aircraft model is no longer manufactured so, in the future, a new aircraft will replace the topdressing fleet. The new design could have an improved capacity to cope with current and future technology. This could include on the go wind measurement from the aircraft, and a computer to carry out ballistics modelling. However, if wind conditions and air flow vary under the aircraft, this may not be sufficient as it would be unfeasible to continually and instantaneously change aircraft heading and swath width.

5.4. Part 3: Fertiliser Placement and Measurement

5.4.1. Data Collection

The sampling methodology is a contributor to the variability of the performance trials' results. Assessing aerial topdressing is expensive (i.e. aircraft, fertiliser, collectors), has large labour requirements, is highly weather dependent, and takes a lot of time to plan and carry out. Since the majority of aerial spreading occurs in hill country, this introduces logistical challenges. The NZCPA collectors are bulky and are transported in a 40 foot container. The container is placed as close as possible to the trial area, but it still takes significant time and resources to place the collectors at the trial site. Selecting a suitable day to complete a trial depends on the weather, the farmer, the rain fall on the farm for the previous week, aircraft and pilot availability, ability to transport and store fertiliser on the farm, and staff and resource availability. These factors impact the success of a trial, and none of the trials were undertaken in perfect conditions. All conditions were typical of those encountered by pilots in the course of their work.

5.4.2. Collector Efficiency

One important issue with data collection in this study was that the whole sample was not fully collected, because particles bounced out of the individual NZCPA collectors. This issue was not discovered until Trial 6. By this time, two performance trials and two validation trials had been

completed. Before the results were corrected, the average field application rate was between 29% and 47% below the target application rate (Table 5.2). The collected data was corrected using coefficients from Trial 6 and 7, with the assumption that the rate of particle bounce between collectors was consistent. The corrected field application rates improved, yet the standard deviation also increased, which meant the coefficient of variation remained approximately the same.

Table 5.2: Original results from Trial 4 and 5. The samples were not adjusted for bounce out of the collectors.

	Trial 4		**Trial 5**	
Target Application Rate (kg ha^{-1})	500	250	284	162
Field Application Rate (kg ha^{-1})	267	176	188	115
% Difference between Field and Target Rate	-46.6	-29.6	-33.8	-29.0
Field Standard Deviation (kg ha^{-1})	151	89	64	62
Coefficient of Variation (%)	56.6	50.6	34.0	54.1

Particle bounce into and out of the collectors was captured at Trial 6 using high speed photometry. A correction value was determined by counting the number of particles that bounced out, and comparing it against the number of particles that remained within the collector. The Trial 6 correction factors assumed that all particle sizes had an equal chance of bouncing out. Trial 7 compared the NZCPA collectors with alternatives. Superphosphate was the only fertiliser studied in this trial, since it was going to be applied in Trial 8. Trial 7 compared the average mass collected for a collector type rather than counting individual particles. The comparison found the percentage difference in the average mass collected by the NZCPA collector lined with bubble wrap was greater than the NZCPA collector with no lining, and the difference was larger than what was measured in Trial 6. It is thought that larger particles were more likely to bounce out than small particles. To confirm this, particle size analysis should be completed using high speed imagery of an NZCPA collector. This was not completed in this study due to time constraints.

When applying a correction factor to the previous collected data, it was assumed each collector experienced the same percentage of fertiliser bouncing out. The transverse spread patterns collected from Trial 1 and 2 were normally distributed. If there were significant variances in the percentage of fertiliser that bounced out of each collector, the distributions would have formed a jagged curve. From Trial 7, the standard deviation of the samples was small (Table 3.6). The NZCPA collectors had the lowest standard deviation compared to the NZAAA (New Zealand Agricultural Aviation Association) and NZCPA with bubble wrap, which indicates that there was insignificant variance in the capturing capability of the NZCPA

collectors. It is unlikely that the full sample is captured by the NZCPA collector lined with bubble wrap, and it is unknown if it is possible to obtain a perfect collection in any field trial. However, the bubble wrap collector is an improvement over the NZAAA collectors used in aerial Spreadmark tests and the original NZCPA collector, and is currently the best option for superphosphate.

5.4.3. Collector Placement

In a variable rate application performance trial, collectors need to be placed in each application rate zone and near boundaries. This is so accuracy, precision, level of off-target application, and capability can be assessed for each application zone. However, the number of collectors limits the trial size and therefore the quality of results. A collector estimates the field application rate over a small area (0.25 – 0.5 m^2), and one collector should not be used to infer the field application rate achieved in a paddock, because the transverse and longitudinal variability can be significant (Figure 2.23 – Figure 2.25). However, it is unknown how many collectors are required to ensure a representative sample is collected.

Generally the greater the number of field collectors, the more reliable the average field application rate and variance. Since there are a limited number of collectors, it is important to consider collector placement, especially as some application zones can be several thousand hectares. A large trial area results in collectors being placed some distance apart to try and capture the whole area's field application rate. This was the grid sampling configuration employed in Trial 4, but it was not possible to explain what contributed to the variance in the results, because wind measurements were not recorded and the collectors were placed too far apart to be able to observe variability between swath widths. Small trial areas, especially if the design is complex (i.e. many application zones, unusual boundaries) will also increase variance because the system may not have sufficient time/distance to react. This was demonstrated in bench testing (Figure 4.21). Therefore, both sampling configuration and collector placement need to be carefully considered, so that the results are meaningful and unbiased.

The transverse spread pattern is normally distributed, which means there are areas of high and low application rates within a swath width. If the set swath width is too wide, there will be insufficient overlap between the field swath widths. A single collector could capture fertiliser of either a high or low application rate, depending on where it is placed. In Trial 4, the flight lines showed that the pilot tried to align to the collector rows (Figure 5.4). As each collector row was 70 m a part and the aircraft was flying a set swath width of 15 m, Pilot A was not able to fully align to each row (70/15 = 4.7 flight lines in between rows). Therefore, the field

application rate may have been under-represented, because the trial was not random. Even in the nested grid sampling trial where randomisation was emphasised, it was uncertain whether the samples were representative of the population. Low application rates indicated either poor collector efficiency, insufficient flow rate out of the hopper, a narrow field swath width or a combination of the above, but it could not be determined from the results which was the main contributor.

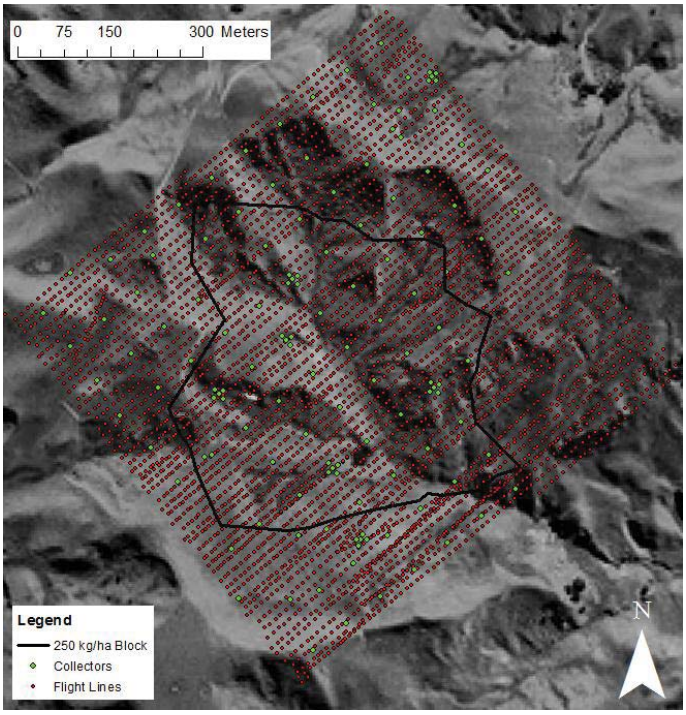


Figure 5.4: Aircraft flight lines recorded every 0.2 s by the VRAT system for Trial 4.

Collectors located near/at boundaries can affect the average field application rate and CV. It is difficult to achieve an even spread at the boundaries because of changing application rates, the forward motion of particles, time it takes for the flow rate to reach the peak stable rate and off-target application due to wind. The hopper door takes 0.18 – 0.37 s to respond to a change in the application zone depending on if a single or dual accumulator is used. If the aircraft is travelling at 56 m s^{-1}, this is an aircraft ground displacement of 11.25 – 23.16 m. As the hopper door opens, the flow rate will change and this will have an effect on the ground fertiliser distribution near the boundaries. It takes 2 – 3 s for the flow to equilibrate to the peak flow rate for that hopper door position, which corresponds to 112 – 168 m. Additionally ballistics modelling, supported by results in Trial 6, demonstrated that particles could travel 20 – 40 m forward of their release point depending on their size. Wind can significantly increase this distance. Therefore, as the aircraft enters a different application zone and the hopper door changes, these factors will introduce variability in to the neighbouring area.

Off-target application into waterways and neighbouring farms is a concern for farmers and applicators. Strict government environmental legislation is in place to regulate the amount of nitrogen/phosphate present in river ways. However, waterways can be less than a meter wide and the current practice is to apply indiscriminately. Pilots do not take action because they are travelling too fast and cannot recognise small features. An objective of the VRAT system is to prevent fertiliser landing in an exclusion zone. However, this is difficult to achieve because of wind conditions, level of accuracy achievable by the aircraft and the VRAT system, forward motion of particles, and a lack of understanding about the stochastic variation in fertiliser application. The VRAT system does have 'edge on' and 'edge off' settings, which could be used to minimise off-target application. When an aircraft enters a zero application zone, the hopper door will close before the boundary. The distance is dependent on the 'edge off' setting and can be a significant distance (approximately 65 m). The 65 m area will have a low field application rate, which can significantly reduce the average field application rate of the application zone. The current practice is to fly along the contour, but it would be more beneficial for pilots to fly parallel around the perimeter of the application zone in order to minimise variance and improve the field distribution.

Collectors are sometimes not placed fully upright in the field because of the topography. The metal spikes of the stand are used to hold the collector in place. For the collector to be level and stable, at least two of the three metal spikes need to be inserted in to the ground. However, in Trial 4 and 8 the steepness of some collector locations only allowed one spike to be inserted. Therefore, the collector had to be angled so that more spikes were inserted. It is unlikely that this had a significant effect on the application rate, but it contributes to the variance in the results.

There is also uncertainty about whether the performance trials were collecting a representative sample of the field application rate. Since a normal fertiliser application occurs over a whole farm, collecting samples from a small part of the application may not be sufficient to understand the variability in aerial topdressing. Collectors are used calibrate the aircraft system and to measure the level of control from the hopper door. However, the question is how many samples are needed. The original assumption was that the application rate collected in this area can be extrapolated to the whole farm, but the results from this study have shown that the field application rate can vary significantly.

The variation in the field application rate is further complicated by the limitations in the VRAT system's accuracy and how accuracy is assessed. The aircraft GPS, delays in system response,

and flow rate equilibration will always be a limitation in boundary recognition and eliminating off-target application. It is possible that a future iteration of the technology may react faster, be more accurate and compensate for environmental conditions. However, it is important at this stage to consider these limitations, and take the appropriate steps to reduce their effects. This includes flying parallel to boundaries when possible, assigning appropriate buffer zones, maintaining a constant aircraft velocity and altitude, and creating an accurate prescription map with precise farm boundaries.

5.4.4. Future Work

It is uncertain the number of trials required to validate a model for aerial topdressing. Two validation trials were carried out for each fertiliser type, yet this was likely an insufficient number of trials. Conditions can differ significantly between farms, application day, time of day and within a flight. One hundred and eighty trials were used to validate AgDRIFT, which were collected for a variety of different aircraft (i.e. Cessna AgHusky 188, Air Tractor AT-502, Aerodyne Wasp), application volume rates (> 0.8 – 38 L ha^{-1}), airspeeds (11 – > 50 m s^{-1}), spray types (nozzle type, nozzle angles, spray pressures and tank mixes), and wind conditions (speed 1.34 – 7.72 m s^{-1}) (Bird et al., 2002; Hewitt et al., 2002). The model and field results did not show a perfect consensus because of stochastic variability. However, the model was able to predict the average field deposition for a variety of conditions.

Hewitt et al. (2002) explained that the Spray Drift Task Force (SDTF) completed the 180 trials so that there was a database available for the quantification of off-target spraying. They created a comprehensive sampling plan by reviewing over 800 reports on spray drift to determine the suitable variables to test, and also considered and tested collector design. All the trials had the same sampling configuration. The application area consisted of four 13.7 m swath widths and a flight length of 792 m; this allowed the collection of a full load. The drift sample area was perpendicular and downwind to the application area, and was 792 m in length with collectors placed 15 m apart. Although there are significant differences between spray and granular application (i.e. particle ballistics and collection method), more than two validation trials should be collected to validate the granular fertiliser ballistics model. A comprehensive trial plan should be made to test for a variety of conditions. However, as shown by Bird et al. (2002), stochastic variability will be a limitation in fully validating the ballistics model.

SDTF tested numerous factors and degrees of freedom. These were determined in their review of the literature and the industry. Different factors and degree of freedoms would be tested in

aerial granular fertiliser application. Not all parameters can be tested so it is important to determine the most common degrees of freedom. There are several aircraft types used in aerial topdressing in New Zealand: PAC 600, PAC Fletcher FU-24 and Gippsland GA200C. Other factors of interest may be spreader type, aircraft velocity, weather conditions, hopper door position, and hopper door type. Ideally, only the factor of interest should vary, while the other factors remain the same, but the issue with factorial trials is there is limited control of other factors.

A complete data set was not collected in this work because of the collectors' limitations. The NZCPA collector lined with bubble wrap had the highest collection efficiency. However it does not have 100% collection efficiency and it is uncertain how much it is failing to collect. Further work is required to fully quantify the amount that bounces out, and assess whether the collection method could be improved. A complete sample could possibly be captured if a NZCPA collector was modified, by lining with bubble wrap, and extending the collar to a height where bounce is no longer an issue. Cardboard could be used to make a simple collar extension. Trial 7 could be repeated comparing the NZCPA collector lined with bubble wrap and the extended collar collectors. High speed photometry could be used to observe an extended collar collector to determine if all the material has been captured. It is not possible to collect data from more than one collector, unless multiple cameras are set up. Therefore, this trial should be completed at least three times for each fertiliser type to get sufficient high speed images, and to ensure the results are repeatable.

The NZAAA collectors are used in Spreadmark certification tests, and their efficiency for all fertiliser types should be tested for reliability. Trial 7 showed that the NZAAA collectors were not as efficient as the NZCPA collectors lined with bubble wrap for superphosphate; therefore, the NZAAA collectors are likely underestimating the field application rates in Spreadmark tests. In Spreadmark tests, the field application rate should be within 30% of the intended application rate for accuracy. It is unlikely that the NZAAA collectors experience more than 30% of fertiliser particles bouncing out based on Trial 7, but the exact efficiency should be determined. If possible, collectors should be redeveloped to improve their collection capability.

Since Spreadmark is the method of assessing accuracy and precision in New Zealand, its validity is held to a higher standard. However, these trials have shown that they have limitations. The NZAAA collectors are small (0.25 m^2) and are set out in three rows to collect a single swath width. This sampling method is not representative of the area. Spreadmark tests

are conducted in ideal conditions on flat land. In an actual application, the swath width is not controlled by the pilots, and is actually highly dependent on the conditions during application. It may be more beneficial to calculate the CV based on multiple swath widths, and to limit the number of runs the pilot can carry out to achieve the maximum swath width. Currently pilots are given unlimited Spreadmark tests to achieve a maximum swath width.

Future performance trials should be designed to answer the objective. However, it might not be possible to have a perfect trial. For example, there is currently no method of assessing the accuracy and precision of a farm application with the number of collectors available. There is too much variability in the application in both the transverse and longitudinal direction to capture over the large areas. The best method of determining the average application area over the farm might be to measure the flow out of the hopper door against time. This will not indicate where the fertiliser lands, but will give the farmer and applicator a general idea of the overall application rate. Weigh cells could be used to measure the remaining load in the hopper.

Line sampling is a good method for collecting multiple swath widths, and there should be replicates of some collectors. Collectors should not be placed more than 3 m apart, which means to cover a large area many collectors are required. Longitudinal variation has not previously been studied in detail, and a possible solution is to set up a field trial to collect a full hopper load. At an application rate of 500 kg ha^{-1}, aircraft velocity of 56 m s^{-1} and swath width of 14 m, it would take 2.6 km for the hopper to empty with a 1.8 T load. Collectors would be placed at regular intervals along this 2.6 km line, and remaining collectors can be used to collect transverse spread patterns. This trial should be completed with no wind present, so that the peak mass can be consistently collected. Because field trials are so expensive and time consuming, trials should be thoroughly planned, and there should be few unknowns (i.e. collector efficiency, hopper door opening and flow rate relationship). This will help to reduce variability in the results, and provide a better understanding of the aircraft's performance.

5.5. Implications of Research

These are the main implications of this research for Ravensdown, the fertiliser industry and the aerial topdressing industry.

- Variable rate application technology for aerial topdressing should be adopted. This study has shown that variable rate application can improve precision over conventional aerial topdressing. The method produces accurate applications and can reduce off-target application if the appropriate settings are used. VRAT is capable of

varying rate, which means it can be used to improve fertiliser utilisation on farms. There are also benefits for the pilot as they can focus more on identifying hazards in the surrounding area, and concentrate less on looking for farm boundaries, since the system is automated and swath tracking is available.

- The VRAT system has performance limitations. Topdressing aircraft travel at 200 – 250 KPH during application, while assessing its location every 0.2 s using GPS. Therefore the ability of the aircraft to deliver fertiliser to a specific area is 11 – 15 m. Mechanical delays are also a limitation as it takes time for the system to register and make an adjustment to the hopper door. Additionally there is the variability in the hopper flow as it equilibrates to the new hopper door opening. These all contribute to variability in the field application rate.
- There should be a re-assessment of how Spreadmark measures aerial topdressing performance. This includes the collectors and sampling configuration used to collect the data. Trials have shown that NZAAA collectors (which are used in Spreadmark) experience fertiliser bounce and that three rows of collectors collecting one swath width is not indicative of the field application rate.
- This study has shown that the level of accuracy and precision achievable in the field is much lower than expected. Therefore it is necessary to determine what the acceptable field application rate is, and whether the current assessments (i.e. Spreadmark) help to achieve these expectations.
- Many trials are required to gain certainty of a model and the VRAT system's performance. Trials are expensive; therefore they need to be well thought out, and thorough analysis should be completed to maximise the value of each trial.
- Ballistics modelling is useful but the simplification of the model inputs limits its accuracy. Since aerial topdressing is a complex process, generalising the model inputs will reduce its prediction value for the current situation. Understandably, it is difficult to collect the information to the resolution required, even in trials. The user should be aware of the model's limitations and expect deviations from the field application rate, when using standardised inputs.
- Aerial topdressing is a highly variable process, which is not well understood. The variance of the data collected in the trials is affected by numerous variables (i.e. wind, topography, aircraft operation, field collection). It is uncertain what level of variability each factor imparts or how they interact. Further study of the factors, in the lab and in the field, is required.

5.6. Improvements to Research Methodology

In review, there were numerous ways to improve the research methodology. The most significant improvement is the sequence in which trials and testing were completed.

1. Literature review

The purpose of a literature review is to gain an understanding of the industry and previous work completed in the study area. It is a beneficial process that should have been completed before any significant field work was undertaken. In this instance, the work was originally assigned through a research based Master of Science (MSc) with an existing test schedule, so a literature review was not completed first. The literature review would have revealed the variability encountered in past aerial topdressing studies, and a number of assumptions that had been made about the VRAT system's performance, which had gone untested. This included the way the field CV was calculated, the efficiency of the field collectors, and the flow characteristics of the fertiliser from the hopper. If the literature review had been carried out first, these assumptions would have been identified and addressed sooner.

2. Test efficiency of collectors and optimise collector

NZCPA collectors were previously assumed to have close to 100% efficiency, but their actual efficiency was not tested. Originally the NZCPA collectors consisted of the stand and cone. Grafton et al. (2012) utilised these collectors and particle bounce out of the collector was observed, but the extent of the issue was not stated. The field application rates found in the Grafton et al. (2012) trial was probably significantly less than the target application rates, and the magnitude of particle bounce would have been greater than in Trial 4 and 5 because without the collar, fertiliser would have been more likely to bounce out of the collectors. Additionally, the standard deviation between collectors may have been large as well, but it is uncertain if this would affect the CV reported. A collar was introduced after the trial, and it was assumed that the addition resolved all issues with particle bounce. This was proven false in Trial 6. Tests to determine the collector's efficiency should have been completed before any trials. As part of scientific research, it is important to determine the efficiency of the sampling method. If the issue was resolved earlier, the proceeding trials and results would have provided greater value and validity. At this stage, it is still unknown whether 100% collection is achievable.

3. Investigate flow rate out of the hopper

The Beverloo equation was used to estimate the flow rate out of the hopper door opening. This was provided by Ravensdown Limited and was based on work completed by Grafton (2010) for lime. However, it was not tested on a standardised PAC 600 hopper. Since it is extremely difficult to measure the flow rate from the hopper during application, it is important that an accurate correlation is found. Testing of the Beverloo equation through static hopper flow tests should have been completed before any trials. Field calibrations, in still weather conditions, were also required to ensure that the correlations were accurate. It may have been necessary to collect the application of a full load. Completing this investigation would have explained some of the variability encountered in the performance trial results, and although it is extremely difficult to achieve constant flow rates, methods to minimise non-constant hopper flow rates could have been found.

4. Bench testing

Bench testing is significantly more inexpensive than performance trials, and should have been better utilised as a tool to assess the variable rate application system. In general, a Satloc Intelligate system could have been set up without the automated hydraulic hopper door to test prescription maps before they are loaded on to the aircraft. Bench testing should have been completed before each trial to ensure the prescription maps were correctly formatted. The bench tests revealed limitations of the Satloc G4 Intelligate system. As specified by Satloc, the prescription maps can handle up to 10,000 vertices. Bench testing revealed that as the prescription maps had more vertices, the accuracy of the VRAT system to open to the correct hopper door position decreased (Table 4.3). This limitation is a concern and should be addressed with Satloc. The system currently has no method to recognise and compensate for angled boundaries, where the aircraft is not entering perpendicular to the boundary. This results in off-target application (Figure 4.17). To compensate, the pilot should either fly perpendicular or parallel to a boundary line.

5. Model validation Trial 1 should have been completed for all fertiliser types including the 70% superphosphate/30% Flexi-N blend

A model validation trial is less logistically challenging and resource intensive than a performance trial. It could have been an introduction to field trials, and issues that emerged from this trial could have been solved for the performance trial. At this point in time, modelling for the fertiliser blend was not a requirement, and was not included until a later date. However, validation data should have been collected at the earliest possibility.

6. First performance trial using line sampling on hill country.

Line sampling was previously completed by Ballard and Will (1971). This sampling method was able to determine accuracy, precision, capability and level of off-target application. It also captures the swath width, and gives an indication of the overall variability of aerial topdressing. However, it does not collect sufficient information on longitudinal variability, which is an issue. Additional collectors could have been planned to collect longitudinal data. The first performance trial was completed in a grid sampling method, and the data was Kriged. However, the collected data was not appropriate for kriging, because spatial variance was not captured at various distances. The pilot also created bias by trying to align to the collectors. Since performance trials were the most expensive component of the project, greater thought and consideration should be given to ensure that appropriate results were collected.

If the first performance trial was completed with tested collectors and calibrated flow rates, the results would have been more reliable. The trial may have given a clearer indication of the areas that needed improvement in the trial and the variable rate system. Unexplained variability could have been investigated in further trials and experiments. In general, all performance trials should have been completed using one fertiliser type applied at 2 – 3 application rates. Trial 5 was completed using a fertiliser mix, which made it difficult to separate its significance in the variance in that trial. Performance trials should be completed on the same farm to try and reduce possible factors that may contribute to variability and, if possible, a spreader should be attached.

5.7. Conclusion

Fertiliser application can be separated into three aspects. The first is its release from the aircraft. This study determined that the main source of variation was the flow dynamics of the fertiliser as it leaves the hopper door, while the aircraft is applying. Previous work in this area has been limited, but it may explain the difference between the results from the static hopper flow tests and Trial 8. To understand the flow dynamics from the hopper door during application, cameras should be attached to observe the fertiliser particles leaving the hopper door.

The second aspect is the motion of the particle through the air, which is known to be significantly affected by wind conditions. The Jones et al. (2008) single particle granular fertiliser model can be used to predict the offset from wind conditions. To make the model more accessible, it was converted to a wind displacement calculator that can be deployed in ArcGIS. However, the calculator is only able to predict the peak offset of the transverse spread

pattern for the average wind velocity and direction; it was simplified to make it more user friendly.

Part three is the placement of fertiliser on the ground and how this is measured. This study encountered issues with collector efficiency and sampling configuration, which affected field results. Further investigation of the NZCPA collectors lined with bubble wrap and NZAAA collectors is required to determine their efficiency. Sampling configurations should be developed around the objectives of a trial.

Overall, to achieve an improved variable rate fertiliser application, this study recommends that the prescription map should have accurate boundaries, and include sufficient buffers. The buffers can be calculated using the ballistic model. Pilots should fly parallel to boundaries, when possible or fly the perimeter of the application area in a race track pattern. This will improve the overall fertiliser distribution in an application zone, mitigate issues surrounding sloped boundaries, and prevent off-target application. Calibration of the application rate leaving the aircraft should be completed before each job, and a method of monitoring the flow rate from the hopper door should be developed and installed. This will help to improve the field application rate. Performance and validation trials should be well planned and sources of variability be limited (i.e. collector efficiency, unknown flow dynamics, fertiliser type). Lastly, multiple trials are required on each farm and under different conditions to ensure robust testing is undertaken.

Chapter 6 - Summary

6.1. Summary

Ravensdown Limited funded this Doctorate of Philosophy to assess a variable rate application technology (VRAT) system that is installed on their Pacific Aerospace Cresco (PAC) 600 aircraft. This project was completion conjunction with their Primary Growth Partnership 'Pioneering to Precision – Application of Fertiliser in Hill Country' with the Ministry of Primary Industries (MPI). The objective of the project is to improve granular fertiliser application to hill country farms, using remotely sensed data and variable rate fertiliser plans. VRAT equipped aircraft are used to execute the fertiliser plans produced. Aerial topdressing is a complex process, and considerable knowledge of its dynamics and ballistics are required to set appropriate hopper door openings for the VRAT plan. While some parts of the process can be consistently controlled through automation, there are other factors that cannot be controlled, and are a source of variation. Wind is the obvious one, where improvements can be made by the wind displacement calculator tool. However, the tool only considers average wind conditions. It is currently not feasible to respond immediately to every variation in the wind conditions. Therefore, automation will reduce operational variability, but it cannot eliminate naturally occurring events.

Chapter 2 presents the validation of a single particle ballistics model formulated by Jones et al. (2008) and further developed by Murray (2007) to determine the transverse spread pattern. Three trials were used to validate the model for superphosphate, urea, di-ammonium phosphate (DAP), and a 70% superphosphate/30% Flexi-N fertiliser blend. Each fertiliser type had two sets of validation data. The point of this is to use the first data set to calibrate the model. The second data set independently validates the model to ensure it has not been over-fitted.

An important part of modelling is selecting accurate model inputs. Incorrect characterisation of the inputs will result in decreased model accuracy. Measuring the initial conditions of aerially applied fertiliser particles is difficult because many particles are applied at once. Furthermore, the use of sensitive equipment is limited by the corrosive property of the fertiliser. Spreaders added greater complexity since they increased the number of possible initial conditions. The characteristics of two spreaders were measured: 11 duct Transland and 9 duct FarmAir ram air spreader. Air flow measurements, using pitot tubes, were taken from the FarmAir spreader and used to estimate the air velocity through a Transland spreader. These values and the aircraft velocity were used to determine the initial discharge velocity of a particle. Inputs, such

as sphericity and the wind power law coefficient, were not fully examined but best estimates were used.

The initial validation was completed for superphosphate because it was applied without a spreader. Superphosphate's modelled transverse spread pattern favoured the left side of the aircraft and did not fit the field data. The lack of fit was attributed to the propeller wash component in the model. In the initial time steps, mass flow occurs out of the hopper door, and the PAC 600 propeller is not powerful enough to separate the particles. Therefore, the particles fall out the propeller wash without being significantly dispersed. After removing the propeller wash component, the modelled transverse spread pattern improved. However, the model does not produce a perfect fit because not all initial conditions are perfectly characterised.

Model validation was completed by comparing the application rates and swath widths of the modelled and field transverse spread patterns, using Spreadmark V17. There was good agreement between the two spread patterns. Model accuracy was also determined using the Kolmogorov-Smirnov (K-S) test. The test indicated that there was no statistically significant difference between the modelled and field transverse spread patterns.

Ravensdown Limited was interested in using the model as a predictor of wind effects on the transverse spread pattern during application. The wind displacement calculator was developed to model the effect of average wind velocity and direction before an application. The calculator produces an offset value that is used to shift the application area to minimise off-target application. The tool was developed using Python and ArcGIS 10.1. Since modelling can take significant time, the tool was further simplified to create wind displacement look up tables. These were developed for superphosphate, urea and DAP. Look up tables were also completed for urea and DAP applied with a Transland and Farmair spreader.

Chapter 3 discussed three sampling configurations used in the performance trials to determine the accuracy, precision, off-target application and capability of the VRAT system. Each trial had different objectives, so the sampling configuration varied. Grid sampling was found to be a poor method of sampling for aerial topdressing. The data collected should not be Kriged, and high variance was observed but unexplained. The nested grid sampling configuration improved the data set for kriging, but did not characterise field variability. Line sampled data was not used for kriging, but the configuration was able to show some sources of variation from within and between swath widths. All three sampling configurations did not examine longitudinal variation down the swath.

The main issue discussed in Chapter 3 is particle bounce out of the collectors. This was discovered in Trial 6 with the help of high speed photometry. The images showed that a significant proportion of the sample bounced out from a New Zealand Centre for Precision Agriculture (NZCPA) collector for superphosphate, urea and DAP, which affects the results from previous trials. Other collectors were investigated to improve the collection efficiency. Trial 7 determined the efficiency of the NZCPA, NZCPA lined with bubble wrap, and New Zealand Agriculture Aviation Association (NZAAA) collectors for superphosphate. The NZCPA collector lined with bubble wrap performed the best. However, it does not have 100% efficiency. The particle bounce out percentage found in Trial 6 and 7 were used to correct previous trial data.

Chapter 4 evaluates the VRAT system for accuracy, precision, off-target application and capability. Trial 4 and 5 showed that the VRAT system applied the field application rate within 30% of the target application rate for both zones. This means it is considered accurate by Spreadmark. These values were corrected for particle bounce out of the collectors. The coefficient of variation (CV) from both trials was lower than the CV found in pilot operated application systems, so VRAT improved precision. One way ANOVA tests showed that there is a statistically significant difference between the field application rate of the two application zones for both Trial 4, 5 and 8. This implies the VRAT system is capable of varying the application rate. Fertiliser was collected in the exclusion zone (i.e. zero application rate) in Trial 8. To minimise off-target application, the prescription map should have an appropriate buffer zone that considers environmental conditions and forward motion of particles. However, wind conditions can shift significantly in a short time, and the ballistics model does not account for outlying granule sizes (< 7 mm and > 0.5 mm); therefore, the pilot should fly parallel to the perimeter of the application zone, when possible.

Bench testing resulted in better understanding of the VRAT system without the added variability of fertiliser flow out of the hopper door, air flow dynamics, and environmental conditions. Bench testing found boundary settings (‘edge on’ and edge off’) that accounted for the system delay. These were validated in the field. Different prescription maps were also tested to find the limitations of the VRAT system. Further investigation of large prescription maps is required (> 10,000 vertices). The bench test results indicated that the greater the number of vertices and polygons, the more inaccurate the hopper door position.

Static hopper flow tests were completed on a standardised PAC 600 hopper. Two hopper doors were tested: clamshell and cantilever. The cantilever hopper door is currently used on

operating topdressing aircraft and replaced the clamshell hopper door. The objective of the static hopper flow test was to determine the relationship between flow rate and the hopper door opening. Flow from the cantilever hopper door was constant after the first 2 – 3 s. The clamshell hopper door produced non-constant flow rates at hopper door openings greater than 0.046 m. From the flow tests, linear flow equations were developed that calculated the expected flow rate out of the hopper door depending on the door opening. Coefficients for the Beverloo equation were also determined. The linear and Beverloo equation calculated similar door openings for a specified application rate. However, these two values were different to what was collected in the field. This suggests that the flow dynamics from the hopper door differs during flight. Further work is required to understand this occurrence so that when the hopper door is automated, the pilot will have confidence that they are applying the correct application rate.

Chapter 5 discussed the sources of variation in this study, aerial topdressing, and its testing. The main issues were the flow dynamics from the hopper door during application, variability of wind conditions, collector efficiency, and sampling configuration. These issues have not been fully resolved, and require further investigation as they have significant effect on the field application rate, CV, and off-target application. Areas of future work are discussed extensively. Several model inputs (i.e. sphericity, wind power law coefficient, spreader discharge parameters) need to be measured, so that a more accurate value is used for the model. Finally, to gain a better understanding of aerial topdressing, more trials are required to determine the effect of different environmental conditions, aircraft type and operation, and sampling configuration.

6.2. Concluding Remarks

This study was the first to undertake performance trials assessing aerial variable rate application of granular fertiliser. The trials were meant to quantify the benefits of the system. However, as the study progressed, it was realised that there is a poor understanding of aerial topdressing in general. There were limited studies completed on aerial topdressing in the past so the accuracy, precision, and level of off-target application of pilot operated application systems is unknown. This makes it difficult to determine the level of improvement aerial topdressing would have from installing the VRAT system. Overall, the variable rate application system improved aerial topdressing, but not to the targets desired. However, the reason that this likely occurred is that the conventional application method was not fully studied, so the starting point is unknown, and the new target is unrealistic. The variability may still have been halved. Spatially dense data was also not collected reliably, so it is unknown whether general

conclusions can be made from the collected data set. It should be noted that very similar data collection methods, to past studies, were used in this study, but in a more complete way. A substantial redesign of the collectors may be required to achieve close to 100% collection.

Part of the issue with previous aerial topdressing studies is that they were based on assumptions that were found to be false. Assumptions include the flow dynamics from the hopper door, repeatability of the swath width, stability of environmental conditions, collection efficiency, and collecting representative samples. There are numerous areas that require further study. The next step is to determine the flow dynamics from the hopper door during application. This could be completed by installing cameras to observe the hopper door. It would also be useful to measure the change in the weight of the hopper load over time, which will indicate the flow rate out of the hopper door opening. Before undertaking the next trial, the collector efficiency should be quantified to ensure a reliable and unbiased data set. To achieve this, a complete fertiliser sample (100% efficiency) should be collected, and compared to the amount captured in the NZCPA collector lined with bubble wrap. A suggestion for collecting a complete sample is to extend the collar of the collector, so that it is too high for fertiliser particles to bounce out.

Although a number of particle ballistic models for aerial granular fertiliser application have been developed, this study created the first commercial wind displacement calculator. Wind is a continuing issue in aerial fertiliser application. In conventional applications, no action is taken to compensate for wind, which results in off-target and inaccurate application. Therefore, the wind displacement calculator has significant value for aerial spreaders. They now have the ability to compensate for average wind conditions measured on the day. The calculator will also predict the field swath width, which can be used to adjust the set swath width, so that there is improved overlap between the transverse spread patterns. However, it should be noted that aerial topdressing is a highly variable and complex process, and care is needed when implementing the model results.

This study has highlighted the highly variable nature of hill country fertiliser application. Currently, a pilot makes decisions based on their experience and what they observe. They make these decisions while travelling at over 200 km h^{-1} and 20 – 40 m above the ground over thousands of hectares. As this occurs, the wind conditions and topography varies. It is, therefore, difficult to foresee and observe where fertiliser will land on the ground and in what quantity. The VRAT system is not meant to replace pilots, but is there to assist them by providing information on aircraft location and farm boundaries, and control flow from the

hopper door. This will allow pilots to focus on their surroundings, which will decrease mistakes and accidents. It will also increase a pilot's control of the hopper door, since adjustments of 1.6 mm can be made automatically. Overall, the VRAT system and ballistic modelling will improve fertiliser application to hill country, by increasing the level of control and understanding of the process.

6.3. Publications

The following is a list of publications that has been produced from this thesis:

Chok, S., Yule, I., and Grafton, M. (2017). *Improving aerial topdressing for hill country through differential rate application technology and modelling.* Paper presented at the International Tri-Conference for Precision Agriculture, Hamilton.

Chok, S. E., Grafton, M. C. E., Yule, I. J. & White, M. (2016). *Accuracy of differential rate application technology for aerial spreading of granular fertilizer within New Zealand.* In Proceedings of the 13th International Conference on Precision Agriculture (unpaginated, online). Monticello, IL: International Society of Precision Agriculture.

Chok, S. E., Grafton, M. C. E., Yule, I. J., and Manning, M. J. (2016). *Capability of ground fertiliser placement when spread from fixed wing aircraft.* (Eds E. R. Thom). Paper presented at the Hill Country Symposium, Rotorua, New Zealand (p 191 – 196). Dunedin, New Zealand: New Zealand Grassland Association.

Chok, S. E., Grafton, M. C. E., Yule, I., White, M., and Manning, M. J. (2016). *Improving aerial topdressing in New Zealand through particle ballistics modelling and accuracy trials.* In: Integrated nutrient and water management for sustainable farming. (Eds L. D. Currie and R. Singh). Occasional Report No. 29. Fertilizer and Lime Research Centre, Massey University, Palmerston North, New Zealand.

Chok, S. E., Grafton, M., and Yule, I. J., (2015). *Validation of model predicting solid fertilizer deposition from a fixed wing aircraft*. Presented at the Proceedings of the 2015 ASABE Annual International Meeting. St. Joseph, MI: American Society of Agricultural and Biological Engineers.

References

Adams, J. R., and Merz, A. R. (1929). Hygroscopicity of fertilizer materials and mixtures. *Industrial & Engineering Chemistry, 21*(4), 305-307.

Akesson, N. B., and Yates, W. E. (1964). Airplane Application of Bulk Fertilizer. *7*(2).

ASAE. (1999). S386.2 Calibration and distribution pattern testing of agricultural aerial application equipment. *ASAE Standards*. St Joseph, Michigan: ASAE.

Ballard, R., and Will, G. (1971). Distribution of aerially applied fertiliser in New Zealand forests. *New Zealand Journal of Forestry Science, 1*, 50-59.

Bansal, R., Walker, J., Gardisser, D., and Grift, T. (1998). Validating FLUENT for the flow of granular materials in aerial spreaders. *Transactions of the ASAE, 41*(1), 29-35.

Bansal, R. K., Walker, J. T., and Gardisser, D. R. (1998a). Computer simulation of urea particle acceleration in an aerial spreader. *Transactions of the Asae, 41*(4), 951-957.

Bansal, R. K., Walker, J. T., and Gardisser, D. R. (1998b). Simulation studies of urea deposition pattern from an aerial spreader. *41*(3).

Barker, P. R. (1979). *Factors affecting aerial distribution of fertilizers to forests.* Paper presented at the Forest Fertilization Conference: September 25-27, 1979, Alderbrook Inn, Union, Washington.

Barringer, J., Pairman, D., and McNeill, S. (2002). *Development of a high resolution digital elevation model for New Zealand*.

Beverloo, W., Leniger, H., and Van de Velde, J. (1961). The flow of granular solids through orifices. *Chemical Engineering Science, 15*(3), 260-269.

Bilanin, A. J., Teske, M. E., Barry, J. W., and Ekblad, R. B. (1989). AgDISP: The aircraft spray dispersion model, code development and experimental validation. *Transactions of the ASAE, 32*(1), 327-0334.

Bird, S. L., Perry, S. G., Ray, S. L., and Teske, M. E. (2002). Evaluation of the AgDISP aerial spray algorithms in the AgDRIFT model. *Environmental Toxicology and Chemistry, 21*(3), 672-681. doi: 10.1002/etc.5620210328

Bohling, G. (2005). *Introduction to geostatistics and variogram analysis.*

BSI. (2013). Test sieves - technical requirements and testing. *Part 2: Tests sieves of perforated metal plate. BS ISO 3310-2:2013* (5 ed.). London, UK: BSI.

Burgess, T., and Webster, R. (1980). Optimal interpolation and isarithmic mapping of soil properties. *Journal of Soil Science, 31*(2), 333-341.

Chan, C. W., Schueller, J. K., Miller, W. M., Whitney, J. D., and Cornell, J. A. (2004). Error sources affecting variable rate application of nitrogen fertilizer. *Precision Agriculture, 5*(6), 601-616. doi: 10.1007/s11119-004-6345-2

Charlton, J. F. L., Sedcole, J. R., and Smith, A. W. J. (1983). Evaluation of devices fitted to a topdressing aircraft to increase fertiliser spread. *New Zealand Journal of Experimental Agriculture, 11*(2), 177-180. doi: 10.1080/03015521.1983.10427750

Chen, Y. C., Bundy, D. S., and Hoff, S. J. (1998). Modeling the variation of wind speed with height for agricultural source pollution control. *ASHRAE Transactions, 104*(1B), 1685.

Chok, S., Grafton, M., Mills, T., and Yule, I. (2014). *The variability in New Zealand single superphosphate granule strength and size, and implications for accurate fertiliser application.* Paper presented at the Fertiliser and Lime Research Workshop, Massey University, Palmerston North.

Counihan, J. (1975). Adiabatic atmospheric boundary layers: a review and analysis of data from the period 1880–1972. *Atmospheric Environment (1967), 9*(10), 871-905.

Craig, I., Woods, N., and Dorr, G. (1998). A simple guide to predicting aircraft spray drift. *Crop Protection, 17*(6), 475-482.

Diacono, M., Rubino, P., and Montemurro, F. (2012). Precision nitrogen management of wheat. A review. *Agronomy for Sustainable Development, 33*(1), 219-241. doi: 10.1007/s13593-012-0111-z

During, C., and Mountier, N. (1967). Sources of error in advisory soil tests: III. Spatial variance. *New Zealand Journal of Agricultural Research, 10*(1), 134-138.

Earls, J., and Dixon, B. (2007). *Spatial interpolation of rainfall data using ArcGIS: A comparative study.* Paper presented at the ESRI User Conference.

Fertiliser Association. (2007). Fact sheet 6: fertiliser use. Retrieved from Fertiliser Storage website: http://www.fertiliser.org.nz/Site/code_of_practice/best_management_practices_considerations/fertiliser_handling/fertiliser_storage.aspx

Geelen, J. (1983). *The topdressers*: Te Awamutu, N.Z. : NZ Aviation Press, 1983.

Gillingham, A., and During, C. (1973). Pasture production and transfer of fertility within a long-established hill pasture. *New Zealand Journal of Experimental Agriculture, 1*(3), 227-232.

Gillingham, A., Gray, M., and Smith, D. (1998). *Pasture responses to phosphorus and nitrogen fertilisers on dry hill country.* Paper presented at the Proceedings of the Conference - New Zealand Grassland Association.

Gillingham, A., Maber, J., Morton, J., and Tuohy, M. (1999). *Precise aerial fertiliser application on hill country.* Paper presented at the Proceedings of the Conference - New Zealand Grassland Association.

Gillingham, A. G., Maber, J. F., Macfarlane, M. J., Korte, C. J., and Manning, M. J. (1985). *Effects of wind and fertiliser characteristics on aerial distribution from an unmodified fixed wing aircraft.* Paper presented at the 20th Technical Workshop and Fertiliser Manufacturers Research Association.

Goense, D. (1997). The accuracy of farm machinery for precision agriculture: A case for fertilizer application. *NJAS Wageningen Journal of Life Sciences, 45*(1), 199-215.

Grafton, M., Yule, I., Davies, C., and Jones, J. (2009). *Incidents and accidents in aerial topdressing in New Zealand*.

Grafton, M., Yule, I., and Watson, R. (2012). *Improving the field CV of aerial topdressing: through computer controlled prescription delivery*. Paper presented at the American Society of Agricultural and Biological Engineers International Meeting, Dallas, Texas. http://elibrary.asabe.org/abstract.asp?aid=41974&t=5

Grafton, M. C. E. (2010). Flow of particulate material from a topdressing aircraft: a thesis presented in partial fulfilment of the requirements of the degree of Doctor of Philosophy in Agricultural Engineering at Massey University, New Zealand.

Grafton, M. C. E., Yule, I. J., Davies, C. E., Stewart, R. B., and Jones, J. R. (2011). Resolving the agricultural crushed limestone flow problem from fixed-wing aircraft. *Transactions of the ASABE, 54*(3), 769-775. doi: 10.13031/2013.37092

Grift, T. (2001). Mass flow measurement of granular materials in aerial application-Part 1: Simulation and modeling. *Transactions of the ASABE, 44*(1), 19-26.

Grift, T. (2011). Picking the low fruit. *Resource, July/August,* 30-31.

Grift, T., and Hofstee, J. (1997). Measurement of velocity and diameter of individual fertilizer particles by an optical method. *Journal of Agricultural Engineering Research, 66*(3), 235-238.

Grift, T., Walker, J., and Hofstee, J. (2001). Mass flow measurement of granular materials in aerial application. Part 2: Experimental model validation. *Transactions of ASAE, 44*(1), 27-34.

Grift, T. E. (2000). Spread Pattern Analysis Tool (SPAT): I. Development and theoretical examples*., 43*(6).

Grift, T. E., and Crespi, C. M. (2008a). Estimating mean particle diameter in free-fall granular particle flow using a Poisson model in space. *Biosystems Engineering, 101*(1), 28-35. doi: https://doi.org/10.1016/j.biosystemseng.2008.06.005

Grift, T. E., and Crespi, C. M. (2008b). Estimation of the flow rate of free falling granular particles using a Poisson model in time. *Biosystems Engineering, 101*(1), 36-41. doi: https://doi.org/10.1016/j.biosystemseng.2008.06.006

Grift, T. E., Walker, J. T., and Gardisser, D. R. (2000). Spread Pattern Analysis Tool (SPAT): II. Examples of aircraft pattern analysis. *43*(6).

Grift, T. E., Walker, J. T., and Hofstee, J. W. (1997). Aerodynamic properties of individual fertilizer particles*., 40*(1).

Gundogdu, M. Y. (2004). Discharge characteristics of polydisperse powders through conical hoppers. Part 1: Predictions for fine, granular, free flowing powders. *Particulate Science and Technology, 22*(4), 339-353.

Haider, A., and Levenspiel, O. (1989). Drag coefficient and terminal velocity of spherical and nonspherical particles. *Powder Technology, 58*(1), 63-70.

Hedderwick, G., and Will, G. M. (1982). *Advances in the aerial application of fertiliser to New Zealand forests: The use of an electronic guidance system and dust-free fertiliser*. Rotorua, New Zealand: Forest Research Institute, New Zealand Forest Service.

Hedley, C. (2014). The role of precision agriculture for improved nutrient management on farms. *Journal of the Science of Food and Agriculture, 95*. http://www.ncbi.nlm.nih.gov/pubmed/24816925 doi:10.1002/jsfa.6734

Hewitt, A., Teske, M., and Thistle, H. (2001). The development of the AgDRIFT® model for aerial application from helicopters and fixed-wing aircraft. *Australasian Journal of Ecotoxicology, 8*, 3-6.

Hewitt, A. J., Johnson, D. R., Fish, J. D., Hermansky, C. G., and Valcore, D. L. (2002). Development of the Spray Drift Task Force database for aerial applications. *Environmental Toxicology and Chemistry, 21*(3), 648-658. doi: 10.1002/etc.5620210326

Hoffmeister, G., Watkins, S. C., and Silverberg, J. (1964). Fertilizer consistency, bulk blending of fertilizer material: effect of size, shape, and density on segregation. *Journal of Agricultural and Food Chemistry, 12*(1), 64-69. doi: 10.1021/jf60131a020

Humby, S., Tüzün, U., and Yu, A. (1998). Prediction of hopper discharge rates of binary granular mixtures. *Chemical Engineering Science, 53*(3), 483-494.

International Organization of Standardization. (1985). 5690/1 Equipment for distributing fertilizers. Test methods. Part 1: Full width fertilizer distributors *International Organization for Standardization, Geneva*.

Johnston, K., Ver Hoef, J. M., Krivoruchko, K., and Lucas, N. (2001). *Using ArcGIS geostatistical analyst* (Vol. 380): Esri Redlands.

Jones, J. R., Murray, R. I., and Yule, I. J. (2008). Modeling the coarse fraction of solid fertilizer deposition from a fixed-wing aircraft: 1. a ballistics model. *Transactions of the ASABE, 51*(3), 857-872.

Justus, C., Hargraves, W., Mikhail, A., and Graber, D. (1978). Methods for estimating wind speed frequency distributions. *Journal of Applied Meteorology, 17*(3), 350-353.

Kiš, I. M. (2016). Comparison of Ordinary and Universal Kriging interpolation techniques on a depth variable (a case of linear spatial trend), case study of the Šandrovac Field. *Rudarsko-geološko-naftni zbornik, 31*(2), 41-58.

Koch, H., Weißer, P., and Stadler, R. (2005). Aspects of wind measurement and the effect of wind on transport and deposition of drift particles during pesticide application. *Nachrichtenblatt-Deutschen Pflanzenschutzdienstes Braunschweig 57*(10), 204-214.

Krige, D. G. (1951). A statistical approach to some mine valuation and allied problems on the Witwatersrand. *Journal of the Southern African Institute of Mining and Metallurgy, 56*(6), 119-139.

Kuntz, M., and Helbich, M. (2014). Geostatistical mapping of real estate prices: an empirical comparison of kriging and cokriging. *International Journal of Geographical Information Science, 28*(9), 1904-1921.

Lambert, M. G., Clark, D. A., and Mackay, A. D. (1990). *Long term effects of withholding phosphate application on North Island hill country: Ballantrae.* Paper presented at the Proceedings of the New Zealand Grasslands Association.

Laslett, G. M. (1994). Kriging and splines: An empirical comparison of their predictive performance in some applications. *Journal of the American Statistical Association, 89*(426), 391-400.

Leopold, U., Heuvelink, G. B., Tiktak, A., Finke, P. A., and Schoumans, O. (2006). Accounting for change of support in spatial accuracy assessment of modelled soil mineral phosphorous concentration. *Geoderma, 130*(3), 368-386.

Lockett, E. (1998). A new system for evaluating the distribution of aerially spread material. *Tasforests 10*, 83-90.

López-Granados, F., Jurado-Expósito, M., Alamo, S., and Garcıa-Torres, L. (2004). Leaf nutrient spatial variability and site-specific fertilization maps within olive (Olea europaea L.) orchards. *European Journal of Agronomy, 21*(2), 209-222.

Macfarlane, M., Korte, C., and Gillingham, A. (1987). *The effect of increasing winds on the distribution of oversown seed and fertiliser.* Paper presented at the Proceedings of the New Zealand Grassland Association.

Mankoc, C., Janda, A., Arévalo, R., Pastor, J. M., Zuriguel, I., Garcimartín, A., and Maza, D. (2007). The flow rate of granular materials through an orifice. *Granular Matter, 9*(6), 407-414. doi: 10.1007/s10035-007-0062-2

Manwell, J. F., McGowan, J. G., and Rogers, A. L. (2010). *Wind energy explained: theory, design and application*: John Wiley & Sons.

Matheron, G. (1963). Principles of geostatistics. *Economic Geology, 58*(8), 1246-1266.

Ministry for Primary Industries. (2012). *Pastoral input trends in New Zealand: A snapshot*. Wellington: Ministry for Primary Industries.

Ministry of Primary Industries. (2017, 19 January 2017). Pioneering to precision - Application of fertiliser in hill country. *Funding and Programmes.* 2017, from https://www.mpi.govt.nz/funding-and-programmes/primary-growth-partnership/primary-growth-partnership-programmes/pioneering-to-precision-application-of-fertiliser-in-hill-country/

Miserque, O., Pirard, E., Schenkel, Y., Mostade, O., and Huyghebaert, B. (2008). Spreading segregation of blended fertilizers: influence of the particles properties. *Applied Engineering in Agriculture, 24*(2), 137-144.

Montero, J. M., Fernández-Avilés, G., and Mateu, J. (2015). *Spatial and spatio-temporal geostatistical modeling and kriging*. Chichester, West Sussex, UK John Wiley and Sons.

Morton, J., Baird, D., and Manning, M. (2000). A soil sampling protocol to minimise the spatial variability in soil test values in New Zealand hill country. *New Zealand Journal of Agricultural Research, 43*(3), 367-375.

Morton, J. D., Stafford, A. D., Gillingham, A. G., Old, A., and Knowles, O. (2016). *The development of variable rate application of fertiliser from a fixed wing topdressing aircraft.* Paper presented at the Hill Country Symposium, Rotorua, New Zealand.

Murray, R. I. (2007). *Variable rate application technology in the New Zealand aerial topdressing industry.* (PhD), Massey University.

Murray, R. I., and Yule, I. J. (2006). *Measuring the application variability of agricultural aircraft: A case study on Limestone Downs.* Paper presented at the Fertiliser and Lime Research Centre Workshop, Massey University, Palmerston North.

Murray, R. I., and Yule, I. J. (2010). Developing variable rate application technology: Economic impact for farm owners and topdressing operators. *New Zealand Journal of Agricultural Research, 50*(1), 65-72.

NZFQC. (2016a). Fertmark code of practice. 2016, from http://fertqual.co.nz/understanding-the-marks/fertmark/

NZFQC. (2016b). Spreadmark codes of practice: New Zealand Fertiliser Quality Council.

O'Connor, M. B., Smart, C. E., and Ledgard, S. F. (1990). *Long term effects of withholding phosphate application on North Island hill country: Te Kuiti.* Paper presented at the Proceedings of the New Zealand Grassland Association.

Oliver, M. A., and Webster, R. (1986). Combining Nested and Linear Sampling for Determining the Scale and Form of Spatial Variation of Regionalized Variables. *Geographical Analysis, 18*(3), 227-242. doi: 10.1111/j.1538-4632.1986.tb00095.x

Pyrcz, M., and Deutsch, C. (2003). The whole story on the hole effect. *Geostatistical Association of Australasia, Newsletter, 18*, 3-5.

Schumann, A. W. (2006). Nutrient management zones for citrus based on variation in soil properties and tree performance. *Precision Agriculture, 7*(1), 45-63.

Scott, R. (1970). Spatial distribution of fertiliser and seed applied from light aircraft. III. Effect of altitude, cross winds and fertiliser material. *New Zealand Journal of Agricultural Research, 13*, 909-920.

Scott, R. S., and Grig, J. L. (1970). Studies into the spatial distribution of fertiliser and seed applied from light aircraft. *New Zealand Journal of Agricultural Research, 13*(1), 12-32. doi: 10.1080/00288233.1970.10421194

Setianto, A., and Triandini, T. (2015). Comparison of kriging and inverse distance weighted (IDW) interpolation methods in lineament extraction and analysis. *Journal of Southeast Asian Applied Geology, 51*(1), 21-29.

Spera, D., and Richards, T. (1979). *Modified power law equations for vertical wind profiles*. Paper presented at the Wind Characteristic and Wind Energy Siting Conference, Portland, Oregon.

Statistics New Zealand. (2012). *Fertiliser and lime applied by farm type (ANZSIC06), during the year ended 30 June 2012*. Statistics New Zealand.

Suckling, F. E. T. (1959). Pasture management trials on unploughable hill country at Te Awa: II. Results for 1951–57. *New Zealand Journal of Agricultural Research, 2*(3), 488-543.

Teske, M. E., Bird, S. L., Esterly, D. M., Curbishley, T. B., Ray, S. L., and Perry, S. G. (2002). AgDrift®: A model for estimating near-field spray drift from aerial applications. *Environmental Toxicology and Chemistry, 21*(3), 659-671.

Teske, M. E., Thistle, H. W., and Grob, I. J. (2007). Determination of dry material physical characteristics for use in dispersion modeling. *Transactions of the ASABE, 50*(4), 1149-1156.

Trayford, R., and Tremayne, E. (1966). *Effect of four factors on the aerial spreading of superphosphate*. Melbourne: Autralian Defence Scientific Service Aeronautical Research Laboratories.

Verhagen, J. (1997). Site specific fertiliser application for potato production and effects on N-leaching using dynamic simulation modelling. *Agriculture, Ecosystems & Environment, 66*(2), 165-175.

Virk, S. S., Mullenix, D. K., Sharda, A., Hall, J. B., Wood, C. W., Fasina, O. O., . . . Fulton, J. P. (2013). Case study: Distribution uniformity of a blended fertilizer applied using a variable-rate spinner disc spreader. *Applied Engineering in Agriculture, 29*(5), 627-636.

Wackrow, A. (2005). *New Zealand fixed wing aviation accidents: A review of all reported New Zealand registered aeroplane accidents from 1995 to 2004.* Civil Aviation Authority of New Zealand.

Wadell, H. (1932). Volume, shape, and roundness of rock particles. *The Journal of Geology, 40*(5), 443-451.

Walker, J., and Gardisser, D. (1988). *Modeling fertilizer particle trajectories*. Paper presented at the NAAA/ASAE Joint Technical Session.

Walker, J., and Gardisser, D. (1989). Using AgDISP for dry material deposition analysis. *Transactions of the ASAE*.

Walker, J., Grift, T., and Hofstee, J. (1997). Determining effects of fertilizer particle shape on aerodynamic properties. *Transactions of the ASAE, 40*(1), 21-27.

Walklate, P. J. (1992). A simulation study of pesticide drift from an air-assisted orchard sprayer. *Journal of Agricultural Engineering Research, 51*, 263-283. doi: http://dx.doi.org/10.1016/0021-8634(92)80042-Q

Yakowitz, S. J., and Szidarovszky, F. (1985). A comparison of kriging with nonparametric regression methods. *Journal of Multivariate Analysis, 16*(1), 21-53. doi: http://dx.doi.org/10.1016/0047-259X(85)90050-8

Yule, I. (2011). *The effect of fertilizer particle size on spread distribution*. Paper presented at the Fertiliser and Lime Research Centre Workshop, Massey University, Palmerston North, New Zealand.

Yule, I., and Pemberton, J. (2009). *Spreader testing for mixing and segregation of blended fertilizers*. Paper presented at the International ASABE Meeting, Reno, Nevada.

Yule, I. J., and Flemmer, R. C. (2005). *Measurement of Vibration in an Aircraft Hopper during Topdressing*. Paper presented at the 1st International Conference on Sensing Technology, Palmerston North.

Yule, I. J., Murray, R. I., Irwin, M., Hedley, M., and Jones, J. (2005). *Variable–Rate Application Technology for Aerial Topdressing Aircraft*. Paper presented at the ASABE International Meeting, Tampa, Florida, USA.

Appendix

	Corrected Wind Angle (°)																																		
Wind Speed (m/s)	**0**	**10**	**20**	**30**	**40**	**50**	**60**	**70**	**80**	**90**	**100**	**110**	**120**	**130**	**140**	**150**	**160**	**170**	**180**	**190**	**200**	**210**	**220**	**230**	**240**	**250**	**260**	**270**	**280**	**290**	**300**	**310**	**320**	**330**	**340**	**350**
0	0	0	0	-1	0	0	-1	0	0	0	0	-1	0	-1	0	0	0	0	0	0	0	-1	0	-1	-1	-1	-1	0	-1	-1	0	0	0	0	-1	0
0.1	-1	-1	-1	-2	-2	-2	-3	-3	-3	-3	-3	-3	-3	-2	-2	-2	-1	-1	0	0	0	1	1	1	2	2	2	2	2	2	2	1	1	1	0	0
0.2	-1	-1	-2	-3	-4	-4	-5	-5	-5	-5	-5	-5	-5	-4	-4	-3	-2	-1	-1	0	1	2	3	3	4	4	5	5	5	4	4	3	3	2	1	0
0.3	0	-2	-3	-4	-6	-6	-8	-8	-8	-9	-8	-8	-7	-7	-5	-4	-3	-2	0	1	2	3	5	4	6	7	7	7	7	7	6	5	4	3	2	1
0.4	0	-2	-4	-5	-7	-8	-9	-10	-11	-11	-11	-10	-10	-9	-7	-5	-4	-2	0	1	3	5	6	8	9	9	10	10	10	9	9	8	6	5	3	1
0.5	0	-3	-5	-7	-9	-11	-12	-11	-13	-14	-13	-12	-11	-10	-8	-7	-5	-3	0	2	4	6	7	10	11	12	12	12	12	12	11	9	8	6	4	2
0.6	0	-3	-6	-8	-10	-12	-13	-15	-15	-16	-16	-15	-14	-12	-10	-9	-6	-3	-1	2	5	8	10	12	12	13	15	15	15	14	13	12	10	7	5	2
0.7	-1	-3	-7	-10	-12	-14	-16	-17	-19	-18	-18	-17	-16	-15	-11	-10	-7	-3	-1	2	5	9	12	14	14	16	16	17	16	15	15	14	11	8	5	2
0.8	0	-4	-7	-11	-14	-15	-18	-19	-19	-20	-20	-20	-17	-17	-14	-11	-8	-4	0	3	6	9	13	15	16	19	19	20	19	19	17	15	13	10	7	3
0.9	-1	-4	-8	-12	-15	-18	-19	-22	-21	-23	-23	-21	-20	-17	-16	-12	-8	-4	0	3	8	12	14	16	19	20	21	22	21	21	18	17	15	12	8	3
1	0	-5	-10	-14	-17	-18	-21	-22	-24	-25	-24	-23	-22	-20	-17	-13	-9	-5	0	4	8	13	16	19	20	22	23	23	23	22	20	19	15	13	9	4
1.1	0	-5	-10	-14	-17	-21	-25	-25	-25	-25	-27	-24	-24	-20	-17	-15	-10	-5	0	5	9	14	17	21	22	23	22	23	23	25	22	20	18	14	10	4
1.2	-1	-6	-12	-16	-19	-22	-26	-24	-26	-28	-29	-28	-25	-23	-20	-14	-11	-6	0	5	10	15	19	21	24	26	28	28	28	26	25	21	18	15	10	4
1.3	-1	-6	-12	-16	-21	-22	-27	-28	-31	-30	-27	-29	-27	-25	-21	-18	-12	-6	0	5	11	16	19	22	26	27	29	27	30	27	27	23	21	16	11	5
1.4	-1	-7	-13	-18	-23	-23	-28	-32	-30	-32	-33	-29	-28	-25	-23	-17	-12	-7	0	6	12	17	21	26	24	28	30	30	31	27	26	25	22	17	12	6
1.5	0	-7	-14	-19	-24	-28	-31	-30	-32	-33	-30	-31	-30	-25	-22	-20	-14	-7	-1	6	13	18	23	27	31	27	29	29	33	30	29	26	22	19	12	6
1.6	0	-8	-15	-20	-25	-28	-32	-30	-37	-35	-35	-32	-30	-27	-26	-20	-14	-7	0	7	14	19	25	24	27	31	32	32	31	31	28	29	24	20	14	7
1.7	0	-8	-15	-21	-25	-30	-32	-37	-34	-36	-36	-33	-34	-32	-27	-22	-15	-7	0	7	14	21	25	30	32	32	32	36	37	31	31	28	25	21	15	7
1.8	0	-9	-16	-22	-25	-29	-34	-33	-36	-36	-36	-33	-38	-31	-29	-23	-16	-9	-1	8	15	22	24	31	32	32	34	37	37	34	31	31	27	21	15	8
1.9	0	-9	-17	-23	-28	-30	-35	-36	-39	-38	-39	-35	-36	-31	-28	-24	-17	-8	-1	7	16	22	28	32	33	40	37	39	36	37	34	30	27	22	16	8
2	0	-10	-18	-24	-30	-31	-35	-37	-39	-40	-40	-38	-35	-31	-30	-23	-18	-9	0	9	17	25	30	33	33	37	40	38	38	40	35	33	29	24	17	9
2.1	0	-10	-18	-27	-30	-34	-38	-41	-43	-45	-44	-39	-38	-34	-27	-25	-19	-9	-1	9	18	24	30	30	35	40	42	41	42	40	37	32	30	25	18	9
2.2	0	-10	-19	-27	-31	-36	-40	-42	-43	-45	-45	-41	-39	-34	-34	-27	-20	-10	0	10	18	25	30	35	36	38	45	44	42	39	37	34	30	26	18	10
2.3	0	-11	-19	-28	-32	-37	-42	-44	-46	-47	-47	-41	-44	-37	-35	-29	-20	-11	0	9	19	24	32	38	41	40	45	46	42	45	42	37	30	27	18	10
2.4	-1	-11	-20	-27	-33	-39	-43	-47	-48	-49	-45	-48	-43	-37	-31	-29	-20	-10	0	11	20	27	35	38	42	43	46	49	50	46	43	38	31	27	19	10
2.5	0	-12	-21	-28	-34	-40	-45	-47	-50	-49	-48	-46	-43	-37	-31	-31	-21	-12	0	10	20	29	34	41	44	46	50	50	50	48	44	38	32	28	21	11
2.6	0	-12	-23	-30	-35	-40	-48	-47	-51	-52	-52	-48	-47	-42	-35	-26	-22	-12	0	11	21	28	35	40	41	46	48	54	49	48	44	41	35	25	19	11
2.7	-1	-13	-23	-30	-38	-45	-48	-53	-52	-56	-52	-51	-45	-42	-38	-30	-23	-13	-1	11	23	27	32	41	44	48	56	52	52	49	47	41	37	30	22	11
2.8	0	-13	-24	-32	-38	-45	-51	-54	-56	-55	-53	-49	-50	-42	-38	-27	-23	-13	-1	12	25	30	35	44	47	49	53	58	56	51	50	41	35	30	23	12
2.9	0	-13	-25	-32	-38	-47	-51	-54	-58	-57	-58	-54	-52	-45	-36	-34	-24	-13	-1	12	23	34	35	48	48	56	56	54	56	50	48	44	37	31	22	12
3	0	-14	-23	-30	-41	-46	-54	-57	-61	-61	-61	-57	-51	-46	-37	-32	-25	-14	0	14	26	35	36	43	50	56	54	59	60	57	49	44	39	30	23	13
3.1	-1	-14	-26	-34	-42	-51	-54	-60	-62	-60	-57	-59	-55	-49	-39	-34	-26	-15	-1	12	22	36	39	45	51	57	59	60	58	58	53	45	39	32	24	13
3.2	0	-14	-26	-34	-45	-51	-56	-61	-62	-62	-63	-59	-56	-50	-38	-32	-25	-13	-1	13	24	32	43	51	53	57	58	64	63	57	57	50	43	33	26	14
3.3	0	-14	-26	-34	-45	-51	-57	-59	-64	-64	-63	-62	-56	-48	-46	-33	-28	-15	0	14	27	33	40	51	56	57	63	66	62	61	59	51	42	33	26	15
3.4	0	-16	-24	-37	-47	-53	-61	-62	-65	-69	-69	-62	-56	-52	-44	-39	-30	-14	0	13	28	33	42	49	58	61	63	62	67	63	60	52	43	36	26	15
3.5	0	-15	-29	-36	-48	-53	-61	-64	-68	-70	-68	-65	-58	-49	-43	-33	-25	-16	0	15	29	38	43	51	60	64	65	68	64	65	63	54	45	36	26	15
3.6	-1	-16	-28	-37	-49	-56	-63	-65	-70	-70	-70	-67	-59	-55	-44	-38	-30	-17	0	16	27	37	45	54	62	65	71	74	68	65	64	55	46	38	26	16
3.7	0	-16	-26	-37	-51	-62	-62	-69	-70	-74	-73	-72	-62	-55	-47	-39	-28	-17	0	16	29	38	46	53	64	69	70	72	72	66	65	60	47	39	26	16
3.8	0	-17	-28	-39	-51	-61	-65	-70	-73	-77	-74	-73	-65	-57	-48	-39	-28	-17	0	16	29	38	48	58	67	71	72	75	73	71	64	58	49	38	27	16
3.9	0	-18	-33	-40	-51	-61	-66	-76	-76	-76	-74	-71	-66	-59	-49	-39	-31	-15	0	16	31	37	50	57	64	70	73	77	75	75	66	59	47	40	30	16
4	0	-18	-28	-43	-53	-62	-74	-73	-80	-81	-76	-72	-66	-58	-51	-38	-32	-19	-1	15	26	39	51	59	65	74	74	80	80	75	69	61	51	41	30	17

Table A. 1: Peak mass transverse displacement look up table for superphosphate (without spreader).

	Corrected Wind Angle (°)																																				
Wind Speed (m/s)	**0**	**10**	**20**	**30**	**40**	**50**	**60**	**70**	**80**	**90**	**100**	**110**	**120**	**130**	**140**	**150**	**160**	**170**	**180**	**190**	**200**	**210**	**220**	**230**	**240**	**250**	**260**	**270**	**280**	**290**	**300**	**310**	**320**	**330**	**340**	**350**
0	9	9	9	9	9	9	9	9	9	9	9	9	9	9	9	9	9	9	9	10	9	9	9	9	9	9	9	9	9	9	9	9	9	9	9	9
0.1	9	9	9	9	9	9	9	10	9	10	9	9	9	10	9	9	9	9	10	9	9	9	9	9	9	9	10	9	9	9	9	9	9	9	9	9
0.2	9	9	9	9	10	9	10	10	10	10	10	10	10	10	10	9	9	9	10	9	10	10	10	10	10	10	10	10	10	10	10	10	9	9	9	9
0.3	9	9	9	9	10	10	11	11	11	11	11	11	11	11	10	10	10	9	10	10	10	10	10	11	11	11	11	11	11	11	10	10	10	9	9	9
0.4	9	9	9	10	10	11	11	11	12	12	12	12	11	11	11	10	10	10	10	10	10	10	11	11	11	12	12	12	12	11	11	11	10	10	9	9
0.5	9	9	9	10	11	11	12	12	13	13	13	13	12	12	11	11	11	10	10	10	10	11	12	12	12	12	13	13	13	12	12	11	10	10	9	9
0.6	9	9	10	11	12	12	13	13	14	14	14	14	13	13	12	11	11	10	10	10	10	11	12	13	13	14	14	14	14	13	13	12	11	10	10	9
0.7	9	9	10	11	12	13	14	14	15	15	15	15	14	14	13	12	11	11	10	10	11	12	12	14	14	15	15	15	15	14	14	13	12	11	10	9
0.8	8	9	10	11	13	14	15	15	16	16	16	16	15	14	13	13	12	11	10	11	11	12	13	14	15	16	17	16	16	15	15	14	12	11	10	9
0.9	8	9	10	11	13	15	16	17	18	18	18	17	17	16	14	13	12	11	11	11	12	13	14	15	17	17	18	18	17	17	16	15	13	12	10	9
1	8	9	11	12	14	16	17	18	19	19	19	18	18	16	15	14	12	11	10	11	12	13	15	16	18	19	19	19	19	18	17	16	14	12	10	9
1.1	8	9	11	13	15	17	18	20	20	20	21	20	19	17	16	14	12	11	11	12	12	14	16	18	19	20	21	21	20	20	18	16	15	12	10	9
1.2	8	9	11	13	15	18	19	21	22	22	22	21	20	19	17	15	13	12	11	12	13	15	17	18	20	21	22	22	22	21	19	18	16	13	11	9
1.3	8	9	11	14	16	19	21	22	23	24	23	22	22	20	18	16	13	12	11	12	13	15	18	20	22	23	23	23	23	22	21	19	16	13	11	9
1.4	8	10	12	14	17	19	22	23	24	25	25	24	23	21	19	17	14	12	11	12	14	16	18	21	23	24	25	25	24	23	22	20	17	14	11	9
1.5	8	9	12	15	18	21	23	25	26	27	26	25	24	22	20	17	15	12	11	13	14	17	19	22	24	25	26	26	26	24	23	21	18	15	12	9
1.6	8	9	12	15	19	22	24	26	27	28	28	27	25	23	21	18	15	13	11	13	15	18	20	23	25	27	28	28	27	26	24	22	19	16	12	9
1.7	8	10	13	16	20	23	25	27	29	29	28	28	27	24	22	19	15	13	12	13	15	18	22	24	26	28	29	29	29	27	25	23	20	16	12	9
1.8	8	9	13	17	20	24	26	29	30	30	30	29	28	25	22	19	16	13	12	13	16	19	23	25	28	29	30	30	30	28	26	23	20	17	13	9
1.9	8	10	14	17	22	24	27	30	30	30	30	30	29	27	24	20	17	14	12	13	16	20	24	26	30	30	30	30	30	29	28	25	21	18	13	9
2	7	10	14	18	22	26	29	30	30	30	30	30	30	28	25	21	17	14	12	14	17	21	25	28	30	30	30	30	30	30	29	26	22	18	14	10
2.1	7	10	14	19	23	26	30	30	30	30	30	30	30	29	26	22	18	14	13	14	17	21	26	29	30	30	30	30	30	30	29	27	23	19	14	10
2.2	7	10	15	19	24	28	30	30	30	30	30	30	30	30	27	22	18	14	12	14	18	22	27	30	30	30	30	30	30	30	30	28	24	19	14	10
2.3	7	10	15	20	25	29	30	30	30	30	30	30	30	30	27	23	19	14	13	14	18	23	28	30	30	30	30	30	30	30	30	29	25	20	15	10
2.4	7	10	16	21	25	30	30	30	30	30	30	30	30	30	29	24	19	15	13	15	19	24	29	30	30	30	30	30	30	30	30	30	26	21	15	10
2.5	7	10	16	21	26	30	30	30	30	30	30	30	30	30	30	25	20	16	13	15	19	25	30	30	30	30	30	30	30	30	30	30	26	21	16	10
2.6	7	10	17	22	27	30	30	30	30	30	30	30	30	30	30	26	20	16	13	16	21	26	30	30	30	30	30	30	30	30	30	30	27	22	16	11
2.7	7	11	17	22	28	30	30	30	30	30	30	30	30	30	30	26	21	16	14	16	21	27	30	30	30	30	30	30	30	30	30	30	28	23	17	10
2.8	7	11	17	23	29	30	30	30	30	30	30	30	30	30	30	27	21	16	14	16	22	27	30	30	30	30	30	30	30	30	30	30	29	23	17	11
2.9	7	11	18	24	30	30	30	30	30	30	30	30	30	30	30	28	22	17	14	17	22	28	30	30	30	30	30	30	30	30	30	30	29	24	18	11
3	7	11	18	24	30	30	30	30	30	30	30	30	30	30	30	29	23	17	15	17	23	29	30	30	30	30	30	30	30	30	30	30	30	25	18	11
3.1	7	11	18	25	30	30	30	30	30	30	30	30	30	30	30	30	24	18	15	17	23	30	30	30	30	30	30	30	30	30	30	30	30	25	18	11
3.2	6	11	18	25	30	30	30	30	30	30	30	30	30	30	30	30	24	18	15	18	24	30	30	30	30	30	30	30	30	30	30	30	30	26	19	12
3.3	6	11	20	26	30	30	30	30	30	30	30	30	30	30	30	30	24	18	15	18	25	30	30	30	30	30	30	30	30	30	30	30	30	27	19	12
3.4	6	12	20	27	30	30	30	30	30	30	30	30	30	30	30	30	25	19	15	19	25	30	30	30	30	30	30	30	30	30	30	30	30	27	20	12
3.5	7	12	20	28	30	30	30	30	30	30	30	30	30	30	30	30	25	19	16	19	26	30	30	30	30	30	30	30	30	30	30	30	30	28	20	12
3.6	6	12	21	28	30	30	30	30	30	30	30	30	30	30	30	30	26	19	16	19	27	30	30	30	30	30	30	30	30	30	30	30	30	28	20	12
3.7	6	12	21	29	30	30	30	30	30	30	30	30	30	30	30	30	27	20	17	20	27	30	30	30	30	30	30	30	30	30	30	30	30	29	21	12
3.8	6	13	21	29	30	30	30	30	30	30	30	30	30	30	30	30	27	20	17	21	28	30	30	30	30	30	30	30	30	30	30	30	30	29	21	12
3.9	6	13	22	30	30	30	30	30	30	30	30	30	30	30	30	30	28	20	17	20	28	30	30	30	30	30	30	30	30	30	30	30	30	30	22	13
4	6	13	22	30	30	30	30	30	30	30	30	30	30	30	30	30	29	21	17	21	29	30	30	30	30	30	30	30	30	30	30	30	30	30	22	13

Table A.2: Swath width of the wind displaced transverse spread pattern to achieve a CV of 25% for superphosphate (without spreader).

	Corrected Wind Angle (°)																																				
Wind Speed (m/s)	**0**	**10**	**20**	**30**	**40**	**50**	**60**	**70**	**80**	**90**	**100**	**110**	**120**	**130**	**140**	**150**	**160**	**170**	**180**	**190**	**200**	**210**	**220**	**230**	**240**	**250**	**260**	**270**	**280**	**290**	**300**	**310**	**320**	**330**	**340**	**350**
0	-1	-1	0	0	-1	-1	-1	0	-1	-1	-1	-1	0	-1	-1	-1	-1	0	0	-1	-1	0	-1	-1	0	0	0	0	0	-1	0	-1	-1	0	0	-1
0.1	0	-1	-1	-1	-2	-2	-2	-2	-2	-2	-2	-2	-2	-2	-2	-1	-1	-1	0	0	0	0	1	1	1	1	1	1	1	1	1	1	1	0	0	0
0.2	0	-1	-2	-2	-3	-3	-4	-4	-4	-4	-4	-4	-4	-3	-3	-2	-2	-1	0	0	1	1	2	2	3	3	3	3	3	3	3	2	2	1	1	0
0.3	-1	-1	-2	-3	-4	-5	-5	-5	-6	-6	-6	-5	-5	-5	-4	-3	-2	-1	-1	0	1	2	3	4	4	5	5	5	5	4	4	4	3	2	1	0
0.4	0	-2	-3	-4	-5	-6	-7	-7	-8	-8	-8	-7	-7	-6	-5	-4	-3	-2	-1	1	2	3	4	5	6	6	7	7	6	6	6	5	4	3	2	1
0.5	0	-2	-4	-5	-6	-7	-8	-9	-9	-9	-9	-9	-8	-7	-6	-5	-3	-2	-1	1	3	4	5	6	7	8	8	8	8	8	7	6	5	4	3	1
0.6	-1	-2	-4	-6	-7	-9	-10	-10	-11	-10	-11	-11	-9	-8	-7	-6	-4	-2	0	1	3	5	6	8	9	9	10	10	10	10	9	7	6	5	3	1
0.7	0	-3	-5	-7	-8	-10	-12	-11	-12	-13	-13	-12	-11	-10	-8	-6	-5	-3	-1	2	4	6	7	9	10	10	12	12	12	11	10	9	7	6	4	2
0.8	0	-3	-5	-7	-9	-11	-13	-13	-14	-14	-14	-13	-13	-11	-9	-7	-5	-3	-1	2	4	7	9	11	11	13	13	13	13	11	12	10	9	6	4	2
0.9	-1	-3	-6	-9	-11	-13	-15	-15	-16	-16	-17	-15	-14	-13	-10	-8	-6	-3	-1	2	5	7	9	12	13	13	15	15	15	15	13	11	10	7	5	2
1	0	-4	-7	-9	-12	-14	-15	-17	-18	-17	-18	-16	-15	-14	-12	-9	-6	-4	-1	3	5	8	11	13	15	16	16	16	15	17	14	13	11	8	6	3
1.1	0	-4	-7	-10	-13	-16	-18	-19	-19	-20	-19	-18	-16	-14	-12	-10	-7	-4	-1	3	6	9	12	14	15	16	16	19	19	18	16	14	12	9	6	3
1.2	-1	-4	-8	-11	-13	-16	-18	-20	-21	-20	-20	-20	-18	-17	-13	-11	-8	-4	-1	3	7	9	13	15	17	19	20	21	20	18	17	16	13	10	7	3
1.3	0	-4	-8	-11	-15	-19	-20	-23	-22	-23	-22	-21	-18	-15	-15	-11	-8	-4	-1	4	7	11	14	16	19	19	22	21	21	19	19	17	15	11	7	3
1.4	0	-5	-9	-13	-17	-20	-22	-25	-23	-25	-25	-23	-22	-18	-17	-12	-9	-5	0	4	8	12	14	18	21	22	23	25	22	22	20	19	15	11	8	4
1.5	-1	-5	-10	-14	-17	-19	-23	-24	-27	-27	-25	-25	-22	-21	-16	-12	-9	-5	0	4	9	12	16	19	21	22	26	26	26	24	22	19	16	13	9	4
1.6	-1	-5	-10	-14	-18	-22	-24	-28	-27	-29	-29	-27	-24	-21	-18	-14	-10	-5	0	4	9	14	16	21	22	24	28	27	26	25	22	21	17	13	9	4
1.7	-1	-6	-10	-15	-20	-24	-27	-28	-29	-32	-30	-28	-27	-23	-20	-14	-9	-6	0	5	10	15	17	21	26	27	28	28	27	26	24	23	20	14	10	5
1.8	0	-6	-11	-17	-20	-25	-26	-28	-31	-33	-29	-28	-27	-23	-19	-17	-11	-6	0	5	10	16	18	22	27	29	31	31	28	28	26	24	19	15	10	5
1.9	-1	-6	-12	-17	-22	-26	-30	-32	-33	-34	-32	-29	-29	-24	-21	-16	-12	-6	0	5	11	14	19	24	27	28	30	31	33	30	28	25	21	16	11	5
2	-1	-7	-13	-18	-23	-29	-31	-35	-34	-34	-35	-32	-29	-26	-22	-18	-13	-7	0	5	12	16	21	26	29	31	33	35	34	31	30	25	23	17	12	6
2.1	0	-7	-14	-19	-24	-28	-32	-34	-36	-38	-36	-35	-32	-29	-24	-18	-13	-7	0	6	12	17	20	27	31	30	35	36	34	34	31	28	23	18	12	6
2.2	0	-7	-14	-19	-26	-31	-33	-34	-38	-39	-37	-35	-32	-28	-23	-19	-13	-7	-1	6	12	17	24	27	31	35	36	38	36	37	31	30	25	18	13	6
2.3	0	-8	-15	-21	-25	-30	-36	-39	-38	-41	-37	-38	-34	-29	-26	-21	-12	-7	0	6	13	18	24	28	32	36	38	39	41	38	34	32	27	20	13	7
2.4	-1	-8	-14	-22	-27	-33	-36	-40	-40	-42	-40	-37	-37	-31	-25	-20	-14	-8	-1	7	13	17	25	29	32	40	41	39	39	38	35	33	27	20	14	7
2.5	0	-8	-16	-23	-29	-34	-37	-42	-43	-42	-43	-40	-37	-33	-27	-19	-14	-8	-1	7	13	19	25	33	36	40	41	42	43	42	36	31	29	21	14	7
2.6	0	-8	-16	-24	-29	-37	-41	-42	-42	-44	-45	-42	-37	-35	-29	-21	-16	-9	0	8	14	20	27	33	38	41	45	45	44	41	38	34	29	23	15	8
2.7	0	-9	-17	-25	-32	-38	-40	-45	-47	-46	-45	-41	-40	-35	-28	-23	-16	-8	0	8	13	22	28	34	38	42	44	46	45	43	40	37	31	23	17	8
2.8	-1	-9	-18	-25	-31	-39	-42	-46	-47	-49	-47	-44	-42	-36	-30	-24	-16	-9	0	8	16	23	28	34	41	42	45	47	50	45	44	38	32	25	16	8
2.9	0	-9	-18	-26	-34	-41	-45	-48	-49	-50	-48	-47	-41	-39	-31	-25	-17	-9	0	9	15	20	30	37	41	47	49	49	51	46	44	40	33	25	17	8
3	-1	-10	-19	-27	-35	-42	-46	-50	-48	-52	-53	-49	-43	-36	-34	-23	-15	-10	0	9	15	23	32	39	45	47	51	52	49	48	46	39	32	27	18	9
3.1	0	-10	-20	-28	-35	-41	-48	-52	-53	-56	-56	-51	-45	-38	-32	-24	-17	-10	0	8	15	23	30	41	43	47	51	51	53	50	48	40	33	27	18	9
3.2	-1	-10	-19	-29	-37	-45	-47	-52	-54	-58	-56	-54	-47	-41	-33	-25	-17	-8	-1	9	17	26	33	37	46	50	54	53	52	51	48	42	36	28	18	9
3.3	0	-11	-19	-29	-37	-45	-52	-55	-58	-59	-59	-52	-52	-40	-35	-28	-19	-10	0	9	17	27	32	42	46	53	53	57	55	53	51	44	37	27	19	10
3.4	-1	-11	-21	-29	-40	-47	-53	-57	-60	-60	-57	-54	-50	-43	-35	-25	-18	-10	-1	10	18	24	35	43	49	53	57	59	56	54	52	46	38	29	20	10
3.5	0	-11	-22	-32	-39	-48	-53	-59	-62	-60	-61	-56	-51	-45	-37	-30	-19	-11	0	10	20	27	35	45	48	55	57	59	59	53	52	48	41	31	22	10
3.6	-1	-12	-22	-31	-42	-50	-55	-57	-61	-61	-62	-58	-52	-46	-37	-28	-20	-11	-1	11	16	27	38	46	51	55	58	62	62	56	54	48	41	32	22	10
3.7	-1	-12	-24	-35	-44	-53	-57	-60	-63	-63	-63	-61	-56	-46	-39	-31	-20	-12	-1	9	20	27	38	44	55	58	63	63	65	61	53	48	41	33	22	11
3.8	-1	-12	-23	-34	-44	-52	-56	-64	-69	-65	-66	-64	-57	-47	-41	-32	-21	-11	-1	11	18	30	39	50	53	62	63	65	64	63	56	52	43	33	22	11
3.9	0	-12	-25	-34	-46	-55	-62	-64	-68	-69	-67	-63	-55	-50	-43	-33	-20	-9	0	11	22	31	41	48	56	65	63	68	65	63	58	52	42	35	23	11
4	0	-13	-25	-35	-45	-55	-60	-67	-69	-71	-69	-63	-57	-50	-43	-31	-21	-10	-1	8	21	29	42	51	56	63	66	65	68	63	57	56	45	37	24	12

Table A.3: Peak mass transverse displacement look up table for DAP (without spreader).

	Corrected Wind Angle (°)																																				
Wind Speed (m/s)	0	10	20	30	40	50	60	70	80	90	100	110	120	130	140	150	160	170	180	190	200	210	220	230	240	250	260	270	280	290	300	310	320	330	340	350
0	12	12	12	12	12	13	13	13	13	13	13	13	11	12	11	12	12	13	12	12	11	11	13	11	12	12	11	13	13	12	11	13	13	12	12	11
0.1	13	12	11	11	12	10	9	12	11	12	11	10	12	11	12	12	10	10	12	10	12	13	11	10	11	12	12	12	12	12	10	11	12	12	10	10
0.2	12	11	11	12	11	11	13	12	12	13	11	11	11	12	12	12	11	11	12	10	11	12	12	11	12	13	13	12	13	12	13	12	12	12	9	11
0.3	11	12	11	11	12	12	12	13	13	12	12	12	12	13	11	12	12	13	12	13	12	13	12	14	12	13	13	13	12	12	13	13	12	11	12	11
0.4	12	11	11	11	12	12	13	13	13	13	13	13	13	14	12	12	11	12	13	12	11	12	13	13	14	14	13	12	12	13	14	12	13	12	11	10
0.5	12	10	11	12	12	13	13	12	13	13	13	14	13	13	13	13	13	11	12	13	13	12	13	13	13	14	13	13	13	14	12	13	11	11	12	10
0.6	11	11	12	12	13	13	14	13	14	14	14	14	14	14	14	13	12	13	13	12	12	14	14	14	14	14	14	13	13	13	13	12	13	12	11	12
0.7	12	11	11	12	13	12	13	14	14	14	14	14	14	14	14	14	13	13	13	13	14	14	14	14	13	14	14	14	14	14	14	13	13	12	12	11
0.8	12	10	11	12	12	13	13	14	14	14	14	15	14	14	14	14	14	13	14	14	13	14	14	15	15	15	14	14	14	14	14	13	13	12	12	11
0.9	11	11	11	13	13	13	13	13	14	15	15	15	15	15	15	15	14	13	13	14	14	14	15	15	15	15	15	15	15	14	14	14	13	13	12	12	11
1	11	10	11	12	12	13	13	14	14	15	15	15	15	15	15	14	14	14	14	14	14	15	15	15	15	15	15	15	15	15	14	14	13	12	12	11
1.1	11	11	11	12	13	12	14	14	15	15	15	15	15	15	15	15	15	13	13	13	15	15	16	15	16	16	16	15	15	15	14	13	13	13	12	11
1.2	11	11	12	13	13	13	14	14	15	16	15	16	15	15	15	15	15	14	14	15	16	15	16	16	16	16	16	16	15	15	14	14	13	12	12	11
1.3	10	11	12	12	13	14	14	15	15	16	16	16	16	16	15	15	15	15	14	15	15	16	16	16	16	16	16	16	16	15	15	14	13	12	12	10
1.4	10	10	12	12	14	14	14	15	16	16	16	17	16	16	16	16	15	15	15	15	15	16	16	16	16	16	16	17	16	16	15	14	14	13	12	11
1.5	10	10	12	13	14	14	15	15	16	16	17	17	16	16	17	16	16	15	14	15	16	16	17	17	17	17	17	17	16	15	15	14	13	13	12	10
1.6	10	11	12	13	14	15	15	16	17	17	17	17	17	17	16	16	15	16	14	16	16	17	17	16	17	18	17	17	16	15	15	15	14	13	12	11
1.7	10	11	12	13	14	15	15	17	16	17	17	17	17	17	17	17	16	16	15	15	16	17	17	17	17	18	18	17	17	16	16	15	14	13	12	11
1.8	10	10	12	13	13	15	16	16	17	17	17	18	18	18	17	17	17	17	16	15	17	17	17	18	18	18	18	18	17	16	16	15	14	13	11	11
1.9	10	10	12	13	14	15	16	17	18	18	18	18	18	18	17	16	17	15	16	16	16	17	18	18	19	19	18	18	17	17	17	16	14	13	12	11
2	10	10	12	13	14	15	17	17	18	18	19	19	18	18	17	17	17	16	17	17	17	17	18	18	19	18	19	19	18	17	17	15	14	13	12	10
2.1	10	10	12	13	15	16	17	17	18	18	19	19	19	19	18	17	17	17	17	17	17	18	18	18	18	19	19	18	18	18	17	16	14	13	12	11
2.2	10	10	12	13	15	16	17	18	19	19	20	20	19	19	17	17	17	16	17	18	18	18	19	19	19	19	20	20	19	19	17	16	15	14	12	11
2.3	9	11	12	14	15	17	18	19	20	20	20	20	20	19	19	18	18	18	16	17	18	19	18	20	20	19	20	20	20	19	17	16	15	13	12	11
2.4	10	10	12	13	15	17	17	19	19	20	20	21	20	19	19	19	18	18	17	18	19	18	19	19	20	21	20	20	19	19	17	16	15	13	12	10
2.5	9	11	12	13	16	17	18	19	20	21	21	21	20	20	19	18	17	19	18	18	19	19	19	20	20	21	21	21	20	19	18	17	15	14	12	10
2.6	9	10	12	14	15	17	19	19	20	21	21	21	20	21	20	19	18	17	19	19	19	19	20	20	21	22	21	21	20	19	19	17	15	14	12	11
2.7	9	10	12	14	15	17	19	20	20	22	22	21	20	20	19	19	18	18	18	18	19	20	20	20	22	22	22	22	20	20	18	17	16	14	12	10
2.8	9	11	12	14	16	17	19	20	22	22	22	22	22	20	20	19	18	19	18	19	19	20	20	21	21	22	22	22	21	20	19	18	16	14	12	10
2.9	8	11	12	14	16	18	19	21	22	23	22	22	21	21	20	19	19	19	18	19	19	19	20	21	22	22	23	22	22	21	19	19	16	14	12	10
3	9	10	12	14	17	18	20	21	23	23	23	23	22	22	20	20	20	19	19	20	19	20	20	22	23	23	24	23	23	21	20	18	16	14	12	11
3.1	9	10	12	15	16	18	20	21	23	23	23	24	22	22	21	20	18	20	19	20	19	20	21	22	23	23	24	23	23	23	20	19	16	14	12	11
3.2	8	11	12	15	17	19	20	23	23	24	24	24	23	22	21	21	19	20	19	20	20	20	21	23	23	24	24	25	23	22	20	19	17	15	13	11
3.3	9	10	12	15	17	19	22	23	23	25	24	24	24	23	21	21	20	20	20	20	20	20	21	23	24	24	24	25	23	22	21	19	17	15	12	10
3.4	8	10	13	15	17	19	21	24	25	24	25	24	24	23	21	21	20	20	20	21	19	20	22	23	24	25	25	25	24	23	21	20	18	15	12	11
3.5	9	10	13	15	18	20	22	24	24	25	26	25	25	24	22	21	20	19	19	21	19	21	23	24	25	25	26	25	24	23	22	20	18	16	13	10
3.6	8	10	12	16	18	21	22	24	25	25	26	25	25	24	22	21	19	21	21	22	21	21	22	24	25	26	26	25	25	24	22	20	18	15	13	11
3.7	8	10	13	15	18	20	23	25	25	27	26	26	25	25	23	21	20	20	21	21	20	21	23	24	25	26	27	26	25	25	23	21	18	15	13	10
3.8	8	11	13	16	18	21	24	26	26	28	27	26	26	24	23	21	21	20	22	22	20	21	24	25	26	26	27	26	26	24	23	21	18	16	13	11
3.9	7	10	13	16	19	22	23	25	26	28	27	27	26	25	24	21	21	19	23	21	21	22	24	25	26	27	26	27	27	25	23	21	19	16	13	11
4	9	10	13	16	19	22	24	26	27	28	28	27	27	25	24	22	19	20	24	22	20	22	24	25	27	28	28	28	27	25	24	22	19	17	13	11

Table A.4: Swath width of the wind displaced transverse spread pattern to achieve a CV of 15% for DAP (without spreader).

	Corrected Wind Angle (°)																																				
Wind Speed (m/s)	**0**	**10**	**20**	**30**	**40**	**50**	**60**	**70**	**80**	**90**	**100**	**110**	**120**	**130**	**140**	**150**	**160**	**170**	**180**	**190**	**200**	**210**	**220**	**230**	**240**	**250**	**260**	**270**	**280**	**290**	**300**	**310**	**320**	**330**	**340**	**350**
0	0	-1	0	0	0	0	-1	0	-1	-1	-1	-1	0	-1	-1	0	0	0	0	-1	0	0	0	0	-1	-1	-1	-1	-1	0	0	0	0	0	0	0
0.1	-1	-1	-1	-1	-2	-2	-2	-2	-2	-2	-2	-2	-2	-2	-2	-2	-1	-1	0	0	0	0	1	1	1	1	1	1	1	1	1	1	1	0	0	0
0.2	0	-1	-2	-2	-3	-3	-4	-4	-4	-4	-4	-4	-4	-3	-3	-2	-2	-1	0	0	1	1	2	2	3	3	3	3	3	3	3	3	2	1	1	0
0.3	0	-2	-3	-3	-4	-5	-5	-6	-6	-6	-6	-6	-6	-5	-4	-3	-2	-1	0	1	1	2	3	4	4	5	5	5	5	5	5	4	3	2	2	1
0.4	0	-2	-3	-4	-5	-6	-7	-8	-8	-8	-8	-8	-7	-6	-5	-4	-3	-2	0	1	2	3	4	5	6	7	7	7	7	7	6	5	4	3	2	1
0.5	-1	-2	-4	-5	-7	-8	-9	-9	-10	-10	-9	-10	-9	-8	-7	-5	-4	-2	-1	1	3	4	6	7	8	8	9	9	9	8	8	7	6	4	3	1
0.6	0	-3	-4	-6	-8	-9	-10	-11	-12	-12	-11	-11	-10	-9	-8	-6	-4	-3	0	2	3	5	7	8	9	10	10	11	10	10	9	8	7	5	3	1
0.7	-1	-3	-5	-7	-9	-11	-12	-13	-14	-13	-14	-13	-12	-11	-9	-7	-5	-3	0	2	4	6	8	9	11	11	12	13	13	12	11	9	8	6	4	2
0.8	0	-3	-6	-8	-10	-12	-14	-15	-16	-15	-16	-15	-14	-12	-10	-8	-6	-3	-1	2	5	7	9	11	12	14	14	15	14	13	12	11	9	7	5	2
0.9	0	-4	-6	-9	-11	-13	-15	-16	-18	-18	-17	-16	-15	-13	-11	-9	-6	-3	-1	2	5	8	10	13	14	14	17	17	17	15	14	13	10	8	5	3
1	-1	-4	-7	-10	-13	-15	-18	-18	-18	-20	-18	-18	-17	-14	-12	-10	-7	-4	0	3	6	9	12	14	15	17	17	18	18	17	15	13	12	9	6	3
1.1	-1	-4	-8	-11	-13	-16	-19	-20	-21	-21	-20	-20	-18	-17	-13	-11	-8	-4	-1	3	7	10	13	16	18	19	21	19	21	19	18	15	12	10	7	3
1.2	-1	-4	-8	-12	-15	-19	-19	-21	-22	-23	-22	-21	-20	-18	-14	-12	-8	-4	0	4	7	11	13	16	18	20	22	22	22	20	19	16	14	11	7	4
1.3	-1	-5	-9	-13	-16	-19	-21	-22	-24	-25	-25	-24	-21	-19	-16	-13	-9	-5	0	4	8	12	15	17	20	22	23	25	23	22	21	19	16	12	8	4
1.4	0	-5	-9	-14	-17	-20	-24	-24	-27	-26	-25	-24	-23	-21	-17	-14	-10	-5	-1	4	8	12	16	20	22	24	25	25	25	24	22	20	15	12	9	4
1.5	-1	-6	-10	-15	-18	-21	-25	-27	-28	-28	-27	-26	-26	-22	-18	-14	-10	-5	-1	4	10	14	17	21	23	25	27	29	28	25	23	21	18	14	9	4
1.6	0	-6	-11	-16	-20	-23	-27	-29	-30	-31	-31	-29	-27	-22	-19	-16	-11	-6	-1	5	10	14	18	22	26	27	28	29	30	27	26	22	19	15	10	5
1.7	0	-6	-11	-16	-20	-25	-29	-30	-32	-33	-32	-30	-28	-24	-20	-16	-12	-6	0	5	10	16	20	24	26	29	30	31	31	29	27	24	20	15	10	5
1.8	0	-6	-12	-17	-21	-26	-30	-32	-34	-33	-34	-32	-30	-27	-22	-17	-11	-6	0	5	11	16	22	25	29	32	31	32	32	31	28	26	22	17	11	6
1.9	0	-7	-13	-18	-23	-28	-31	-32	-35	-35	-33	-34	-31	-26	-24	-18	-12	-7	0	6	11	17	22	26	29	33	34	35	35	32	31	27	22	17	12	6
2	0	-7	-13	-20	-25	-29	-34	-37	-38	-39	-37	-36	-32	-28	-24	-19	-13	-7	0	6	13	17	23	27	31	34	35	37	38	36	32	28	23	19	13	6
2.1	-1	-7	-14	-20	-26	-30	-33	-37	-40	-38	-40	-36	-34	-30	-25	-19	-14	-7	0	6	13	19	23	28	33	36	38	38	39	34	32	28	25	19	14	7
2.2	0	-8	-15	-22	-27	-32	-37	-40	-42	-41	-42	-39	-37	-31	-26	-21	-14	-8	0	7	13	20	25	30	33	38	38	43	41	38	36	31	26	20	14	7
2.3	0	-8	-15	-22	-29	-35	-36	-41	-43	-43	-42	-40	-36	-32	-28	-22	-14	-8	-1	7	13	21	26	31	36	41	40	43	43	41	36	33	27	21	15	7
2.4	0	-8	-16	-23	-30	-36	-40	-40	-45	-46	-43	-40	-37	-32	-27	-23	-16	-8	-1	7	15	22	28	33	38	39	42	46	42	41	38	35	28	23	15	7
2.5	0	-9	-17	-24	-30	-37	-41	-44	-45	-48	-46	-45	-39	-36	-30	-23	-17	-9	0	8	15	23	28	35	39	43	44	44	45	43	40	37	29	22	16	8
2.6	-1	-9	-17	-24	-33	-38	-42	-44	-47	-50	-50	-46	-42	-38	-31	-23	-16	-9	-1	8	16	22	29	35	39	45	48	46	50	45	43	36	31	25	16	8
2.7	-1	-9	-17	-25	-34	-41	-43	-48	-49	-51	-47	-48	-42	-39	-29	-25	-17	-9	-1	8	17	24	30	36	42	45	48	50	49	47	44	39	32	25	16	8
2.8	0	-10	-18	-27	-35	-40	-45	-49	-51	-52	-51	-50	-44	-38	-35	-26	-19	-9	-1	8	17	26	31	37	45	49	47	52	51	47	44	40	34	27	18	9
2.9	0	-10	-19	-27	-36	-43	-48	-50	-53	-53	-52	-51	-45	-40	-34	-25	-19	-10	-1	9	18	25	34	39	43	49	51	54	54	49	47	41	35	26	18	9
3	0	-10	-19	-29	-37	-44	-48	-54	-58	-55	-54	-52	-50	-41	-34	-25	-19	-10	0	9	18	27	33	43	46	50	54	53	55	52	49	43	37	28	19	9
3.1	0	-11	-21	-30	-36	-47	-51	-55	-59	-57	-56	-51	-51	-45	-36	-30	-19	-10	0	10	19	27	36	42	50	53	56	57	57	54	50	43	37	28	20	10
3.2	-1	-11	-21	-32	-40	-46	-51	-57	-57	-59	-61	-55	-53	-43	-37	-28	-20	-11	0	9	19	28	37	42	49	54	58	57	58	57	51	45	38	30	20	10
3.3	-1	-11	-22	-32	-40	-47	-56	-58	-61	-62	-60	-58	-52	-45	-41	-30	-20	-11	0	10	19	30	37	46	51	57	60	60	61	57	52	47	38	30	22	10
3.4	0	-12	-23	-32	-43	-50	-55	-60	-63	-63	-60	-60	-54	-47	-42	-30	-20	-10	-1	9	17	30	39	45	54	55	61	62	65	60	55	47	42	31	22	11
3.5	0	-12	-24	-35	-45	-52	-57	-61	-64	-68	-61	-60	-56	-49	-41	-31	-22	-12	0	10	20	29	37	47	54	59	62	64	64	62	55	49	42	33	23	12
3.6	-1	-12	-24	-35	-44	-54	-58	-63	-69	-68	-66	-60	-56	-49	-43	-32	-22	-12	-1	11	20	30	42	49	58	62	62	66	66	63	59	51	43	33	23	11
3.7	0	-13	-25	-35	-45	-53	-60	-63	-71	-70	-70	-64	-58	-50	-41	-30	-23	-13	0	12	21	31	43	51	59	61	66	70	68	65	59	52	43	36	23	12
3.8	-1	-13	-25	-38	-49	-56	-62	-65	-72	-71	-71	-70	-62	-54	-45	-32	-23	-13	0	10	23	30	44	54	58	67	69	68	68	66	63	53	47	35	24	12
3.9	-1	-13	-25	-38	-49	-56	-65	-69	-69	-75	-71	-68	-64	-56	-45	-33	-22	-13	-1	12	21	34	43	55	63	66	72	73	73	68	62	58	47	36	26	12
4	0	-14	-26	-38	-50	-57	-66	-72	-73	-78	-72	-70	-64	-56	-45	-33	-24	-12	0	10	21	36	46	55	63	66	74	73	73	69	65	59	49	39	25	13

Table A.5: Peak mass transverse displacement look up table for urea (without spreader).

	Corrected Wind Angle (°)																																				
Wind Speed (m/s)	**0**	**10**	**20**	**30**	**40**	**50**	**60**	**70**	**80**	**90**	**100**	**110**	**120**	**130**	**140**	**150**	**160**	**170**	**180**	**190**	**200**	**210**	**220**	**230**	**240**	**250**	**260**	**270**	**280**	**290**	**300**	**310**	**320**	**330**	**340**	**350**
0	7	7	8	8	7	6	8	7	7	8	8	8	8	6	8	9	8	8	7	7	9	8	8	8	8	7	8	9	6	8	7	8	8	7	9	8
0.1	9	7	8	7	6	5	7	7	8	8	8	7	7	5	7	8	6	5	8	5	5	8	6	5	5	6	8	8	7	6	6	4	6	7	4	5
0.2	6	6	6	8	6	8	7	8	9	7	7	9	6	8	7	9	5	6	8	5	6	8	8	9	9	8	8	8	8	7	8	9	7	6	4	5
0.3	6	8	6	8	8	7	9	9	10	9	9	9	9	9	7	9	9	8	6	8	8	9	8	7	10	9	9	9	10	7	8	7	8	8	7	8
0.4	7	4	6	7	8	9	9	10	10	8	10	10	10	9	9	9	8	7	8	4	6	10	10	10	9	10	10	9	10	9	10	8	8	9	6	5
0.5	7	6	6	9	8	9	10	10	10	11	10	11	11	11	10	9	8	6	9	6	9	9	9	11	11	10	10	11	10	10	10	9	9	8	8	6
0.6	7	8	8	9	10	10	10	10	11	11	11	11	11	11	10	10	9	8	8	9	9	9	10	11	11	11	11	11	11	11	10	10	9	8	9	7
0.7	6	5	9	9	10	9	10	11	11	11	11	11	12	11	11	11	9	8	9	8	8	11	11	11	11	11	11	11	11	11	11	11	9	9	8	5
0.8	7	6	7	9	9	11	11	10	12	12	12	11	11	12	11	10	10	8	9	7	10	11	12	12	12	12	12	12	11	11	11	11	9	9	7	6
0.9	6	7	7	9	10	11	12	12	12	12	12	12	12	12	11	12	11	9	8	8	10	11	12	12	12	13	13	12	11	12	11	10	10	9	8	7
1	8	7	8	9	10	11	11	12	12	13	13	13	13	12	12	11	12	8	10	8	11	12	12	12	12	13	13	13	12	12	12	11	10	9	9	5
1.1	5	6	9	10	10	11	11	13	13	13	13	13	13	13	13	12	11	9	10	9	11	12	12	12	13	13	12	13	13	12	11	12	11	10	8	7
1.2	6	6	9	10	11	11	12	13	13	13	14	13	13	13	13	12	11	11	10	11	11	12	13	14	14	14	14	14	13	13	13	12	11	10	9	8
1.3	5	8	9	10	11	12	12	13	14	14	14	14	14	13	13	13	11	11	8	11	12	13	13	14	14	14	14	14	13	13	13	11	11	10	9	6
1.4	6	6	9	10	11	12	13	13	14	14	15	14	14	14	13	13	12	12	10	11	13	13	13	14	14	14	14	14	14	13	13	12	11	10	10	7
1.5	6	7	9	10	11	12	13	14	14	15	15	15	15	14	14	13	13	8	10	10	12	13	14	15	15	15	15	15	14	14	14	12	12	10	9	8
1.6	7	8	9	10	11	13	13	14	15	15	15	15	16	15	14	13	13	12	11	11	13	14	14	15	15	16	16	16	15	14	14	13	11	11	9	7
1.7	7	6	9	11	11	13	14	15	15	16	16	16	16	15	15	14	14	12	10	12	14	15	14	15	16	15	16	16	15	15	14	13	12	10	9	7
1.8	6	7	9	11	12	13	14	15	15	16	16	16	16	15	15	14	14	11	9	12	14	14	15	16	16	17	17	16	16	15	15	13	12	11	9	8
1.9	6	7	10	11	12	13	15	16	17	16	17	17	16	16	15	14	14	12	11	12	14	14	15	16	16	17	17	17	16	16	15	14	12	11	10	8
2	7	7	9	11	12	14	15	15	16	17	17	17	17	16	15	14	14	13	11	13	13	15	15	16	17	17	17	17	17	16	15	14	13	11	10	8
2.1	5	7	10	11	12	14	16	17	16	17	18	18	17	17	16	15	14	13	12	13	15	15	16	17	17	17	18	17	17	16	16	14	13	11	10	8
2.2	7	8	10	12	13	14	16	17	18	18	18	18	18	17	16	15	14	13	12	14	15	15	16	16	18	18	19	19	18	17	16	15	13	12	10	8
2.3	5	8	10	12	13	15	16	17	18	19	19	19	18	18	16	15	15	13	10	13	16	15	17	18	18	19	18	19	18	17	17	15	13	12	10	8
2.4	6	8	10	12	13	15	16	18	19	19	19	19	18	18	17	16	16	14	9	14	16	16	17	18	19	20	20	19	19	18	17	16	14	12	10	8
2.5	6	7	10	12	14	16	17	19	19	19	19	19	19	18	17	16	15	15	12	14	16	16	17	18	19	20	20	19	19	18	17	16	14	12	10	8
2.6	6	8	10	12	14	16	18	19	20	21	20	20	19	19	18	17	15	15	14	15	16	16	18	19	20	20	20	20	19	19	18	16	14	12	10	8
2.7	5	8	11	12	15	16	18	19	20	21	20	21	20	19	18	17	16	15	13	15	17	17	18	19	19	21	20	20	20	20	18	17	14	12	10	9
2.8	5	8	10	13	14	17	19	19	21	22	22	20	20	19	18	17	16	15	15	15	16	17	19	19	20	21	22	21	21	20	18	16	15	13	11	8
2.9	5	8	10	13	15	17	19	20	21	22	22	21	21	20	19	18	16	15	14	16	16	18	19	20	21	22	22	22	21	20	19	17	15	13	10	8
3	5	8	10	13	15	17	18	21	22	23	22	22	21	20	19	18	17	15	15	16	17	18	19	21	21	22	22	22	21	21	19	18	15	13	11	8
3.1	4	8	11	13	15	17	19	21	22	22	22	22	22	21	19	18	17	17	14	16	17	18	19	21	21	22	23	23	23	21	19	17	15	13	11	8
3.2	5	8	11	13	16	18	20	22	23	23	23	23	22	21	19	19	17	17	14	17	17	18	20	21	22	23	23	22	22	22	21	17	16	13	11	8
3.3	6	8	10	13	16	19	20	22	24	24	24	23	23	21	20	19	17	17	14	17	17	20	20	21	23	24	24	24	23	22	20	18	16	14	11	9
3.4	5	8	11	14	16	19	21	22	23	25	24	24	23	22	21	19	17	17	15	18	18	19	21	22	23	24	25	24	23	22	21	19	17	14	11	8
3.5	6	8	11	14	17	19	21	24	24	25	25	25	23	22	21	19	18	17	16	18	18	19	21	22	24	25	25	25	24	24	21	19	17	14	12	8
3.6	5	8	11	14	17	20	22	23	25	26	26	25	24	22	21	20	18	17	16	17	19	20	21	23	24	24	25	26	25	24	22	19	17	14	12	8
3.7	5	9	11	14	17	19	23	24	26	25	26	26	24	23	21	20	19	17	17	18	18	21	22	23	25	26	27	26	25	24	22	20	17	14	11	8
3.8	5	8	11	15	17	21	23	24	26	28	27	25	25	23	22	20	19	18	17	19	20	20	22	23	25	26	26	27	27	25	23	20	17	15	11	9
3.9	4	9	11	14	17	21	23	25	26	26	27	26	25	24	22	20	18	18	17	19	19	20	22	24	26	27	27	27	25	25	23	21	18	15	12	8
4	5	9	11	15	19	21	24	26	27	29	28	28	26	24	23	20	19	18	18	19	19	21	22	25	26	27	28	28	28	25	23	22	18	15	12	9

Table A.6: Swath width of the wind displaced transverse spread pattern to achieve a CV of 15% for urea (without spreader).

	Corrected Wind Angle (°)																																				
Wind Speed (m/s)	**0**	**10**	**20**	**30**	**40**	**50**	**60**	**70**	**80**	**90**	**100**	**110**	**120**	**130**	**140**	**150**	**160**	**170**	**180**	**190**	**200**	**210**	**220**	**230**	**240**	**250**	**260**	**270**	**280**	**290**	**300**	**310**	**320**	**330**	**340**	**350**
0	2	0	0	0	2	2	2	0	1	2	2	0	2	2	2	2	2	0	2	2	2	2	2	2	2	2	2	0	2	2	0	2	1	0	2	2
0.1	2	1	-1	1	0	1	0	1	1	0	0	1	-2	1	1	1	-1	1	2	0	2	3	1	1	1	3	3	2	3	1	1	1	1	3	2	0
0.2	1	-1	1	0	0	-1	-1	-1	-1	-1	-1	-1	0	0	0	1	1	-1	2	2	1	2	2	3	3	3	3	4	3	3	3	3	2	2	1	0
0.3	2	1	0	-1	-1	-1	-2	-6	-3	-3	-6	-6	-2	-2	-1	0	0	2	2	3	2	3	3	4	5	5	5	5	5	5	5	4	3	3	2	2
0.4	1	1	0	-1	-2	-2	-7	-3	-8	-8	-4	-4	-7	-2	-2	-1	0	-2	0	1	2	4	5	5	6	7	7	7	7	7	6	5	5	3	2	1
0.5	1	-2	0	-2	-3	-4	-5	-9	-6	-6	-5	-9	-4	-4	-2	-1	0	1	2	1	3	4	6	7	8	8	9	9	9	8	8	7	6	4	3	1
0.6	0	0	-2	-6	-4	-9	-10	-11	-6	-7	-7	-7	-10	-9	-4	-2	0	1	2	2	4	5	7	8	9	10	11	11	10	10	9	8	7	5	4	2
0.7	2	0	-2	-7	-9	-10	-8	-8	-8	-9	-9	-8	-11	-6	-9	-7	-1	0	2	2	4	6	8	10	11	12	12	12	12	12	11	10	8	6	4	2
0.8	1	-1	-2	-5	-10	-12	-13	-10	-14	-11	-10	-14	-8	-7	-10	-8	-2	0	2	2	5	7	9	11	12	13	14	14	14	13	12	11	9	7	5	2
0.9	1	-1	-3	-9	-11	-13	-14	-12	-12	-12	-12	-11	-10	-8	-5	-4	-2	0	2	3	5	8	10	12	14	15	16	16	16	15	14	12	10	8	5	3
1	1	-4	-4	-10	-12	-10	-12	-13	-14	-14	-18	-14	-11	-10	-7	-5	-7	0	2	3	6	9	11	14	15	16	17	17	17	16	16	13	12	9	6	3
1.1	0	-1	-4	-11	-14	-16	-13	-16	-15	-18	-19	-18	-13	-11	-9	-6	-3	0	2	3	7	10	13	15	17	18	18	19	18	18	17	15	13	10	7	3
1.2	1	-1	-8	-11	-14	-17	-17	-18	-20	-20	-17	-18	-14	-12	-9	-6	-4	-1	2	4	7	11	14	16	17	20	20	20	20	19	18	16	14	11	7	4
1.3	0	-2	-9	-12	-14	-17	-21	-20	-22	-19	-20	-17	-18	-13	-9	-8	-4	-1	2	4	8	11	15	17	20	21	22	23	21	21	19	18	15	11	8	4
1.4	1	-2	-9	-13	-17	-16	-22	-20	-22	-21	-21	-21	-18	-15	-11	-7	-5	-1	2	4	9	12	16	18	20	21	22	23	23	23	21	19	16	12	9	4
1.5	1	-3	-10	-14	-17	-21	-20	-24	-25	-26	-23	-21	-19	-17	-10	-7	-5	-2	3	5	9	13	16	19	21	24	24	24	24	24	22	20	17	13	9	5
1.6	0	-6	-11	-12	-19	-20	-22	-25	-26	-25	-27	-24	-21	-18	-13	-8	-6	-1	2	5	10	14	18	21	22	24	26	26	26	26	24	21	18	14	10	5
1.7	0	-6	-11	-16	-20	-22	-26	-27	-27	-27	-26	-26	-24	-18	-14	-8	-6	-2	2	5	10	15	19	22	24	26	28	27	28	27	25	23	19	15	10	5
1.8	1	-4	-12	-17	-21	-22	-25	-29	-30	-30	-29	-28	-24	-20	-15	-10	-6	-1	2	6	11	15	19	21	25	27	29	30	28	28	25	22	21	16	11	6
1.9	1	-7	-12	-17	-23	-25	-28	-31	-32	-33	-32	-30	-27	-21	-16	-12	-7	-1	3	6	11	16	21	22	27	28	29	31	30	30	26	24	21	17	12	6
2	1	-7	-13	-18	-23	-27	-30	-31	-34	-35	-33	-30	-29	-23	-19	-12	-6	-2	3	6	12	17	21	24	27	30	30	32	33	31	29	25	21	17	12	6
2.1	1	-4	-14	-19	-24	-27	-32	-35	-35	-36	-33	-33	-29	-23	-19	-12	-7	-1	2	6	13	17	22	24	27	32	34	34	34	31	30	26	22	18	13	7
2.2	0	-8	-14	-21	-24	-29	-33	-34	-38	-36	-37	-35	-30	-24	-21	-12	-7	-2	3	7	13	18	21	26	30	32	35	36	37	34	31	27	25	19	13	7
2.3	1	-8	-15	-20	-26	-31	-34	-39	-40	-38	-39	-35	-32	-27	-20	-15	-8	-2	3	7	14	16	23	26	31	34	38	37	36	36	33	30	25	20	14	7
2.4	1	-8	-15	-22	-27	-31	-37	-39	-42	-41	-42	-36	-34	-29	-23	-15	-7	-2	3	7	14	18	23	28	33	35	38	40	41	38	34	31	26	21	14	7
2.5	1	-9	-15	-23	-27	-34	-38	-42	-43	-43	-41	-40	-35	-29	-23	-15	-8	-1	3	8	14	17	23	29	35	38	39	41	40	41	35	32	26	22	15	8
2.6	0	-9	-17	-23	-29	-35	-39	-43	-44	-46	-43	-39	-36	-32	-24	-18	-9	-2	4	8	14	18	25	31	35	38	42	44	41	41	39	33	29	22	16	8
2.7	0	-9	-17	-24	-30	-37	-40	-44	-46	-45	-43	-40	-38	-33	-27	-18	-9	-3	4	8	15	18	27	31	36	42	44	44	45	44	40	35	30	23	17	8
2.8	1	-9	-18	-26	-32	-38	-42	-46	-47	-47	-47	-44	-41	-35	-26	-19	-10	-3	3	8	15	19	27	32	38	42	46	46	47	44	41	36	30	24	17	9
2.9	1	-10	-18	-26	-33	-40	-44	-46	-49	-50	-48	-46	-40	-36	-29	-20	-10	-2	4	9	15	18	26	34	39	45	45	49	49	47	43	38	31	25	17	9
3	0	-10	-19	-27	-35	-40	-44	-49	-51	-54	-49	-48	-43	-35	-30	-20	-11	-2	4	9	16	19	28	35	41	46	48	50	50	49	45	39	33	26	18	9
3.1	1	-10	-19	-26	-36	-42	-49	-52	-54	-53	-50	-48	-43	-38	-31	-22	-12	-2	4	9	13	21	29	37	44	48	50	50	51	50	46	40	35	26	19	9
3.2	1	-11	-20	-29	-36	-43	-50	-52	-55	-55	-53	-49	-45	-40	-31	-22	-12	-1	11	10	13	22	30	36	43	51	52	53	53	54	49	43	35	27	19	10
3.3	0	-11	-21	-29	-37	-44	-50	-53	-58	-56	-55	-51	-46	-40	-32	-23	-13	-2	5	10	13	23	30	38	45	50	53	57	56	53	49	45	36	28	19	10
3.4	0	-11	-22	-31	-40	-45	-50	-56	-57	-59	-57	-52	-47	-42	-33	-23	-14	-2	10	10	15	24	32	41	48	55	55	58	57	56	51	46	37	29	21	11
3.5	1	-12	-21	-31	-40	-48	-53	-58	-60	-60	-58	-57	-49	-42	-34	-25	-14	-2	11	1	15	25	33	42	48	56	59	59	59	57	52	48	39	30	21	11
3.6	0	-12	-22	-33	-42	-50	-55	-59	-62	-62	-62	-56	-51	-44	-36	-27	-14	-3	10	1	14	25	36	43	49	57	61	62	61	59	56	47	38	30	22	11
3.7	0	-12	-23	-33	-43	-50	-57	-62	-63	-65	-62	-57	-52	-45	-37	-28	-15	-4	10	2	16	25	36	44	50	58	61	63	61	61	56	49	41	30	23	12
3.8	1	-12	-24	-35	-44	-51	-58	-62	-65	-66	-62	-60	-54	-48	-38	-26	-14	-4	-11	2	16	27	35	45	54	61	63	62	66	62	57	52	43	32	23	12
3.9	1	-13	-24	-35	-44	-54	-60	-64	-65	-68	-63	-63	-56	-48	-38	-29	-17	-5	-11	24	18	28	38	45	56	62	66	64	65	63	59	53	43	34	24	12
4	1	-13	-25	-36	-46	-55	-63	-67	-68	-69	-68	-61	-55	-50	-41	-29	-16	-5	-11	3	17	28	39	49	57	62	67	68	66	64	61	53	46	34	23	12

Table A.7: Peak mass transverse displacement look up table for DAP (with 9 duct FarmAir spreader).

	Corrected Wind Angle (°)																																				
Wind Speed (m/s)	0	10	20	30	40	50	60	70	80	90	100	110	120	130	140	150	160	170	180	190	200	210	220	230	240	250	260	270	280	290	300	310	320	330	340	350
0	27	27	27	27	27	27	27	27	27	27	27	27	27	27	27	27	27	27	27	27	27	27	27	27	27	27	27	27	27	27	27	27	27	27	27	27
0.1	26	26	26	27	27	27	27	27	27	27	27	27	27	27	27	27	27	27	27	26	27	27	27	26	27	27	27	26	27	26	26	26	26	27	26	26
0.2	26	26	26	26	26	26	26	26	27	27	27	27	27	27	27	27	27	27	27	27	27	27	26	27	26	26	26	26	26	26	26	26	25	26	26	26
0.3	26	26	26	26	26	26	26	26	26	26	26	27	27	27	27	28	28	28	28	28	28	27	26	26	26	26	26	25	25	25	25	25	25	26	26	26
0.4	26	26	26	26	26	26	26	26	26	26	27	27	27	27	27	28	28	28	28	27	27	27	27	26	26	26	25	25	25	25	25	25	25	25	25	25
0.5	25	25	25	25	26	25	26	26	26	26	27	27	27	27	28	28	28	28	28	28	27	27	27	26	26	25	24	24	24	24	24	24	24	24	25	25
0.6	25	25	25	25	25	25	25	26	26	26	27	27	27	27	28	28	29	29	29	29	28	27	26	26	26	24	24	24	24	24	23	23	24	24	24	25
0.7	25	25	25	25	25	25	25	26	26	26	27	27	27	28	28	28	29	29	29	29	28	27	26	25	24	24	24	23	23	23	22	23	23	23	24	24
0.8	25	25	25	25	25	25	26	26	26	26	26	27	27	27	28	28	29	29	29	29	28	27	27	26	24	21	24	23	23	23	23	22	22	23	23	24
0.9	24	25	24	24	25	25	25	26	26	26	27	27	27	28	28	29	29	30	30	29	28	27	26	19	25	24	24	23	23	23	23	23	23	22	23	24
1	24	24	24	24	24	25	25	26	26	26	27	27	27	28	28	29	29	30	30	29	28	27	26	21	20	23	24	25	24	23	23	22	22	22	23	23
1.1	24	24	24	24	25	25	25	25	26	26	27	27	27	28	28	29	30	30	30	30	28	26	19	25	23	24	25	25	24	24	23	22	23	22	22	23
1.2	24	24	24	24	24	25	25	26	26	26	27	27	27	28	28	29	30	30	30	30	28	19	19	21	25	26	26	25	25	24	23	22	23	21	22	23
1.3	23	24	24	24	24	25	25	26	26	26	27	27	27	28	28	29	30	30	30	30	28	27	19	21	26	26	26	26	25	25	24	23	22	21	22	22
1.4	23	23	23	24	24	24	25	25	26	27	27	27	27	27	28	29	30	30	30	30	28	20	20	26	26	26	26	26	26	25	24	23	22	21	21	22
1.5	23	23	23	24	24	25	25	26	26	27	27	27	27	28	28	29	30	30	30	30	28	19	20	25	27	27	27	26	26	25	24	23	22	21	21	22
1.6	23	23	23	23	24	25	25	26	26	27	27	27	28	27	28	29	30	30	30	30	19	19	20	27	27	27	27	27	26	26	25	25	23	22	21	21
1.7	22	23	23	23	24	25	25	26	26	27	27	27	27	27	21	20	30	30	30	30	19	19	20	27	28	27	27	27	27	26	26	25	24	23	21	21
1.8	22	22	23	23	24	24	25	26	26	27	27	27	27	27	21	20	19	30	30	30	19	19	20	27	28	28	28	27	26	26	25	24	23	21	21	21
1.9	22	22	23	23	24	25	25	26	27	27	27	27	28	27	21	20	19	30	30	30	19	19	21	28	28	28	27	27	26	26	25	24	23	21	20	21
2	22	22	22	23	24	25	25	26	26	27	28	28	28	27	21	20	19	30	30	30	19	19	21	28	28	28	28	27	27	26	25	24	23	22	20	20
2.1	22	22	22	23	24	25	25	26	27	27	28	28	28	27	22	20	19	30	30	30	19	19	21	28	29	28	28	27	27	26	25	24	23	21	20	21
2.2	22	22	22	23	24	25	25	26	27	27	27	28	28	27	22	20	19	30	30	30	19	19	22	28	29	28	28	27	27	26	25	24	23	22	20	20
2.3	21	22	22	23	24	25	26	26	27	28	28	28	28	27	22	19	19	30	30	30	19	19	22	29	29	29	28	28	27	26	25	24	23	22	20	20
2.4	21	21	22	23	24	25	26	26	27	28	28	28	28	28	22	19	19	19	30	19	19	19	21	29	29	29	28	28	27	26	25	24	23	22	20	19
2.5	21	21	22	23	24	25	26	26	27	28	28	28	28	27	22	20	19	18	30	19	19	18	27	29	29	29	28	28	27	26	25	24	23	22	20	19
2.6	21	21	22	23	24	25	26	27	27	28	28	29	28	28	23	19	19	18	30	19	19	18	27	29	29	29	28	28	27	26	25	24	23	22	20	19
2.7	21	21	22	23	24	25	26	26	28	28	29	29	29	28	23	20	19	18	30	19	19	18	27	30	29	29	28	28	27	26	25	24	24	22	20	19
2.8	20	21	22	23	24	25	26	27	28	28	29	29	29	28	23	20	19	18	19	19	18	18	28	30	29	29	29	28	27	27	25	24	23	22	20	19
2.9	20	21	22	23	24	25	26	27	28	29	29	29	29	28	24	20	19	18	18	19	18	17	28	29	30	29	29	28	27	27	26	25	23	22	20	19
3	20	21	21	23	24	25	26	27	28	29	29	29	29	28	25	20	19	18	18	19	18	18	29	29	30	29	29	28	28	27	26	25	23	22	20	18
3.1	20	20	21	23	24	25	27	27	28	29	29	30	30	28	24	20	18	18	18	19	18	17	28	30	30	29	29	28	28	27	26	25	23	22	20	19
3.2	20	20	21	23	24	25	27	28	29	29	29	29	29	29	26	20	18	18	18	19	13	17	28	30	30	29	29	29	28	27	26	25	24	22	20	18
3.3	20	20	21	23	24	26	27	28	29	29	30	30	30	29	26	20	18	18	18	18	12	18	29	30	29	30	30	29	29	27	26	25	24	22	20	18
3.4	20	20	21	23	24	26	27	28	29	30	30	30	29	29	25	20	18	18	18	19	13	18	29	30	30	30	29	29	29	28	26	25	24	22	20	18
3.5	19	20	21	23	24	26	27	28	29	30	30	30	30	29	26	20	18	18	18	18	13	18	29	30	30	30	30	30	29	28	27	25	24	22	20	18
3.6	19	20	21	23	24	26	27	29	30	30	30	30	29	29	26	20	18	18	18	18	13	19	29	30	30	30	30	30	29	28	27	25	24	22	20	18
3.7	19	20	21	22	24	26	27	28	30	30	30	30	30	30	27	21	18	18	17	18	13	19	30	30	30	30	30	30	29	28	27	25	24	22	20	17
3.8	19	20	21	22	24	26	28	29	30	30	30	30	30	30	27	21	18	17	17	18	13	19	30	30	30	30	30	30	30	28	27	26	24	22	20	18
3.9	19	20	21	22	24	27	28	29	30	30	30	30	30	30	28	21	18	17	17	18	13	19	29	30	30	30	30	30	30	29	27	26	24	22	20	17
4	19	19	21	23	25	26	28	29	30	30	30	30	30	30	28	21	18	17	17	18	14	20	30	30	30	30	30	30	30	30	28	26	24	22	20	17

Table A.8: Swath width of the wind displaced transverse spread pattern to achieve a CV of 15% for DAP (with 9 duct FarmAir spreader).

	Corrected Wind Angle (°)																																				
Wind Speed (m/s)	0	10	20	30	40	50	60	70	80	90	100	110	120	130	140	150	160	170	180	190	200	210	220	230	240	250	260	270	280	290	300	310	320	330	340	350
0	0	0	0	0	0	0	0	0	0	0	0	0	0	0	0	0	0	0	0	0	0	0	0	0	0	0	0	0	0	0	0	0	0	0	0	0
0.1	0	-1	-1	-1	-2	-2	-2	-2	-2	-2	-2	-2	-2	-2	-2	-1	-1	-1	0	0	0	1	1	1	2	2	2	2	2	2	1	1	1	1	0	0
0.2	0	-1	-2	-2	-3	-4	-4	-4	-2	-5	-5	-4	-4	-4	-3	-2	-2	-1	0	0	1	2	2	3	3	4	4	4	4	4	3	3	2	2	1	0
0.3	0	-1	-2	-4	-4	-5	-6	-6	-6	-7	-6	-6	-6	-5	-5	-1	-2	-1	0	1	2	3	4	4	5	5	6	6	6	5	5	4	4	3	2	1
0.4	0	-2	-3	-5	-6	-7	-7	-8	-8	-8	-8	-8	-7	-7	-6	-5	-3	-2	0	1	3	4	5	6	7	7	7	8	7	7	7	6	5	4	3	1
0.5	0	-2	-4	-6	-7	-8	-9	-10	-10	-10	-10	-10	-9	-8	-7	-6	-4	-2	0	1	3	5	6	7	8	9	9	9	9	9	8	7	6	5	3	2
0.6	0	-3	-5	-6	-8	-9	-11	-11	-12	-12	-12	-11	-10	-9	-8	-7	-5	-3	0	2	4	6	7	9	10	11	11	11	11	11	10	9	7	6	4	2
0.7	0	-3	-5	-7	-9	-11	-12	-13	-14	-14	-13	-13	-12	-11	-9	-7	-5	-3	0	2	5	7	8	10	11	12	13	13	13	12	11	10	8	7	5	2
0.8	0	-3	-6	-8	-11	-12	-14	-15	-16	-16	-15	-15	-14	-12	-10	-8	-6	-3	0	3	5	8	10	11	13	14	15	15	15	14	13	12	10	8	5	3
0.9	0	-4	-7	-9	-11	-14	-15	-17	-17	-17	-17	-16	-15	-14	-12	-9	-7	-4	0	3	6	8	11	13	15	16	16	17	16	16	15	13	11	9	6	3
1	0	-4	-7	-10	-13	-15	-17	-18	-19	-19	-19	-18	-17	-15	-13	-10	-7	-4	0	3	6	10	12	14	16	17	18	18	18	18	16	14	12	9	7	3
1.1	0	-4	-8	-11	-14	-17	-18	-19	-21	-20	-21	-20	-18	-17	-14	-11	-8	-4	0	4	7	10	13	16	17	19	20	21	20	19	18	16	13	10	7	4
1.2	0	-5	-9	-12	-15	-18	-20	-22	-22	-22	-23	-21	-20	-17	-15	-12	-9	-5	0	4	8	11	14	17	19	21	21	22	21	21	19	17	14	11	8	4
1.3	0	-5	-9	-13	-17	-20	-21	-23	-24	-24	-24	-21	-21	-19	-16	-13	-9	-5	0	4	8	12	15	18	21	22	23	23	23	22	21	18	15	12	8	4
1.4	0	-5	-10	-14	-17	-21	-22	-25	-27	-27	-26	-25	-22	-20	-17	-13	-10	-6	0	5	9	13	17	19	21	24	25	25	24	24	23	19	17	13	9	5
1.5	0	-6	-11	-15	-18	-22	-25	-27	-28	-27	-26	-26	-24	-21	-15	-15	-11	-6	0	5	10	14	18	21	23	25	25	26	27	25	24	21	18	14	10	5
1.6	0	-6	-11	-16	-20	-23	-27	-30	-29	-28	-30	-28	-24	-21	-16	-15	-11	-6	0	5	10	15	19	22	25	25	27	28	28	28	25	22	19	15	10	5
1.7	0	-6	-12	-16	-21	-24	-27	-31	-32	-31	-31	-29	-27	-22	-18	-17	-12	-7	0	6	11	16	19	23	26	28	31	30	29	28	27	24	20	16	11	6
1.8	0	-7	-12	-18	-22	-26	-29	-31	-33	-32	-32	-31	-28	-23	-22	-13	-7	-7	0	6	12	17	21	25	26	30	31	32	32	30	27	25	21	17	12	6
1.9	0	-7	-13	-19	-23	-28	-31	-33	-34	-36	-33	-33	-30	-24	-20	-13	-7	-7	0	6	12	17	22	26	28	32	32	33	33	33	30	26	23	17	12	6
2	0	-7	-13	-19	-25	-29	-32	-35	-37	-38	-37	-35	-31	-27	-24	-14	-8	-7	0	7	13	17	23	27	30	32	35	35	35	33	31	28	24	19	13	7
2.1	0	-8	-14	-21	-26	-30	-34	-36	-39	-39	-39	-36	-32	-29	-22	-17	-8	-8	0	7	13	18	23	27	31	34	36	37	35	36	32	29	25	19	13	7
2.2	0	-8	-15	-21	-26	-32	-36	-39	-40	-40	-39	-36	-34	-32	-23	-17	-8	-8	0	7	13	20	25	28	32	36	38	39	38	38	35	30	26	20	14	7
2.3	0	-8	-16	-22	-28	-33	-38	-41	-43	-41	-42	-40	-36	-32	-25	-17	-8	-3	0	7	14	20	24	29	35	38	41	42	41	39	38	32	27	21	15	8
2.4	0	-9	-16	-23	-29	-35	-38	-42	-43	-44	-43	-40	-38	-33	-24	-19	-8	-2	0	8	15	21	26	32	35	40	43	44	44	42	36	33	28	22	16	8
2.5	0	-9	-17	-24	-31	-36	-41	-42	-46	-46	-44	-43	-41	-34	-29	-18	-11	-3	0	8	16	22	26	33	37	44	44	45	45	43	40	35	29	23	16	8
2.6	0	-9	-18	-25	-32	-38	-42	-46	-50	-48	-47	-44	-39	-35	-28	-21	-12	-4	0	8	16	21	28	33	38	43	48	46	47	46	42	37	30	24	17	9
2.7	0	-10	-18	-25	-33	-39	-44	-47	-51	-49	-50	-46	-42	-38	-29	-21	-11	-4	0	9	17	22	29	36	41	44	48	51	49	47	44	38	31	25	17	9
2.8	0	-10	-18	-26	-34	-40	-45	-48	-52	-53	-51	-47	-44	-38	-31	-22	-12	-4	2	9	17	23	29	36	43	48	51	51	52	49	47	41	34	25	18	9
2.9	0	-10	-19	-28	-36	-42	-47	-50	-53	-53	-53	-50	-45	-39	-31	-21	-13	-4	3	9	18	23	31	36	44	50	54	52	54	51	46	41	36	26	18	10
3	0	-11	-20	-29	-38	-43	-50	-53	-54	-55	-54	-51	-48	-41	-33	-23	-14	-4	4	10	17	24	32	38	46	49	54	53	54	51	48	43	36	27	19	10
3.1	0	-11	-21	-30	-37	-45	-51	-54	-59	-59	-57	-53	-49	-41	-35	-24	-14	-5	3	10	17	26	31	43	47	51	54	57	56	53	50	44	38	28	20	10
3.2	0	-11	-22	-31	-39	-47	-52	-58	-59	-59	-58	-56	-50	-42	-35	-26	-15	-4	9	10	17	26	34	40	50	54	57	59	58	55	53	47	39	30	20	10
3.3	0	-12	-22	-32	-40	-47	-54	-57	-59	-60	-59	-57	-51	-43	-35	-28	-14	-5	9	10	17	27	33	45	49	56	61	60	59	57	53	48	39	30	21	11
3.4	0	-12	-22	-33	-42	-50	-57	-61	-63	-62	-62	-58	-55	-47	-39	-27	-15	-5	9	11	18	26	37	44	52	58	61	62	60	59	54	48	41	30	21	11
3.5	0	-12	-23	-33	-44	-52	-56	-61	-67	-65	-62	-61	-53	-47	-40	-28	-17	-5	9	22	18	28	36	47	54	59	62	64	63	61	57	52	43	33	22	11
3.6	0	-13	-24	-34	-44	-53	-61	-65	-66	-65	-65	-61	-55	-48	-39	-29	-18	-6	9	22	18	27	36	48	57	61	63	65	65	64	60	51	44	34	23	12
3.7	0	-13	-24	-36	-46	-54	-61	-65	-68	-68	-68	-63	-58	-51	-42	-30	-18	-6	9	23	18	30	39	50	56	63	67	69	65	64	59	53	45	34	24	12
3.8	0	-13	-26	-37	-47	-57	-63	-66	-69	-70	-69	-65	-59	-51	-42	-32	-19	-6	9	23	19	30	39	50	60	65	67	71	69	67	63	56	46	35	24	12
3.9	0	-13	-26	-38	-48	-56	-64	-70	-73	-71	-71	-67	-60	-52	-43	-31	-20	-6	9	23	20	31	42	51	60	66	69	71	72	67	64	56	48	37	25	13
4	0	-14	-27	-38	-49	-58	-66	-69	-74	-74	-74	-68	-64	-55	-43	-32	-20	-6	9	23	21	31	44	53	62	67	71	74	73	71	65	58	48	38	25	13

Table A.9: Peak mass transverse displacement look up table for urea (with 9 duct FarmAir spreader).

	Corrected Wind Angle (°)																																				
Wind Speed (m/s)	**0**	**10**	**20**	**30**	**40**	**50**	**60**	**70**	**80**	**90**	**100**	**110**	**120**	**130**	**140**	**150**	**160**	**170**	**180**	**190**	**200**	**210**	**220**	**230**	**240**	**250**	**260**	**270**	**280**	**290**	**300**	**310**	**320**	**330**	**340**	**350**
0	22	22	22	22	22	22	22	22	22	22	22	22	22	22	22	22	22	22	22	22	22	22	22	22	22	22	22	22	22	22	22	22	22	22	22	22	22
0.1	22	21	21	22	22	22	22	22	22	22	22	22	22	22	22	22	22	22	22	21	22	22	21	21	21	21	21	21	21	21	21	21	20	21	21	21	21
0.2	21	21	21	22	22	22	22	22	22	22	22	22	22	22	22	23	23	22	22	22	21	22	21	21	20	20	20	20	20	20	19	20	20	21	20	21	21
0.3	21	21	21	21	21	22	21	22	22	22	22	22	22	23	23	23	23	23	23	22	22	21	21	20	19	19	19	18	18	19	19	19	19	20	20	20	20
0.4	21	21	21	21	21	21	21	22	22	22	22	22	22	23	23	23	23	23	23	22	22	22	20	20	19	18	17	17	18	17	19	18	19	19	20	20	20
0.5	20	21	21	21	21	21	22	22	22	22	22	23	23	23	23	23	23	23	23	23	21	19	19	18	18	19	18	18	18	19	18	17	18	18	18	20	20
0.6	20	20	21	21	21	21	21	22	22	22	22	22	23	23	23	23	24	24	24	23	22	21	20	19	19	18	19	18	19	18	17	17	17	17	18	19	19
0.7	20	20	20	21	21	21	21	22	22	22	23	23	23	23	23	24	24	24	24	23	21	19	19	19	19	20	20	20	20	19	18	17	18	17	18	19	19
0.8	20	20	20	20	21	21	21	22	22	22	23	23	23	23	23	24	24	24	24	23	22	17	18	20	21	21	20	21	20	20	18	18	17	16	17	19	19
0.9	20	20	20	20	21	21	21	22	22	22	23	23	23	24	24	24	24	25	24	23	22	18	18	18	21	22	21	21	21	20	19	18	17	16	17	18	18
1	19	20	20	20	21	21	21	22	22	23	23	23	23	24	24	24	25	25	25	23	18	17	19	20	21	22	22	22	21	21	21	20	19	18	17	16	18
1.1	19	19	20	20	21	21	22	22	22	23	23	23	24	24	24	24	25	25	25	24	18	17	17	22	22	22	22	22	22	21	20	19	18	17	17	17	17
1.2	19	19	19	20	20	21	22	22	22	23	23	24	24	24	24	25	25	26	26	24	18	18	22	23	23	23	23	23	22	21	21	20	19	18	16	17	17
1.3	19	19	19	20	21	21	22	22	23	23	24	24	24	24	24	25	25	26	26	24	17	17	22	23	23	23	23	23	22	22	21	20	19	17	16	16	16
1.4	18	19	19	20	21	21	22	22	23	23	24	24	24	24	25	25	26	26	26	24	17	18	22	24	24	24	23	23	23	22	21	20	19	18	16	17	17
1.5	18	19	19	20	20	21	22	23	23	24	24	24	24	25	25	25	26	27	27	25	17	18	23	24	24	24	24	23	23	22	21	21	19	18	16	16	16
1.6	18	18	19	20	20	21	22	23	23	24	24	25	24	24	25	25	26	27	27	24	17	17	24	25	25	24	24	24	23	22	22	21	19	18	16	15	15
1.7	18	19	19	20	20	21	22	23	23	24	24	25	25	25	25	25	26	27	27	17	17	18	24	25	25	25	24	24	24	23	23	22	21	20	18	16	16
1.8	17	18	19	20	21	21	22	23	24	24	25	25	25	25	25	25	26	27	28	17	17	18	25	25	25	25	25	24	23	23	22	21	20	18	16	15	15
1.9	17	18	19	20	21	21	22	23	24	25	25	25	25	25	25	25	26	27	28	17	17	18	25	26	25	25	25	24	24	23	22	21	20	18	16	15	15
2	17	18	19	20	21	22	22	23	24	25	25	25	25	25	26	25	27	28	29	17	17	19	26	26	26	25	25	24	24	23	22	21	20	19	16	15	15
2.1	17	18	19	20	21	22	23	24	24	25	25	26	26	26	25	25	26	28	29	17	17	19	26	26	26	25	25	25	24	23	22	21	20	19	17	15	15
2.2	17	18	19	20	21	22	23	24	24	25	25	26	26	26	25	19	17	28	29	17	17	18	26	26	26	26	25	25	24	23	22	21	20	19	17	15	15
2.3	17	18	19	20	21	22	23	24	25	25	26	26	26	26	26	18	17	28	30	16	17	18	26	26	26	26	26	25	24	24	22	22	20	19	17	14	14
2.4	16	18	19	20	21	22	23	24	25	25	26	26	26	26	25	20	17	28	30	16	17	20	26	27	26	26	26	25	24	24	23	21	20	19	17	15	15
2.5	16	17	18	20	21	22	23	24	25	26	26	27	27	26	26	19	17	28	30	16	17	19	27	27	27	26	26	26	25	24	23	22	20	19	17	14	14
2.6	16	17	18	20	21	22	23	24	25	26	26	27	26	26	25	19	17	29	30	16	17	20	26	27	27	26	26	25	25	24	23	22	20	19	17	15	15
2.7	16	17	18	20	21	22	24	25	26	26	27	27	27	27	26	19	17	28	30	16	17	19	27	27	27	27	27	26	25	24	23	22	20	19	17	15	15
2.8	16	17	18	20	21	23	24	25	26	27	27	27	27	27	27	19	17	16	30	16	17	20	27	27	27	27	27	26	26	25	23	22	21	19	17	14	14
2.9	16	17	18	20	21	23	24	25	26	27	27	27	27	27	26	19	17	16	30	16	16	19	27	27	27	27	27	26	26	25	24	22	21	19	17	14	14
3	16	17	18	20	21	23	24	25	27	27	28	28	27	27	26	19	17	16	30	16	16	19	28	27	27	27	27	27	26	25	24	22	21	19	17	14	14
3.1	15	17	18	20	21	23	25	26	27	27	28	27	28	27	27	19	17	16	30	16	16	18	28	27	27	28	28	27	27	26	24	23	21	19	17	14	14
3.2	15	17	18	20	21	23	24	26	27	28	28	28	28	27	26	19	17	16	30	16	16	19	27	27	28	28	28	28	27	26	24	23	21	19	17	14	14
3.3	15	17	18	20	22	24	25	26	28	28	28	28	28	28	27	20	16	16	30	16	11	19	28	28	28	28	28	28	27	26	25	23	21	19	17	14	14
3.4	15	17	18	20	22	24	25	26	28	28	28	29	29	27	27	20	16	16	30	16	11	19	28	28	28	28	29	28	28	26	25	23	21	19	17	14	14
3.5	15	17	18	20	22	24	26	28	28	29	29	29	29	27	27	20	16	15	30	16	12	20	28	28	29	29	28	29	28	27	25	24	21	19	17	14	14
3.6	15	16	18	20	22	24	26	28	29	30	30	29	28	28	27	21	16	15	30	16	12	20	28	28	29	28	29	29	29	28	26	24	21	20	17	15	15
3.7	15	16	18	20	22	24	26	28	29	30	30	29	29	28	27	21	16	15	30	16	12	20	28	29	29	29	29	29	28	28	26	24	22	20	18	14	14
3.8	15	16	18	20	22	24	26	28	29	30	30	29	29	28	27	21	16	15	30	16	12	26	28	28	28	30	30	29	29	28	27	24	22	19	17	14	14
3.9	14	16	18	20	22	25	27	28	30	30	30	30	29	28	27	23	16	15	30	16	13	25	28	28	29	30	30	30	30	28	27	25	22	20	17	14	14
4	14	16	18	20	23	25	27	29	30	30	30	30	30	29	27	22	16	15	30	15	13	26	28	29	30	30	30	30	30	29	27	25	22	20	17	14	14

Table A.10: Swath width of the wind displaced transverse spread pattern to achieve a CV of 15% for urea (with 9 duct FarmAir spreader).

	Corrected Wind Angle (°)																																				
Wind Speed (m/s)	**0**	**10**	**20**	**30**	**40**	**50**	**60**	**70**	**80**	**90**	**100**	**110**	**120**	**130**	**140**	**150**	**160**	**170**	**180**	**190**	**200**	**210**	**220**	**230**	**240**	**250**	**260**	**270**	**280**	**290**	**300**	**310**	**320**	**330**	**340**	**350**
0	1	1	-3	2	1	1	-2	1	-2	-1	1	-1	-2	-2	-2	-2	1	-1	1	-1	-1	-2	-1	-2	-1	-2	-2	2	-1	-3	-1	-1	-2	-2	1	1
0.1	-1	-1	1	-2	-2	-2	0	-3	-3	-3	-3	-3	-2	-2	-2	-2	1	-1	-3	2	2	-2	1	1	-1	-1	-1	-1	-1	-1	-1	1	-1	2	-2	-2
0.2	-1	1	-2	-3	-3	-4	-4	-4	-4	-5	-4	-4	-4	-4	-3	-3	-2	1	2	0	1	3	2	3	3	3	4	4	4	3	3	3	2	2	1	-2
0.3	-1	-2	-3	-4	-4	-5	-6	-6	-6	-6	-6	-6	-6	-5	-4	-4	-3	-2	-1	-2	-1	3	4	4	5	5	5	5	5	5	5	4	3	3	2	-2
0.4	1	-2	-3	-5	-6	-6	-7	-8	-8	-8	-8	-8	-7	-6	-6	-5	-3	-2	-3	1	-1	4	5	6	6	7	7	7	7	7	6	6	5	4	2	1
0.5	-1	-3	-4	-5	-7	-8	-9	-9	-10	-10	-10	-9	-9	-8	-7	-5	-4	-3	-3	-2	3	5	6	7	8	8	9	9	9	8	8	7	6	5	3	-1
0.6	-1	-3	-5	-6	-8	-9	-10	-11	-12	-12	-11	-11	-10	-9	-8	-6	-5	-3	-3	-1	4	5	7	8	9	10	10	11	10	10	9	8	7	5	4	2
0.7	-1	-3	-5	-7	-9	-10	-12	-13	-13	-13	-13	-13	-12	-10	-9	-7	-5	-3	-3	2	4	6	8	10	11	12	12	12	12	12	11	9	8	6	4	2
0.8	1	-3	-6	-8	-10	-12	-13	-14	-15	-15	-15	-14	-13	-12	-10	-8	-6	-3	-3	3	5	7	9	11	12	13	14	14	14	13	12	11	9	7	5	3
0.9	-1	-4	-6	-9	-11	-13	-15	-16	-17	-17	-17	-16	-15	-13	-11	-9	-6	-4	2	3	6	8	10	12	14	15	15	15	15	15	14	12	10	8	6	3
1	1	-4	-7	-10	-12	-15	-17	-17	-18	-19	-18	-17	-16	-15	-13	-10	-7	-4	2	3	6	9	11	13	15	16	17	16	17	16	15	14	11	9	6	3
1.1	1	-4	-8	-11	-14	-16	-18	-19	-20	-20	-20	-20	-18	-16	-13	-11	-8	-4	-1	4	7	10	12	15	16	17	18	18	17	18	17	15	12	10	7	4
1.2	-1	-5	-8	-12	-15	-17	-19	-20	-22	-22	-22	-21	-19	-17	-15	-12	-8	-5	2	4	7	11	13	16	18	19	19	18	20	19	17	16	14	11	7	4
1.3	1	-5	-9	-13	-16	-19	-21	-22	-24	-24	-24	-22	-20	-19	-16	-13	-9	-5	2	4	8	12	14	17	19	20	21	21	21	20	20	17	15	11	8	4
1.4	1	-5	-9	-13	-17	-19	-22	-25	-24	-24	-25	-23	-21	-20	-17	-14	-9	-5	2	4	9	12	15	17	19	21	22	23	22	22	19	18	16	12	9	4
1.5	-1	-6	-10	-14	-18	-21	-24	-26	-27	-27	-26	-26	-24	-21	-17	-14	-10	-6	2	5	9	13	16	18	21	22	24	23	23	23	21	19	17	13	9	5
1.6	-1	-6	-11	-15	-19	-23	-25	-27	-28	-28	-28	-27	-24	-22	-19	-15	-11	-6	-2	5	10	14	17	19	23	24	25	25	25	24	23	20	18	14	10	5
1.7	-1	-6	-11	-16	-21	-24	-26	-29	-29	-30	-29	-28	-26	-23	-20	-16	-11	-6	-2	5	10	15	18	20	23	25	26	27	28	25	23	22	19	15	10	6
1.8	-1	-7	-12	-17	-22	-25	-28	-30	-32	-32	-31	-29	-28	-25	-22	-17	-12	-7	2	6	11	15	18	20	25	26	27	29	30	27	26	24	20	16	11	6
1.9	1	-7	-12	-18	-22	-26	-29	-30	-33	-33	-34	-29	-26	-25	-20	-18	-12	-7	-3	6	12	17	18	22	26	28	30	31	30	28	27	23	20	17	12	6
2	1	-7	-13	-19	-23	-28	-31	-34	-35	-34	-33	-32	-29	-24	-20	-18	-13	-7	-3	6	12	12	20	22	27	29	31	31	33	30	30	26	22	17	12	7
2.1	-1	-7	-14	-20	-25	-28	-33	-35	-36	-36	-35	-34	-31	-26	-24	-19	-14	-7	-3	7	13	18	19	26	28	31	34	35	34	33	31	27	22	18	12	7
2.2	-1	-8	-14	-20	-25	-30	-35	-36	-38	-37	-37	-36	-32	-28	-24	-20	-14	-8	-4	7	13	17	20	26	30	32	37	36	34	35	32	28	23	19	13	7
2.3	-1	-8	-15	-21	-26	-32	-35	-39	-39	-41	-40	-37	-33	-30	-26	-21	-15	-8	-4	7	14	19	22	27	30	34	38	37	39	37	34	29	25	20	14	7
2.4	1	-8	-16	-22	-28	-32	-37	-39	-41	-41	-39	-38	-35	-30	-26	-21	-15	-8	-4	7	14	17	24	27	33	36	40	40	42	40	34	32	26	20	14	7
2.5	-1	-9	-16	-23	-29	-34	-38	-41	-44	-44	-41	-40	-35	-30	-28	-22	-16	-9	-4	8	15	18	25	30	36	38	40	43	42	40	37	33	27	21	15	8
2.6	-1	-9	-17	-24	-29	-36	-41	-44	-44	-44	-44	-41	-38	-34	-27	-22	-17	-9	-4	8	15	20	25	32	36	41	42	45	45	44	39	33	28	21	16	8
2.7	-1	-9	-18	-25	-32	-37	-41	-45	-46	-47	-46	-42	-37	-33	-28	-22	-17	-9	-3	8	11	20	26	31	36	41	44	47	47	45	39	35	30	22	16	8
2.8	-1	-10	-18	-26	-32	-38	-43	-46	-48	-49	-48	-45	-41	-35	-27	-22	-11	-10	-4	9	12	20	25	34	39	44	46	47	47	44	43	36	30	24	17	9
2.9	-1	-10	-19	-26	-33	-39	-46	-49	-50	-51	-48	-47	-41	-37	-31	-23	-11	-10	-6	9	10	21	29	33	40	45	47	49	49	47	44	38	31	24	17	9
3	-1	-10	-20	-27	-35	-40	-46	-50	-53	-53	-50	-50	-43	-37	-30	-22	-11	-10	-5	9	12	21	28	36	44	45	52	51	50	50	46	38	33	25	17	9
3.1	-1	-11	-20	-28	-35	-42	-48	-51	-53	-53	-53	-50	-45	-38	-30	-23	-13	-11	-4	2	13	23	31	37	44	50	53	55	51	51	46	43	34	26	18	10
3.2	-1	-11	-20	-29	-37	-44	-47	-53	-54	-56	-55	-51	-46	-40	-33	-24	-13	-11	-5	10	14	23	31	40	47	51	55	54	53	53	49	42	36	27	19	10
3.3	-1	-11	-21	-29	-37	-45	-50	-55	-56	-58	-57	-55	-50	-42	-34	-24	-13	-4	-6	3	12	23	33	40	49	54	56	57	55	53	49	44	38	28	19	10
3.4	-1	-11	-21	-31	-38	-48	-52	-55	-59	-61	-59	-53	-49	-44	-35	-25	-14	-3	-5	4	15	23	33	41	49	55	58	58	59	57	52	47	37	29	20	10
3.5	-1	-12	-22	-32	-41	-47	-54	-59	-61	-62	-59	-56	-50	-43	-35	-27	-15	-4	-7	3	15	26	34	42	51	54	58	61	59	58	54	47	38	31	20	11
3.6	-1	-12	-23	-33	-42	-49	-56	-59	-64	-64	-61	-59	-52	-45	-36	-28	-17	-3	-5	2	14	26	36	43	51	57	61	60	61	58	56	48	41	31	22	11
3.7	-1	-12	-24	-34	-43	-52	-58	-62	-66	-66	-63	-62	-54	-46	-38	-27	-17	-4	-5	4	15	25	36	47	53	59	62	65	62	61	55	51	42	33	22	11
3.8	1	-13	-24	-34	-44	-52	-59	-62	-66	-69	-67	-64	-53	-47	-40	-29	-17	-4	11	3	15	26	38	48	54	61	64	65	65	65	57	53	43	33	23	12
3.9	-1	-13	-24	-35	-44	-53	-60	-64	-69	-68	-67	-62	-55	-47	-40	-30	-18	-4	-6	3	17	27	40	49	57	63	66	68	67	65	59	54	44	34	24	12
4	-1	-13	-26	-37	-46	-55	-61	-65	-70	-71	-70	-65	-58	-50	-42	-30	-19	-4	11	4	19	28	40	49	58	62	67	71	69	66	62	54	46	36	23	12

Table A.11: Peak mass transverse displacement look up table for DAP (with 11 duct Transland spreader).

	Corrected Wind Angle (°)																																				
Wind Speed (m/s)	0	10	20	30	40	50	60	70	80	90	100	110	120	130	140	150	160	170	180	190	200	210	220	230	240	250	260	270	280	290	300	310	320	330	340	350
0	26	26	26	26	26	26	26	26	26	26	26	26	26	26	26	26	26	26	26	26	26	26	26	26	26	26	26	26	26	26	26	26	26	26	26	26
0.1	26	26	26	26	26	26	26	26	26	26	26	26	26	26	26	26	26	26	26	26	26	26	26	26	26	26	26	26	26	26	26	26	26	26	26	26
0.2	25	25	25	25	25	25	25	25	26	26	26	26	26	26	26	26	26	26	26	26	26	26	26	26	26	26	25	25	25	25	25	25	25	25	25	25
0.3	25	25	25	25	25	25	25	25	25	26	26	26	26	26	26	26	27	27	27	27	26	26	26	26	25	25	25	25	25	25	25	25	25	25	25	25
0.4	25	25	25	25	25	25	25	25	25	26	26	26	26	26	26	27	27	27	27	27	27	26	26	25	25	25	25	25	24	24	24	24	25	25	25	25
0.5	25	25	25	25	25	25	25	25	25	26	26	26	26	26	26	27	27	27	27	27	27	26	26	25	25	25	25	24	24	24	24	24	24	24	24	24
0.6	25	25	25	24	25	25	25	25	26	26	26	26	26	26	27	27	27	28	27	27	27	26	26	26	25	25	25	24	24	24	24	24	24	24	24	24
0.7	24	24	24	24	24	25	25	25	25	26	26	26	26	27	27	27	27	27	28	27	27	26	26	26	25	25	25	25	24	24	24	23	23	23	24	24
0.8	24	24	24	24	24	24	25	25	25	26	26	26	26	27	27	27	28	28	28	28	27	26	26	26	25	25	25	25	24	24	24	24	23	23	23	24
0.9	24	24	24	24	24	24	25	25	25	25	26	26	27	27	27	28	28	28	28	28	27	27	26	26	26	26	25	25	25	24	24	24	23	23	23	24
1	24	23	24	24	24	25	25	25	25	26	26	26	27	27	27	28	28	28	29	28	27	26	26	26	26	26	26	25	25	25	24	24	23	23	23	23
1.1	23	23	23	24	24	24	25	25	25	26	26	26	27	27	27	28	28	29	29	28	27	27	26	27	26	26	26	26	25	25	24	24	23	23	23	23
1.2	23	23	23	23	24	24	24	25	25	26	26	27	27	27	28	28	28	29	29	29	27	27	27	26	27	26	26	26	25	25	24	24	23	23	22	23
1.3	23	23	23	23	24	24	25	25	25	26	26	26	27	27	28	28	29	29	29	29	28	27	27	27	27	27	26	26	26	25	24	24	23	22	22	22
1.4	23	23	23	23	24	24	25	25	26	26	26	27	27	27	28	28	29	29	30	29	28	27	27	27	27	27	27	26	26	25	25	24	23	23	22	22
1.5	23	23	23	23	24	24	25	25	26	26	26	26	27	28	28	29	29	30	30	29	28	27	28	27	27	27	27	27	26	25	25	24	23	22	22	22
1.6	22	22	23	23	23	24	25	25	26	26	27	27	27	28	28	29	29	30	30	30	28	28	28	28	27	27	27	27	26	26	25	24	23	22	22	22
1.7	22	22	23	23	23	24	25	25	26	27	27	27	27	28	28	29	30	30	30	30	28	28	28	28	28	27	27	27	26	26	25	24	23	23	21	21
1.8	22	22	22	23	23	24	25	26	26	27	27	27	28	28	28	29	30	30	30	30	28	28	28	28	28	28	27	27	26	26	25	24	24	22	22	22
1.9	22	22	22	23	23	24	25	26	26	27	27	28	28	28	28	29	30	30	30	30	28	28	28	28	28	28	28	27	27	26	25	24	24	23	22	21
2	22	22	22	23	23	24	25	26	27	27	28	28	28	28	28	29	30	30	30	30	29	28	29	29	28	28	28	27	27	26	25	24	24	23	21	21
2.1	22	22	22	23	24	24	25	26	27	27	28	28	28	28	29	29	30	30	30	30	28	29	29	29	29	28	28	27	27	26	25	25	24	23	21	21
2.2	22	22	22	22	24	24	25	26	27	28	28	28	28	28	29	29	30	30	30	30	29	29	29	29	29	29	28	28	27	26	26	25	24	23	21	21
2.3	21	21	22	22	23	24	26	26	27	28	28	29	29	29	28	29	30	30	30	30	29	28	29	29	29	29	28	28	27	26	25	24	24	23	21	21
2.4	21	21	22	22	24	25	25	26	27	28	28	29	29	29	29	29	30	30	30	30	18	29	30	30	29	29	29	28	27	26	26	25	24	23	21	20
2.5	21	21	22	22	24	25	26	27	28	28	29	29	29	29	29	29	30	30	30	30	18	29	30	30	29	29	28	28	27	27	26	25	24	23	21	20
2.6	21	21	22	22	24	25	26	27	28	28	29	29	29	29	29	29	30	30	30	30	18	29	30	30	29	29	29	28	27	27	26	25	24	23	21	20
2.7	21	21	21	22	24	25	26	27	28	29	29	29	29	29	29	29	30	30	30	30	18	29	30	30	30	29	29	28	28	27	26	25	24	23	21	20
2.8	21	21	21	22	24	25	26	27	28	29	29	30	30	29	29	29	30	30	30	30	18	29	30	30	30	30	29	29	28	27	26	25	24	23	21	20
2.9	20	21	21	22	24	25	26	28	28	29	30	30	30	30	29	27	30	30	30	18	18	30	30	30	30	29	29	28	28	27	26	25	24	23	21	20
3	20	20	21	22	24	25	27	28	29	29	30	30	30	30	29	26	22	30	30	18	18	30	30	30	30	30	29	29	28	27	26	25	24	23	21	20
3.1	20	20	21	23	24	26	27	28	29	29	30	30	30	30	29	27	22	30	30	18	18	29	30	30	30	30	30	29	28	28	26	25	24	23	21	20
3.2	20	20	21	22	24	25	27	28	29	30	30	30	30	30	29	25	21	30	30	18	18	20	30	30	30	30	30	30	29	28	26	26	24	23	21	19
3.3	20	20	21	23	24	26	27	28	30	30	30	30	30	30	29	24	21	20	30	18	18	20	30	30	30	30	30	30	29	28	27	25	24	23	21	19
3.4	20	20	21	23	24	26	27	29	30	30	30	30	30	30	29	24	22	20	30	18	18	20	30	30	30	30	30	30	29	28	27	25	24	23	21	19
3.5	20	20	21	23	24	26	28	29	30	30	30	30	30	30	29	24	21	20	30	18	18	21	30	30	30	30	30	30	30	29	27	26	24	23	21	19
3.6	20	20	21	23	25	26	28	29	30	30	30	30	30	30	29	24	21	20	19	18	18	21	30	30	30	30	30	30	30	29	27	26	24	23	21	19
3.7	19	20	21	23	25	26	28	29	30	30	30	30	30	30	30	24	21	20	19	18	18	22	30	30	30	30	30	30	30	29	28	26	24	23	21	19
3.8	19	19	21	23	25	27	28	30	30	30	30	30	30	30	30	25	21	20	19	18	18	21	30	30	30	30	30	30	30	29	28	26	24	23	21	19
3.9	19	20	21	23	25	27	29	30	30	30	30	30	30	30	30	24	21	20	19	18	18	22	30	30	30	30	30	30	30	29	28	26	25	23	21	19
4	19	19	21	23	25	27	29	30	30	30	30	30	30	30	30	24	21	20	19	18	18	23	30	30	30	30	30	30	30	30	28	27	25	23	21	19

Table A.12: Swath width of the wind displaced transverse spread pattern to achieve a CV of 15% for DAP (with 11 duct Transland spreader).

	Corrected Wind Angle (°)																																				
Wind Speed (m/s)	**0**	**10**	**20**	**30**	**40**	**50**	**60**	**70**	**80**	**90**	**100**	**110**	**120**	**130**	**140**	**150**	**160**	**170**	**180**	**190**	**200**	**210**	**220**	**230**	**240**	**250**	**260**	**270**	**280**	**290**	**300**	**310**	**320**	**330**	**340**	**350**
0	-1	-1	-1	-1	-1	-1	-1	-1	-1	-1	-1	-1	-1	-1	-1	-1	-1	-1	-1	-1	-1	-1	-1	-1	-1	-1	-1	-1	-1	-1	-1	-1	-1	-1	-1	-1
0.1	-1	-1	-1	-2	-2	-2	-3	-3	-3	-3	-3	-3	-3	-2	-2	-2	-2	-1	-1	0	0	1	1	1	2	2	2	2	2	2	2	1	1	1	0	0
0.2	-1	-2	-2	-3	-3	-4	-4	-5	-5	-5	-5	-5	-4	-4	-3	-3	-2	-2	-1	0	1	2	2	3	3	4	4	4	4	4	3	3	2	2	1	0
0.3	-1	-2	-3	-4	-5	-5	-6	-6	-7	-7	-7	-6	-6	-5	-5	-4	-3	-2	-1	1	2	3	4	4	5	5	6	6	6	5	5	4	4	3	2	1
0.4	-1	-2	-4	-5	-6	-7	-7	-8	-8	-8	-8	-8	-8	-7	-6	-5	-4	-2	-1	1	3	4	5	6	7	7	7	8	8	7	7	6	5	4	3	1
0.5	-1	-3	-4	-6	-7	-8	-9	-10	-10	-10	-10	-10	-9	-8	-7	-6	-4	-3	-1	2	3	5	6	7	8	9	9	9	9	9	8	7	6	5	3	2
0.6	-1	-3	-5	-7	-8	-10	-11	-12	-12	-12	-12	-11	-11	-10	-8	-7	-5	-3	-1	2	4	6	7	9	10	11	11	11	11	10	10	9	7	6	4	2
0.7	-1	-3	-5	-8	-9	-11	-12	-13	-14	-14	-14	-13	-12	-11	-9	-8	-5	-3	-1	2	5	7	8	10	11	12	13	13	13	12	11	10	8	7	5	2
0.8	-1	-4	-6	-9	-11	-12	-14	-15	-16	-16	-16	-15	-14	-12	-11	-8	-6	-4	-1	3	5	8	10	11	13	14	14	15	15	14	13	12	10	8	5	3
0.9	-1	-4	-7	-9	-12	-14	-15	-17	-17	-18	-18	-17	-16	-14	-12	-9	-7	-4	-1	3	6	9	11	13	14	15	16	16	16	15	15	13	11	8	6	3
1	-1	-4	-7	-10	-13	-15	-17	-19	-19	-20	-19	-19	-17	-15	-13	-10	-7	-4	-1	3	6	9	12	14	16	17	18	18	17	17	16	14	12	9	7	3
1.1	-1	-5	-8	-11	-14	-17	-19	-20	-21	-21	-21	-20	-19	-16	-14	-11	-8	-5	-1	4	7	10	13	16	17	19	19	20	20	19	17	15	13	10	7	4
1.2	-1	-5	-9	-12	-16	-18	-20	-22	-23	-23	-23	-21	-21	-18	-15	-12	-9	-5	-1	4	8	11	14	17	19	20	21	21	21	20	19	17	14	11	8	4
1.3	-1	-5	-9	-13	-17	-20	-22	-24	-24	-25	-24	-24	-21	-20	-16	-13	-9	-5	-1	4	8	12	15	17	19	21	23	23	23	22	21	18	15	12	8	4
1.4	-1	-6	-10	-14	-18	-21	-23	-25	-27	-27	-27	-26	-24	-21	-18	-14	-10	-6	-1	5	9	13	16	19	21	23	25	25	24	24	22	20	16	13	9	5
1.5	-1	-6	-11	-15	-19	-22	-25	-27	-28	-29	-29	-27	-25	-22	-20	-15	-11	-6	-1	5	10	14	18	21	22	26	26	26	26	25	24	21	17	14	10	5
1.6	-1	-6	-11	-16	-20	-23	-27	-30	-30	-31	-30	-28	-26	-24	-20	-16	-11	-6	-1	5	10	15	18	21	25	27	28	29	29	27	25	22	19	15	10	5
1.7	-1	-7	-12	-17	-21	-25	-28	-31	-32	-32	-32	-30	-28	-24	-21	-17	-12	-7	-1	6	11	15	19	23	26	27	30	30	30	29	26	23	20	15	11	6
1.8	-1	-7	-12	-18	-23	-27	-31	-32	-34	-34	-34	-32	-29	-27	-22	-17	-13	-7	-1	6	11	16	21	23	27	30	31	33	32	30	28	25	21	17	11	6
1.9	-1	-7	-13	-19	-23	-28	-32	-33	-35	-36	-34	-33	-31	-28	-23	-19	-13	-7	-1	6	12	17	22	24	29	32	35	32	34	33	29	27	22	17	12	6
2	-1	-7	-14	-20	-25	-29	-32	-36	-37	-38	-37	-35	-32	-29	-24	-19	-14	-8	-1	7	13	18	22	25	30	34	34	36	35	35	32	29	24	18	13	7
2.1	-1	-8	-15	-21	-26	-30	-35	-37	-38	-39	-37	-36	-34	-29	-25	-20	-14	-8	-1	7	13	19	23	27	32	35	37	38	38	36	33	30	24	19	13	7
2.2	-1	-8	-15	-22	-27	-32	-37	-40	-41	-41	-42	-38	-36	-32	-27	-21	-15	-8	-1	7	14	19	25	30	35	36	40	41	41	38	35	30	26	20	14	7
2.3	-1	-8	-16	-22	-28	-34	-38	-41	-42	-44	-42	-41	-38	-32	-28	-22	-16	-8	-1	8	14	20	25	30	35	38	41	42	41	39	38	32	27	21	14	8
2.4	-1	-9	-16	-24	-29	-35	-41	-42	-43	-45	-44	-41	-38	-33	-29	-23	-16	-9	-1	8	15	21	25	30	37	41	43	45	44	42	39	35	27	22	15	8
2.5	-1	-9	-17	-24	-31	-38	-41	-45	-47	-47	-46	-45	-38	-35	-28	-24	-17	-9	-1	8	15	21	27	32	39	44	44	46	45	42	40	36	29	23	16	8
2.6	-1	-10	-18	-25	-32	-38	-42	-46	-47	-49	-47	-46	-41	-35	-31	-25	-17	-9	-1	8	16	21	28	33	40	46	48	48	48	45	43	36	31	24	16	8
2.7	-1	-10	-18	-26	-33	-39	-46	-47	-50	-51	-50	-46	-43	-38	-30	-25	-18	-10	-1	9	16	21	28	37	42	46	49	51	51	48	44	39	33	25	17	9
2.8	-1	-10	-19	-27	-34	-43	-46	-50	-51	-52	-52	-50	-45	-38	-33	-23	-18	-10	-1	9	17	22	31	36	45	46	53	52	53	51	46	40	33	26	18	9
2.9	-1	-10	-20	-28	-35	-44	-48	-52	-54	-55	-54	-50	-46	-42	-34	-24	-19	-10	-1	9	18	23	31	39	44	51	53	54	54	51	48	43	34	27	18	9
3	-1	-11	-20	-30	-36	-45	-51	-53	-57	-57	-56	-52	-48	-42	-33	-28	-19	-11	-1	10	18	24	32	41	47	52	54	56	56	53	48	43	37	28	19	10
3.1	-1	-11	-21	-29	-39	-46	-52	-57	-58	-58	-56	-53	-50	-43	-37	-29	-20	-11	-3	10	17	25	33	42	49	55	58	59	57	55	51	46	37	29	19	10
3.2	-1	-11	-22	-32	-40	-48	-54	-57	-60	-61	-58	-56	-51	-44	-37	-29	-21	-11	-3	10	18	27	34	42	52	56	57	61	58	57	53	47	39	29	20	10
3.3	-1	-12	-22	-32	-41	-48	-54	-58	-62	-64	-60	-56	-51	-45	-37	-29	-21	-12	-5	11	17	27	36	46	52	59	60	60	61	58	54	49	41	31	21	11
3.4	-1	-12	-23	-33	-42	-49	-57	-62	-63	-64	-63	-57	-54	-46	-38	-29	-21	-12	-4	11	18	27	38	45	53	57	60	62	62	60	54	49	42	31	22	11
3.5	-1	-12	-23	-34	-44	-53	-59	-62	-64	-66	-64	-61	-54	-48	-38	-32	-20	-12	-5	11	18	28	38	49	55	61	62	65	64	62	58	51	42	33	22	11
3.6	-1	-13	-24	-34	-44	-54	-60	-65	-67	-68	-65	-65	-58	-51	-42	-32	-19	-6	-5	5	19	28	38	48	56	64	65	66	67	63	60	52	44	34	22	11
3.7	-1	-13	-25	-35	-47	-56	-62	-65	-69	-73	-67	-64	-59	-53	-41	-32	-19	-13	-6	5	19	28	41	51	58	64	69	69	70	65	60	54	46	34	23	12
3.8	-1	-13	-26	-37	-47	-56	-63	-68	-73	-72	-71	-66	-62	-52	-42	-35	-20	-13	9	6	19	29	42	51	61	67	69	72	70	67	62	55	45	37	24	12
3.9	-1	-14	-26	-37	-48	-58	-65	-70	-74	-73	-71	-68	-62	-53	-44	-34	-20	-6	9	6	19	30	41	54	61	66	70	71	71	69	63	57	47	37	25	13
4	-1	-14	-27	-39	-49	-60	-67	-72	-74	-76	-74	-69	-66	-56	-44	-35	-20	-6	9	6	21	33	43	56	63	71	74	74	73	69	67	59	49	37	25	13

Table A.13: Peak mass transverse displacement look up table for urea (with 11 duct Transland spreader).

	Corrected Wind Angle (°)																																				
Wind Speed (m/s)	0	10	20	30	40	50	60	70	80	90	100	110	120	130	140	150	160	170	180	190	200	210	220	230	240	250	260	270	280	290	300	310	320	330	340	350
0	21	21	21	21	21	21	21	21	21	21	21	21	21	21	21	21	21	21	21	21	21	21	21	21	21	21	21	21	21	21	21	21	21	21	21	21
0.1	21	21	21	21	21	21	21	21	21	21	21	21	21	21	21	21	21	21	21	21	21	21	21	21	21	21	21	21	21	21	21	21	21	21	21	21
0.2	20	21	20	20	20	21	21	21	21	21	21	21	21	21	21	21	21	22	22	21	21	21	21	21	21	21	21	20	20	20	20	20	20	20	20	20
0.3	20	20	20	20	20	20	20	20	21	21	21	21	21	21	21	21	22	22	22	22	21	21	21	20	20	20	20	20	20	20	20	20	20	20	20	20
0.4	20	20	20	20	20	20	20	21	21	21	21	21	21	21	21	22	22	22	22	22	22	21	21	20	20	20	20	20	20	20	20	20	19	20	20	20
0.5	20	20	20	20	20	20	20	20	21	21	21	21	21	21	22	22	22	22	22	22	21	21	21	21	21	20	20	20	20	20	19	19	19	19	20	20
0.6	20	20	19	20	20	20	20	21	21	21	21	21	21	22	22	22	22	22	22	22	22	21	21	21	21	21	21	21	20	20	20	19	19	19	19	19
0.7	19	19	19	20	20	20	20	21	21	21	21	22	22	22	22	22	22	23	23	22	22	21	21	21	21	21	21	21	21	21	20	20	19	19	19	19
0.8	19	19	19	20	20	20	20	21	21	21	22	22	22	22	22	22	23	23	23	23	22	22	22	22	22	22	22	21	21	21	20	20	19	19	18	19
0.9	19	19	19	19	20	20	20	21	21	21	22	22	22	22	23	23	23	23	23	23	22	22	22	22	22	22	22	22	21	21	21	20	19	19	18	19
1	19	19	19	19	20	20	21	21	21	22	22	22	22	23	23	23	23	23	23	23	22	22	22	22	23	22	22	22	22	21	21	20	20	19	18	18
1.1	19	19	19	19	20	20	21	21	22	22	22	23	23	23	23	23	23	24	24	23	22	22	23	23	23	23	23	22	22	21	21	20	20	19	18	18
1.2	19	18	19	19	20	20	21	21	22	22	22	23	23	23	23	23	23	24	24	23	22	23	23	23	23	23	23	23	22	22	21	20	20	19	18	18
1.3	18	18	19	19	20	20	21	22	22	22	23	23	23	23	23	23	24	24	24	23	23	23	23	24	24	23	23	23	22	22	21	21	20	19	18	18
1.4	18	18	18	19	20	20	21	22	22	23	23	23	24	23	24	24	24	24	25	24	23	23	24	24	24	24	23	23	23	22	21	21	20	19	18	18
1.5	18	18	18	19	20	21	21	22	23	23	23	24	24	24	24	24	24	25	25	24	23	24	24	24	24	24	24	23	23	22	22	21	20	19	18	17
1.6	18	18	18	19	20	21	21	22	23	23	24	24	24	24	24	24	25	25	25	24	24	24	24	24	24	24	24	23	23	22	22	21	20	19	18	17
1.7	18	18	18	19	20	21	21	22	23	23	24	24	24	24	24	24	25	25	26	24	24	24	25	25	24	24	24	24	23	23	22	21	20	19	18	17
1.8	18	18	18	19	20	21	22	23	23	24	24	24	24	24	25	25	25	25	26	25	24	25	25	25	25	24	24	24	23	23	22	21	20	19	18	17
1.9	17	17	18	19	20	21	22	23	24	24	24	25	25	25	25	25	25	26	26	25	25	25	25	25	25	25	24	24	23	23	22	21	20	19	18	17
2	17	17	18	19	20	21	22	23	24	24	25	25	25	25	25	25	25	26	26	25	25	25	26	25	25	25	25	24	24	23	22	21	20	19	18	17
2.1	17	17	18	19	20	21	22	23	24	25	25	26	25	25	25	25	26	26	27	25	25	26	26	26	26	25	25	24	24	23	22	21	20	19	18	17
2.2	17	17	18	19	20	21	23	24	24	25	26	26	26	26	25	26	26	27	27	25	25	26	26	26	26	26	26	25	24	23	23	22	21	19	18	17
2.3	17	17	18	19	21	22	23	24	25	26	26	26	26	26	26	26	26	27	28	25	26	26	26	26	26	26	26	25	25	24	23	22	20	19	18	16
2.4	17	17	18	19	21	22	23	24	25	25	26	26	26	26	26	26	26	27	28	26	26	26	26	26	26	26	26	25	24	24	23	22	21	19	18	16
2.5	17	17	18	19	21	22	23	25	25	26	26	27	26	27	26	26	26	27	28	26	26	27	27	27	27	26	26	26	25	24	23	22	21	19	18	17
2.6	16	17	18	19	21	22	24	25	26	26	27	27	27	27	26	26	27	28	29	26	26	27	27	27	27	27	27	26	25	24	23	22	21	19	18	16
2.7	16	17	18	19	21	22	24	25	26	26	27	27	27	27	27	26	27	28	29	27	26	27	27	27	27	27	27	26	25	25	23	22	21	20	18	16
2.8	16	17	18	19	21	22	24	25	26	27	27	27	28	27	27	26	27	28	29	27	26	27	27	27	27	27	27	27	26	25	24	23	21	19	18	16
2.9	16	16	18	20	21	23	24	25	27	27	28	28	28	27	27	26	27	29	30	27	27	27	28	28	27	27	28	27	26	25	24	23	21	20	18	16
3	16	16	18	20	21	23	25	26	27	28	28	28	28	28	27	27	27	29	30	16	27	28	28	28	28	28	28	27	26	26	24	23	21	20	18	16
3.1	16	16	18	20	21	23	25	27	27	28	28	29	28	28	28	27	27	29	30	16	26	28	28	28	28	28	28	27	27	26	25	23	21	20	18	16
3.2	16	16	18	20	22	24	25	27	28	28	28	29	29	28	28	27	27	29	30	16	26	28	28	28	28	29	28	28	27	26	25	23	22	20	18	16
3.3	16	16	18	20	22	23	25	27	28	29	29	29	29	28	28	27	21	29	30	16	17	28	28	29	29	29	29	28	27	27	25	23	22	20	18	16
3.4	15	16	18	20	22	24	26	27	29	29	30	29	29	29	28	27	20	30	30	16	17	28	28	29	29	29	29	29	28	26	25	23	22	20	18	16
3.5	15	16	18	20	22	24	26	28	28	30	30	30	29	29	28	27	21	30	30	16	17	28	29	29	29	29	29	29	28	27	25	24	22	20	18	16
3.6	15	16	18	20	22	25	26	28	29	30	30	30	30	29	29	27	20	30	30	16	17	28	29	29	29	29	29	30	29	28	26	24	22	20	18	16
3.7	15	16	18	20	22	25	27	28	29	30	30	30	30	30	29	27	20	30	30	16	17	28	29	30	29	30	30	30	29	28	26	24	22	20	18	16
3.8	15	16	18	20	23	25	26	29	30	30	30	30	30	29	28	27	20	30	30	16	17	28	29	29	30	30	30	30	30	29	27	24	22	20	18	16
3.9	15	16	18	20	23	25	27	29	30	30	30	30	30	29	29	27	20	30	30	16	17	28	29	30	30	30	30	30	30	28	27	25	23	20	18	16
4	15	16	18	21	23	25	28	30	30	30	30	30	30	30	29	27	19	18	30	16	17	29	29	29	30	30	30	30	30	30	27	25	23	20	18	16

Table A.14: Swath width of the wind displaced transverse spread pattern to achieve a CV of 15% for urea (with 11 duct Transland spreader).

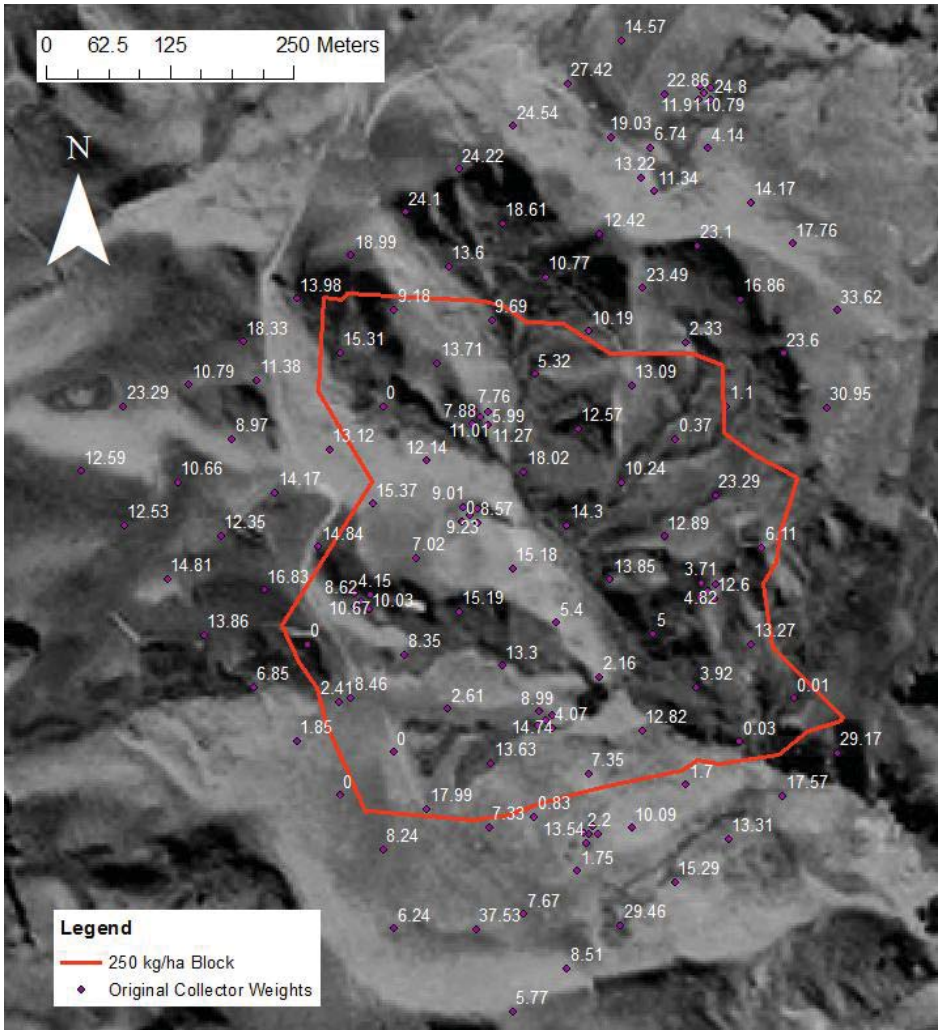


Figure A.1: Collected masses (in grams) from Trial 4 (uncorrected).

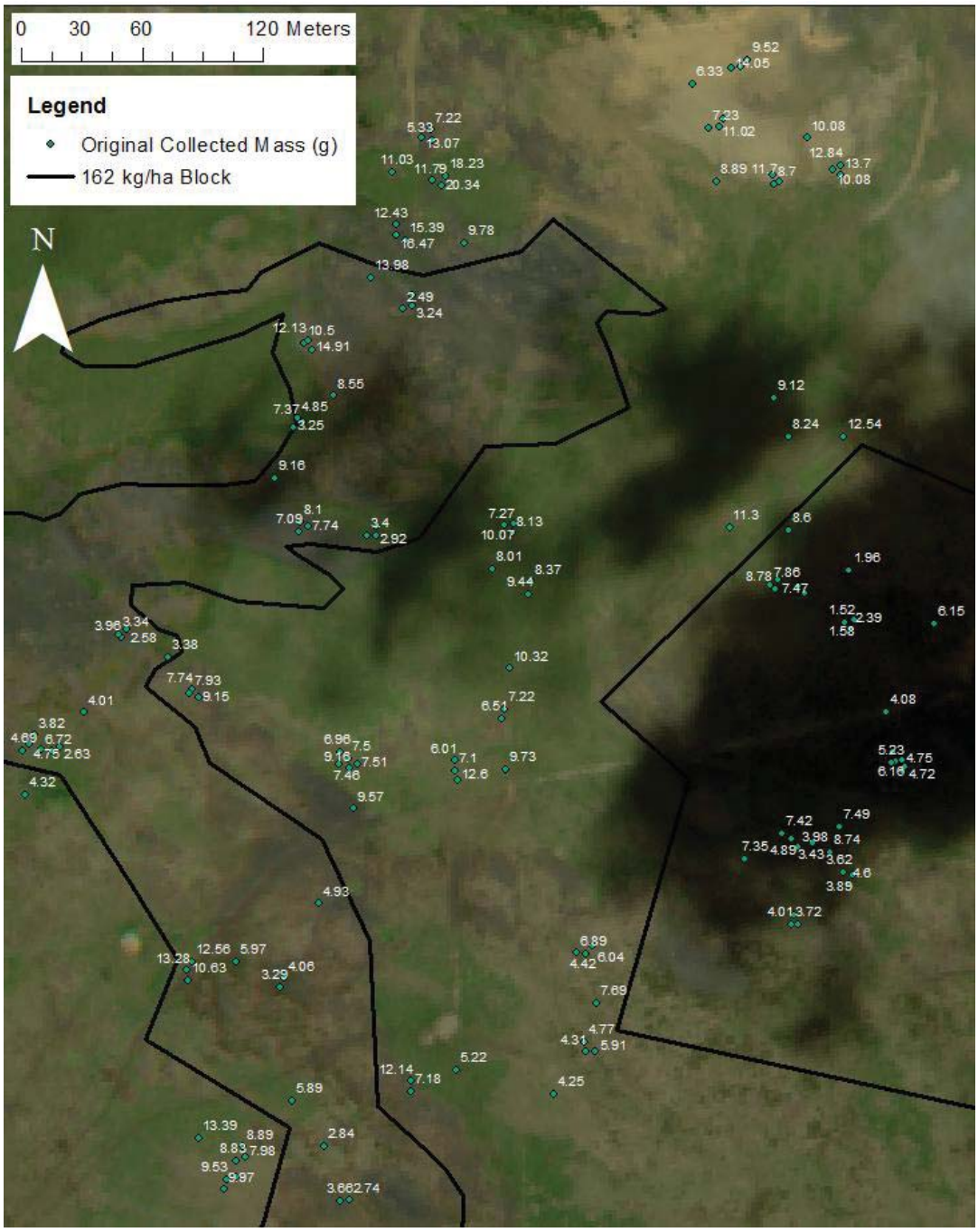


Figure A.2: Collected masses (in grams) from Trial 5 (uncorrected).

Table A.15: Raw and adjusted data for Trial 6 Objective 1 for Urea Area 1.

Flight	1				**Fert/Area**	Urea/1
Collector	**Distance (m)**	**R1 (g)**	**R2 (g)**	**R3 (g)**	**Average (g)**	**Bounce Adjusted (g)**
1	-22	0	0	0	0	0
2	-16	0	0	0	0	0
3	-10	0	0	0	0	0
4	-4	1.14	1.26	1.45	1.283	1.525
5	2	6.8	9.1	8.34	8.080	9.599
6	8	7.13	9.57	9.63	8.777	10.427
7	14	4.33	4.69	4.94	4.653	5.528
8	20	0.98	1.02	1.18	1.060	1.259
9	26	0.12	0.15	0.19	0.153	0.182

Flight	2				**Fert/Area**	Urea/1
Collector	**Distance (m)**	**R1 (g)**	**R2 (g)**	**R3 (g)**	**Average (g)**	**Bounce Adjusted (g)**
1	-21	0	0	0	0	0
2	-15	0	0	0	0	0
3	-9	0	0	0	0	0
4	-3	0.29	0.25	0.11	0.217	0.257
5	3	2.74	2.45	2.77	2.653	3.152
6	9	3.26	3.96	3.72	3.647	4.332
7	15	4.2	4.14	3.29	3.877	4.606
8	21	2.23	2.42	1.79	2.147	2.550
9	27	0.86	0.78	0.75	0.797	0.946

Flight	3				**Fert/Area**	Urea/1
Collector	**Distance (m)**	**R1 (g)**	**R2 (g)**	**R3 (g)**	**Average (g)**	**Bounce Adjusted (g)**
1	-24	0	0	0	0	0
2	-18	0	0	0	0	0
3	-12	0	0	0	0	0
4	-6	1.21	0.5	1.53	1.080	1.283
5	0	3.13	3.63	3.43	3.397	4.035
6	6	3.1	4.11	4.53	3.913	4.649
7	12	1.75	2.16	2.94	2.283	2.713
8	18	0.7	0.86	1.13	0.897	1.065
9	24	0.45	0.21	0.35	0.337	0.400

Flight	4				Fert/Area	Urea/1
Collector	**Distance (m)**	**R1 (g)**	**R2 (g)**	**R3 (g)**	**Average (g)**	**Bounce Adjusted (g)**
1	-24	0	0	0	0	0
2	-18	0	0	0	0	0
3	-12	0	0.15	0.04	0.063	0.075
4	-6	1.48	1.43	1.96	1.623	1.929
5	0	2.88	3.93	4.97	3.927	4.665
6	6	3.94	4.12	4.56	4.207	4.998
7	12	3.25	2.71	2.6	2.853	3.390
8	18	1.71	1.31	1.05	1.357	1.612
9	24	0.68	0.52	0.49	0.563	0.669

Table A.16: Raw and adjusted data for Trial 6 Objective 1 for DAP Area 1.

Flight	1				Fert/Area	DAP/1
Collector	**Distance (m)**	**R1 (g)**	**R2 (g)**	**R3 (g)**	**Average (g)**	**Bounce Adjusted (g)**
1	-24	0	0	0	0	0
2	-18	0	0	0	0	0
3	-12	0	0	0	0	0
4	-6	0	0	0.3	0.100	0.154
5	0	2.42	3.14	4.62	3.393	5.222
6	6	10.02	12.62	12.9	11.847	18.230
7	12	9.63	10.64	9.01	9.760	15.019
8	18	3.76	3.16	2.4	3.107	4.781
9	24	1.24	0.57	0.36	0.723	1.113

Flight	2				Fert/Area	DAP/1
Collector	**Distance (m)**	**R1 (g)**	**R2 (g)**	**R3 (g)**	**Average (g)**	**Bounce Adjusted (g)**
1	-24	0	0	0	0	0
2	-18	0	0	0	0	0
3	-12	0	0	0	0	0
4	-6	0.16	0	0.09	0.083	0.128
5	0	2.42	1.66	1.34	1.807	2.780
6	6	3.13	3.38	3.46	3.323	5.114
7	12	3.04	3.6	2.96	3.200	4.924
8	18	2.5	2.39	2.59	2.493	3.837
9	24	1.19	1.03	1.08	1.100	1.693

Flight	3				Fert/Area	DAP/1
Collector	**Distance (m)**	**R1 (g)**	**R2 (g)**	**R3 (g)**	**Average (g)**	**Bounce Adjusted (g)**
1	-21	0	0	0	0	0
2	-15	0	0	0	0	0
3	-9	0.21	0	0.19	0.133	0.205
4	-3	3.15	3.43	3.65	3.410	5.248
5	3	6.5	7.18	7.84	7.173	11.039
6	9	7.36	6.58	8.18	7.373	11.347
7	15	3.32	3.67	3.17	3.387	5.212
8	21	1	0.75	0.72	0.823	1.267
9	27	0.08	0.25	0.17	0.167	0.256

Flight	4				Fert/Area	DAP/1
Collector	**Distance (m)**	**R1 (g)**	**R2 (g)**	**R3 (g)**	**Average (g)**	**Bounce Adjusted (g)**
1	-25	0	0	0	0	0
2	-19	0	0	0	0	0
3	-13	0	0.24	0.02	0.087	0.133
4	-7	1.11	2.21	4.56	2.627	4.042
5	-1	5.3	7.5	13.7	8.833	13.593
6	5	6.35	8.48	13.14	9.323	14.347
7	11	4.01	4.06	4.62	4.230	6.509
8	17	1.76	1.21	1.07	1.347	2.072
9	23	0.32	0.29	0.26	0.290	0.446

Table A.17: Raw and adjusted data for Trial 6 Objective 1 for Superphosphate Area 1.

Flight	1				Fert/Area	Super/1
Collector	**Distance (m)**	**R1 (g)**	**R2 (g)**	**R3 (g)**	**Average (g)**	**Bounce Adjusted (g)**
1	-24	0	0	0	0	0
2	-18	0	0	0	0	0
3	-12	0	0	0	0	0
4	-6	0	0	0	0	0
5	0	0.52	1.23	1.13	0.960	1.325
6	6	9.55	15.56	14.17	13.093	18.069
7	12	8.51	8.65	7.68	8.280	11.426
8	18	1.14	1.53	1.09	1.253	1.730
9	24	0.15	0.28	0.05	0.160	0.221

Flight 2 **Fert/Area** Super/1

Collector	Distance (m)	R1 (g)	R2 (g)	R3 (g)	Average (g)	Bounce Adjusted (g)
1	-24	0	0	0	0	0
2	-18	0	0	0	0	0
3	-12	0	0	0	0	0
4	-6	0	0	0	0	0
5	0	6.81	6.26	4.16	5.743	7.926
6	6	14.72	18.05	19.72	17.497	24.145
7	12	6.32	6.66	8.96	7.313	10.092
8	18	1.57	2.21	2.75	2.177	3.004
9	24	0.65	0.66	0.57	0.627	0.865

Flight 3 **Fert/Area** Super/1

Collector	Distance (m)	R1 (g)	R2 (g)	R3 (g)	Average (g)	Bounce Adjusted (g)
1	-24	0	0	0	0	0
2	-18	0	0	0	0	0
3	-12	0	0	0	0	0
4	-6	0	0	0.11	0.037	0.051
5	0	3.48	7.11	9.01	6.533	9.016
6	6	20.94	23.81	31.14	25.297	34.909
7	12	6.08	6.13	6.38	6.197	8.551
8	18	1.48	0.92	1.31	1.237	1.707
9	24	0.33	0.24	0.3	0.290	0.400

Flight 4 **Fert/Area** Super/1

Collector	Distance (m)	R1 (g)	R2 (g)	R3 (g)	Average (g)	Bounce Adjusted (g)
1	-24	0	0	0	0	0
2	-18	0	0	0	0	0
3	-12	0	0	0	0	0
4	-6	0	0.03	0	0.010	0.014
5	0	2.98	6.2	6.81	5.330	7.355
6	6	19.85	28.41	29.97	26.077	35.986
7	12	7.38	8.57	6.28	7.410	10.226
8	18	1.88	1.3	1.47	1.550	2.139
9	24	0.52	0.39	0.37	0.427	0.589

Table A.18: Raw and adjusted data for Trial 6 Objective 1 for Urea Area 2.

Flight	1				**Fert/Area**	Urea/2
Collector	**Distance (m)**	**R1 (g)**	**R2 (g)**	**R3 (g)**	**Average (g)**	**Bounce Adjusted (g)**
1	18	0	0	0	0	0
2	12	0	0	0	0	0
3	6	0	0	0	0	0
4	0	0.11	0.1	0.25	0.153	0.182
5	-6	1.8	2.55	2.63	2.327	2.764
6	-12	3.04	4.35	3.89	3.760	4.467
7	-18	4.72	5.59	5.67	5.327	6.328
8	-24	3.92	3.53	2.98	3.477	4.130
9	-30	2.2	1.64	1.49	1.777	2.111

Flight	2				**Fert/Area**	Urea/2
Collector	**Distance (m)**	**R1 (g)**	**R2 (g)**	**R3 (g)**	**Average (g)**	**Bounce Adjusted (g)**
1	24	0	0	0	0	0
2	18	0	0	0	0	0
3	12	0	0	0	0	0
4	6	0.04	0	0	0.013	0.016
5	0	1.63	1.39	2.51	1.843	2.190
6	-6	3.48	3.64	3.13	3.417	4.059
7	-12	3.6	4.63	4.91	4.380	5.204
8	-18	3.04	3.37	3.81	3.407	4.047
9	-24	1.47	1.39	1.58	1.480	1.758

Flight	3				**Fert/Area**	Urea/2
Collector	**Distance (m)**	**R1 (g)**	**R2 (g)**	**R3 (g)**	**Average (g)**	**Bounce Adjusted (g)**
1	24	0	0	0	0	0
2	18	0	0	0	0	0
3	12	0	0	0	0	0
4	6	0	0	0	0	0
5	0	0.62	0.95	1	0.857	1.018
6	-6	5.47	5.83	6.79	6.030	7.164
7	-12	9.18	9.25	13.11	10.513	12.490
8	-18	5.9	5.87	9.58	7.117	8.455
9	-24	1.47	2.04	3.48	2.330	2.768

Flight	4				Fert/Area	Urea/2
Collector	**Distance (m)**	**R1 (g)**	**R2 (g)**	**R3 (g)**	**Average (g)**	**Bounce Adjusted (g)**
1	24	0	0	0	0	0
2	18	0	0	0	0	0
3	12	0	0	0	0	0
4	6	0.62	1.11	0.73	0.820	0.974
5	0	6.26	7.34	10.57	8.057	9.572
6	-6	13.5	17.42	15.62	15.513	18.431
7	-12	8.06	7.89	5.89	7.280	8.649
8	-18	1.62	1.92	1.77	1.770	2.103
9	-24	0.21	0.09	0.14	0.147	0.174

Table A.19: Raw and adjusted data for Trial 6 Objective 1 for DAP Area 2.

Flight	1				Fert/Area	DAP/2
Collector	**Distance (m)**	**R1 (g)**	**R2 (g)**	**R3 (g)**	**Average (g)**	**Bounce Adjusted (g)**
1	25	0	0	0	0	0
2	19	0	0	0	0	0
3	13	0.12	0.17	0.07	0.120	0.185
4	7	1.27	1.73	1.88	1.627	2.503
5	1	3.07	2.96	3.31	3.113	4.791
6	-5	4.66	3.83	3.91	4.133	6.361
7	-11	3.62	3.73	3.85	3.733	5.745
8	-17	1.87	1.62	1.31	1.600	2.462
9	-23	0.66	0.41	0.4	0.490	0.754

Flight	2				Fert/Area	DAP/2
Collector	**Distance (m)**	**R1 (g)**	**R2 (g)**	**R3 (g)**	**Average (g)**	**Bounce Adjusted (g)**
1	24	0	0	0	0	0
2	18	0	0	0	0	0
3	12	0	0.07	0	0.023	0.036
4	6	1.75	1.77	1.86	1.793	2.760
5	0	3.45	3.53	3.48	3.487	5.366
6	-6	5.02	5.04	5.24	5.100	7.848
7	-12	4.95	4.29	4.13	4.457	6.858
8	-18	2.02	2.27	2.17	2.153	3.314
9	-24	0.36	0.5	0.5	0.453	0.698

Flight	3				Fert/Area	DAP/2
Collector	**Distance (m)**	**R1 (g)**	**R2 (g)**	**R3 (g)**	**Average (g)**	**Bounce Adjusted (g)**
1	24	0	0	0	0	0
2	18	0	0	0	0	0
3	12	0	0	0	0	0
4	6	0.09	0	0.13	0.073	0.113
5	0	2.47	2.98	5.01	3.487	5.366
6	-6	7.19	8.49	8.99	8.223	12.655
7	-12	8.54	8.86	11.16	9.520	14.650
8	-18	5.75	4.93	4.6	5.093	7.838
9	-24	1.91	1.45	1.28	1.547	2.380

Flight	4				Fert/Area	DAP/2
Collector	**Distance (m)**	**R1 (g)**	**R2 (g)**	**R3 (g)**	**Average (g)**	**Bounce Adjusted (g)**
1	24	0	0	0	0	0
2	18	0	0	0	0	0
3	12	0.0175	0	0.14	0.053	0.081
4	6	1	1.45	1.52	1.323	2.036
5	0	5.5	6.07	7.66	6.410	9.864
6	-6	0	11.6	10.7	7.433	11.439
7	-12	6.83	6.85	8.13	7.270	11.188
8	-18	2.74	2.57	2.89	2.733	4.206
9	-24	0.74	0.35	0.67	0.587	0.903

Table A.20: Raw and adjusted data for Trial 6 Objective 1 for Superphosphate Area 2.

Flight	1				Fert/Area	Super/2
Collector	**Distance (m)**	**R1 (g)**	**R2 (g)**	**R3 (g)**	**Average (g)**	**Bounce Adjusted (g)**
1	24	0	0	0	0	0
2	18	0	0	0	0	0
3	12	0	0	0	0	0
4	6	0	0	0	0	0
5	0	9.09	5.68	8.23	7.667	10.580
6	-6	29.73	25.96	26.49	27.393	37.803
7	-12	17.07	16.14	15.57	16.260	22.439
8	-18	4.71	4.62	4.76	4.697	6.481
9	-24	1.24	1.57	1.04	1.283	1.771

Flight	2				Fert/Area	Super/2
Collector	**Distance (m)**	**R1 (g)**	**R2 (g)**	**R3 (g)**	**Average (g)**	**Bounce Adjusted (g)**
1	24	0	0	0	0	0
2	18	0	0	0	0	0
3	12	0	0	0	0	0
4	6	0	0	0	0	0
5	0	0.93	2.17	1.05	1.383	1.909
6	-6	13.76	11.24	8.52	11.173	15.419
7	-12	8.3	7.43	10.63	8.787	12.126
8	-18	2	2.49	3	2.497	3.445
9	-24	0.36	0.43	0.54	0.443	0.612

Flight	3				Fert/Area	Super/2
Collector	**Distance (m)**	**R1 (g)**	**R2 (g)**	**R3 (g)**	**Average (g)**	**Bounce Adjusted (g)**
1	22.5	0	0	0	0	0
2	16.5	0	0	0	0	0
3	10.5	0	0	0	0	0
4	4.5	0	0	0	0	0
5	-1.5	4.49	1.82	4.17	3.493	4.821
6	-7.5	22.78	21.05	18.74	20.857	28.782
7	-13.5	12.48	8.08	9.74	10.100	13.938
8	-19.5	3.35	3.02	3.19	3.187	4.398
9	-25.5	1.11	0.62	0.84	0.857	1.182

Flight	4				Fert/Area	Super/2
Collector	**Distance (m)**	**R1 (g)**	**R2 (g)**	**R3 (g)**	**Average (g)**	**Bounce Adjusted (g)**
1	24	0	0	0	0	0
2	18	0	0	0	0	0
3	12	0	0	0	0	0
4	6	0	0	0	0	0
5	0	2.71	5.75	5.1	4.520	6.238
6	-6	28.09	28.86	32.29	29.747	41.050
7	-12	12.21	11.59	10.35	11.383	15.709
8	-18	2.29	3.3	2.27	2.620	3.616
9	-24	0.48	0.85	0.44	0.590	0.814

Table A.21: Raw and adjusted data for Trial 6 Objective 1 for Urea Area 3.

Flight	1				**Fert/Area**	Urea/3
Collector	**Distance (m)**	**R1 (g)**	**R2 (g)**	**R3 (g)**	**Average (g)**	**Bounce Adjusted (g)**
1	-21	0	0	0	0	0
2	-15	0	0	0	0	0
3	-9	0	0	0	0	0
4	-3	0.25	0.3	0.93	0.493	0.586
5	3	10.19	7.88	11.18	9.750	11.583
6	9	20.32	15.95	21.35	19.207	22.818
7	15	9.2	11.27	11.37	10.613	12.609
8	21	1.53	1.81	2.27	1.870	2.222
9	27	0.22	0.14	0.18	0.180	0.214

Flight	2				**Fert/Area**	Urea/3
Collector	**Distance (m)**	**R1 (g)**	**R2 (g)**	**R3 (g)**	**Average (g)**	**Bounce Adjusted (g)**
1	-24	0	0	0	0	0
2	-18	0	0	0	0	0
3	-12	0	0	0	0	0
4	-6	0.04	0.07	0.15	0.087	0.103
5	0	3.05	2.73	2.88	2.887	3.429
6	6	5.47	5.23	4.44	5.047	5.996
7	12	6.39	6.23	4.69	5.770	6.855
8	18	2.91	2.39	1.98	2.427	2.883
9	24	0.65	0.64	0.54	0.610	0.725

Flight	3				**Fert/Area**	Urea/3
Collector	**Distance (m)**	**R1 (g)**	**R2 (g)**	**R3 (g)**	**Average (g)**	**Bounce Adjusted (g)**
1	-24	0	0	0	0	0
2	-18	0	0	0	0	0
3	-12	0	0	0	0	0
4	-6	0	0.1	0.08	0.060	0.071
5	0	4.21	4.07	5.1	4.460	5.299
6	6	22.42	25.47	34.47	27.453	32.616
7	12	17.26	21.09	27.71	22.020	26.161
8	18	2.72	3.87	5.44	4.010	4.764
9	24	0.48	0.37	0.57	0.473	0.562

Flight	4				Fert/Area	Urea/3
Collector	**Distance (m)**	**R1 (g)**	**R2 (g)**	**R3 (g)**	**Average (g)**	**Bounce Adjusted (g)**
1	-24	0	0	0	0	0
2	-18	0	0	0	0	0
3	-12	0	0	0	0	0
4	-6	0.48	0.8	0.69	0.657	0.780
5	0	3.15	4.2	4.58	3.977	4.724
6	6	5.83	6.6	6.98	6.470	7.687
7	12	4.5	6.87	7.6	6.323	7.512
8	18	1.96	2.53	2.94	2.477	2.942
9	24	0.72	0.53	0.94	0.730	0.867

Table A.22: Raw and adjusted data for Trial 6 Objective 1 for DAP Area 3.

Flight	1				Fert/Area	DAP/3
Collector	**Distance (m)**	**R1 (g)**	**R2 (g)**	**R3 (g)**	**Average (g)**	**Bounce Adjusted (g)**
1	-24	0	0	0	0	0
2	-18	0	0	0	0	0
3	-12	0	0.05	0.07	0.040	0.062
4	-6	0.71	1.52	2.6	1.610	2.478
5	0	17.92	13.38	17.34	16.213	24.950
6	6	19.38	22.04	19.35	20.257	31.172
7	12	2.67	5.04	4.32	4.010	6.171
8	18	0.28	0.66	0.52	0.487	0.749
9	24	0	0.02	0.06	0.027	0.041

Flight	2				Fert/Area	DAP/3
Collector	**Distance (m)**	**R1 (g)**	**R2 (g)**	**R3 (g)**	**Average (g)**	**Bounce Adjusted (g)**
1	-24	0	0	0	0	0
2	-18	0	0	0	0	0
3	-12	0	0	0	0	0
4	-6	0	0	0	0	0
5	0	0.88	0.03	0.34	0.417	0.641
6	6	9.15	7.96	7.16	8.090	12.449
7	12	13.16	11.12	13.17	12.483	19.210
8	18	6.63	7.94	10.1	8.223	12.655
9	24	2.13	1.47	2	1.867	2.873

Flight	3				Fert/Area	DAP/3
Collector	**Distance (m)**	**R1 (g)**	**R2 (g)**	**R3 (g)**	**Average (g)**	**Bounce Adjusted (g)**
1	-24	0	0	0	0	0
2	-18	0	0	0	0	0
3	-12	0	0	0.05	0.017	0.026
4	-6	0.17	0.34	0.68	0.397	0.610
5	0	3.81	6.12	9.99	6.640	10.218
6	6	15.84	21.73	19.9	19.157	29.480
7	12	15.47	16.54	14.72	15.577	23.970
8	18	3.67	2.96	2.6	3.077	4.735
9	24	0.57	0.17	0.18	0.307	0.472

Flight	4				Fert/Area	DAP/3
Collector	**Distance (m)**	**R1 (g)**	**R2 (g)**	**R3 (g)**	**Average (g)**	**Bounce Adjusted (g)**
1	-24	0	0	0	0	0
2	-18	0	0	0	0	0
3	-12	0	0	0	0	0
4	-6	1.48	0.18	0.41	0.690	1.062
5	0	11.03	7.02	9.53	9.193	14.147
6	6	18.01	16.19	23.04	19.080	29.362
7	12	8.81	9.17	10.71	9.563	14.717
8	18	1.64	1.39	1.89	1.640	2.524
9	24	0.15	0.1	0.16	0.137	0.210

Table A.23: Raw and adjusted data for Trial 6 Objective 1 for Superphosphate Area 3.

Flight	1				Fert/Area	Super/3
Collector	**Distance (m)**	**R1 (g)**	**R2 (g)**	**R3 (g)**	**Average (g)**	**Bounce Adjusted (g)**
1	-21	0	0	0	0	0
2	-15	0	0	0	0	0
3	-9	0	0	0	0	0
4	-3	0.53	0.23	1.06	0.607	0.644
5	3	9.26	10.47	13.1	10.943	11.608
6	9	16.07	15.16	15.18	15.470	16.410
7	15	2.82	3.37	3.96	3.383	3.589
8	21	0.58	0.56	0.58	0.573	0.608
9	27	0.15	0.38	0.26	0.263	0.279

Flight 2 **Fert/Area** Super/3

Collector	Distance (m)	R1 (g)	R2 (g)	R3 (g)	Average (g)	Bounce Adjusted (g)
1	-20	0	0	0	0	0
2	-14	0	0	0	0	0
3	-8	0	0.39	0	0.130	0.179
4	-2	0.57	0.16	0.17	0.300	0.414
5	4	14.21	10.91	12.3	12.473	17.213
6	10	28.91	25.78	25.62	26.770	36.943
7	16	7.7	6.93	6.82	7.150	9.867
8	22	1.42	0.99	1.2	1.203	1.661
9	28	0.3	0.11	0.12	0.177	0.244

Flight 3 **Fert/Area** Super/3

Collector	Distance (m)	R1 (g)	R2 (g)	R3 (g)	Average (g)	Bounce Adjusted (g)
1	-21.5	0	0	0	0	0
2	-15.5	0	0	0	0	0
3	-9.5	0	0	0	0	0
4	-3.5	0.56	0.92	1.2	0.893	1.233
5	2.5	20.18	21.66	28.06	23.300	32.154
6	8.5	19.27	21.61	20.04	20.307	28.023
7	14.5	3.56	3.26	2.92	3.247	4.480
8	20.5	0.33	0.81	0.72	0.620	0.856
9	26.5	0	0.45	0.17	0.207	0.285

Flight 4 **Fert/Area** Super/3

Collector	Distance (m)	R1 (g)	R2 (g)	R3 (g)	Average (g)	Bounce Adjusted (g)
1	-24	0	0	0	0	0
2	-18	0	0	0	0	0
3	-12	0	0	0	0	0
4	-6	0	0	0	0	0
5	0	0.09	0.14	0.42	0.217	0.299
6	6	13.34	14.11	18.54	15.330	21.155
7	12	11.89	12.36	14.17	12.807	17.673
8	18	1.56	1.96	2.21	1.910	2.636
9	24	0.15	0.1	0.18	0.143	0.198

Table A.24: Raw data for Flight 1 of Trial 7.

Flight 1		
Collector Masses (g)		
NZAAA	Bubble	Control
11.17	9.4	9.3
11.17	13.24	9.85
11.65	13.92	9.88
11.85	13.39	10.4
12.05	13.35	11.27
12.66	15.65	11.11
13.07	15.83	9.28
13.32	14	10.15
13.58	12.19	11.99
14.33	13.83	12.48
14.40	13.79	9.63
14.53	15.37	9.15
14.57	15.18	10
14.69	15.43	10.85
14.84	16.33	10.67
16.69	16.12	10.27
17.08	17.27	11.42
17.84	16.26	11.57
	14.8	11.57
	17.84	11.25
	14.36	10.94
	12.84	10.23
	13.76	10.68
	14.03	11.56
	15.69	10.24
	13.5	12.43
	13.68	9.41
	14.71	10.48
	15.9	10.92
	17.8	9.82

Table A.25: Raw data for Flight 2 of Trial 7.

Flight 2		
Collector Masses (g)		
NZAAA	Bubble	Control
15.99	22.8	13.25
16.76	21.52	14.03
18.22	24.27	14.39
20.01	23.93	14.61
20.25	23.73	14.71
20.57	22.02	14.8
20.75	22.12	14.95
20.86	22.1	15.08
21.94	20.09	15.09
22.66	19.63	15.29
22.93	19.35	15.52
23.92	24.59	16.27
	22.64	16.37
	19.09	16.38
	22.46	16.42
	22.63	16.65
	21.77	16.66
	22.1	17.21
	21.15	17.87
	22.77	18.44
	20.3	19.82
	19.58	
	18.78	
	21.62	
	23.33	
	23.46	
	23.92	
	20.59	
	25.27	
	22.21	